ASPECTS OF HOMOGENEOUS NUCLEATION

Thesis by

Barbara Ellen Wyslouzil

In Partial Fulfillment of the Requirements

for the Degree of

Doctor of Philosophy

California Institute of Technology

Pasadena, California

1992

(Defended August 23, 1991)

iii

ACKNOWLEDGEMENTS

ABSTRACT

Experimental investigations of vapor phase binary nucleation were carried out for both the methanesulfonic acid-water and the sulfuric acid-water systems. A rapid mixing device produced acid-water aerosols under isothermal conditions and at relative acidities (Ra), $0.04 < Ra < 0.65$, relative humidities (Rh), $0.01 < Rh < 0.65$, and temperatures, $T = 20$, 25 and 30 °C. The number concentration of the aerosol at the exit of the nucleation and growth tube is extremely sensitive to the binary nucleation rate. Thus at low particle concentrations, when condensation did not significantly change the saturation levels, the binary nucleation rates were estimated from the number concentration data as a function of Ra, Rh and temperature. Particle size distributions were also measured and found to vary with the amount of acid and water present. An integral model considering both nucleation and growth simulated the experimental system and predicted the total number of particles, the total mass in the aerosol phase, and the mass average diameter at the exit of the nucleation and growth tube. The simulations reproduced the experimental results quite well for the methansulfonic acid-water binary, if the nucleation rate was adjusted by a temperature dependent correction factor which ranged from 10^{-8} at $T = 19$ °C to 10^{-4} at 30 °C. Further analysis showed that the ratio of experimental to theoretical nucleation rates for both acid-water systems was a strong function of the predicted number of acid molecules in the critical nucleus.

Classical homogeneous nucleation theory was extended to nonisothermal conditions by simultaneously solving cluster mass and energy balances. In vapor phase nucleation, the steady state nucleation rate was lower than the corresponding isothermal rate and this discrepancy increased as the pressure of the background gas decreased. After the initial temperature transients decayed, subcritical clusters were found to have temperatures elevated with respect to that of the background gas.

TABLE OF CONTENTS

Chapter 3 : Binary Nucleation in acid-water systems II.
Sulfuric acid-water and a comparison with
methanesulfonic acid-water   70

Chapter 4 : Nonisothermal Homogeneous Nucleation   111

LIST OF FIGURES

Chapter 2

Appendix : Supplementary Material to Chapter 2

Chapter 3

Appendix : Supplementary Material to Chapter 3

Chapter 4

xvi

Appendix A

Figure 1. : Schematic of the TSI 3020 condensation nucleus counter.   163

Figure 2 : Detection efficiency of the TSI 3020 condensation nucleus
counter.   164

Figure 3 : Particle detection efficiency for the TSI 3760 condensation nucleus
counter alone and combined with the TSI 3071 differential mobility analyzer.   165

Figure 4 : Schematic of the differential mobility analyzer.   166

Figure 5 : Sheath air calibration for the 3071 differential mobility analyzer.   167

Figure 6 : Sheath air calibration for the short body (L^B = 10 cm) differential
mobility analyzer.   168

Figure 7 : Combined detection efficiency for the 3020 condensation
nucleus counter and the short body differential mobility analyzer.   169

Figure 8 : Linearizing circuit for the AD590 series thermistor.   170

Figure 9 : Schematic diagram of the thermistor placement.   171

Figure 10 : Schematic of the capillary flowmeters.   172

Appendix B

LIST OF TABLES

CHAPTER 1

Introduction

The formation of a new phase and the rate at which it appears in a supersaturated parent phase has long been a topic of practical as well as theoretical interest. One such class of phase transitions, perhaps the most apparent in daily experience, is the gas to particle or gas to liquid phase transition. Examples of this process include new aerosol formation in the atmosphere, ash and soot production during combustion, the manufacture of high quality ceramic powders, and the appearance of water droplets formed as the water vapor exiting a boiling kettle cools, supersaturates and nucleates. To control these phase transitions in order to use them advantageously, it is necessary to predict both the conditions for onset and the rate at which particles of the new phase appear. Both of these issues are addressed by classical nucleation theory and explored by nucleation experiments.

First developed by Volmer[1] and Becker and Doering[2] to describe the gas to liquid phase transition in the absence of particles or other surfaces, classical nucleation theory successfully predicts the major trends of single component nucleation phenomena and does a reasonable job of anticipating the onset of significant nucleation. The theory has been modified to address such issues as including the effects of the rotational and translational free energy of the new phase clusters,[3] the effect of using a size dependent surface tension term[4] and accounting for association of the monomer in the parent phase.[5] The theory has also been extended to describe more complex situations of interest, for example particle formation involving multiple condensing species, which Reiss[6] first developed for the case of two component, or binary, nucleation. Experimental methods employing the thermal upward diffusion chamber, fast expansion chambers and shock tubes, have been developed

to measure the nucleation rate as a function of the saturation level and temperature. As the quality and quantity of available data continues to improve, more stringent tests of the theory may be posed leading to a better understanding of the fundamental physical processes involved.

This thesis explores two areas of nucleation phenomena and theory. The first section of the thesis, Chapters 2 and 3, describes detailed experimental studies of binary nucleation in acid-water systems. As a consequence of the added complexity of working with two components rather than one, far fewer data exist for binary systems and only very limited data exist for acid-water binaries because of the difficulty associated with working with these highly corrosive materials. The two acids used in the experiments, sulfuric acid (H_2SO_4) and methanesulfonic acid (CH_3HSO_4), are of great interest because they are both naturally occurring atmospheric species that can nucleate in the presence of water vapor to form new particles, even when both species are unsaturated. Dimethylsulfide produced by marine phytoplankton oxidizes in the atmosphere to produce methanesulfonic acid. Sulfuric acid is formed as the oxidation product of SO_2, which is emitted by both natural and anthropogenic sources. The sulfuric acid-water system is of particular interest because it is the system traditionally used to test various forms of the binary nucleation rate expression The data collected in the present experiments are the first measurements of nucleation rates for H_2SO_4-H_2O binary systems at subsaturated conditions and in the absence of chemical reaction. Furthermore, these experiments represent the first systematic study of the temperature dependence in binary nucleation.

The experiments use a fast mixing apparatus to produce an aerosol consisting of acidic solution droplets. Both the number concentration of the particles produced and the resultant particle size distributions in these two acid-water systems are measured as functions of relative humidity, relative acidity and temperature. When the rate of particle production is low enough the nucleation rates are calculated from the observed number

concentration and compared to the rates predicted by classical nucleation theory. For higher particle production rates, the experiments are modelled using an integral model that considers both nucleation and condensation. The measured particle size behavior is compared to the predictions of the integral model and provides additional insight into the competition between nucleation and condensation in binary systems.

Classical nucleation theory assumes that new particles appear from the supersaturated vapor phase by the growth of liquid-like clusters of monomer. Clusters grow or decay by the addition or loss of a monomer, and the equations used to describe the time rate of change of the cluster distribution may be solved to yield both the steady state cluster distribution and the steady state particle flux or nucleation rate. Chapter 4 of this thesis investigates the effects of solving these mass balance equations in the presence of a second set of differential equations that describe the energy changes that arise because the phase transition is necessarily accompanied by a change in energy. The energy released or required by the phase transition may have a dramatic effect on the mass balance equations since the two sets of equations are strongly coupled. Both the transient and steady state behavior are discussed and compared to the isothermal results using the vapor to liquid phase transition of water as a model system.

In Chapter 5 the results and conclusions of the work presented in this thesis are summarized.

References

[1]M. Volmer, Z. Phys. Chem., **25**, 555 (1929).

[2]R. Becker and W. Doering, Ann. Phys. (Leipzig), **24**, 719 (1935).

[3]J. Lothe and G.M. Pound, J. Chem. Phys., **36**, 2080 (1962).

[4]B.V. Derjaguin and A.V. Prokhorov, J. Colloid Interface Sci., **46**, 283 (1974).

[5]J.L. Katz, H. Saltsburg and H. Reiss, J. Colloid Interface Sci., **21**, 560 (1966).

[6]H.J. Reiss, J. Chem. Phys., **18**, 840 (1950).

CHAPTER 2

Binary Nucleation in Acid - Water Systems
I. Methanesulfonic Acid - Water

B.E. Wyslouzil, J.H. Seinfeld and R.C. Flagan,

Department of Chemical Engineering,

California Institute of Technology,

Pasadena California 91125

and

K. Okuyama

Department of Chemical Engineering,

Hiroshima University,

Saijo-cho, Higashi-Hiroshima,

Japan

ABSTRACT

Experimental measurements of binary nucleation between methanesulfonic acid (MSA) and water vapor were carried out for relative acidities (Ra), $0.05 < Ra < 0.65$, and relative humidities (Rh), $0.06 < Rh < 0.65$, using a continuous flow mixing-type device. The number concentration of particles leaving the nucleation and growth tube was measured as a function of the initial relative humidity and the relative acidity in the temperature range from 20 to 30 ° C. Particle size distributions were also measured and found to vary with the amount of water and acid present. The system was simulated to predict the total number of particles and the total mass of acid in the aerosol phase using a simple integral model and classical binary nucleation theory allowing for the formation of acid-water hydrates in the gas phase. At low particle concentrations, condensation rates did not significantly change the saturation levels and the nucleation rates were estimated from the total number concentration data as functions of Ra, Rh and temperature. The values of experimental and theoretical nucleation rates differed significantly, with J_{exp}/J_{theor} changing as a function of temperature from 10^{-8} to 10^{-4} as temperature varied from 20 to 30 ° C. This work represents the first systematic experimental study of the temperature dependence of binary nucleation.

I. INTRODUCTION

Significant particle formation by heteromolecular, homogeneous nucleation between an acid gas and water vapor was first predicted for sulfuric acid and water by Doyle[1] using the binary nucleation theory developed by Reiss[2]. Since then, only three acid - water systems have been studied experimentally; these are sulfuric acid (H_2SO_4) - water, nitric acid (HNO_3) - water, and methanesulfonic acid (CH_3HSO_4) - water.

Reiss, et al.[3] had limited success using an expansion chamber to study nucleation in the sulfuric acid and water systems, encountering problems related to corrosion and the low vapor pressure of H_2SO_4. The high expansion ratios required in their experiments produced low final temperatures (- 28.5 ° C to - 51.7 ° C) which makes comparison with theory difficult because the measured thermodynamic data exist only at much higher temperatures. On further analysis, Shelling and Reiss[4] concluded that expansion chambers or nozzles were not well suited for measuring the critical supersaturation ratios in H_2SO_4 - water vapor mixtures.

Boulaud et al.[5] mixed varying amounts of SO_3 and water vapor in a 200 l vessel and measured the resulting particle concentration as a function of time, from which they estimated the nucleation rates. The change in nucleation rate, J, with respect to time, due to changes in the saturation level of the acid in the vessel, was not considered and so their data represent at best an estimate of J_{avg} for the first 150 s of the experiments.

Mirabel and Clavelin[6] used an upward thermal diffusion chamber to measure the onset of nucleation (nucleation rate, $J = 2 - 3$ $cm^{-3}s^{-1}$) in both the nitric acid - water and sulfuric acid - water systems. They were able to investigate the nitric acid - water system for

$0 < $ Rh $ < 3$ and at two temperatures, 5 ° C and 25 ° C, but they did not comment on the effect of temperature on the critical saturation ratios. In the case of sulfuric acid - water they investigated only $T = 25$ ° C, and values of Rh < 1 were not possible because of the low vapor pressure of H_2SO_4. Nucleation rate measurements represent a more sensitive test of the theory than simple measurements of the onset of nucleation, and thermal diffusion chambers have only recently been used for this purpose in the case of single component nucleation[7].

Nucleation in the methanesulfonic acid - water system was first studied experimentally by Kreidenweis et al.[8] for $T = 25$ ° C and Ra, Rh < 1.0. Methanesulfonic acid is a naturally occurring oxidation product of biogenically produced dimethyl sulfide, and recent interest has focussed on estimating the contribution of this material to the formation of non-sea-salt aerosols over the remote pacific, its potential as a source of cloud condensation nuclei, and its role in the overall global sulfur budget[9,10]. Measured nucleation rates for this system are therefore of interest, both in their own right, as well as for comparison with those of sulfuric acid which is also considered a major source of atmospheric aerosol particles. This comparison will be made in Part II where the data from H_2SO_4 - water nucleation experiments are presented.

The MSA - water nucleation measurements of Kreidenweis et al.[8] employed a continuous-flow mixing-type device first applied to binary nucleation studies by Okuyama et al.[11]. In this device particle-free gas streams saturated with the desired acid and water vapor are rapidly mixed at known temperatures and pressures to create well characterized initial conditions. The mixed stream is then allowed to nucleate, and the particles grow while flowing through an isothermal flow tube. The number concentration of particles produced is measured at the outlet of the nucleation and growth tube using a high resolution particle counter and provides a sensitive measure of the binary nucleation rate. Although

the continuous flow experimental approach has some drawbacks, for instance at very high nucleation rates mixing and nucleation may be occurring over comparable timescales, it appears to be the simplest available method for generating consistent and reliable nucleation rate data in acid-water systems under controlled, isothermal, and subsaturated conditions.

The present work expands on that of Kreidenweis et al.[8], incorporating several changes to the apparatus that allow for better control of the experimental flows and temperatures. These modifications are reflected in the improved repeatability of the results which makes it possible to distinguish real variations in nucleation rates, due to changes in such variables as temperature, from problems in experimental repeatability. In addition, the effects of temperature on the nucleation process are systematically investigated and particle size distributions are measured to further elucidate the competition between nucleation and condensation in such systems. The experimental data are then evaluated against classical binary nucleation theory.

II. THE CONTINUOUS FLOW MIXING DEVICE AND EXPERIMENTAL PROCEDURES

Figure 1 shows a schematic of the experimental apparatus used in the nucleation experiments. The equipment is similar to that used by Kreidenweis et al.[8] but it has been modified in several key areas. In particular, improvements have been made in flow control and measurement, the design of the acid bubbler has been changed to reduce pressure buildup during experiments and to facilitate cleaning, and the use of a single large water bath gives better temperature control.

Extra-dry bottled air is used as the carrier gas in the experiments. After passing the air through a conditioning column containing silica gel, a 10 Å molecular sieve, and a high capacity Teflon filter with a 0.2 μm pore size, the pressure is reduced from 275 kPa to about 100 kPa. The flow is then split into the three streams required in the experiments; a stream of air to be saturated with water, F_h, a stream to be saturated with acid, F_a, and a stream of air for dilution, F_d. The flowrates of these streams are measured using flowmeters consisting of glass capillary tubes and 0 - 10 torr differential pressure transducers. The flows are controlled by needle valves placed at the downstream end of the flow capillaries. Thus the pressure in the capillary tubes is maintained and is relatively insensitive to downstream pressure fluctuations. The calibrated range of each flow capillary is 20 - 1000 $cm^3 min^{-1}$. All of the lines used for air transfer are dehydrated copper, Teflon or polyflow tubing. All of the surfaces in contact with acid or acid gas are glass, Teflon or Viton. Swagelok^{TM} fitting are used throughout the apparatus.

The air is saturated with water by bubbling the air stream through a series of two water bubblers containing ultrapure water. The first bubbler is at room temperature while the second bubbler is fully immersed in the large water bath. Calibrated thermistors are used to measure temperatures throughout the system, and the temperature of the final humidification stage is measured by a thermistor (T1) encased in a glass tube submerged in the liquid. The pressure inside the water bubbler is measured at a pressure tap located near the top of the bubbler. At the exit of the bubbler a filter assembly containing two 0.2 μm pore size Teflon filters, eliminates the entrained liquid water droplets.

Dry dilution air is added to the humid stream at the tee between the water bubbler and the mixer. This stream allows the relative acidity and relative humidity to be varied while still maintaining a constant total flow rate through the nucleation and growth tube. The temperature of the mixed humid stream is measured just before it enters the mixer (T3), to

confirm that the temperature of this stream is the same as the bath and the acid stream temperatures.

The air to be saturated with acid enters the bottom of the acid bubbler and bubbles through a pool of acid supported on a 60 mm wide fine frit. A thermistor *(T2)* enclosed in a glass tube measures the temperature of the acidified air near the top of the bubbler. The pressure inside the bubbler is measured at a nearby pressure tap. A filter assembly containing two 41 mm diameter Teflon filters with pore size of 0.2 μm, removes entrained acid particles without imposing a large pressure drop between the acid bubbler and the mixer.

Figure 2 illustrates the overall acid bubbler, mixer and nucleation and growth tube assembly. The mixer is machined entirely of Teflon and is located directly above the acid bubbler. The acidic air enters the central chamber from the bottom, while the humid air is injected through eight 0.5 mm diameter holes surrounding the chamber. The distance from the top of the acid filters to the center of the mixing chamber is less than 1.5 cm to minimize vapor loss between the position where equilibrium of the acid is assumed and where the two vapor streams combine. The rapid mixing promoted by the geometry of the mixer gives rise to the desired initial conditions of relative humidity and relative acidity. Above the mixer, a 51 mm diameter glass tube with a volume of 280 cm^3, provides time for the nucleation and growth of the particles. A thermistor in the water bath just outside the tube and about halfway down *(T4)*, measures the temperature at which nucleation occurs.

The flow from the nucleation and growth tube exits to a 10 mm (3/8") glass tube. The level of the water in the temperature-regulated bath is maintained at this height. A 6 mm (1/4") Teflon tube leads from the tube exit, through the wall of the bath to a TSI model

3020 condensation nucleus counter (CNC). The CNC draws 300 cm^3 min^{-1} of the flow and the excess flow is vented.

Particles size distributions are measured using the Scanning Electrical Mobility Spectrometer (SEMS)[12] when the particle concentration is high enough ($\geq$ 5x10^3 cm^{-3}) . This instrument rapidly scans the entire particle size distribution by exponentially ramping the collector rod voltage of a TSI model 3071 differential mobility analyzer (DMA) with the transmitted particles being counted by a TSI model 3076 CNC. An IBM AT computer controls the collector rod voltage of the DMA, counts the particles detected by the CNC in successive time intervals, and displays the calculated size distribution. Particle size distributions were taken at two to six different conditions during an experiment and ten scans were taken at each condition to assure a representative distribution. The 3076 CNC requires a flow of ~1.6 l min^{-1} and experiments were generally run at 1.0 l min^{-1} total flow, therefore clean filtered room air is drawn into the line between the classifier and the CNC to make up the difference in flows. The use of lab air at this point will not change the number of particles measured by the CNC because the experiments are all run at low relative humidity.

The experiments all used a total flow rate of 1.0 l min^{-1} (measured at STP) to maintain a constant residence time of about 18 seconds in the nucleation and growth tube. In each experiment a value of relative acidity or relative humidity was selected and then the value of the other variable was changed to obtain conditions where total number concentrations ranged from near zero to as high as possible. Generally it was possible to observe a change in total particle concentration of five to seven orders of magnitude. Experiments were started either at a high or low number concentration and the relative saturation level of interest was changed in increments of 0.01 to 0.05. The total number of particles was recorded when the new conditions had stabilized, 2 to 5 min after selecting a new

condition. This time corresponded to 7 to 18 times the residence time of the nucleation and growth tube. Total number concentration measurements were then recorded manually for several minutes with 8 to 30 values recorded at each setting from which a mean value was subsequently calculated. Before taking any measurements, the equipment was run for more than 10 h after the addition of acid to assure stable operating conditions.

Figure 3 shows a schematic of the type of data curves generated, and indicates the different operating regimes that exist during a complete nucleation experiment. The fundamental principle of the continuous flow nucleation experiments is that at small observed number concentration condensation rates are sufficiently low that the acid saturation level, and hence the nucleation rate, remains constant from the time of mixing until the particles are counted. Thus in this regime the nucleation rate may be calculated by dividing the observed number concentration by the length of time over which nucleation occurs. Because of the low vapor pressure of the acid with respect to that of water, the saturation level of water will be constant even at high nucleation rates. The initial steep increase in the observed number concentrations with saturation level corresponds to the constant nucleation rate regime.

As the saturation level of one component and the observed number concentration increase further, condensation begins to compete effectively with nucleation and reduces the acid saturation so that nucleation is rapidly quenched after the initial mixing. Because the length of time during which constant nucleation is occurring cannot be easily determined, these data points cannot be used to calculate nucleation rates. They do however provide additional test points with which to compare the results from an integral model that accounts for both nucleation and condensation. This regime is analogous to that described by Hung et al.[7] when measuring nucleation rates using an upward thermal

diffusion cell, where above a certain threshold value of J, the assumption of negligible mass loss is no longer valid and rates cannot be deduced from the observed particle flux.

At the highest saturation levels, initial nucleation rates are extremely high and the timescales of mixing, nucleation and coagulation become comparable. These points correspond to the extremely flat region in the observed number concentration versus saturation curves.

A. Calculation of relative humidity and relative acidity

The relative humidity and acidity of the combined streams is calculated based on a simple mass balance, the assumption of equilibrium in the bubblers at the temperature, and the pressure recorded inside each bubbler at a given condition.

The relative humidity after mixing is

$$Rh = \frac{p_l \, Y_w \, F_h}{p_w(T_m) \, [(1+Y_w)F_h + F_d + F_a]} \tag{1}$$

where F_h, F_d and F_a are the humid, dry and acidic flows, p_l is the absolute pressure in the laboratory, $p_w(T_m)$ is the saturation vapor pressure of water at the temperature inside the mixer. T_m is equal to the temperature in the nucleation and growth tube as measured by thermistor $T4$ since mixing is isothermal. Y_w, the ratio of the moles of water to the moles of dry air is

$$Y_w = \frac{p_w(T_{wb})}{p_{wb} - p_w(T_{wb})} \tag{2}$$

Here $p_w(T_{wb})$ is the saturation vapor pressure of water at the temperature inside the water bubbler and p_{wb} is the actual measured pressure inside the water bubbler.

Likewise the relative acidity after mixing is

$$Ra = \frac{p_1\, p_a(T_{ab})\, F_a}{p_{ab}\, p_a(T_m)\, [(1+Y_w)F_h + F_d + F_a]} \tag{3}$$

where p_{ab}, $p_a(T_{ab})$ and $p_a(T_m)$ are the actual acid bubbler pressure, the saturation vapor pressure of the acid at the temperature in the acid bubbler and the saturation vapor pressure of acid at the temperature of the mixer. Furthermore the ratio of moles of acid to moles of air, Y_a, is approximately equal to zero because the vapor pressure of the acid is on the order of 1 ppm.

B. Acid Purity

The methanesulfonic acid used in all of the experiments was purchased from the Alfa Chemical Company with an assayed acid purity of 99.5% established by titration. This acid was not purified further and ranged in color from a pale straw color to light brown. On further discussion with the manufacturer of the acid, Penwalt Chemical Company, the major impurities were given as dimethyl disulfide at <10 ppm and methyl methane thiosulfonate at <5 ppm with some indication of chloromethyl sulfone at <1 ppm. This is the same material used in the experiments by Kreidenweis et al.[8].

III. NUCLEATION RATES AND PARTICLE SIZE BEHAVIOR

Experiments were performed at relative acidities of 0.33, 0.15 and 0.075 and relative humidities of 0.30 and 0.15. The three temperatures investigated were 19, 25 and 30 °C. Table 1 summarizes the conditions employed in the set of experiments presented here.

The measured total number concentrations of particles as functions of Rh are summarized in Figures 4 through 6 for the three different temperatures. Horizontal error bars represent the computed uncertainty in the Rh due to uncertainties in the flow and temperature control. This uncertainty has been estimated as ± 5%, due mainly to the uncertainties in flow calibrations which are each ± 3%. Vertical error bars represent the range of values observed after the system had stabilized for a given condition, with the symbol located at the calculated mean value. The broken lines are the result of simulating the experiments and will be discussed subsequently. The equivalent curves generated for experiments in which Rh was constant and Ra was varied are available in the supplementary material submitted to PAPS[13].

The extent to which the experiments are repeatable when working with a given batch of acid, is illustrated in Figure 4 where data for the two runs at Ra = 0.33 were taken three days apart, and in Figure 6 where data for the two runs at Ra = 0.075 were taken about 5 hours apart. Consistency of the data set is very good and is illustrated in each of the figures by * symbols. In these figures data points collected during tests at constant relative humidity were added to the graphs of tests at constant relative acidity to show that the measured number concentration is insensitive to the way the particular combination of Ra and Rh was approached.

The total number concentration data follow the major trends predicted by binary nucleation theory. At low levels of one component particle concentrations less than 0.1 cm^{-3} are observed, which indicates that nucleation is not occurring at a measurable rate. At moderate degrees of saturation, a slight increase in the level of one of the components leads to an exponential increase in the total number of particles observed. This reflects the exponential increase in nucleation rate with saturation level that is characteristic of nucleation processes. As the saturation is increased further, the total number concentration curves begin to level off, indicating that the available acid vapor is rapidly depleted by condensation onto the newly formed particles and the nucleation process is quenched. With the production of large numbers of particles initially, condensation competes effectively for the remaining acid vapor and quickly reduces the relative nucleation rate. Thus large changes in the saturation level lead to relatively small changes in the total number of particles observed. Total particle concentrations generally vary from 5 to 7 orders of magnitude over the course of an experiment. On the steepest curves, this large increase is achieved over a change in relative saturation of only 0.3. As relative acidity decreases, a higher level of relative humidity is required before particles are observed. Equivalent results are observed as relative humidity decreases. Figures 7 through 9 summarize the relative saturation levels that correspond to nucleation rates of $J = 0.01$, 1, and $100 \text{ cm}^{-3}\text{s}^{-1}$ that were derived from the total number concentration data at each temperature.

The increase in nucleation rates with temperature is clearly illustrated by comparing equivalent curves in Figures 4 through 6, where a 5 °C increase in temperature generally corresponds to a two order of magnitude increase in the nucleation rate. This increase in nucleation rate with temperature is consistent with observations in single component nucleation experiments.

Figures 10 and 11 illustrate typical particle size distributions. Figure 10 shows that as Rh increases at fixed Ra, particle size generally decreases. Physically, as the nucleation rate increases with Rh more particles are being formed from the same initial amount of acid. Thus there is simply less acid available for particle growth and the particle size must generally be smaller. On the other hand, Figure 11 shows that as Ra increases at fixed Rh, particle size first increases and later decreases. Here the situation is more complex. Although an increase in nucleation rate should decrease particle size, an increase in the amount of acid also allows for greater particle growth by condensation. Thus it appears that increases in condensation initially dominate and it is only at the highest saturation levels that increases in the nucleation rate produce enough particles to reduce the average particle size.

Many of the particle size curves display a bimodal distribution with a broad main peak and a smaller secondary peak located at approximately one half the diameter of the main peak. The main peak is believed to represent those particles that are formed by nucleation between MSA and water vapor which then grow by the subsequent condensation of MSA and water in the nucleation and growth tube. Because of the great excess of water present, particles are in equilibrium with the local relative humidity at all times, and growth is limited by the number of acid molecules added to the droplet. The main peak is always present. The second peak is most pronounced at high saturation levels of both components and at the highest temperatures. In about half of the distributions this second peak is not present.

From the measured number distributions, $dN/d\ln D_p$, volume distribution, $dV/d\ln D_p$, curves were constructed. The peak diameter of the volume distribution curves, which is equivalent to the peak diameter in the mass distribution, was within the measuring range of the DMA for about half of the distributions. This value is important because it is predicted

by the model that will be used to simulate the experiments. Figures 12 and 13 further illustrate the behavior of the peak diameter in the number distribution under varying conditions of relative humidity and relative acidity. The broken lines are intended as visual aids only and do not represent numerical fits of the data points. In Figure 12 the largest changes in peak diameter are found in the curve for Ra = 0.33. By comparing the conditions of these tests to the appropriate number concentration curves, it is clear that the larger decrease in diameter at Ra = 0.33 corresponds to a larger increase in number concentration than is observed for the conditions at Ra = 0.075, where essentially no change in peak diameter is observed.

The effect of changing Ra for fixed Rh is illustrated for $T = 30 \, ^\circ$ C in Figure 13. The curves at two levels of Rh exhibit the same type of behavior, an increase in peak diameter with an increase in Ra followed by a sharp decrease at the highest level of Ra. As in Figure 12, the particles produced at higher relative humidity are smaller. This behavior was also observed at $T = 19$ and $25 \, ^\circ$ C.

Although the model used predicts only a single mass average diameter, Figure 14 shows that for the range of data collected, the peak in the mass distribution is related to the peak in the number distribution in a straightforward manner. Thus the curves illustrating the behavior of the number distribution peaks should be equivalent to the behavior in the mass distribution peaks with a suitable change in the scaling. In addition, the slope of this curve gives an estimate of the polydispersity factor α_p. This factor will be required in the integral model equation describing the condensation of the acid vapor onto the existing aerosol. Because the model assumes a monodisperse aerosol, condensation will be overpredicted if α_p is set equal to 1. Okuyama et al.[11] showed that the polydispersity factor $\alpha_p = D_{pN} / D_{pm}$ where D_{pN} and D_{pm} are the number and mass average diameters respectively. In Figure 14 this corresponds to the slope of the data and is about $\alpha_p = 0.6$.

IV. INTEGRAL MODEL OF NUCLEATION AND GROWTH

The measured total number concentrations do not yield nucleation rates directly. Rather they measure the total number of particles that result from the competition between nucleation and condensation along the length of the nucleation and growth tube. When the total number of particles is small, condensation should not change the saturation level of the acid significantly, and the nucleation rate may be calculated from the total number concentration by dividing by the length of time over which nucleation is occurring. In order to determine when condensation begins to dominate and to compare experimental results to the predictions of theory over the entire range of experimental results, it is necessary to integrate the changes occurring in the gas and aerosol phases along the length of the nucleation and growth tube. The fact that the total number of particles is a strong function of the nucleation rate provides the basic validity of the experimental approach; it is expected that simulating the experiments should yield sensitive information regarding the adequacy of the binary nucleation rate expression over the range of conditions studied.

An integral nucleation and growth model that predicts the basic variables of interest, i.e., the total number of particles formed and the mass average particle diameter, was developed by Okuyama et al.[11] and is the model applied to these experiments. The model describes the saturation level of the acid in the vapor phase, S_a, the total number of particles, N_a, and the total mass of acid in the aerosol phase, M_a, and will therefore be referred to as the SNM model. The model assumes that the formation and growth of the aerosol does not change the amount of water present because the vapor pressure of the water is much higher than that of the acid.

The three differential equations that describe the evolution of the aerosol in the absence of coagulation and wall losses from either the vapor or aerosol phase are

$$\frac{dS_a}{dt} = \frac{dR_a}{dt} = \frac{-(N_A \, g^* \, J + R_c) \, RT}{p_a^\circ} \tag{4}$$

$$\frac{dM_a}{dt} = M_{wa} (g^* J + R_c) \tag{5}$$

$$\frac{dN_a}{dt} = J \tag{6}$$

where N_A is Avogadro's Number, g^* is the number of acid molecules in a critical cluster, J is the rate of binary nucleation, R_c is the rate of condensation and M_{wa} is the molecular weight of the acid. The equations are integrated for 18 s, which corresponds to the residence time of the nucleation and growth tube under the conditions employed. The mass of each droplet at any point in the tube is calculated by taking the total mass of acid in the aerosol phase, dividing by the total number of particles and then adding water to achieve equilibration at the local relative humidity. The mass and composition of the droplet determine the mass average diameter. The property data correlations for the MSA - water binary used in the simulations are those developed by Kreidenweis et al.[8].

A. The Rate of Binary Nucleation

The generalized rate expression for binary nucleation is

$$J = C \exp(-\Delta G^*/kT) \tag{7}$$

where ΔG^* is the free energy of formation of the critical cluster from the vapor phase and C is a slowly varying pre-exponential factor. The critical cluster corresponds to the saddle

point in the cluster free energy surface. Later work refined the original expression of Reiss[2] to better reflect the kinetics of the process[14], to locate the saddle point more accurately[15-17], and to reflect the effect due to the presence of hydrates in the gas phase[18-20].

Hydrate formation can have a relatively large effect on the nucleation rate by changing the shape of the free energy surface and therefore the location and value of ΔG at the saddle point. Traditionally, the free energy surface is described as a function of the number of acid molecules, n_1, and the number of water molecules, n_2, by

$$\Delta G(n_1, n_2) = n_1(\mu_1 - \phi_1) + n_2(\mu_2 - \phi_2) + \sigma A \tag{8}$$

where μ and ϕ are the chemical potentials of the species in the liquid and gas phases, σ is the surface tension of the cluster and A is the surface area of the cluster.

Jaecker-Voirol and Mirabel[19] showed that the free energy surface, ΔG, could be modified to produce a new surface $\Delta G'$, reflecting the presence of hydrates. Their expression relating the two surfaces is

$$\exp\left(\frac{-\Delta G'}{kT}\right) = \left[\frac{1 + K_1' p_w + \quad + K_1' K_2' \ldots (p_w)^h}{1 + K_1' p_1 + \quad + K_1' K_2' \ldots (p_1)^h}\right]^{n_2} \exp\left(\frac{-\Delta G}{kT}\right) \tag{9}$$

Here p_w is the partial pressure of water vapor above a droplet of composition n_1 waters and n_2 acids, and p_1 is the vapor pressure of water in the system. The values of K_h' are the equilibrium constants for the reactions

$$H_2O + ACID \cdot hH_2O \leftrightarrow ACID \cdot (h+1)H_2O \tag{10}$$
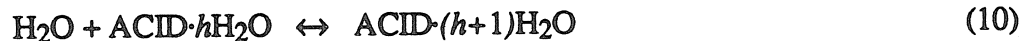
and are found by looking at the free energy change on addition of a water molecule,

$$K_h' = \exp\left(\frac{-\Delta G_h{}^\circ}{kT}\right) \qquad (11)$$

with

$$\Delta G_h{}^\circ = kT \ln p_w + \frac{2\,\sigma\,v_1}{r} \qquad (12)$$

p_w is expressed in atmospheres, σ is the surface tension, v_1 is the partial molecular volume of water (partial molar volume/N_A), and r is found from

$$\frac{4}{3}\pi r^3 = (n_1 + n_2)\,v \qquad (13)$$

where v is the molecular volume of the mixture[21]. The first ten hydration constants were calculated by Jaecker-Voirol and Mirabel[19] for sulfuric acid and water. Table 2 shows the equivalent values for the MSA - water binary at 25 ° C calculated using equations (11) - (13). With $K_1' = 142$ for MSA versus 1360 for sulfuric acid, the effect of hydration is not as strong for MSA, but it is still significant, especially at higher relative humidities.

Hydrate distributions were calculated for relative humidities of 0.1, 0.5 and 1.0. Above Rh = 0.10, the concentration of hydrates containing one acid molecule becomes significant with respect to the total acid concentration. The concentration of hydrates containing 2 or 3 acid molecules is always many orders of magnitude smaller than the equivalent hydrate containing only one acid molecule, and may therefore be ignored.

Including the effect of hydrates, the general nucleation rate expression still takes the form

$$J = C \exp\left(-\Delta G'^*/kT\right) \tag{14}$$

but now $\Delta G'^*$ is the saddle point of the modified free energy surface. The frequency factor C previously had the form

$$C = \frac{\beta_2 A^* N_1 Z}{\sin^2 \phi} \tag{15}$$

where β_2 is the rate of acid impingement, A^* is the surface area of the critical nucleus, N_1 is the number density of water vapor and Z is the non-equilibrium factor, equivalent to the Zeldovitch factor in single component nucleation. The angle ϕ is the angle between the direction of growth and the n_1 axis. In cases when the critical nucleus in not dilute with respect to either component, Jaecker-Voirol and Mirabel[20] have suggested that this angle may be approximated by

$$\tan \phi = \frac{n_2^*}{n_1^* + n_2^*} \tag{16}$$

It can be shown that this assumption is valid for the conditions of interest in the MSA - water system. To account for hydrates, the term $\beta_2 A^*$ is replaced by

$$\tau = (8\pi kT)^{1/2} \sum_{h=0}^{h=h_{max}} \delta^2 \gamma^{-1/2} N_h \tag{17}$$

where δ is the sum of the radii of the critical nucleus and the hydrate, γ is the reduced mass of the critical nucleus and the hydrate and N_h is the number density of the hydrates containing h water molecules.

The effect that hydration has on the nucleation rate in the region of interest for the experiments carried out here, is illustrated in Figure 15, where rates calculated without accounting for hydrates are compared to those predicted by the hydrated theory. At Rh = 0.10, the rate is reduced by about 2 orders of magnitude, while at Rh = 1.0 J_{unhydr}/J_{hydr} $\cong 10^{-6}$. The value of Z has been taken as 0.25.[20] The saddle point of the free energy surface has been determined by a numerical search that limits clusters to integral numbers of water and acid molecules.

B. Rate of Condensation

Once particles have formed in the gas phase, nucleation must compete with condensation, which will quickly dominate the mass transfer process from the gas to the aerosol phase. The condensation rate is approximated by a continuum expression which is modified for non-continuum effects by an expression due to Dahneke,[22]

$$R_c = 2\pi D_{AB} p_a{}^{\circ} \int_{D_p{}^*}^{\infty} D_p\, n(D_p)\, [\, S_a - a_a \exp\left(\frac{4\sigma \bar{v}_a}{D_p RT}\right)\,]\, f(Kn)\, dD_p \tag{18}$$

$$= \alpha_p \{\, 2\pi D_{AB} p_a{}^{\circ} \bar{D}_p [\, S_a - a_a \exp\left(\frac{4\sigma \bar{v}_a}{\bar{D}_p RT}\right)\,]\, f(\overline{Kn})\, \}\, N \tag{19}$$

with the average Knudsen number, $\overline{Kn} = \dfrac{\lambda_{AB}}{\overline{D}_p}$, $\overline{D}_p$ the average particle diameter and

$$f(\overline{Kn}) = \frac{(1 + \overline{Kn})}{(1 + 2\,\overline{Kn}\,(1 + \overline{Kn})\, /\, \alpha_s)} \tag{20}$$

Here D_{AB} is the binary diffusion coefficient of acid gas in air, a_a is the acid activity, $\overline{v}_a$ is the partial molar volume of the acid and λ_{AB} is the mean free path of the acid molecules in air. A factor α_s has been added to account for the sticking probability of an acid molecule, and a second factor α_p accounts for the polydispersity of the the aerosol. Because the aerosol is modelled as being monodisperse, condensation will be overpredicted if α_p is set equal to 1. However, from the data of D_{pN} vs D_{pm} it is possible to estimate a value for $\alpha_p = D_{pN}/D_{pm}$ as about 0.6. The term α_s represents the sticking probability or accommodation coefficient of an acid molecule as it strikes the surface of a growing droplet. The value of this parameter has not been measured for MSA. Recent work by Van Dingenen[23] concluded the value of α_s for sulfuric acid lies in the range $0.024 < \alpha_s < 0.064$ with a geometric mean value of 0.04, but in the absence of any other data $\alpha_s = 1.0$ will be used in the MSA modelling.

If the presence of hydrates is included in the nucleation calculation, their effect on the rate of condensation should also be considered. The change in the average value of D_{AB} and λ_{AB} due to hydrates is of greatest concern. Table 3 summarizes the estimated values of these parameters for the first five hydrates, and weights them with respect to the relative number distribution of the hydrates at relative humidities of 0.50 and 0.10 to estimate an average value. The diffusivities were estimated using the Chapman-Enskog equation with the first order approximation of the collision parameter, $\Omega = 1,$ [24]

$$D_{AB} = \frac{0.00266 \, T^{3/2}}{p \, M_{AB}^{1/2} \, \sigma_{AB}^2} \tag{21}$$

with p, the pressure in bars, $M_{AB} = 2 \left[\frac{1}{M_A} + \frac{1}{M_B} \right]^{-1}$ and σ_{AB} the characteristic length

is given by $\sigma_{AB} = (\sigma_A + \sigma_B)/2$ in Angstroms. The value of σ_B for air was taken as 3.711

Å from Reid et al.[23] and the values of σ_A for MSA and the hydrates was estimated from the

molecular volume of the liquid phase. The mean free path λ_{AB} may be estimated for the

dilute species A = free acid molecule or hydrate as [25]

$$\lambda_{AB} = \frac{32 \, D_{AB}}{3 \, \pi \, \bar{c}_A \left(1 + \frac{M_A}{M_B} \right)} \tag{22}$$

$$\bar{c}_A = \left(\frac{8 \, R \, T}{\pi \, M_A} \right)^{1/2} \tag{23}$$

where $\bar{c}_A$ is the mean speed of the hydrate.

Although the presence of hydrates does change the average value of the diffusivity,

the change is only on the order of 20 %, which is well within the uncertainty of the

estimation method. The only available experimental estimate of the diffusivity of MSA is

due to Tang[26]. When measuring the vapor pressure of MSA, the value of a temperature

independent parameter

$$b = \left(\frac{\rho R T_0^2}{8 M_W D_0} \right) \tag{24}$$

was estimated as 1.7856×10^8 torr K s cm^{-2}. With a value of $R = 6.237 \times 10^4$ torr cm^3

gmol^{-1} K^{-1}, this gives $D_{AB} = 0.06$ cm^2 s^{-1} at $T_0 = 298$ K. The estimate is within 30% of

the theoretical value, but because the experiment was not designed to measure D_{AB}, the theoretical value will be used in the model calculations.

C. Effect of Temperature on Nucleation Rates, Changes in Property Data

Changes were made in the MSA property correlations developed by Kreidenweis *et al.*[8] to allow for variation with temperature. Density data were taken from Teng and Lenzi[27] and extrapolated to give $\rho_{30}/\rho_{25} = \rho_{25}/\rho_{20} = 1.002$ for pure MSA. The variation of vapor pressure with temperature was taken from the correlation presented by Tang and Munkelwitz.[28] Diffusivity was varied with temperature as $D_{ij} = D_{ij}^{\circ}\left(\dfrac{T}{T^{\circ}}\right)^2$ as suggested by Tang and Munkelwitz.[28]

The variation of surface tension with temperature for pure MSA was estimated using a group contribution method[21] and was found to give $\sigma_{25}/\sigma_{30}=1.007$ and $\sigma_{19}/\sigma_{25} = 1.009$. This was combined with the known variation in the surface tension of water with temperature and the variation of surface tension with composition at 25 ° C, to give an estimate of surface tension over the range of temperatures and compositions required for modelling the experiments. When the change in surface tension with temperature was estimated for sulfuric acid and subsequently compared to the measured values, the ratio of estimated/measured was approximately 3. Thus the estimated change in surface tension with temperature for MSA may be somewhat high.

To vary the activity, a_i, with temperature, the partial molar heats of mixing, $\bar{h_i}$, are required. The first approximation for this change is then given by [24]

$$\ln(a_i\,(T)) \;=\; \ln(a_i\,(T^\circ)) \,-\, \frac{\overline{h_i}}{R}\left(\frac{1}{T}-\frac{1}{T^\circ}\right) \tag{25}$$

The change in activity coefficients with temperature is important because the increase in nucleation rates with temperature due to decreases in surface tension and increases in the vapor pressure may be offset in part, or entirely, by an increase in the activity coefficient. No heat of mixing data are available for the MSA-water binary system. As a first estimate therefore, the values for sulfuric acid[29] have been used.

Figure 16 shows the results of temperature variation on the calculated nucleation rates for relative humidities of 0.50 and 0.10. The sensitivity of the rate calculations to the extrapolated physical properties is illustrated by letting the surface tension variation of pure MSA be reduced to 1/3 of the estimated change and the heats of mixing be reduced by 1/2. These changes show that, despite the uncertainty in extrapolation, the calculated nucleation rates at 20 and 30 ° C are known to within a factor of 10, relative to the nucleation rates at 25 ° C. The major effect of temperature is to steepen the rate curves, thus the curves must cross at some value of Ra and Rh.

V. COMPARISON OF THE EXPERIMENTAL DATA WITH BINARY NUCLEATION THEORY AND THE INTEGRAL MODEL

The experimental nucleation rate data were first simulated at 25 ° C, where physical property data are well known. As illustrated in Figure 17, nucleation rate data for Ra = 0.33 and 0.075 do not agree with classical binary nucleation theory by several orders of magnitude. This was also the case for the data at

$T = 19$ and 30 ° C.

The use of a correction factor to reconcile the differences between observed and predicted nucleation rates has been a reasonably successful approach and Table 4 summarizes typical values observed for J_{exp}/J_{theor} in both unary and binary nucleation . For $T = 25\,°$ C, a single correction factor of 1×10^{-6} is found to adequately fit the MSA-water rate data, Figure 17, as well as all of the total number concentration data, Figure 4. Similarly, as illustrated in Figure 5, the $T = 19\,°$ C data are very well described by a correction factor of 1×10^{-8}. Only the $T = 30\,°$ C data, Figure 6, are not easily fit using this method, with a large mismatch between the data curves and the model still apparent even when the best correction factor, 1×10^{-4}, is used. We can think of no reason to reject the $T = 30\,°$ C data as less reliable than the data at 25 or $19\,°$ C. Although the discrepancy is greatest at total number concentrations of less than $1\ cm^{-3}$, a region where repeatability is generally more difficult, the data for Ra = 0.075 includes the results of two experiments that agree well even in this region. Indeed the mismatch arises because the model predicts very similar slopes at $30\,°$ C for Ra = 0.33 and Ra = 0.075, while, as illustrated in Figure 6, the experiments show these slopes are different.

Despite these difficulties, the excellent predictions generated at the two lower temperatures justifies the use of this approach as appropriate in light of the simplicity of the overall model. Of interest is the behavior of the ratio J_{exp}/J_{theor} as a function of temperature. Previous work has found this that ratio generally decreases with an increase in temperature, while this work shows that in the MSA-water system the opposite is true. Even if the rate calculations at $T = 19$ and $30\,°$ C are incorrect by an order of magnitude due to uncertainties in the property data, a reasonable maximum uncertainty as estimated previously, this trend would still hold.

Given the correction factor at each temperature, nucleation rate profiles and saturation levels were calculated along the length of the nucleation and growth tube to confirm that the assumptions made that these were relatively constant at particle concentrations $\leq 10^3$, were indeed acceptable. Figure 18 illustrates the variation of the normalized nucleation rate, J/J°, and the normalized relative acidity, Ra/Ra°, along the length of the flow tube for $Ra = 0.33$ and initial nucleation rates of $J^\circ = 10$ and 100 cm^{-3}s^{-1}. Certainly at $J^\circ = 10$ cm^{-3}s^{-1}, the nucleation rate after 18 s of integration time is better than 80% of the initial rate and the acid saturation level has dropped by less than 2%. Lower values of J° show even less acid vapor depletion, and thus the assumption of constant nucleation rates appears to be valid for $J^\circ < 10$ cm^{-3}s^{-1}.

At $J^\circ = 100$ cm^{-3}s^{-1}, the nucleation rate is only 10% of the initial rate after t = 18 s, corresponding to a 20% decrease in the initial acid saturation. This means that the points corresponding to $J = 100$ cm^{-3}s^{-1} in Figures 7 through 9, must be reinterpreted slightly to reflect the fact that these points really represent $J_{avg} = 100$ cm^{-3}s^{-1}. At the indicated saturation levels therefore, the initial rate J° must be somewhat higher than 100 cm^{-3}s^{-1} in order to compensate for reduced nucleation further along the tube.

The particle size results generated by the model using the appropriate correction factor for each temperature were then examined to see if there was qualitative agreement with the size data collected. To make the comparison easier, the mass average particle diameter predicted by the model was multiplied by the polydispersity factor, $\alpha_p = 0.6$, to give an estimate of the number average particle diameter.

Figure 19 illustrates the predicted and observed variation in the particle diameter as a function of Rh for the three levels of Ra at $T = 30\,^\circ$ C, and the corresponding experimental results. The major trends are clearly followed. The decrease in particle diameter predicted

with an increase in Rh is apparent for the Ra = 0.33 and Ra = 0.15 experimental data points, although the predicted variations are much larger than those observed. However the predicted variation at Ra = 0.075 over the change in Rh from 0.46 to 0.66 is a factor of three, while the data show no change. Figure 20, again for $T = 30$ ° C, illustrates the corresponding variation of the particle diameter with Ra for two levels of Rh. The same features are apparent in the previously presented Figure 13, albeit for different values of Rh.

The current version of the model does not predict the actual particle sizes very well, although it does confirm that the variations observed are consistent with predictions made using classical nucleation theory and a simple condensation calculation. The incorporation of a sticking probability $\alpha_s < 1.0$ could improve the agreement with observations by reducing both the maximum particle size predicted and the maximum predicted range (D_{pmax}/D_{pmin}). However at this point the introduction of a second adjustable parameter is not warranted. A more detailed aerosol model that is capable of predicting size distributions is required and would add more insight to the competing processes of nucleation and condensation.

A. Comparison with Previous Work

The only previous experimental work on the MSA-water system is that of Kreidenweis et al.[8]. Conditions in those experiments were somewhat different than in the experiments completed here, but it should be possible to compare results by simulating the data using the experimental nucleation rate correction factor found for the current work at T = 25 ° C and a polydispersity factor of 0.6. As was the case here, including a correction factor to reduce the nucleation rate greatly improved the agreement between experiments and data. With a correction factor of 10^{-6}, good agreement was achieved for the Ra = 0.39

and 0.34 data. Most of the remaining data were still overestimated by about two orders of magnitude and it appears that a correction factor of about 10^{-8} would give the best overall fit of these data.

B. Vapor and Particle Losses in the Experimental System, Impact on Modelling

Terms to account for the loss of vapor and particles in the experimental system have not been included in the model. To estimate the particle loss, flow through the tube was modelled as a Graetz problem using the solution given by Brown[35]. The smallest particles will be on the order of the critical cluster, ~ 2 nm, and for these C_{avg}/C_0 was reduced by 30% by the tube exit, which does not represent a significant change in the total particle concentration observed.

The vapor loss term is more critical than the particle loss term because of the strong dependence of the nucleation rate on the saturation level. The solution to the Graetz problem assumes that the walls act as perfect sinks and therefore severely overestimates the vapor loss that will occur. There was no visible condensation in any of the experiments even after 7 days of continuous flow through the nucleation tube. In addition, the good repeatability of experiments performed as much as 3 days apart, argues that after the initial conditioning period, vapor losses to the walls are not significantly influencing the nucleation rates.

VI. SUMMARY AND CONCLUSIONS

Number concentrations of particles produced by binary nucleation between MSA and water were measured over a wide range of Ra <1 and Rh <1, and at three different temperatures. From these data, nucleation rates J_{exp} were estimated as a function of Ra, Rh and T. As in the case of homogeneous nucleation, binary nucleation rates were found to increase with an increase in temperature. This represents the first systematic study of the effect of temperature on binary nucleation rates.

Comparison with J_{theor}, calculated using the classical binary nucleation theory and accounting for the presence of hydrates, shows that J_{theor} does not agree with J_{exp} by up to 8 orders of magnitude and that a temperature dependent correction factor is required. Including the effect of hydrates in the rate calculation reduces the disagreement between theory and experiment but does not eliminate it. Once the correction factor is incorporated into the model for nucleation and growth, the original number concentration data are reasonably well described. The change in the correction factor with temperature, from 10^{-8} at 19 ° C to 10^{-4} at 30 ° C, is opposite to that found by others[7,30,31] for homomolecular, homogeneous nucleation.

The observed particle size distributions varied with changes in Ra and Rh in a manner that was consistent with a simple model of nucleation and growth. The competition between the two processes was clearly illustrated in Figure 13, where increases in Ra first increase the average particle size (condensation dominates), and then decrease the average particle size (nucleation dominates). A more sophisticated aerosol model is required to better predict the experimental particle size data.

The continuous flow mixing apparatus provides an excellent tool for studying binary nucleation processes at saturation levels less than one, and seems to be the best way to work with such corrosive and difficult systems as acid and water.

ACKNOWLEDGEMENT

REFERENCES

[1]G.J. Doyle, J. Chem. Phys. 35, 795 (1961).

[2]H. Reiss, J. Chem. Phys. 18, 840 (1950).

[3]H. Reiss, D.I. Margolese and F.J. Schelling J. Coll. Int. Sci. 56, 511 (1976).

[4]F.J. Schelling and H. Reiss, J. Coll. Int. Sci 83, 246 (1981).

[5]D. Boulaud, G. Madelaine, D. Vilga and J. Bricard, J. Chem. Phys. 66, 4854 (1977).

[6]P. Mirabel and J.L. Clavelin, J. Chem. Phys. 68, 5020 (1978).

[7]C.H. Hung, M.J. Krasnopoler and J.L. Katz, J. Chem. Phys. 90, 1856 (1989).

[8]S. Kreidenweis, R. Flagan, J. Seinfeld and K. Okuyama, J. Aer. Sci. 20, 585 (1989).

[9]R.J. Charlson, J.E. Lovelock, M.O. Andreae and S.G. Warren, Nature 326, 655 (1987).

[10]S.E. Schwartz, Nature 336, 441 (1988).

[11]K. Okuyama, Y. Kousaka, S. Kreidenweis, R.C. Flagan and J.H. Seinfeld, J. Chem. Phys. 89, 6442 (1988).

[12]S.C. Wang and R.C. Flagan, Aerosol Sci. Technol. 13, 230 (1990).

[13]See AIP document no. PAPS JCPSA-94-6827-15 for 15 pages of supplementary material. Order by PAPS number and journal reference from American Institute of Physics, Physics Auxiliary Publication Service, 335 East 45th Street, New York, NY 10017. The price is $1.50 for each microfiche (98 pages) or $5.00 for photocopies up to

30 pages, and $0.15 for each additional page over 30 pages. Airmail additional. Make checks payable to the American Institute of Physics.

[14] D. Stauffer, J. Aer. Sci. 7, 319 (1976).

[15] R.G. Renninger, F.C. Hiller and R.C. Bone, J. Chem. Phys. 75, 1584 (1981).

[16] G. Wilemski, J. Chem. Phys. 80, 1370 (1984).

[17] P. Mirabel and H. Reiss, Langmuir, 3, 228 (1986).

[18] R.H. Heist and H. Reiss, J. Chem. Phys. 61, 573 (1974).

[19] A. Jaecker-Voirol, P.Mirabel and H.Reiss, J. Chem. Phys. 87, 4849 (1987).

[20] A. Jaecker-Voirol and P.Mirabel, J. Chem. Phys. 88, 3518 (1987).

[21] P. Mirabel, Personal Communication (1990).

[22] B. Dahneke, In *Theory of Dispersed Multiphase Flow*, R.E. Meyer (Ed.), Academic Press, New York, 97(1983).

[23] R. Van Dingenen, PhD Thesis, State University Ghent (1990).

[24] R.C Reid, J.M. Prausnitz and B.E. Poling, *The Properties of Gases and Liquids*, McGraw Hill, New York (1987).

[25] J.H. Seinfeld, *The Atmospheric Chemistry and Physics of Air Pollution*, John Wiliey and Sons, (1986).

[26] I.N. Tang, Personal Communication, (1990).

[27] T.T. Teng and F. Lenzi, J. Chem. Engng. Data 20, 432 (1975).

[28]I.N. Tang and H.R.Munkelwitz, J. Coll. Inter. Sci. 141, 109 (1991).

[29]W.F. Giauque, E.W. Hornung, J.E. Kunzler and T.R. Rubin, J. Am. Chem. Soc. 82, 62 - 70 (1960).

[30]R. Strey, P.E. Wagner and T. Schmeling, J. Chem. Phys. 84, 2325 (1986).

[31]P.E. Wagner and R. Strey, J. Chem. Phys. 80, 5266 (1984).

[32]G.W. Adams, J.L. Schmitt and R.A. Zalabsky, J. Chem. Phys. 81, 5074 (1984).

[33]C. Flageollet, M.D. Cao and P. Mirabel, J. Chem. Phys. 72, 544 (1980).

[34]J.P. Garnier and P. Mirabel, J. Chem. Phys. 77, 2035 (1982).

[35]G.M. Brown, AIChE J. 6, 179 (1960).

Table 1 : Experimental conditions investigated in the MSA-water nucleation experiments.

Experiment Number	Temperature (°C)	Relative Acidity, Ra	Relative Humidity, Rh
16.02	29.6	0.329 - 0.332	0.066 - 0.461
16.03	29.8	0.148 - 0.154	0.083 - 0.655
16.04	29.9	0.075 - 0.076	0.134 - 0.655
16.05	29.9	0.051 - 0.656	0.301 - 0.307
16.06	29.9	0.075 - 0.656	0.152 - 0.156
16.07	29.9	0.074 - 0.076	0.151 - 0.654
16.08	18.9	0.328 - 0.331	0.183 - 0.449
16.09	18.9	0.149 - 0.154	0.277 - 0.641
16.10	18.9	0.075 - 0.078	0.385 - 0.635
16.11	18.8	0.128 - 0.649	0.294 - 0.297
16.12	18.9	0.363 - 0.652	0.149 - 0.150
16.01	25.2	0.331 - 0.334	0.084 - 0.457
16.13	24.6	0.327 - 0.330	0.116 - 0.456
16.14	24.7	0.149 - 0.153	0.199 - 0.648
16.15	24.9	0.075 - 0.076	0.297 - 0.644
16.16	24.9	0.076 - 0.654	0.297 - 0.317
16.17	25.0	0.291 - 0.650	0.151 - 0.152

Table 2 : Values of the first 10 K_h' constants for MSA - water at 25 °C

h	1	2	3	4	5	6	7	8	9	10
K_h'	142.9	31.2	15.6	10.7	8.80	7.79	7.24	6.91	6.71	6.59

Table 3 : Diffusivity, mean speed and mean free path of the MSA-H_2O hydrates.

h	Hydrate Distribution		Molecular Mass	Mole fraction MSA	ρ g cm^{-3}	D_{AB} cm^{2}s^{-1}	$\bar{c}_A$ cm s^{-1} (x 10^{-4})	λ_{AB} cm (x10^6)
Rh =	0.5	0.1						
0	0.08	0.67	96.11	1.00	1.507	0.0884	2.56	2.71
1	0.26	0.29	114.13	0.50	1.426	0.0790	2.35	2.30
2	0.39	0.04	132.14	0.33	1.363	0.0718	2.19	2.00
3	0.20		150.16	0.25	1.317	0.0661	2.05	1.76
4	0.06		168.17	0.20	1.276	0.0616	1.94	1.58
5	0.01		186.19	0.17	1.245	0.0578	1.84	1.43
weighted averages : Rh = 0.5						0.0728	2.21	2.05
Rh = 0.1						0.0850	2.48	2.56

Table 4 : Experimental Correction Factors to Classical Nucleation Theory

Single Component Nucleation

Species	Temperature (K)	J_{exp}/J_{theor}	Reference
N-alcohols			
n-hexanol	256 - 296	$10^7 - 10^1$	Strey et al.[30]
$\downarrow$			
methanol	230 - 274	$10^{-4} - 10^{-11}$	Strey et al.[30]
n-nonane	233 - 315	$10^7 - 10^{-4}$	Hung et al.[7]
	203 - 238	$10^7 - 10^0$	Wagner et al.[31]
	217 - 266	$10^5 - 10^0$	Adams et al.[32]
Dioctylphthalate	312 - 317	10^5	Okuyama et al.[11]
Dibutylphthalate	312 - 317	$10^6 - 10^7$	Okuyama et al.[11]

Binary Nucleation

Species	Temperature (K)	J_{exp}/J_{theor}	Reference
Dioctylphthalate/ Dibutylphthalate	312 - 317	10^3	Okuyama et al.[11]
n-propanol/water	298	$< 10^{-6}$	Flageollet et al.[33]
methanol/water	298	$< 10^{-4}$	Flageollet et al.[33]
n-alcohol/n-alcohol	298	$< 10^{-2}$	Garnier et al.[34]
methanesulfonic acid /water	292 - 303	$10^{-8} - 10^{-4}$	present work
sulfuric acid/water	293 - 303	$10^{-12} - 10^7$	present work, Part II
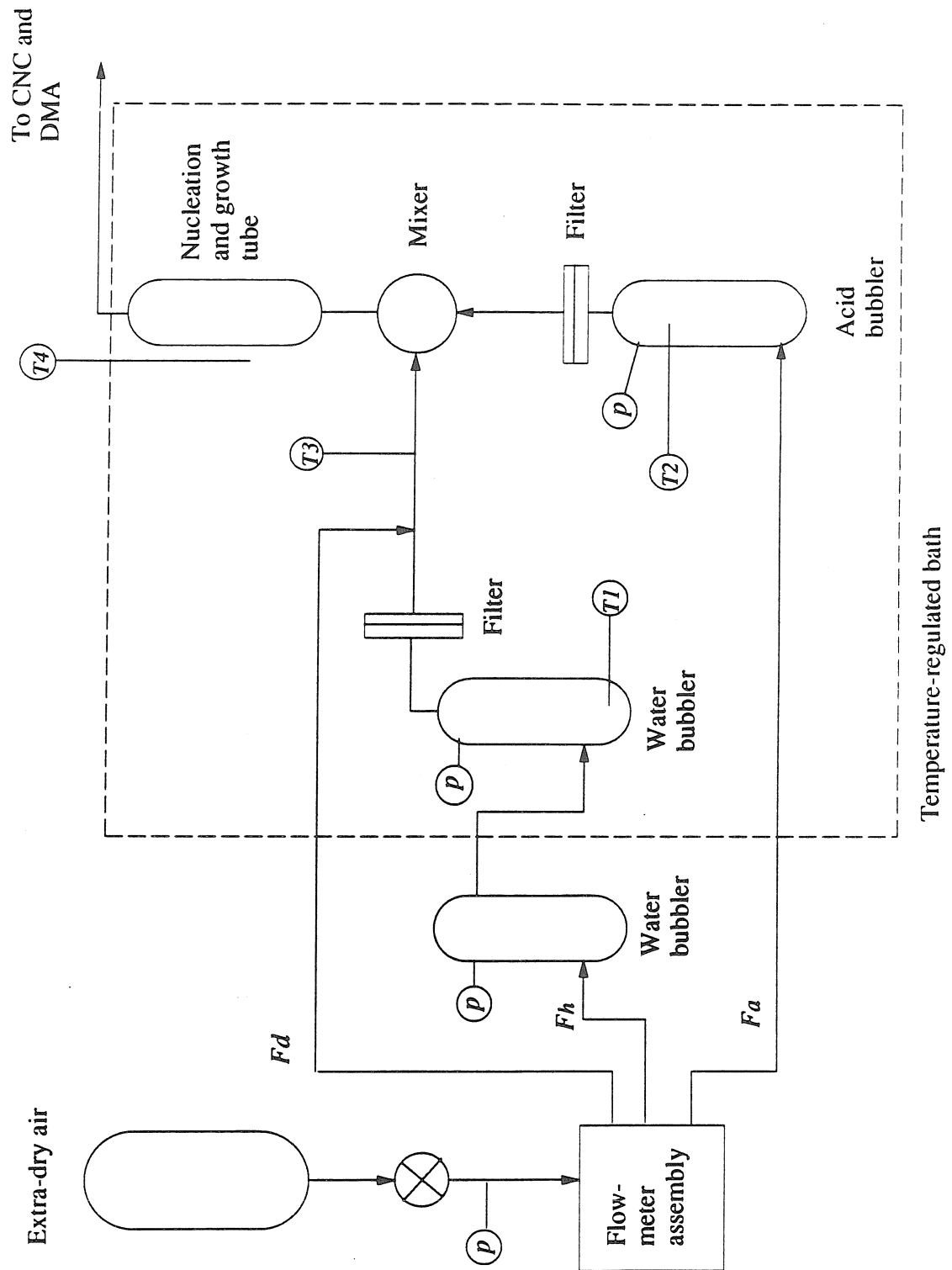
Figure 1 : Schematic of the experimental equipment.

Mixer Detail

0.5 mm
ports (8)

Fh

Filter

Fa

to CNC and
DMA

$T4$

Nucleation and
growth tube

Dilution air
stream, Fd

Humid air
stream, Fh

$T3$

Mixer

$T2$

Acidic air
stream, Fa

p

$T1$

p

Acid
bubbler

Water
bubbler
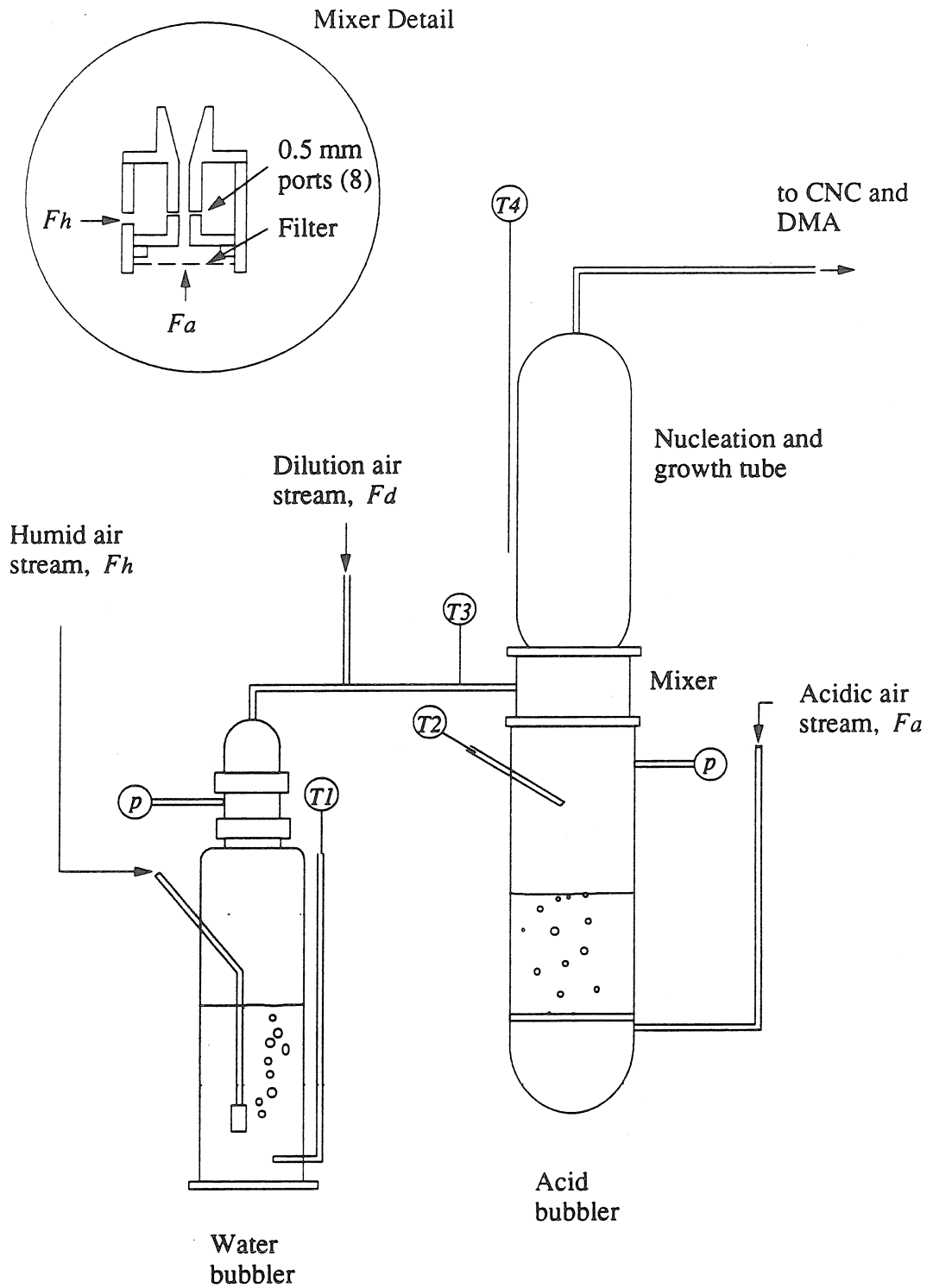
Figure 2 : Details of the continuous flow mixing type nucleation system.
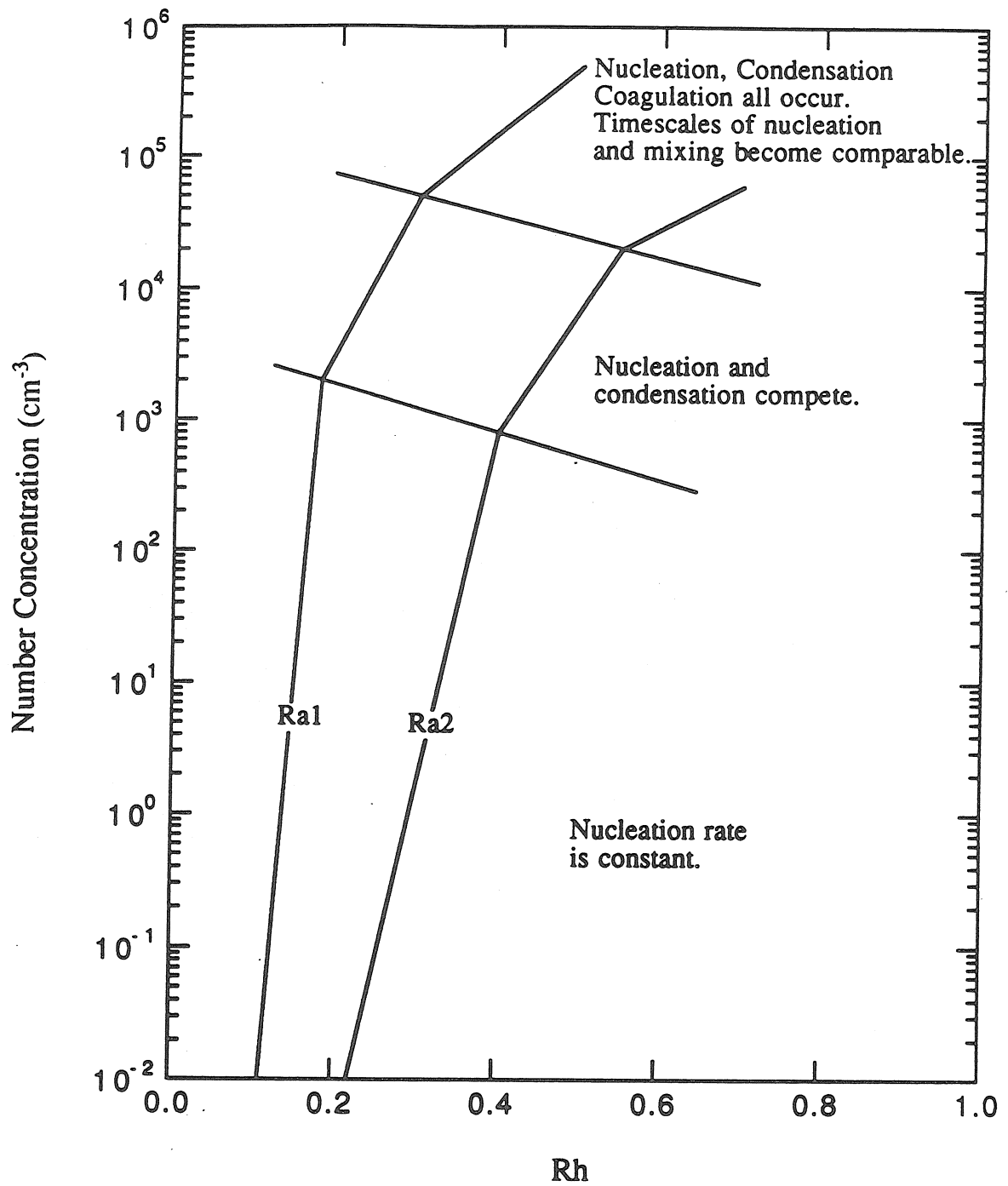
Figure 3 : Typical operating regimes for the continuous flow mixing type nucleation system.
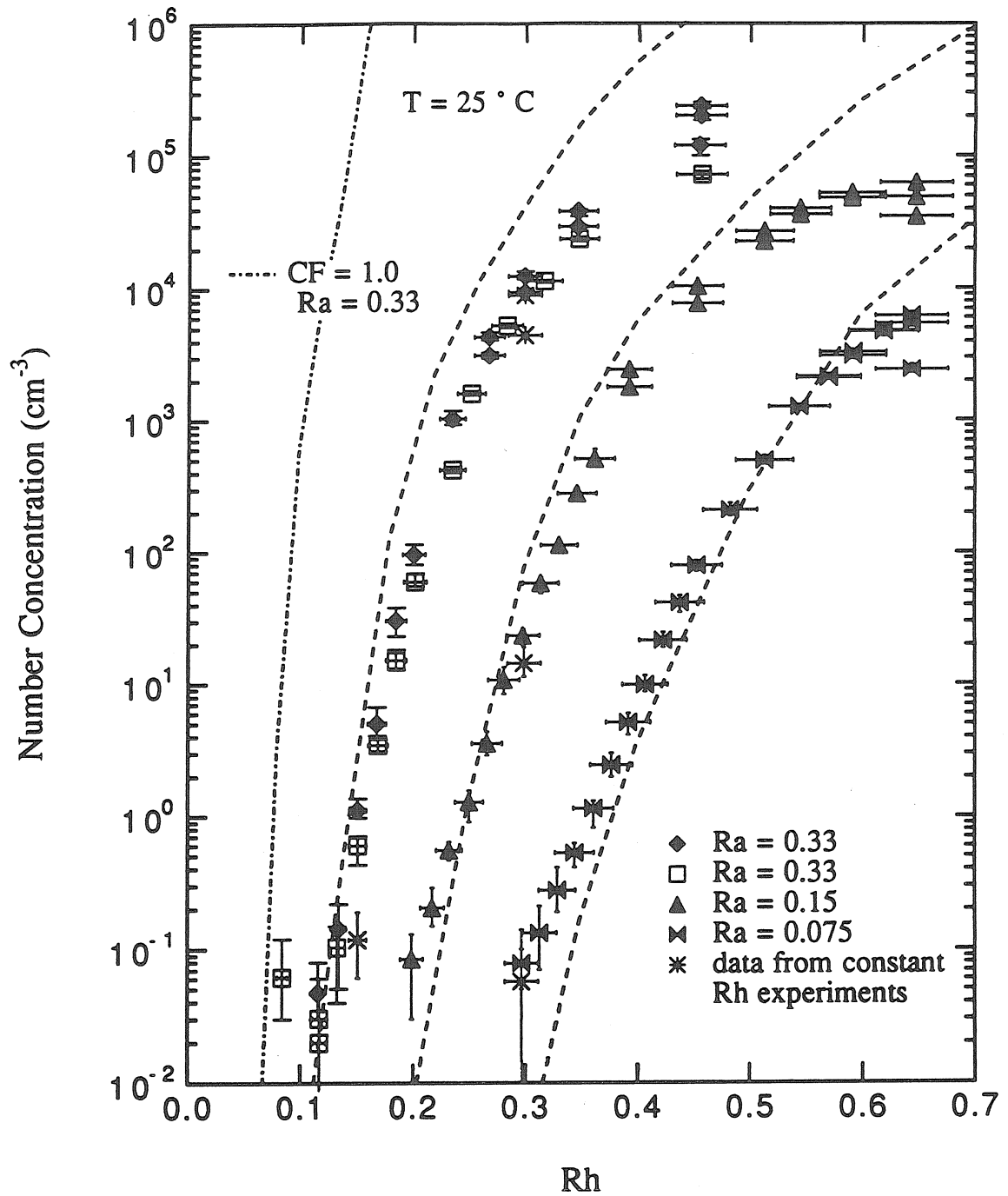
Figure 4 : Observed number concentrations as a function of relative humidity at $T = 25\,^{\circ}$ C.

Broken lines are the predicted number concentrations from the integral model using

$\alpha_p = 0.6$, $\alpha_s = 1.0$ and a correction factor, $CF = 10^{-6}$.
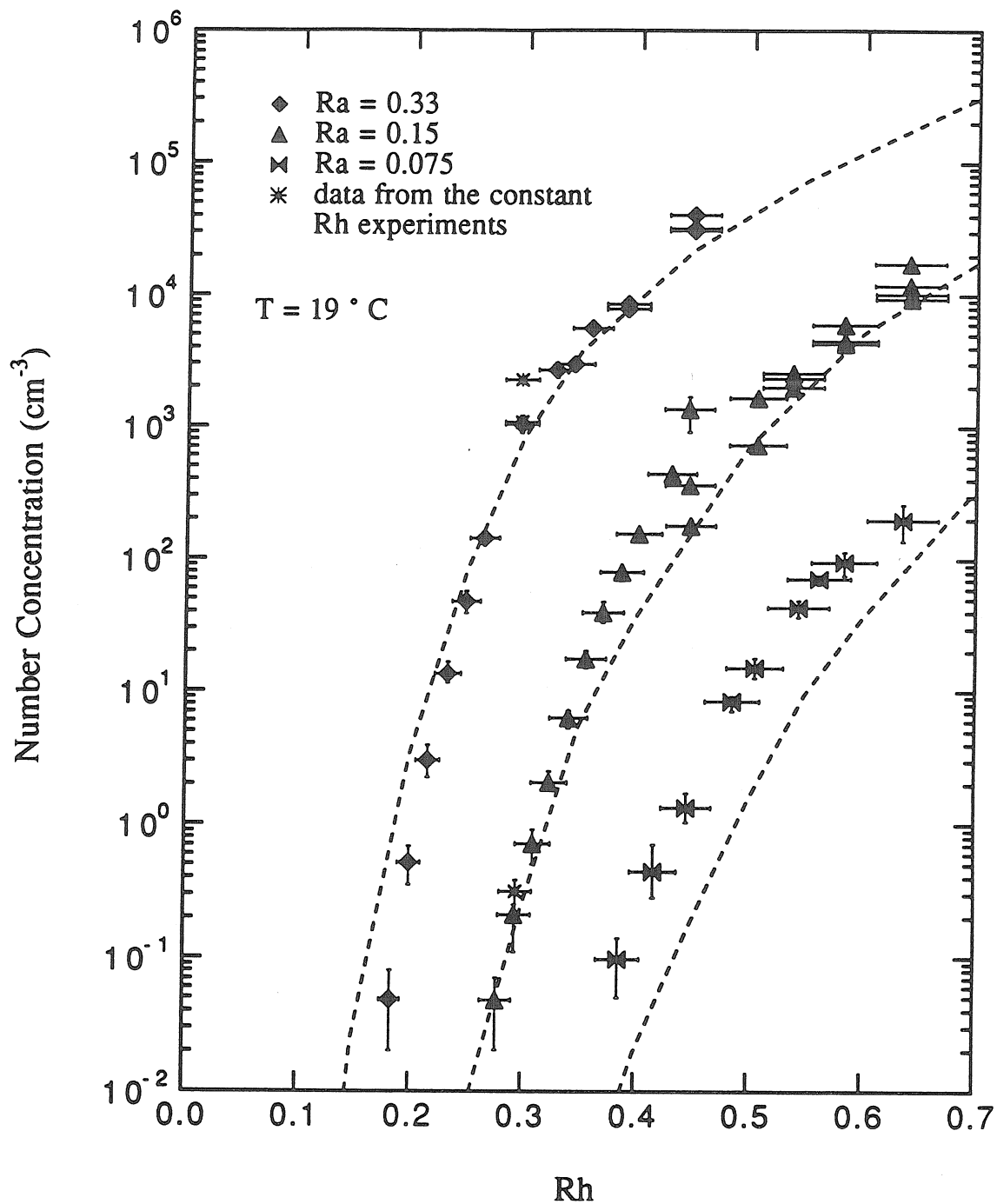
Figure 5 : Observed number concentrations as a function of relative humidity at $T = 19 °$ C.

Broken lines are the predicted number concentrations from the integral model using
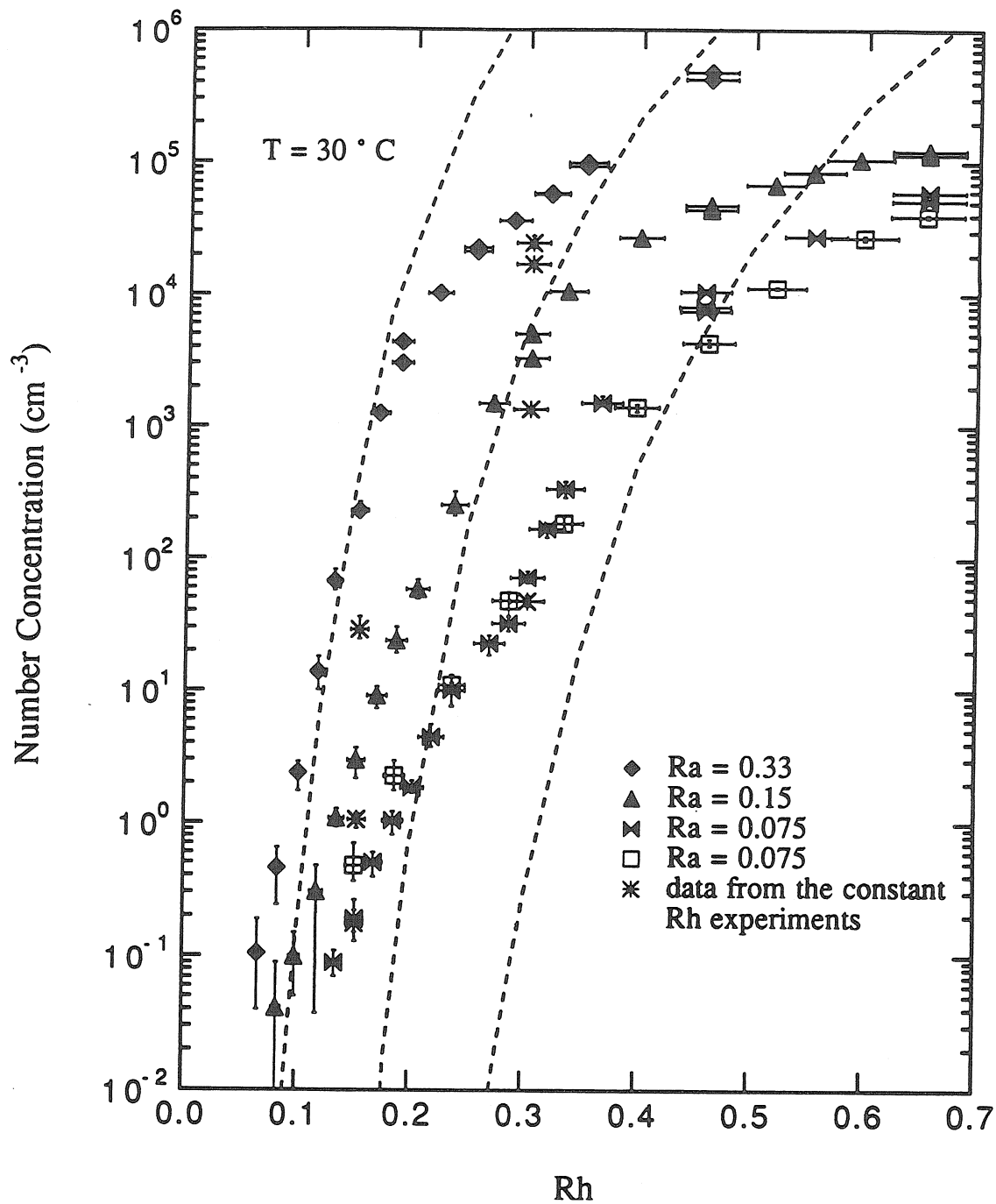
$\alpha_p = 0.6$, $\alpha_s = 1.0$ and $CF = 10^{-8}$.

Figure 6 : Observed number concentrations as a function of relative humidity at $T = 30$ ° C. Broken lines are the predicted number concentrations from the integral model using $\alpha_p = 0.6$, $\alpha_s = 1.0$ and $CF = 10^{-4}$.
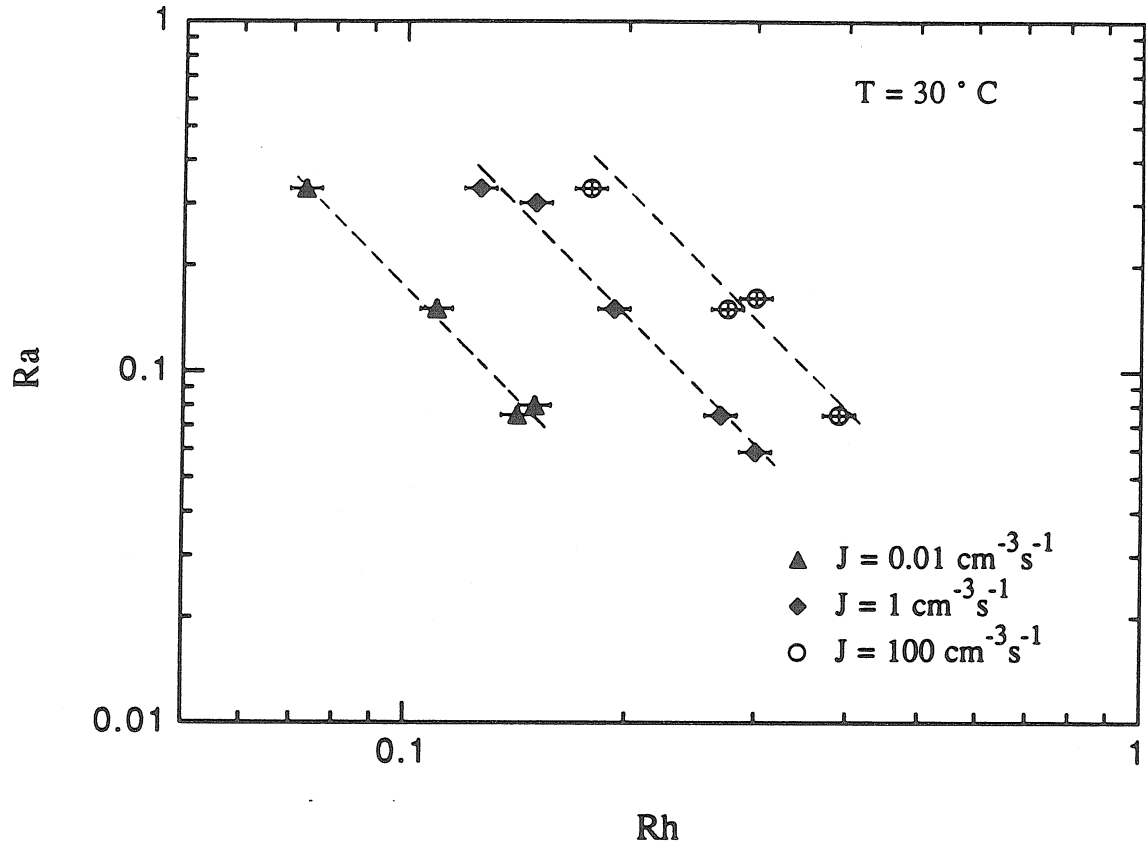
Figure 7 : The variation of nucleation rates with saturation level for the MSA-water binary system at $J = 0.01$, 1 and 100 cm^{-3}s^{-1} and $T = 30°$ C.
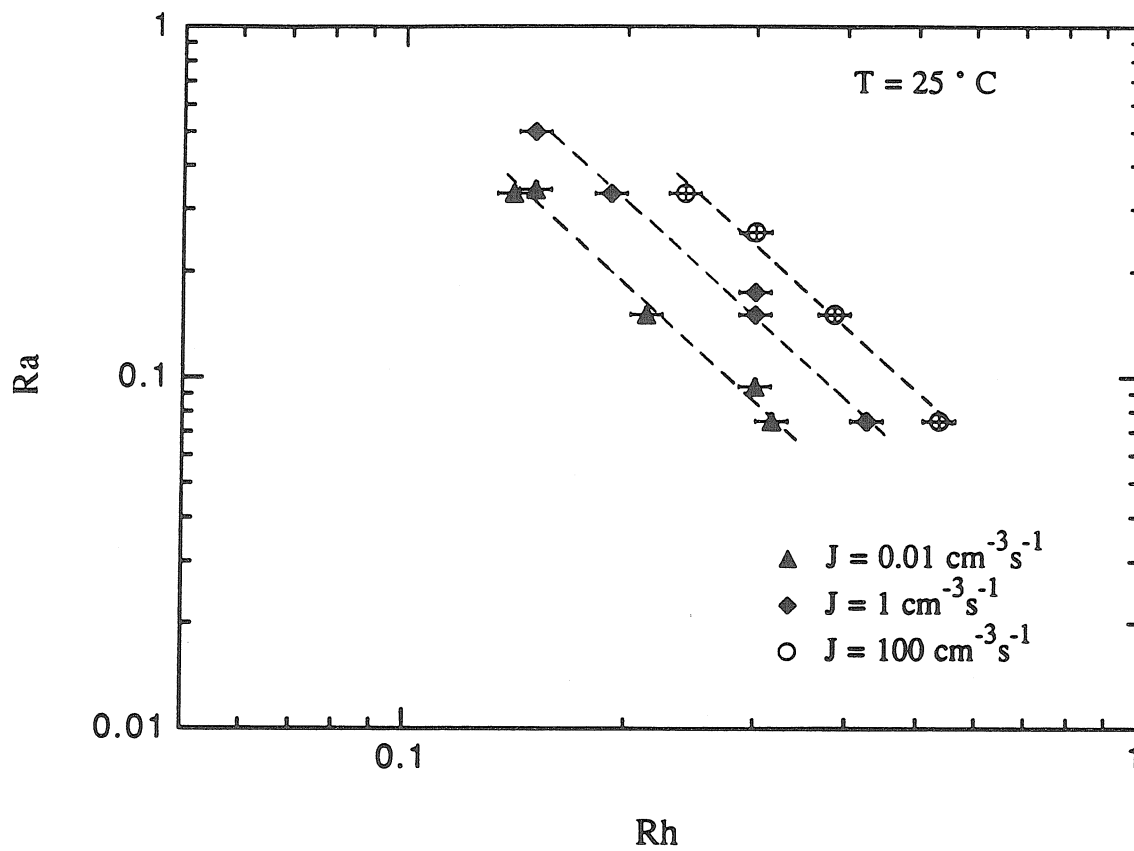
Figure 8 : The variation of nucleation rates with saturation level for the MSA-water binary system at $J = 0.01$, 1 and 100 cm^{-3}s^{-1} and $T = 25°$ C.
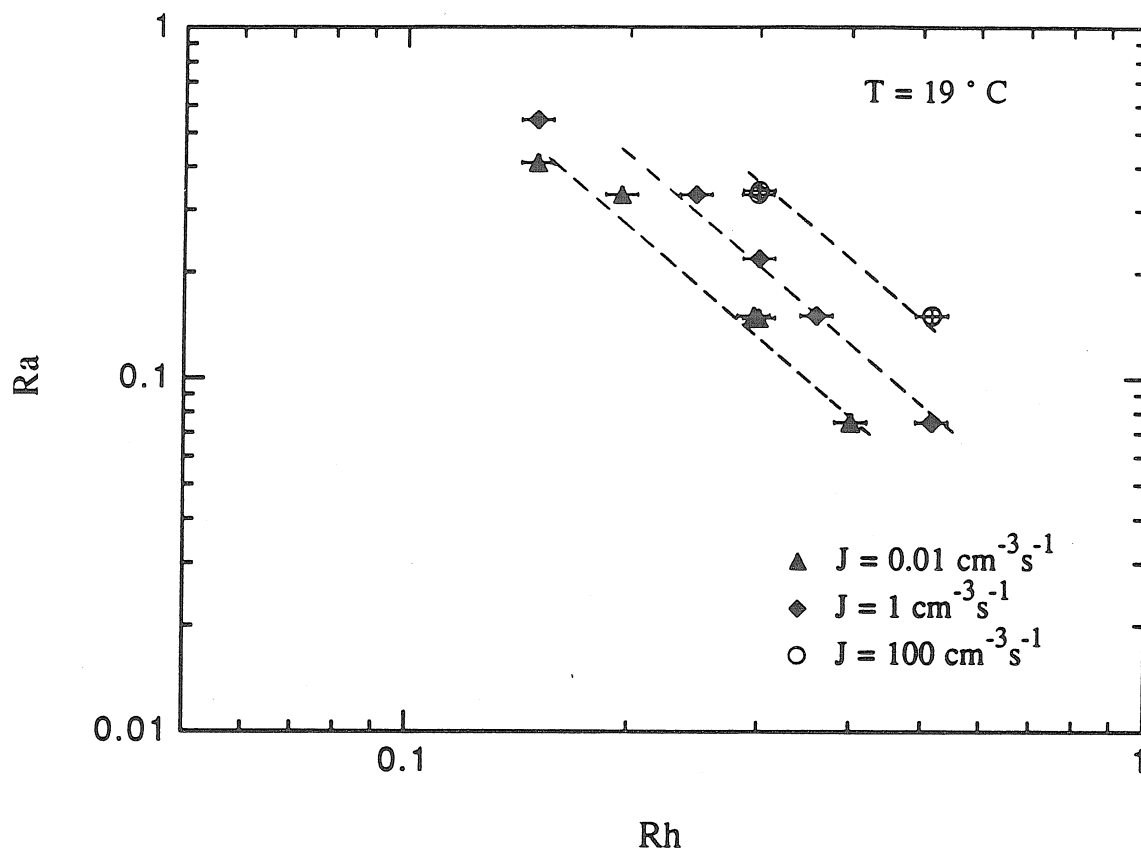
Figure 9 : The variation of nucleation rates with saturation level for the MSA-water binary system at $J = 0.01$, 1 and 100 cm^{-3}s^{-1} and $T = 19°$ C.
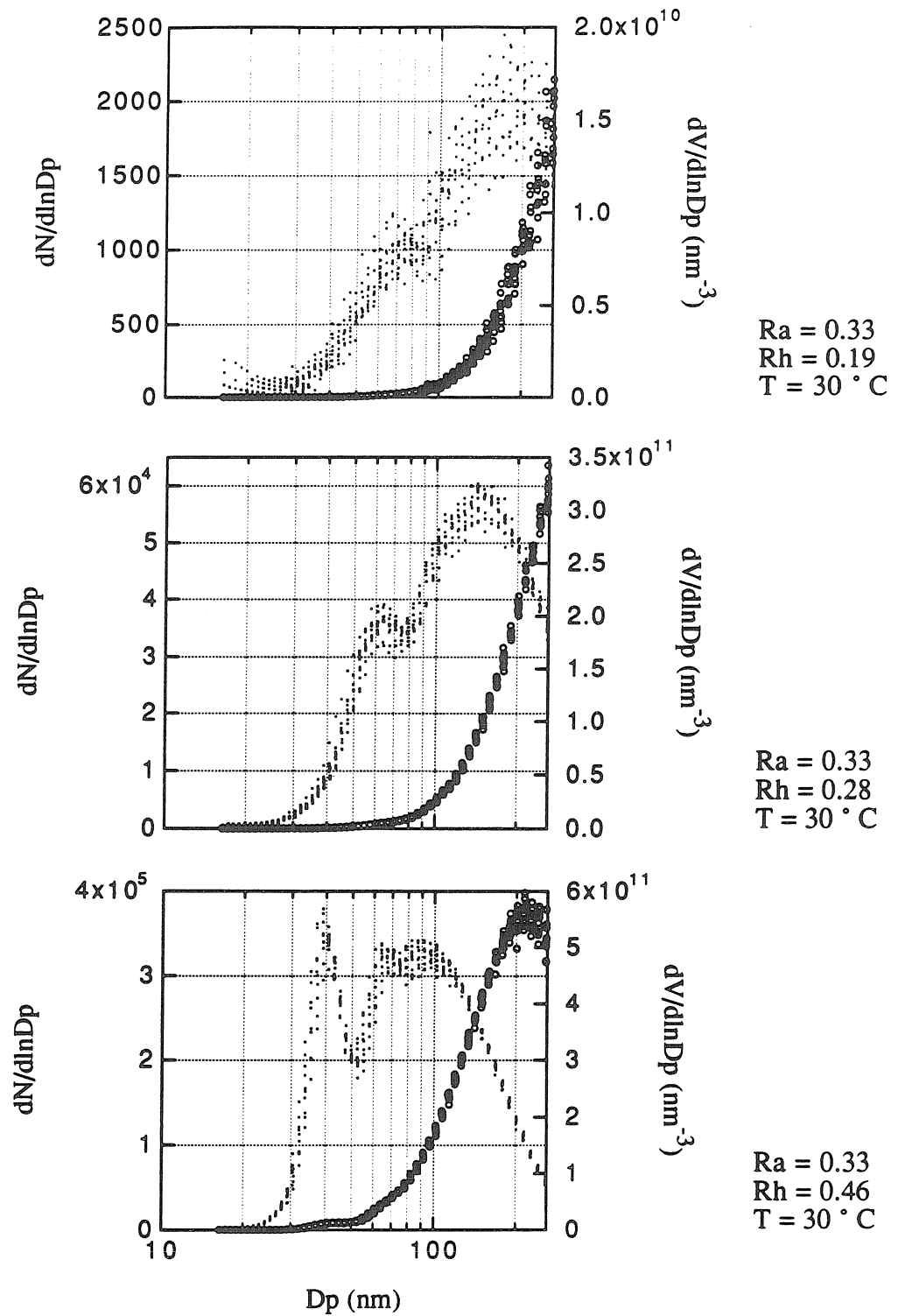
Figure 10 : The observed change in the particle size distributions with increasing nucleation rates due to increases in Rh.
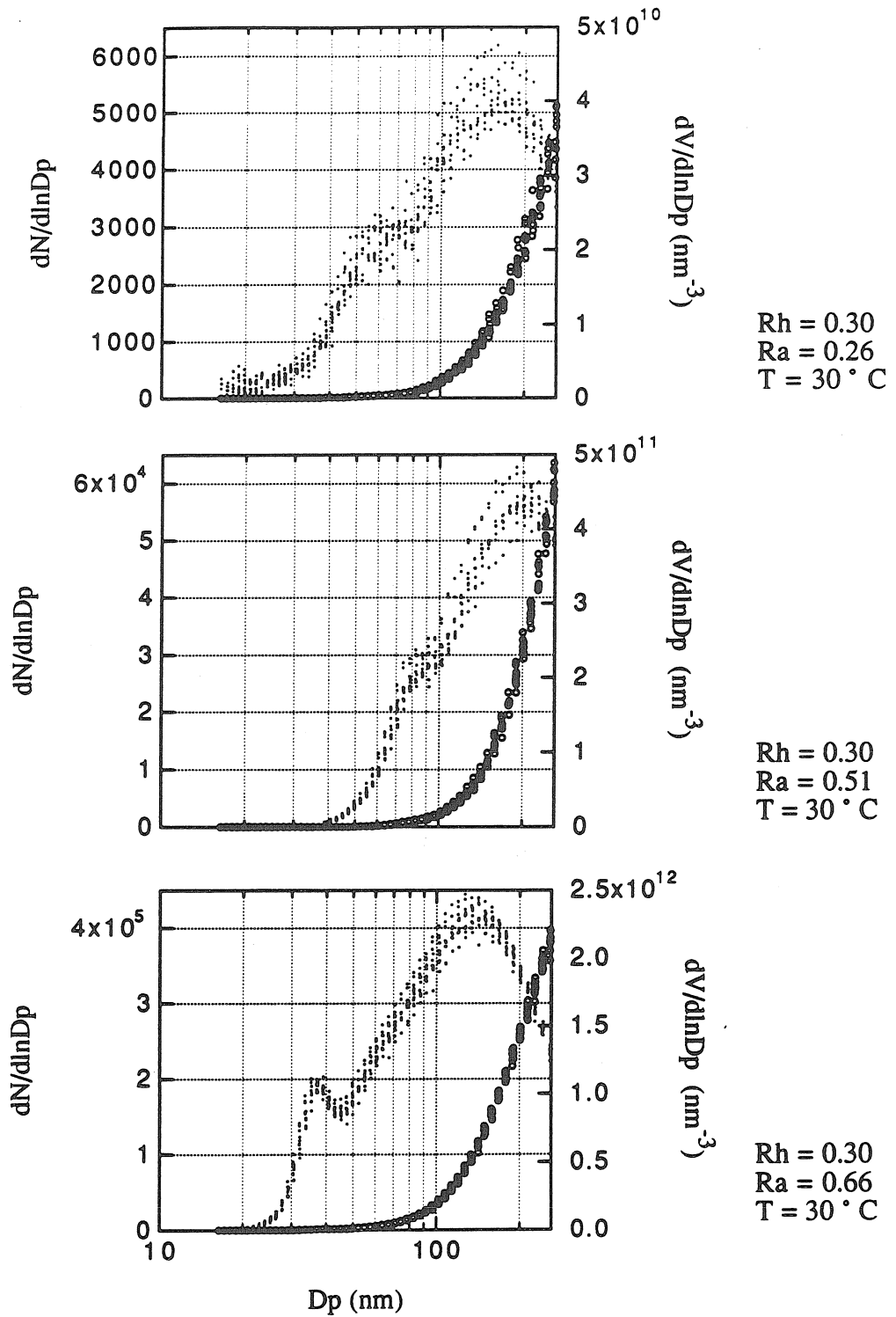
Figure 11 : The observed change in the particle size distributions with increasing nucleation rates due to increases in Ra.
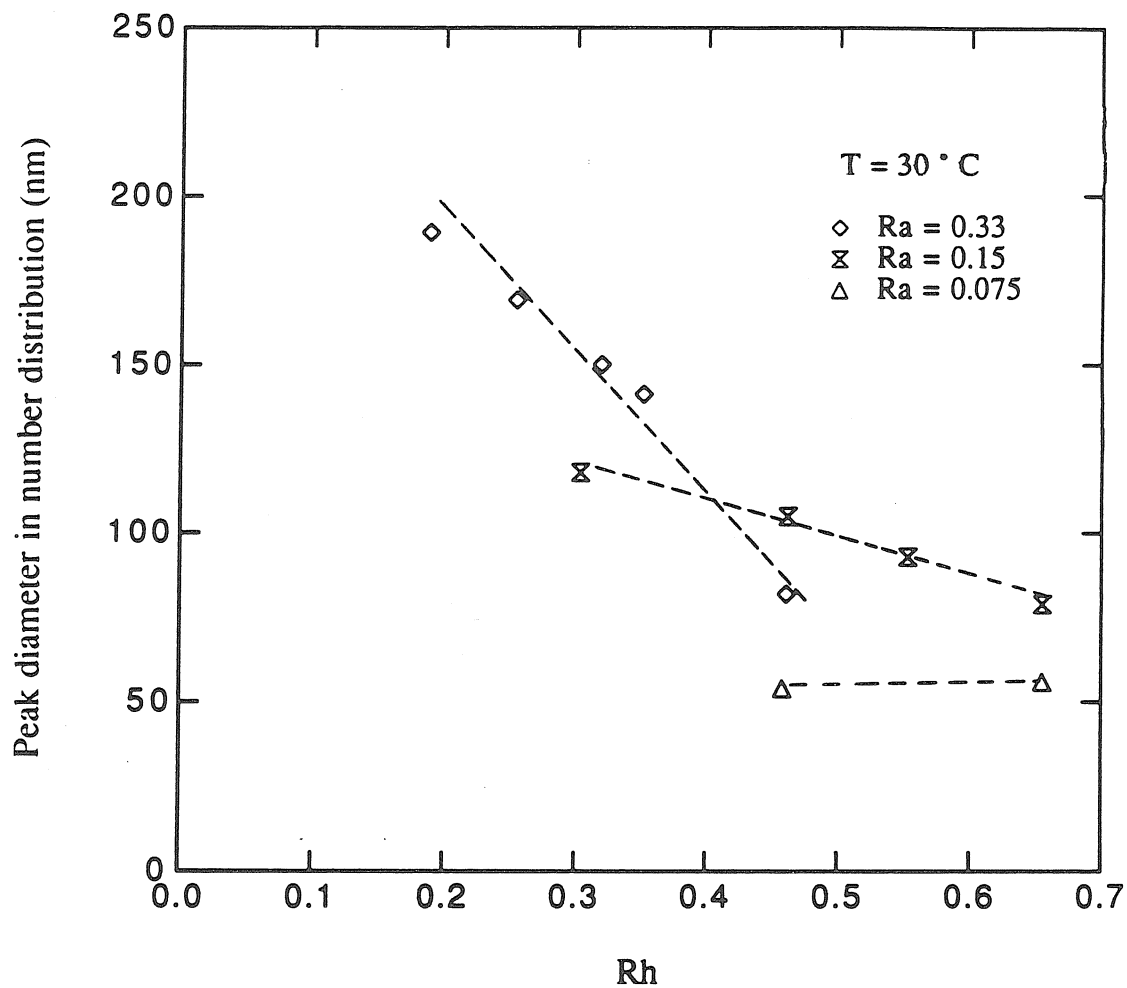
Figure 12 : Variation in the peak diameter of the number distribution with Rh for three values of Ra at $T = 30°$ C. The broken lines indicate the trend in the data only.
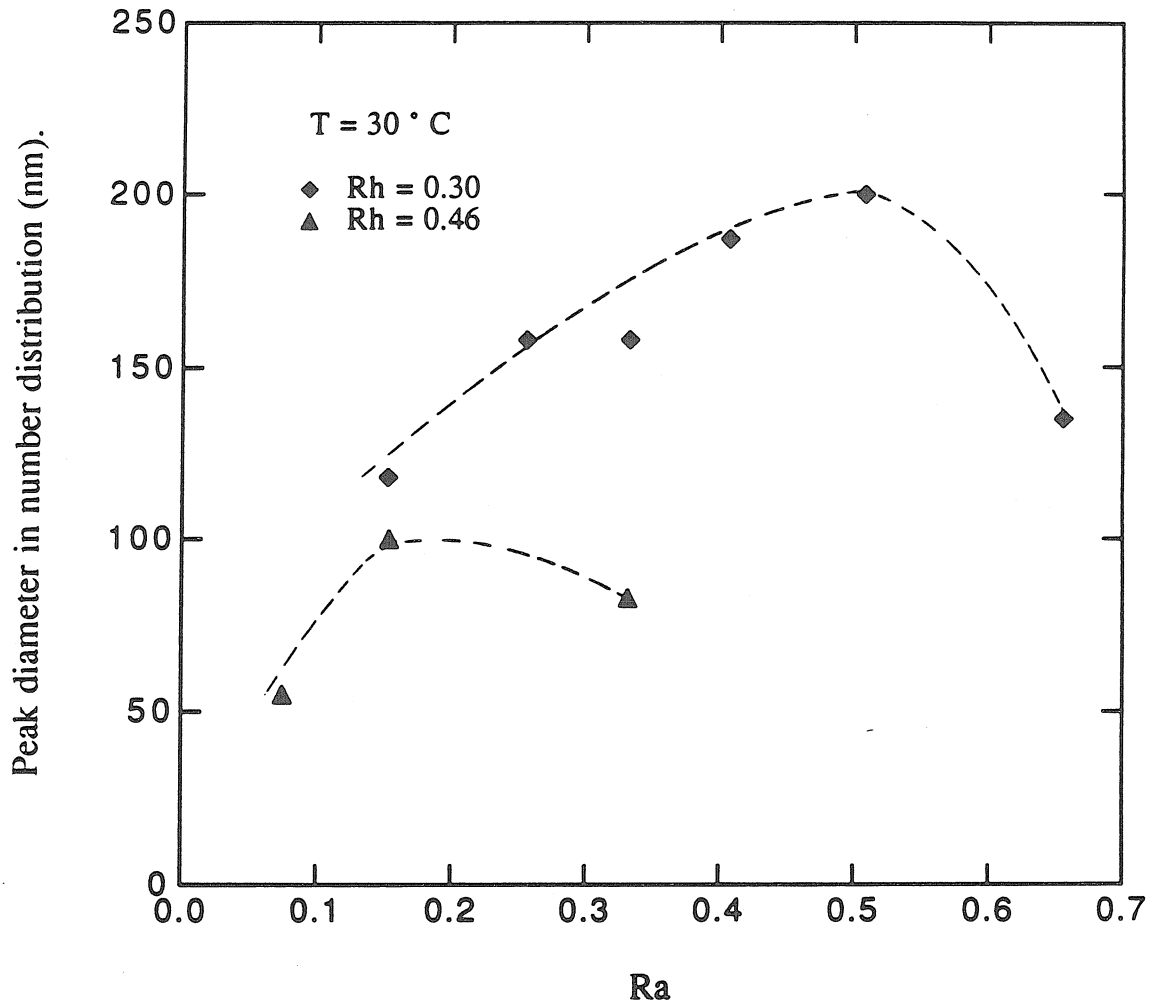
Figure 13 : Variation in the peak of the number distribution with Ra for two values of Rh at $T = 30°$ C. The broken lines indicate the trend in the data only.
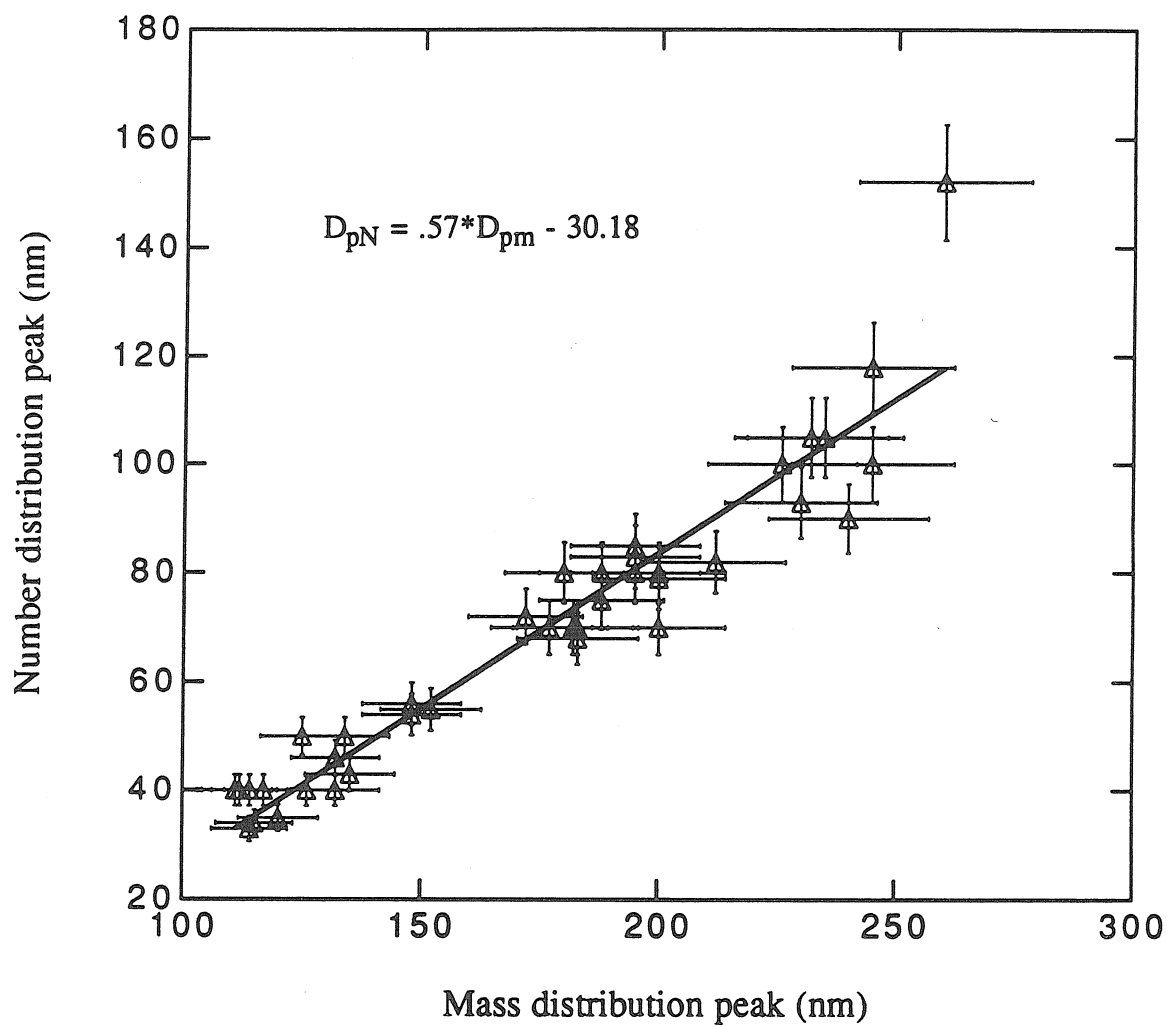
Figure 14 : Variation in the peak of the number distribution with the peak in the mass distribution. The slope of the line is an estimate of the polydispersity factor, α_p.
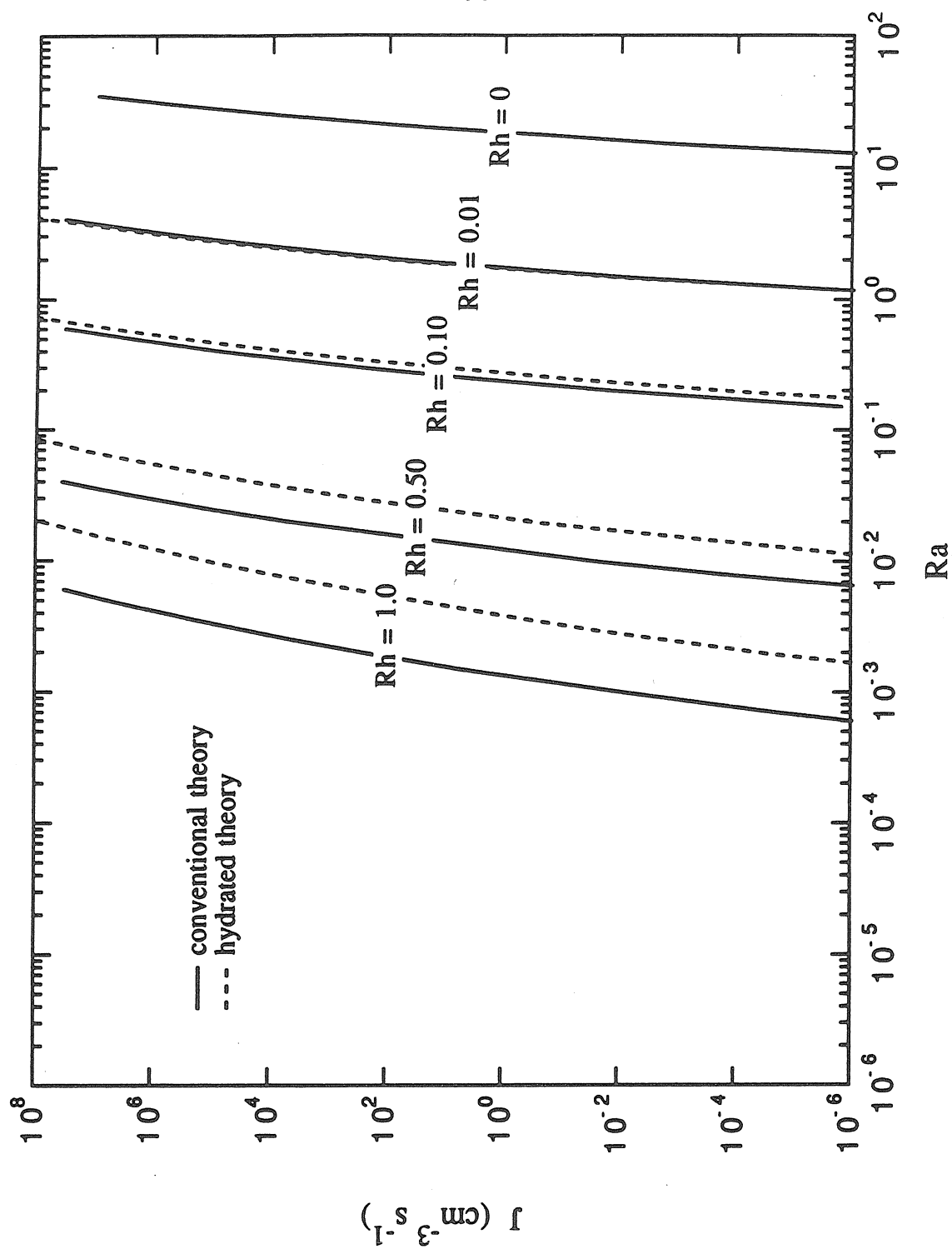
Figure 15 : The reduction in nucleation rates as a function of relative humidity when the effect of hydrates is included in the classical nucleation theory.
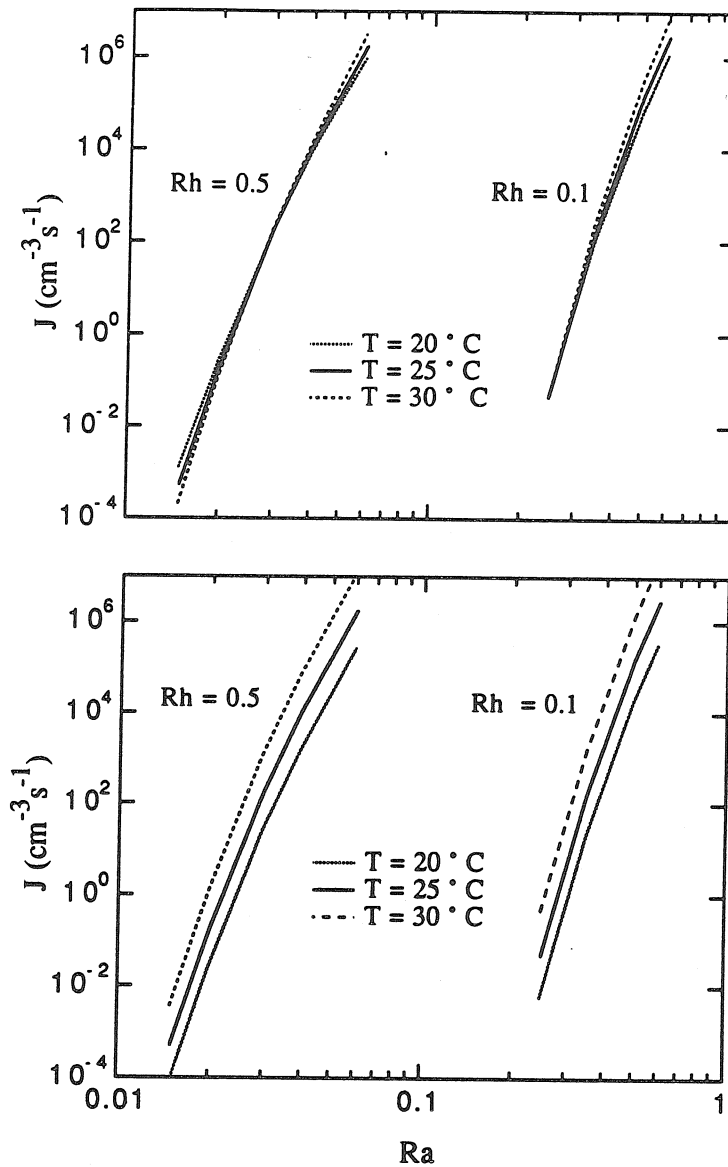
Figure 16 : The changes in the nucleation rate with temperature as predicted by binary nucleation theory and the sensitivity of these to uncertainties in the property values. a) The temperature dependence of the surface tension of MSA has been estimated using a group contribution method and the heats of mixing are those of sulfuric acid. b) The temperature dependence of the surface tension of MSA has been estimated as 1/3 of that estimated by the group contribution method and the heats of mixing are 1/2 of the values for sulfuric acid.
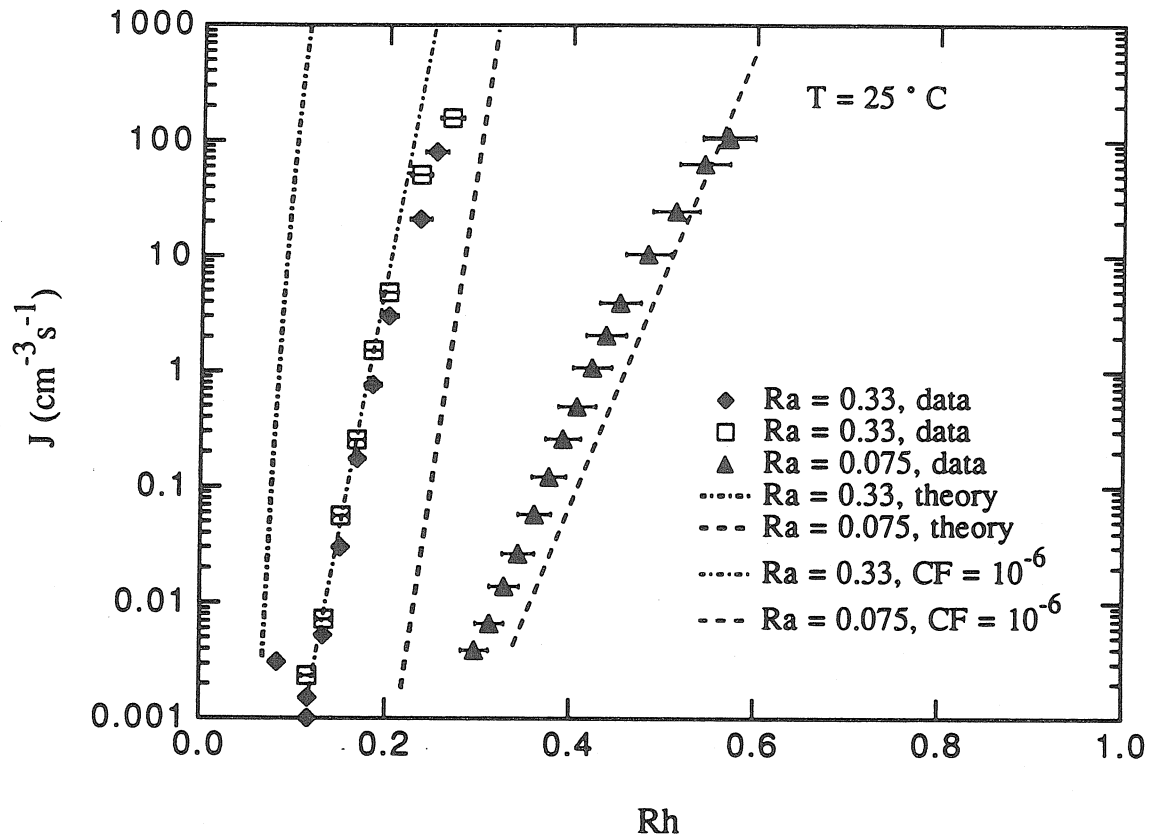
Figure 17 : A comparison of the experimental nucleation rates with classical binary nucleation theory and with the empirically corrected theoretical curves.
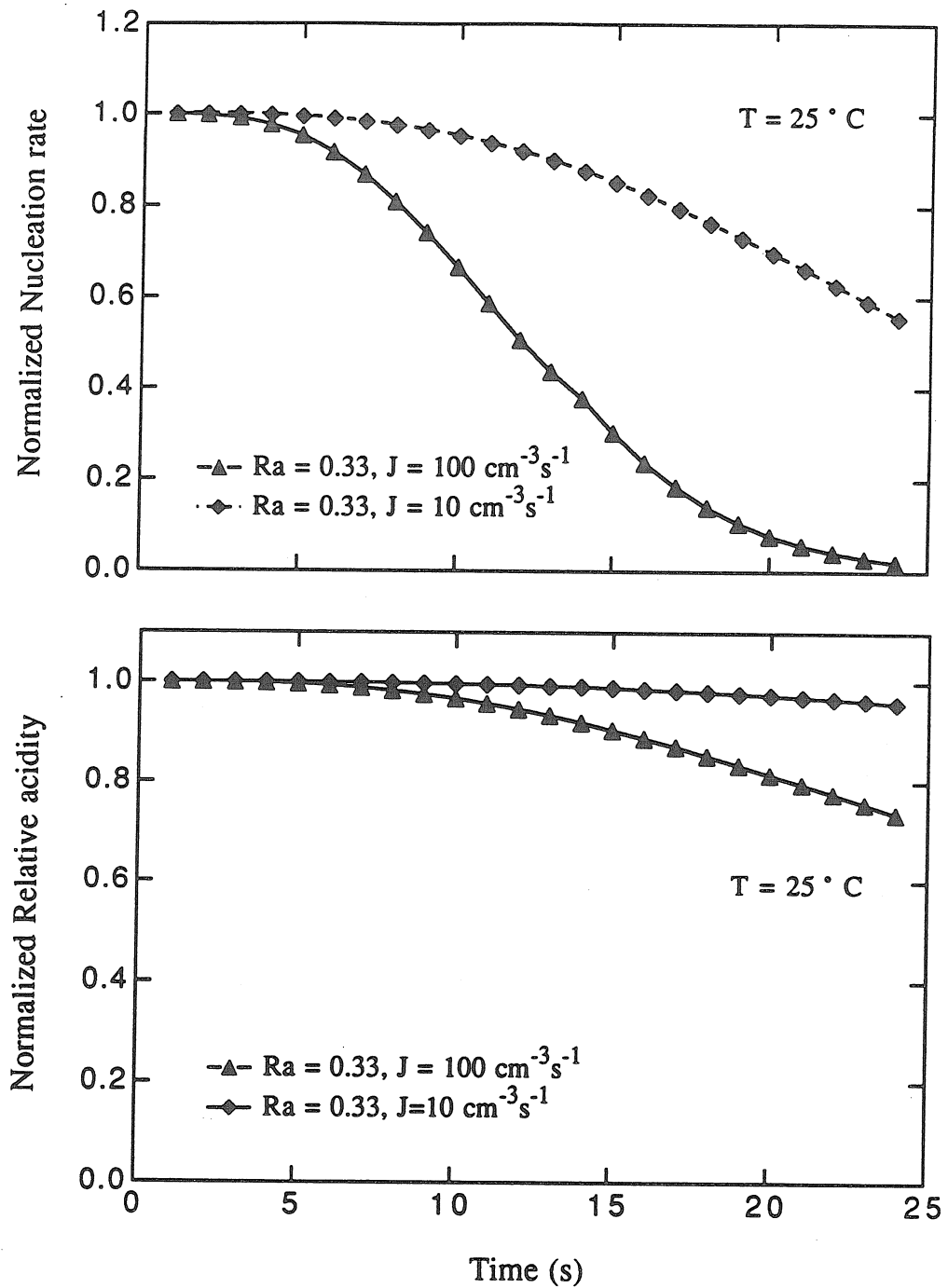
Figure 18 : Simulated profiles along the nucleation path for the MSA -water experiments showing the predicted changes in the normalized nucleation rate and the normalized relative acidity for $J° = 100$ and 10 $cm^{-3}s^{-1}$.
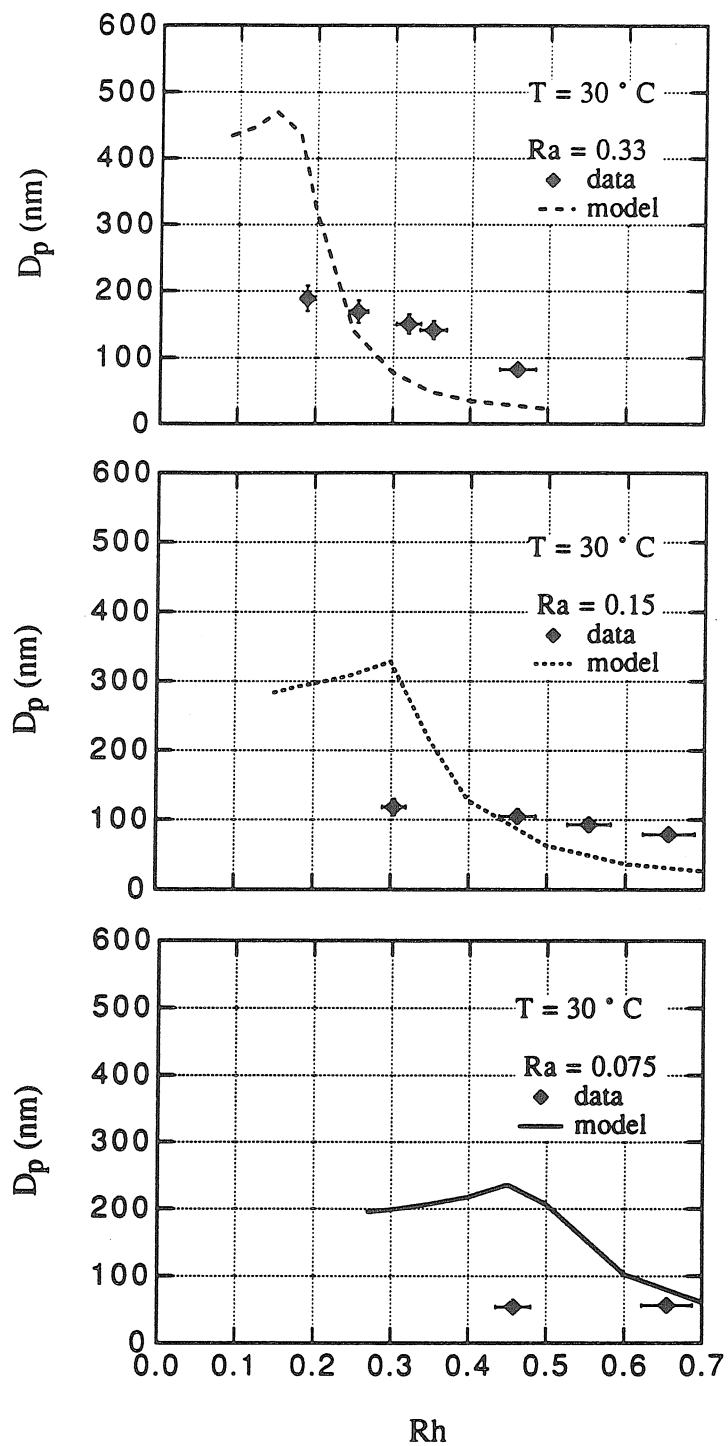
Figure 19 : The predicted particle size at the end of 18 s of simulation is compared to the observed peak diameter in the number distributions at $T = 30 \,^\circ$ C. Simulations used the values $\alpha_p = 0.6$, $\alpha_s = 1.0$ and $CF = 10^{-4}$.
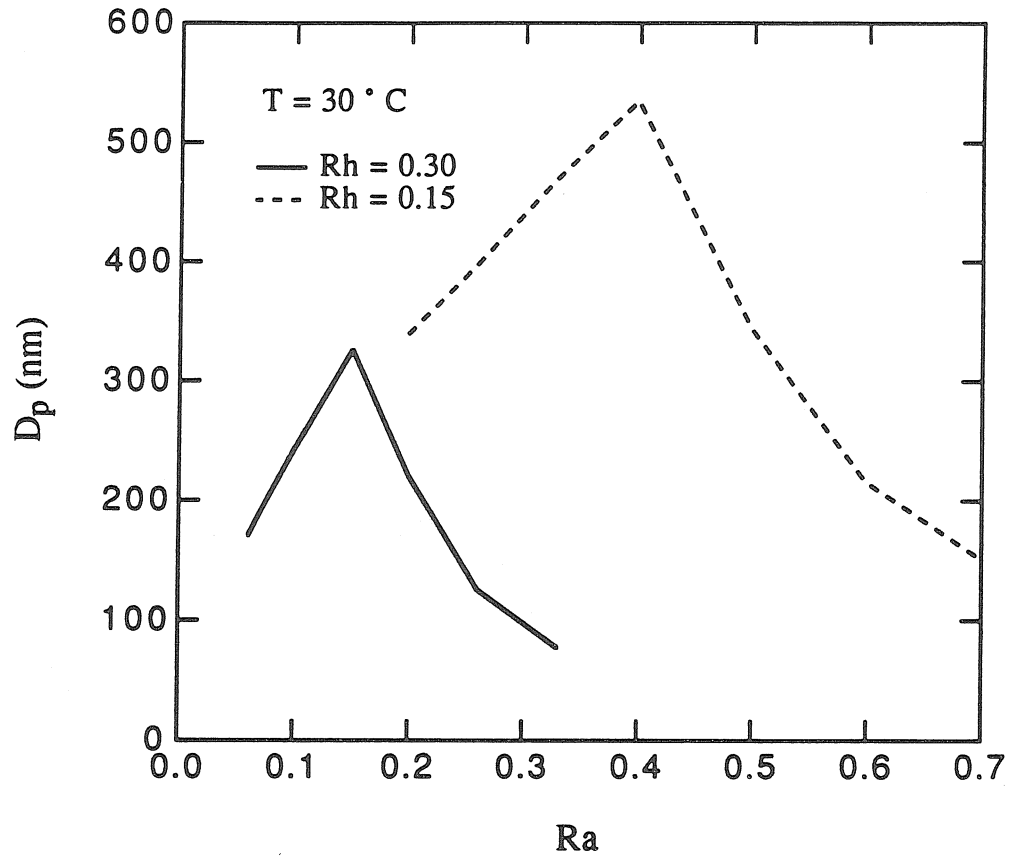
Figure 20 : The predicted variation in the particle diameter with changes in Ra for two levels of Rh. The particles formed at higher relative humidity are predicted to be smaller. This Figure should be compared with the data in Figure 13.

Appendix :

Supplementary Material to Chapter 2

The figures in this Appendix constitute the supplementary material deposited as AIP document no. PAPS JCPSA-94-6827-15 and listed as Reference 13 in the paper *Binary nucleation in acid-water systems. I. Methanesulphonic acid-water.*, B. E. Wyslouzil, J. H. Seinfeld, R. C. Flagan and K. Okuyama, J. Chem. Phys. **94**, 6827 (1991).

Binary Nucleation in Acid - Water Systems
I. Methanesulfonic Acid - Water

B.E. Wyslouzil, J.H. Seinfeld and R.C. Flagan,

Department of Chemical Engineering,

California Institute of Technology,

Pasadena California 91125

and

K. Okuyama

Department of Chemical Engineering,

Hiroshima University,

Saijo-cho, Higashi-Hiroshima,

Japan
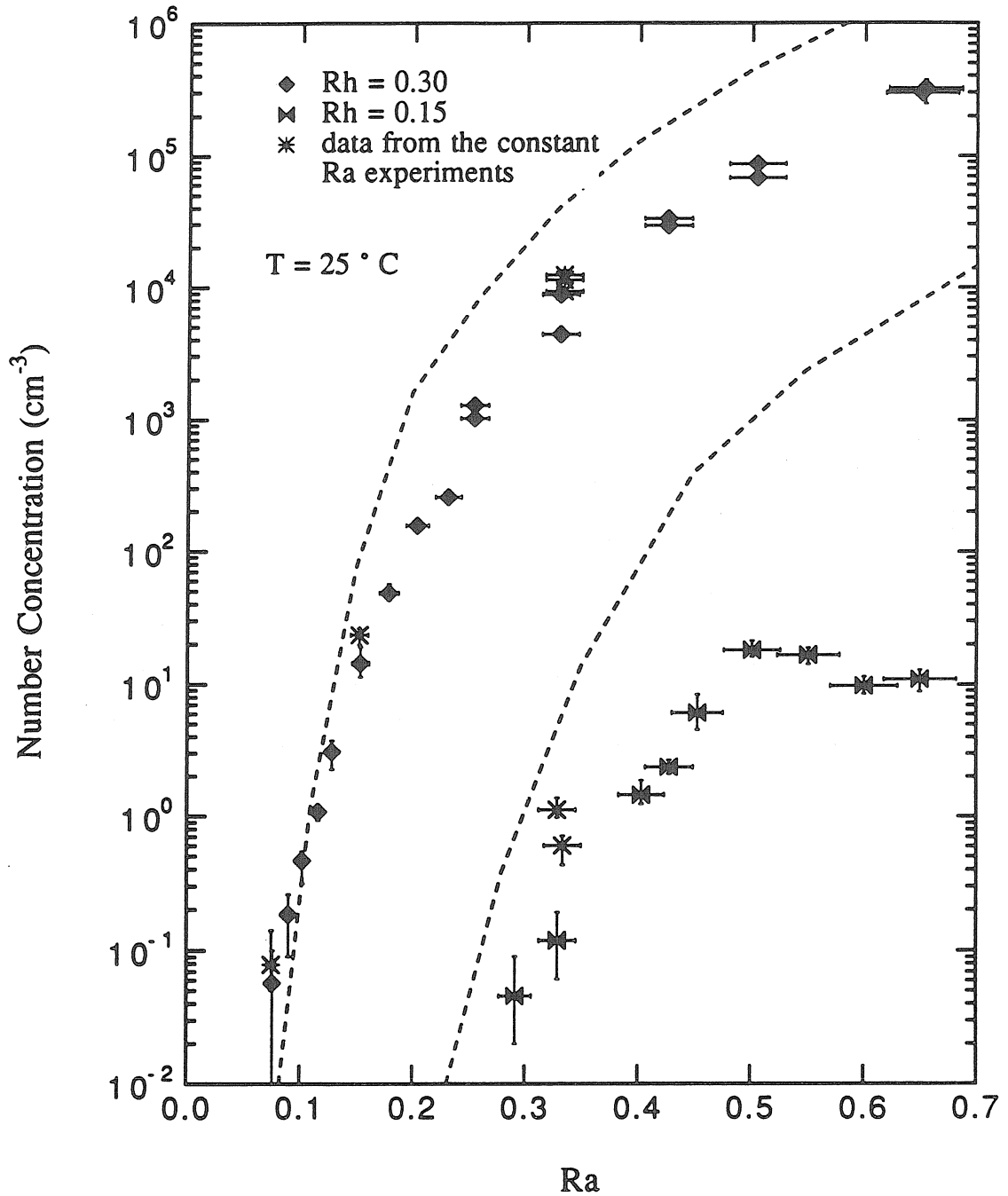
Figure 1 : Observed number concentrations as a function of relative acidity at $T = 25\,^\circ$ C.

Broken lines are the predicted number concentrations from the integral model using

$\alpha_p = 0.6$, $\alpha_s = 1.0$ and a correction factor, $CF = 10^{-6}$.
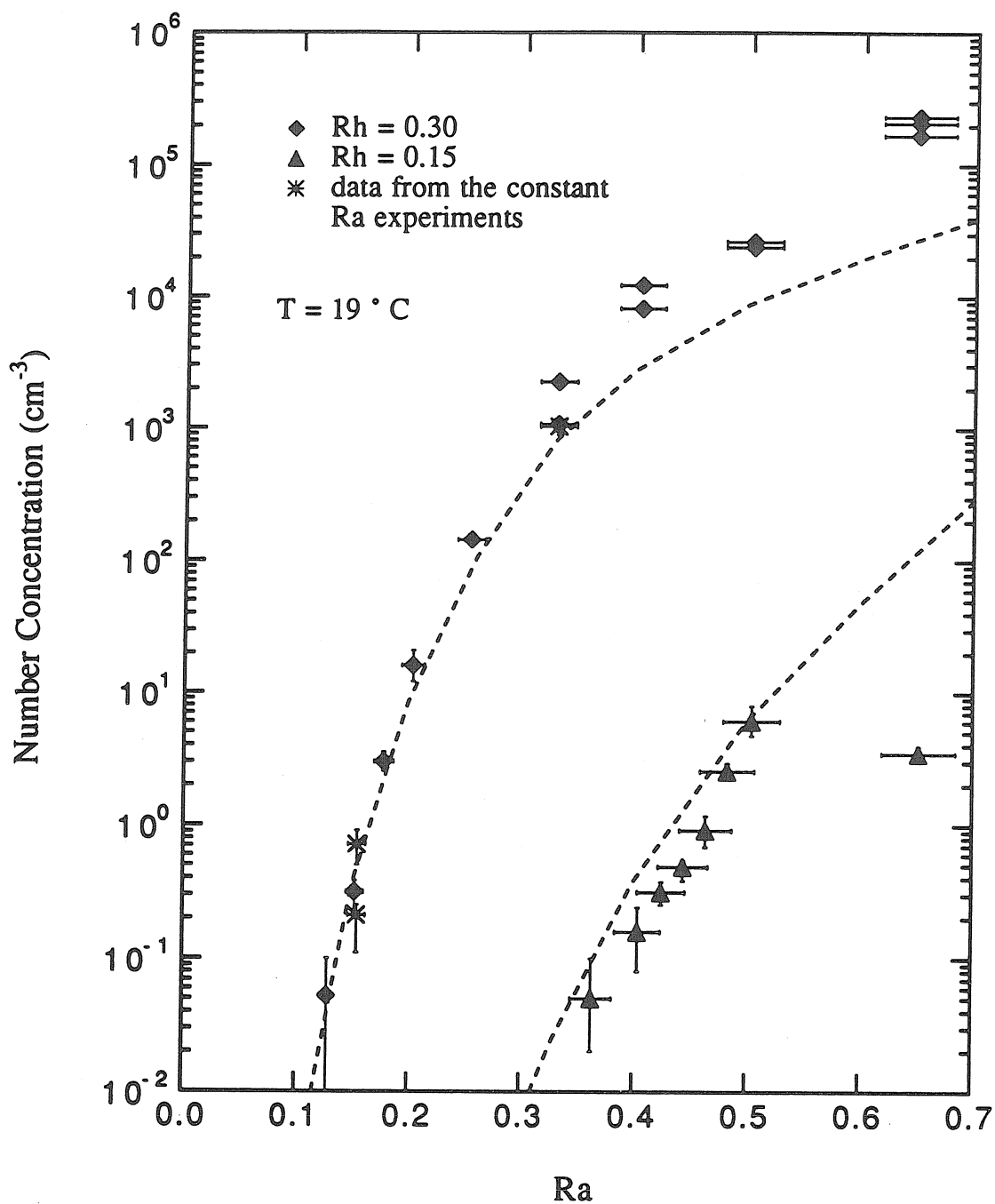
Figure 2 : Observed number concentrations as a function of relative acidity at $T = 19\,^{\circ}$ C.

Broken lines are the predicted number concentrations from the integral model using
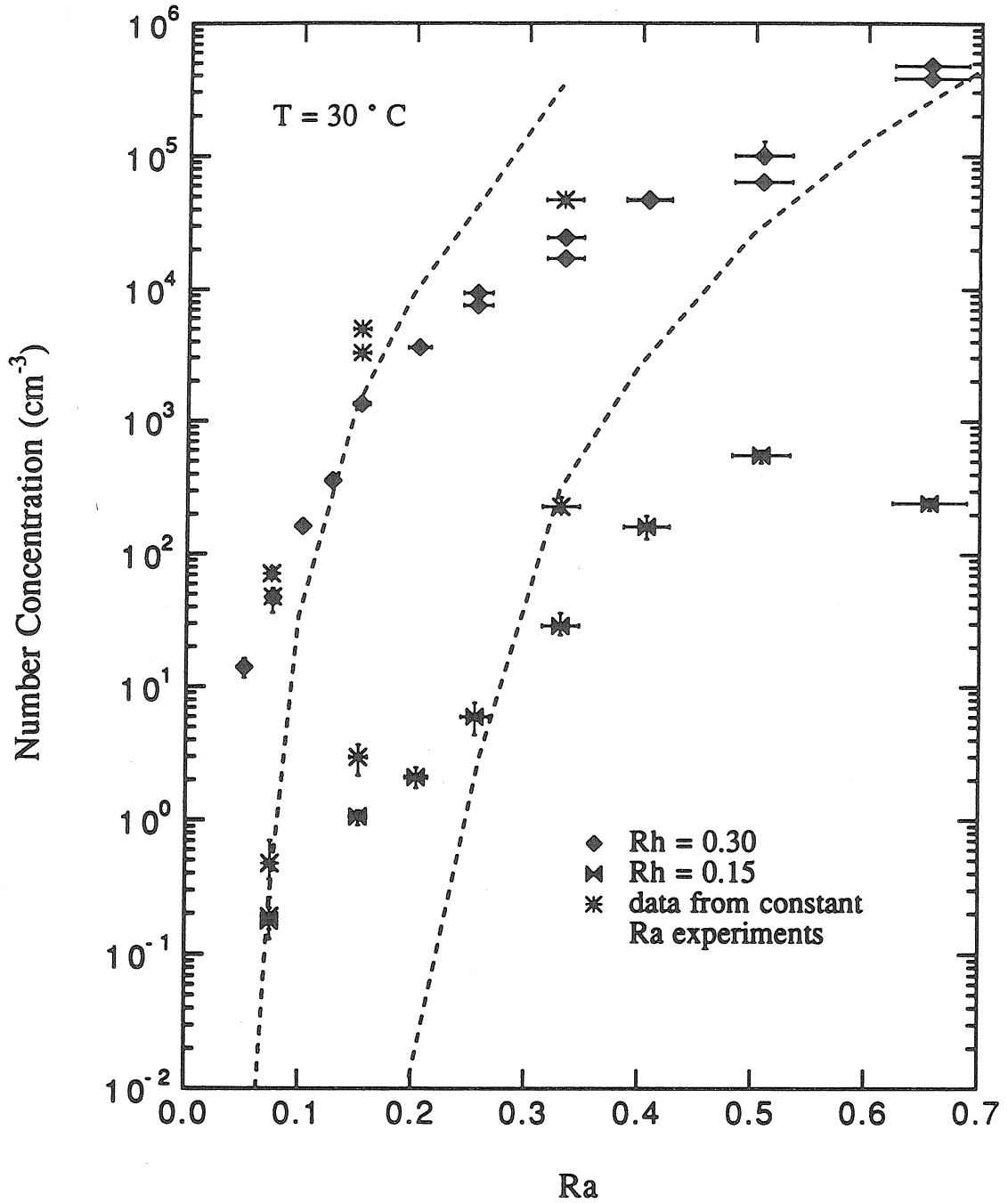
$\alpha_p = 0.6$, $\alpha_s = 1.0$ and $CF = 10^{-8}$.

Figure 3 : Observed number concentrations as a function of relative acidity at $T = 30\,^{\circ}$ C. Broken lines are the predicted number concentrations from the integral model using $\alpha_p = 0.6$, $\alpha_s = 1.0$ and $CF = 10^{-4}$.
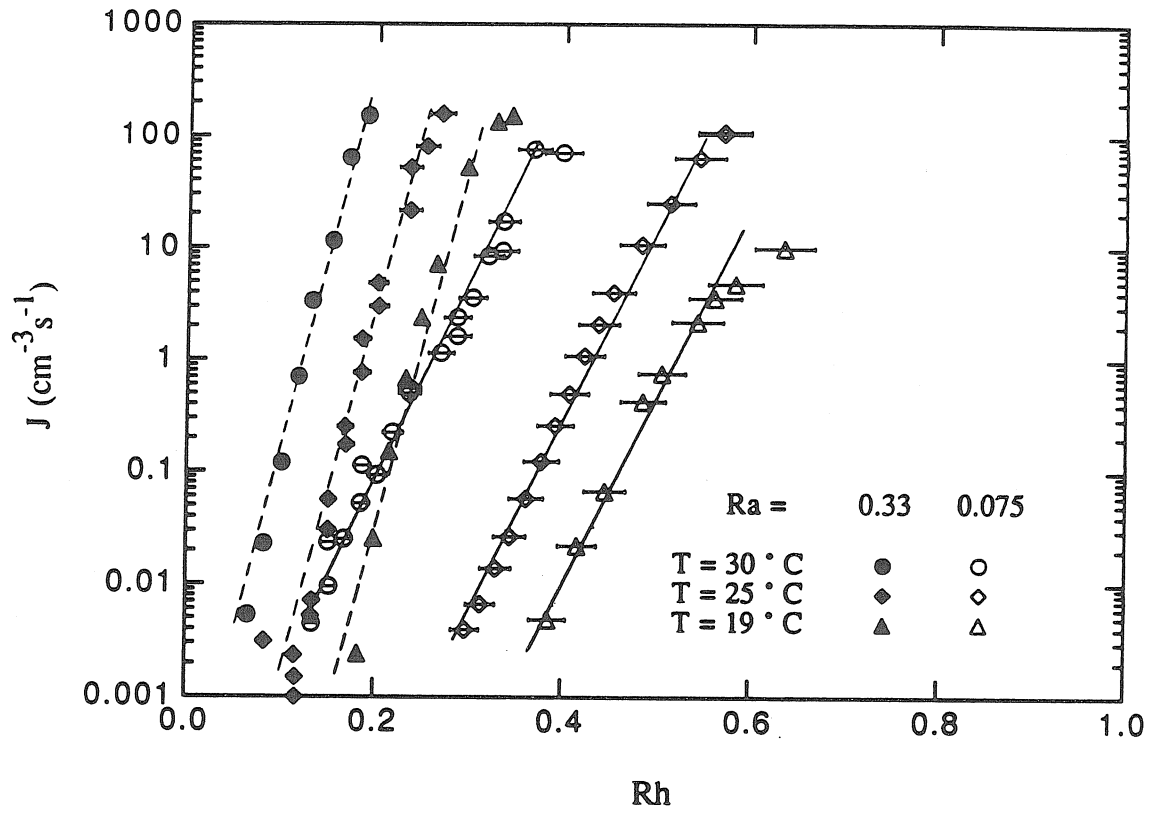
Figure 4 : The variation of nucleation rates for MSA-water with relative humidity for Ra = 0.33 and 0.075. The lines indicate the trends in the data only.
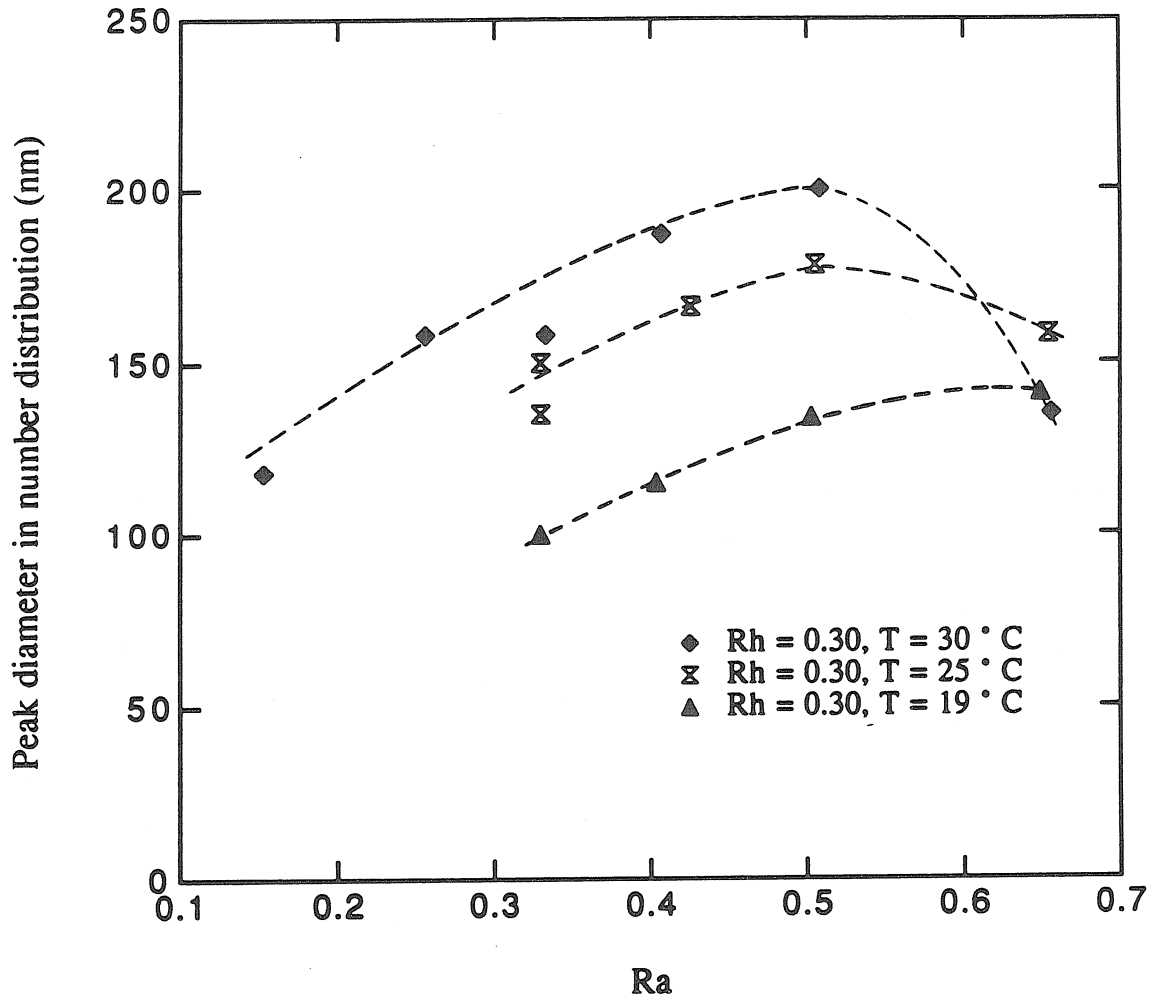
Figure 5 : Variation in the peak of the number distribution with Ra for Rh = 0.30 at three temperatures.
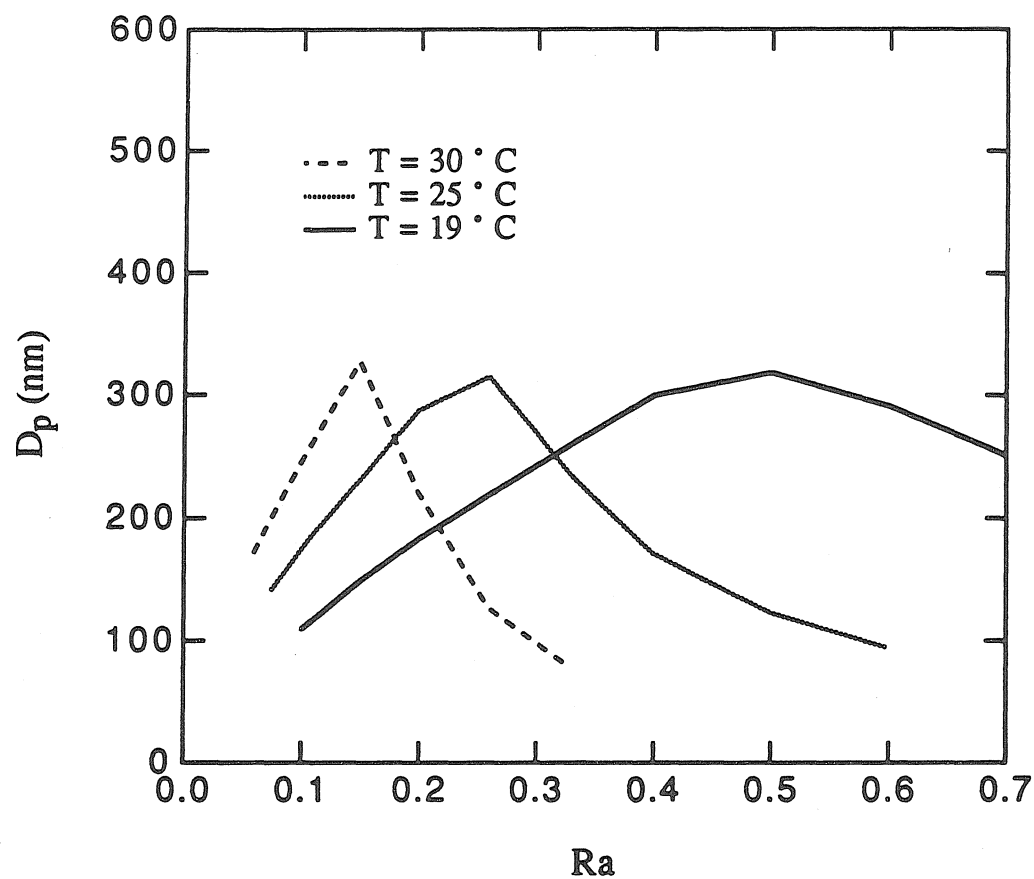
Figure 6 : The predicted variation of the particle diameter with Ra and temperature for Rh = 0.30. The empirical correction factors appropriate for each temperature have been applied and this figure should be compared with the data in Fig. 5.

CHAPTER 3

Binary Nucleation in Acid - Water Systems II. Sulfuric Acid - Water and a Comparison with Methanesulfonic Acid - Water

B.E. Wyslouzil, J.H. Seinfeld and R.C. Flagan,

Department of Chemical Engineering,

California Institute of Technology,

Pasadena California 91125

and

K. Okuyama

Department of Chemical Engineering,

Hiroshima University,

Saijo-cho, Higashi-Hiroshima,

Japan

ABSTRACT

This work presents a systematic investigation of binary nucleation rates for sulfuric acid and water and the effect of temperature on these rates at isothermal, subsaturated conditions. The results from nucleation rate measurements for the sulfuric acid (H_2SO_4) - water system are discussed and compared to those previously presented for methanesulfonic acid (MSA) - water [B. E. Wyslouzil, J. H. Seinfeld, R. C. Flagan, and K. Okuyama, J. Chem. Phys. 94, 6827 (1991)]. Experiments were conducted at relative humidities (Rh) ranging from $0.006 < Rh < 0.65$, relative acidities (Ra) in the range of $0.04 < Ra < 0.46$, and at three temperatures, $T = 20, 25$ and $30 °C$, in the continuous flow mixing - type apparatus described in Paper I. Particles were formed by binary nucleation and grew by condensation as the mixed stream flowed through an isothermal glass tube. Number concentrations observed at the exit of the nucleation and growth tube as a function of Rh and Ra are extremely sensitive to the binary nucleation rate, and from these data the nucleation rate was estimated as a function of saturation level and temperature. Particle size distributions were also measured using a specially constructed Differential Mobility Analyzer. As anticipated, the H_2SO_4 particles formed by nucleation and growth are much smaller than those formed in the MSA - water experiments, but particle size distribution measurements confirm that most of the particles formed are being observed. The ratio of experimental to theoretical nucleation rates, J_{exp}/J_{theor}, was found to be a strong function of the predicted number of acid molecules in the critical nucleus for both the H_2SO_4 - water and MSA - water systems.

I. INTRODUCTION

The sulfuric acid - water binary has been the traditional model for theoretical studies of the binary nucleation rate expression.[1-4] It is an important system in the atmosphere, because H_2SO_4 is the product of the oxidation of SO_2 as well as other naturally occurring sulfur species. The system does present intrinsic experimental difficulties, related to its corrosive properties and its extremely low vapor pressure. Property values are however reasonably well known over essentially the entire range of composition at temperatures near 25 ° C. Even the vapor pressure of sulfuric acid has been determined recently to within a factor of about four by Ayers[5] and Roedel.[6]

The first measurements of nucleation rates in the H_2SO_4 - H_2O system were the expansion chamber results of Reiss *et al.*[7] Later however, Schelling and Reiss[8] concluded that expansion chambers were not appropriate for working with the acid water system in part because of the long times scales required to set up the steady-state cluster distributions relative to the sensitive time of the chamber. Boulaud *et al.*[9] observed particle formation between SO_3 and water vapor as a function of time, but on the timescale of their experiments nucleation, condensation and coagulation are all important. Finally, Mirabel and Clavelin[10] measured the onset of nucleation at 25 ° C using a thermal upward diffusion chamber, but only measurements at Rh > 1 were possible because of the low vapor pressure of H_2SO_4. In single component homogeneous nucleation, rate data are a considerably more stringent test of theory than simply determining the critical supersaturation. This is certainly the case in binary nucleation as well, and provides the motivation for the current work.

The continuous flow mixing device used to measure nucleation rates in the MSA-water system,[11] is used here to investigate nucleation in the H_2SO_4 - water system. The effect of

temperature on the nucleation process is investigated for Ra and Rh < 1 in the range from 20 to 30 ° C. At very low values of Ra, conditions should approach those that can exist in the atmosphere. Particle size distributions are measured to better understand the competing processes of nucleation and condensation, and to ensure that the majority of the particles produced are large enough to be observed. The nucleation rate data are then compared to the predictions of classical binary nucleation theory and the deviation of the ratio J_{exp}/J_{theor} from 1 is investigated.

II. CHANGES TO THE CONTINUOUS FLOW MIXING DEVICE

Since detailed descriptions of the experimental procedures and apparatus appear in paper I, only the basic concept and the changes made in order to work with the H_2SO_4 - water system will be discussed here.

In the continuous flow mixing device particle-free gas streams saturated with the desired acid and water vapor are rapidly mixed at known temperatures and pressures to create well characterized initial conditions. The mixed stream flows through an isothermal tube in which particles nucleate and grow. The number concentration of particles produced is measured at the outlet of the reactor using a high resolution condensation nucleus counter (CNC) and provides a sensitive measure of the binary nucleation rate. When the number of particles produced is low, condensation rates will not deplete the acid vapor significantly, and nucleation rates may be derived by dividing the total number concentration by the length of time over which nucleation occurs.

The principal difference in the experimental setup from that previously described is in the method used to measure the particle size distributions. A short column (10 cm) DMA[12]

was used in conjunction with the TSI 3020 CNC to improve the lower cutoff for the < 50 nm particles produced in the experiment. The shorter column length allows the high mobility fine particles to be classified at reasonable voltages and sheath air flow rates, the use of a brass rather than Teflon outlet port reduces the loss of particles by electrostatic charging, and the 3020 CNC has a lower detection limit than the 3076 CNC used previously. The DMA was run in stepping mode, with voltages changed manually. At least six number concentrations were recorded at each voltage, once steady state was achieved, which were then averaged as part of the inversion process. At particle diameters (D_p) less than 20 nm, the data were corrected for the decreased counting efficiency of the CNC using the data of Ahn and Liu,[13] Keady et al.[14] and Bartz et al.,[15] and for diffusional losses in the DMA using the data of Adachi et al.[16] Before starting the experiments, it was also necessary to let the equipment run for several days in order to achieve steady and reproducible data. After this initial conditioning period, experimental results were extremely reproducible.

The sulfuric acid used in all of the experiments was 'Ultrex' high purity H_2SO_4 (Aldrich Chemicals) assayed at 97.5 wt%. Because the source of H_2SO_4 vapor is a mixture containing 2.5 wt% water, the expression for Ra must be corrected for acid composition. Equation (3) of Paper I therefore becomes

$$Ra = \frac{a_a\, p_l\, p_a(T_{ab})\, F_a}{p_{ab}\, p_a(T_m)\, [(1+Y_w)F_h + F_d + F_a]} \tag{1}$$

Here a_a is the acid activity over a 97.5 wt% solution of H_2SO_4. As in Paper I, p_l, p_{ab}, $p_a(T_{ab})$ and $p_a(T_m)$ are the absolute pressure in the laboratory, the measured acid bubbler pressure, the saturation vapor pressure of the acid at the temperature in the acid bubbler and the saturation vapor pressure of acid at the temperature of the mixer. F_h, F_d

and F_a are the flow rates of the humid, dry and acidic streams respectively, and Y_w is the ratio of moles of water vapor per mole of dry air flowing through the water bubbler. The assumption has been made that the ratio of moles of acid to moles of air, Y_a, is approximately equal to zero because the vapor pressure of the acid at 25 ° C is on the order of 1.4×10^{-4} torr. The values for a_a are based on the data of Giauque *et al.*[17]

Although some water vapor will be present at equilibrium with the H_2SO_4 solution, at 97.5 wt% H_2SO_4 the activity of water, $a_w \approx 10^{-4}$, is negligible compared to the amount of water vapor entering with the humid stream. Therefore the value of Rh is still calculated using Equation (1) from Paper I.

III. NUCLEATION RATES AND PARTICLE SIZE BEHAVIOR

Experiments with the H_2SO_4 - water binary were performed at relative acidities of 0.45, 0.25, 0.15 and 0.10, relative humidities of 0.28 and 0.14, and temperatures of 20, 25 and 30 ° C. All of the experimental conditions investigated are summarized in Table 1.

Figure 1 shows typical data collected on the variation of number concentration as a function of the saturation level and temperature for $T = 25$ ° C. The symbols represent the average of all the values observed at the given conditions, with the extremes indicated by the vertical error bars. Horizontal error bars represent the calculated uncertainty in the saturation levels, ($\pm$ 5%), which is the result of the uncertainties in the flow and temperature controls. The uncertainties in the flows dominate the total uncertainty, since each flow is accurate to $\pm$ 3%. Data represented by *'s show the internal consistency of the data and demonstrate that the number concentration observed at a given set of conditions is independent of the direction of approach to that condition. The repeatability of the

experiments, once steady operating conditions have been achieved, is illustrated in Fig. 1 where experiments at Ra = 0.45 and 0.25 were repeated one and three days apart, respectively. At the same conditions of saturation and temperature, measured number concentrations agree to within a factor of three or four.

It is clear from the data presented here that the number of particles produced is extremely sensitive to both the saturation levels and temperature. Because the vapor pressure of water is so much higher than that of the acid, even high nucleation rates will not perturb the relative humidity of the mixed stream. Furthermore, if the production of particles is low, nucleation and condensation will not deplete the acid vapor significantly on the time scale of the experiment. In this case, the nucleation rate can be estimated by dividing the number concentration of particles produced by the length of time over which nucleation occurs. With the low final number concentration and a residence time of only 18 s, coagulation will not occur to any significant extent, and as discussed previously,[11] losses of particles or vapor to the walls can also be neglected.

The initial steep increase in the number concentration curves (Fig. 1), from $N < 0.1$ cm^{-3} up to about $N = 1000$ cm^{-3}, corresponds to the region of constant nucleation rate along the nucleation and growth tube. At higher levels of saturation, the curves flatten out, as the available acid vapor is depleted and nucleation is quenched well within the flow tube. These data cannot be used to derive nucleation rates because the time over which significant nucleation is occurring is unknown.

Figures 2 through 7 illustrate the variation of the nucleation rates with saturation level derived from the experimental number concentrations. The data for a given constant saturation level all fall on straight lines, except for a few points at $T = 30\,°C$. These points, corresponding to Rh < 0.02, actually fall below the lower limit of the flowmeter

calibrations and uncertainty in the actual value of Rh requires that these points be discarded from further analysis. Figures 8 through 10 illustrate the saturation levels that correspond to $J = 0.01$, 1 and 100 $cm^{-3}s^{-1}$ that have been derived from the experimental nucleation rate data. Figure 10 clearly shows the rapid increase in the level of Ra required to maintain a given nucleation rate as Rh decreases, indicative of the approach to single component nucleation.

The effect of temperature on the nucleation rate is clearly demonstrated in Fig. 11, where experimental and theoretical rates corresponding to Rh = 0.28 at $T = 20, 25$ and 30 ° C are plotted. A temperature increase of 5 ° C corresponds to an increase in the observed nucleation rate of two to four orders of magnitude. This observation differs significantly from the behavior predicted by classical binary nucleation theory, where the only discernable change is a slight increase in the steepness of the rate curves as temperature increases, however it does agree with the observations in single component nucleation.

The binary nucleation rate expression used to calculated the nucleation rate at the initial mixed stream conditions was that developed by Jaecker-Voirol and Mirabel[4] and described in detail in Paper I. The saddle point of the free energy surface was found by a discrete search that allowed only integral numbers of acid and water molecules in the critical cluster, and which included the effect of hydrate formation in the gas phase. The data correlation programs developed by Kreidenweis and Seinfeld[19] and the vapor pressure of pure sulfuric acid measured by Ayers[5] were used in all of the calculations.

Particle size distributions were measured for only a limited number of cases. Volume distributions $dV/dlnD_p$, were calculated from the measured number distributions, $dN/dlnD_p$. Figure 12 illustrates a typical particle size distribution. As in almost all of the

cases observed, the peak in the number distribution appears to be within the measuring range of the instrumentation even with the corrections due to diffusion losses and counting efficiency of the CNC for particles < 20 nm. Although there is not enough data to perform a thorough analysis of the behavior of the peak diameter with respect to changes in Ra and Rh, the distributions do imply that most of the particles produced are being counted and that the nucleation rate measurements are not significantly affected by particles not visible to the TSI 3020 CNC.

The particle size distributions are well described by log-normal distributions and from the value of σ_g, the standard deviation obtained from the fit of the volume distribution curves, a value of the polydispersity factor, $\alpha_p = \exp(-\ln^2(\sigma_g))$, was estimated as $\alpha_p = 0.7$. The polydispersity factor is used in the integral model for nucleation and growth, described in Paper I, to correct for the overestimation of the condensation rate that occurs because the aerosol is assumed to be monodisperse. The value of α_p for the H_2SO_4 - H_2O is higher than that found for the MSA - H_2O aerosols, where $\alpha_p = 0.6$, reflecting the more monodisperse size distributions observed.

A major objective of the present work is to compare measured nucleation rates with the predictions of classical binary nucleation theory. The plots of the experimental nucleation rates against the theoretical nucleation rates on log-log coordinates, Figs. 13 through 15, show that a straight line relationship exists between the two rates for each constant saturation level experiment conducted. However at a given temperature, the data from the different experiments do not all fall on a single straight line, and experiments at constant Ra have distinctly different slopes from those at constant Rh. Thus the application of a single correction factor to the binary nucleation rate expression at a given temperature, which was found to give a reasonable description of the experimental results in the case of MSA - water, cannot describe the H_2SO_4 - H_2O data.

In each of the figures, however, a clear trend emerges. As the initial level of acidity increases, the value of the ratio J_{exp}/J_{theor} increases. This suggests that J_{exp}/J_{theor} should be a function of a characteristic concentration. One concentration available is that of the critical nucleus as predicted by classical binary nucleation theory. Although J_{exp}/J_{theor} was found to vary with the mole fraction of acid in the critical nucleus, a strong correlation was found by plotting J_{exp}/J_{theor} against the number of acid molecules in the critical nucleus. As illustrated in Fig. 16, there is a strong relationship between the two variables of interest, and the data from all three temperatures fall on a single band with good agreement in the regions of overlap.

The line for perfect agreement between theory and experiment, $J_{exp}/J_{theor} = 1$, has been included in Fig. 16 for reference. The discrepancy between experiment and theory ranges over more than 20 orders of magnitude as the predicted number of acid molecules in the critical nucleus varies from about 4 to 30. A decrease in the number of acid molecules in the critical nucleus corresponds to increasing nucleation rates, thus this graph confirms that overall in the H_2SO_4 - H_2O system the predicted rates increase far more rapidly than the observed rates. Figure 16 represents a useful way to present the discrepancy between the experimental and theoretical nucleation rates when the true critical nucleus composition is unknown.

In retrospect it should not be surprising to find a compositional dependence of J_{exp}/J_{theor}. In single component nucleation the critical nucleus composition is well defined, while in binary nucleation this composition corresponds to that at the saddle point of the free energy surface, a function that depends strongly on the number of acid molecules present. Work with the dioctylphthalate (DOP) - dibutylphthalate (DBP) system by Okuyama et al.[19] showed that the best overall correction factor for the binary nucleation

measurements could also be quite different from that of either of the individual components, with no smooth transition between the two. This in some senses also implies a dependence of J_{exp}/J_{theor} on the critical nucleus composition.

Although Fig. 11 shows that the experimental nucleation rates depend strongly on the temperature, the compositional dependence of J_{exp}/J_{theor} clearly dominates any temperature dependence of this function over the range of temperatures investigated in this study. A wider range of temperatures would be required to try and separate the two effects.

A. Comparison with Previous Data on the Nucleation of H_2SO_4 - H_2O

The only available data with which to compare the present results are the 25 ° C H_2SO_4 - H_2O experiments of Mirabel and Clavelin.[10] The strong dependence of nucleation rate on temperature precludes a comparison with the results of Reiss et al.,[6] where experimental conditions were far below room temperature. Figure 17 presents the current data for $J = 1$ cm^{-3}s^{-1} as a function of acid and water saturation levels, along with the first few points taken from Fig. 3 of Mirabel and Clavelin[10]. The curve[10] suggested for extrapolating these data to lower Rh has also been included to facilitate comparison with the present data set.

As Rh approaches zero, the present data show the expected sharp increase in the Ra which corresponds to the approach to single component nucleation. If the present data set is extrapolated in a simple manner to higher values of Rh, they lie about 1 order of magnitude above the data of Mirabel and Clavelin.[10] This agreement is not unreasonable, considering the difficulty involved in working with the H_2SO_4 - H_2O system.

B. Comparison between H_2SO_4 and MSA

To ascertain whether MSA behaves in a manner analogous to that of H_2SO_4, a chemically similar compound, the measured nucleation rates for MSA-water from Paper I were compared to the corresponding theoretical rates. As illustrated in Fig. 18 , there are good straight line relationships between the two rates on logarithmic coordinates. As anticipated, at $T = 19\,°$ C all of the data lie close to a single straight line corresponding to $J_{exp}/J_{theor} = 10^{-8}$. The close correspondence of all the data to the single line $J_{exp}/J_{theor} = 10^{-8}$, is consistent with the good modelling fit possible with a single correction factor found for this temperature in Paper I. In similar plots at $T = 25$ and $30\,°$ C (available as supplementary material from PAPS[20]), the data were spread out, as was the case for H_2SO_4, but the trend was different. However, if all of the data are plotted, in Fig. 19, as J_{exp}/J_{theor} versus the number of acid molecules in the critical nucleus, the same behavior is found as in the case of H_2SO_4 . Once again compositional effects dominate the changes in J_{exp}/J_{theor} over the temperature range investigated in these experiments.

From classical nucleation theory, we expect nucleation rates for the H_2SO_4 - H_2O binary to be substantially higher than for the MSA - H_2O binary. In general this was found to be true and Fig. 20 compares the experimental and predicted results for Rh $= 0.15$ and $T = 25\,°$ C. Once again the experiments and theory show the same trends, albeit severely offset in terms of the actual values.

C. Simulation of the Continuous Flow Apparatus

The integral model described in Paper I was used here to ascertain that the assumptions regarding constant nucleation rates along the length of the reactor were valid. With the strong dependence of the correction factor on composition it is not possible to model the

system in the same way as for MSA. Several test cases were run for $J° = 100$ and

$10 \, cm^{-3}s^{-1}$ using the correction factors found for the given initial conditions. In all cases the nucleation rates and acid saturations remained essentially constant along the length of the nucleation and growth tube, thus verifying the assumption that in these situations condensation onto the nucleating particles is not dominating the gas to particle conversion process.

IV. SUMMARY AND CONCLUSIONS

The nucleation rates measured using a continuous flow mixing type device were presented for the H_2SO_4 - water binary for Ra and Rh <1 and as a function of temperature for $T = 20, 25$ and $30 °C$. The nucleation rates varied from $J = 0.01$ to $100 \, cm^{-3}s^{-1}$ and were strong functions of both saturation level and temperature, increasing with temperature by two to four orders of magnitude for a temperature increase of $5 °C$. In contrast to single component nucleation, the temperature dependent behavior was much stronger than that predicted by classical nucleation theory.

For the H_2SO_4 - water binary plots of $log(J_{exp})$ vs $log(J_{theor})$ were linear for a given saturation level, however at a single temperature the ratio of J_{exp}/J_{theor} was clearly not constant. Rather, the ratio J_{exp}/J_{theor} was a strong function of the predicted number of acid molecules in the critical nucleus. Overall, the ratio J_{exp}/J_{theor} was a stronger function of composition than temperature over the range of temperature investigated. The same results held for the MSA-water binary when these data were analyzed in a similar manner.

As anticipated, when comparing the results for the two acid-water systems, the nucleation rates of H_2SO_4 - water were much higher than those of MSA - water in the

range of values investigated. The slopes of the rate curves were also steeper, again in agreement with theory, and the average particle size was much smaller for the H_2SO_4 - water aerosol than for the MSA - water aerosol.

ACKNOWLEDGEMENTS

REFERENCES

[1] G.J. Doyle, J. Chem. Phys. 35, 795 (1961).

[2] W.J. Shugard, R.H.Heist and H. Reiss, J. Chem. Phys. 61, 5298 (1974).

[3] A. Jaecker-Voirol, P.Mirabel and H.Reiss, J. Chem. Phys. 87, 4849 (1987).

[4] A. Jaecker-Voirol and P.Mirabel , J. Chem. Phys. 88, 3518 (1987).

[5] G.P. Ayers, R.W. Gillett and J.L. Gras, Geophys. Res. Lett., 7, 433 (1980).

[6] W. Roedel, J. Aerosol Sci., 10, 375 (1979).

[7] H. Reiss, D.I. Margolese and F.J. Schelling J. Coll. Int. Sci. 56, 511 (1976).

[8] F.J. Schelling and H. Reiss, J. Coll. Int. Sci 83, 246 (1981).

[9] D. Boulaud, G. Madelaine, D. Vilga and J. Bricard, J. Chem. Phys. 66, 4854 (1977).

[10] P. Mirabel and J.L. Clavelin, J. Chem. Phys. 68, 5020-5027 (1978).

[11] B.E. Wyslouzil, J.H.Seinfeld, R.C. Flagan and K. Okuyama, J. Chem. Phys. 94, 6827 (1991).

[12] Y. Kousaka, K. Okuyama, M. Adachi and T. Mimura, J. Chem. Eng. Japan, 19, 401 (1986).

[13] K. H. Ahn and B.Y.H. Liu, J. Aerosol Sci., 21, 263 (1990).

[14]P.B. Keady, V.L. Denler, G.J. Sem, M.R. Stolzenburg and P.H. McMurray, in *Atmospheric Aerosols and Nucleation*, Wagner, P.E. and G. Vali Eds., 190 (Springer Verlag, 1988)

[15]H. Bartz, H. Fissan, C. Helsper, Y. Kousaka, K. Okuyama, N. Fukishima, P.B. Keady, S. Kerrigan, S.A. Fruin, P.H. McMurray, D.Y. Pui and M.R. Stolzenburg, J. Aerosol Sci., 16, 443 (1985).

[16]M. Adachi, K. Okuyama, Y. Kousaka, S.W. Moon and J.H. Seinfeld, Aerosol Sci. Techn., 12, 225 (1990).

[17]W.F. Giauque, E.W. Hornung, J.E. Kunzler and T.R. Rubin, J. Am. Chem. Soc. 82, 62 (1960).

[18]S. Kreidenweis and J. H. Seinfeld, Atmos. Environ., 22, 283 (1988).

[19]K. Okuyama, Y. Kousaka, S. Kreidenweis, R.C. Flagan and J.H. Seinfeld, J. Chem. Phys., 89, 6442-6453, (1988).

[20]See AIP document no. PAPS JCPSA-94-6842-9 for 9 pages of supplementary material. Order by PAPS number and journal reference from American Institute of Physics, Physics Auxiliary Publication Service, 335 East 45th Street, New York, NY 10017. The price is $1.50 for each microfiche (98 pages) or $5.00 for photocopies up to 30 pages, and $0.15 for each additional page over 30 pages. Airmail additional. Make checks payable to the American Institute of Physics.

Table 1 : Experimental conditions investigated in the total number experiments.

Experiment Number	Temperature (° C)	Relative Acidity	Relative Humidity
20.09	25.1	0.454-0.455	0.012-0.286
20.10	24.7	0.453-0.454	0.012-0.291
20.11	25.0	0.246-0.249	0.028-0.434
20.12	25.0	0.150-0.156	0.094-0.601
20.13	24.9	0.113-0.116	0.156-0.644
20.14	24.9	0.114-0.456	0.140-0.144
20.15	25.1	0.087-0.456	0.281-0.284
20.28	25.4	0.245-0.248	0.046-0.444
20.16	20.2	0.455-0.456	0.044-0.333
20.17	19.8	0.247-0.250	0.045-0.432
20.18	19.7	0.147-0.154	0.109-0.560
20.19	19.7	0.113-0.115	0.397-0.647
20.20	19.7	0.153-0.455	0.141-0.143
20.21	19.7	0.116-0.456	0.280-0.283
20.22	29.5	0.448-0.450	0.006-0.274
20.23	29.8	0.245-0.248	0.006-0.419
20.24	30.0	0.150-0.156	0.011-0.479
20.25	30.1	0.112-0.116	0.027-0.417
20.26	30.0	0.046-0.453	0.136-0.139
20.27	30.2	0.039-0.454	0.268-0.272
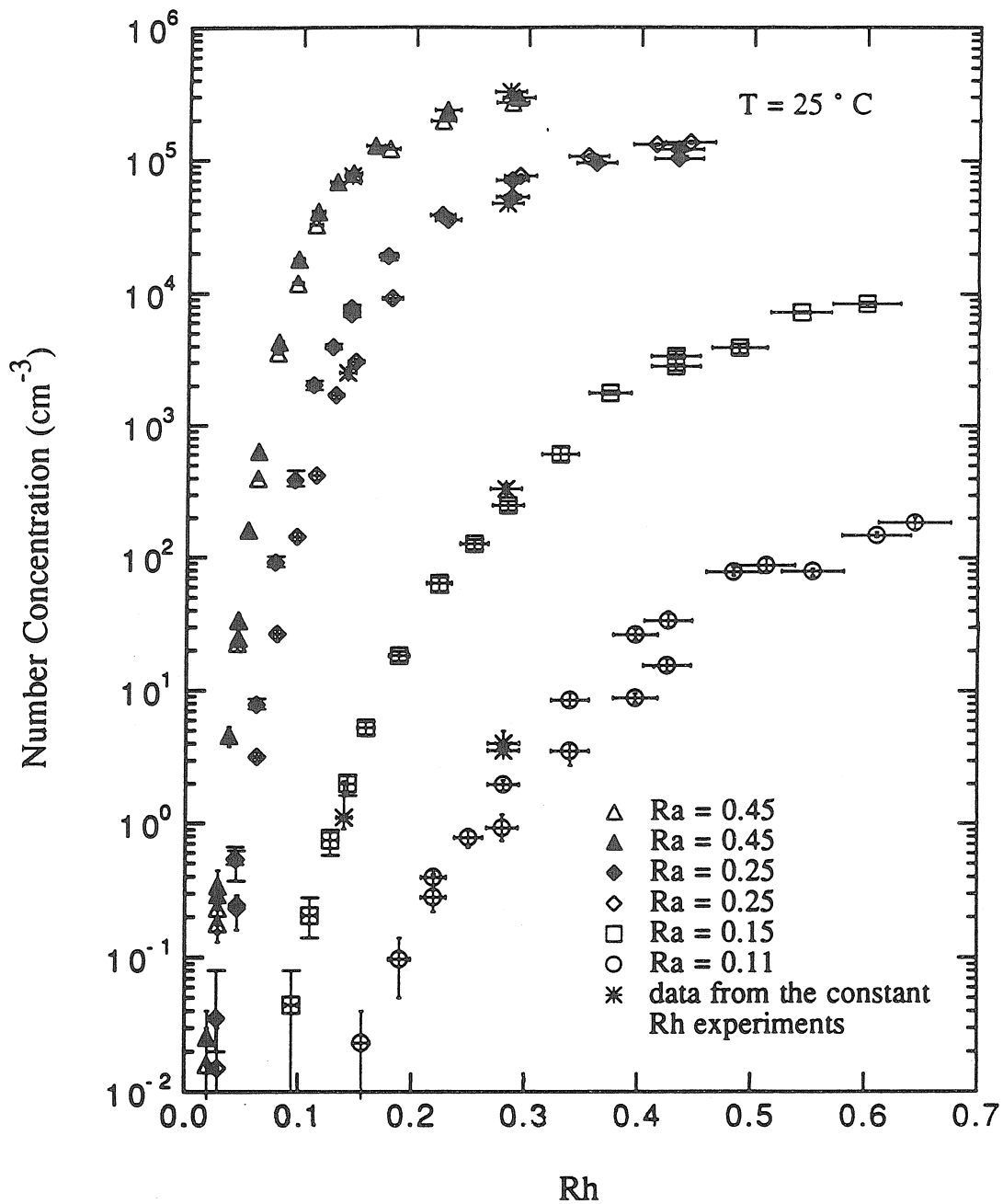
Figure 1 : The observed number concentrations as a function of relative humidity at $T = 25\,°C$.
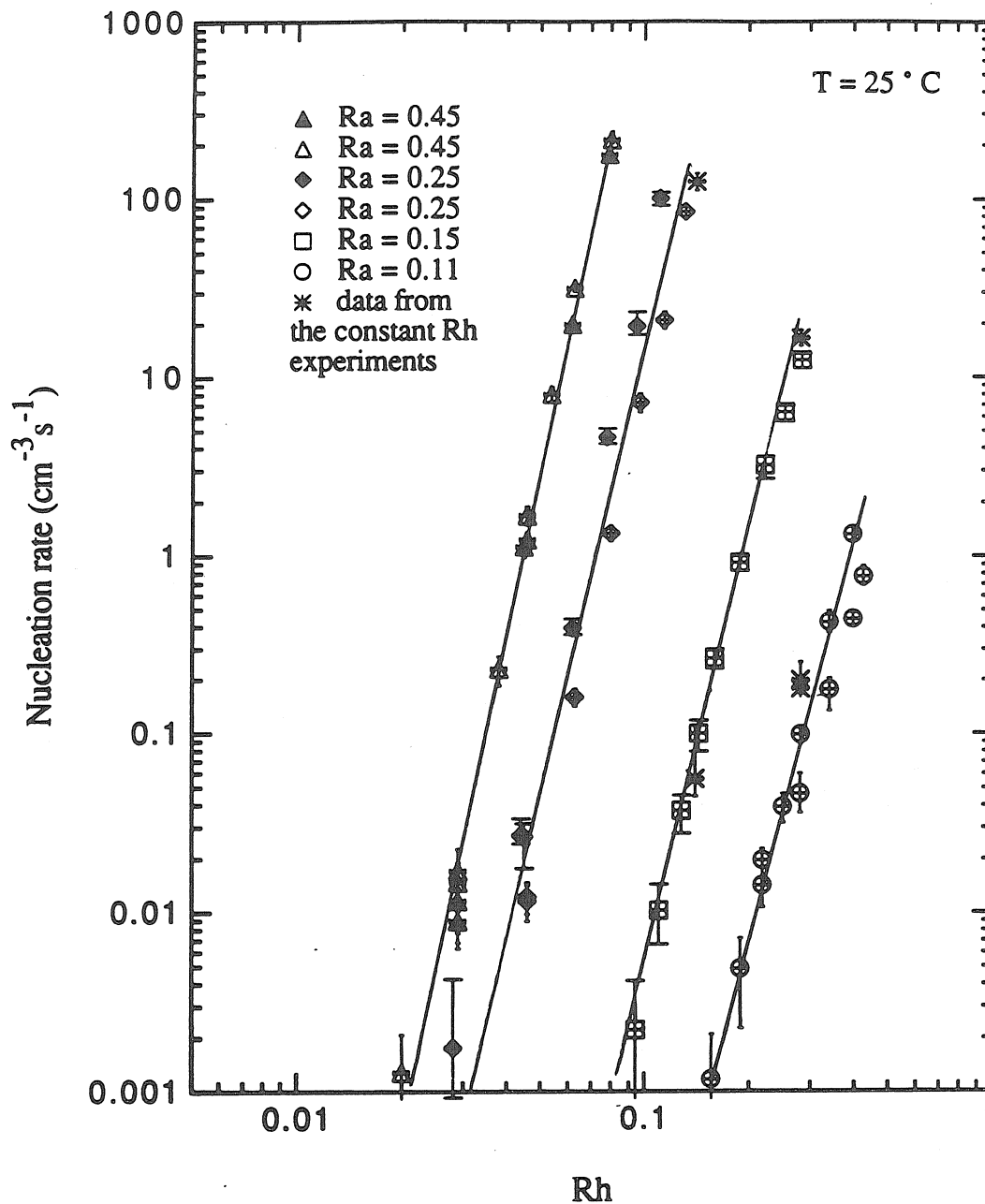
Figure 2 : Nucleation rates of H_2SO_4 - H_2O as a function of relative humidity at four different relative acidities and $T = 25$ ° C. The repeatability of the experiments is illustrated by the two experiments at Ra = 0.45, where data were taken one day apart, and the two experiments at Ra = 0.25 where data were taken three days apart. The lines connect the data points only.
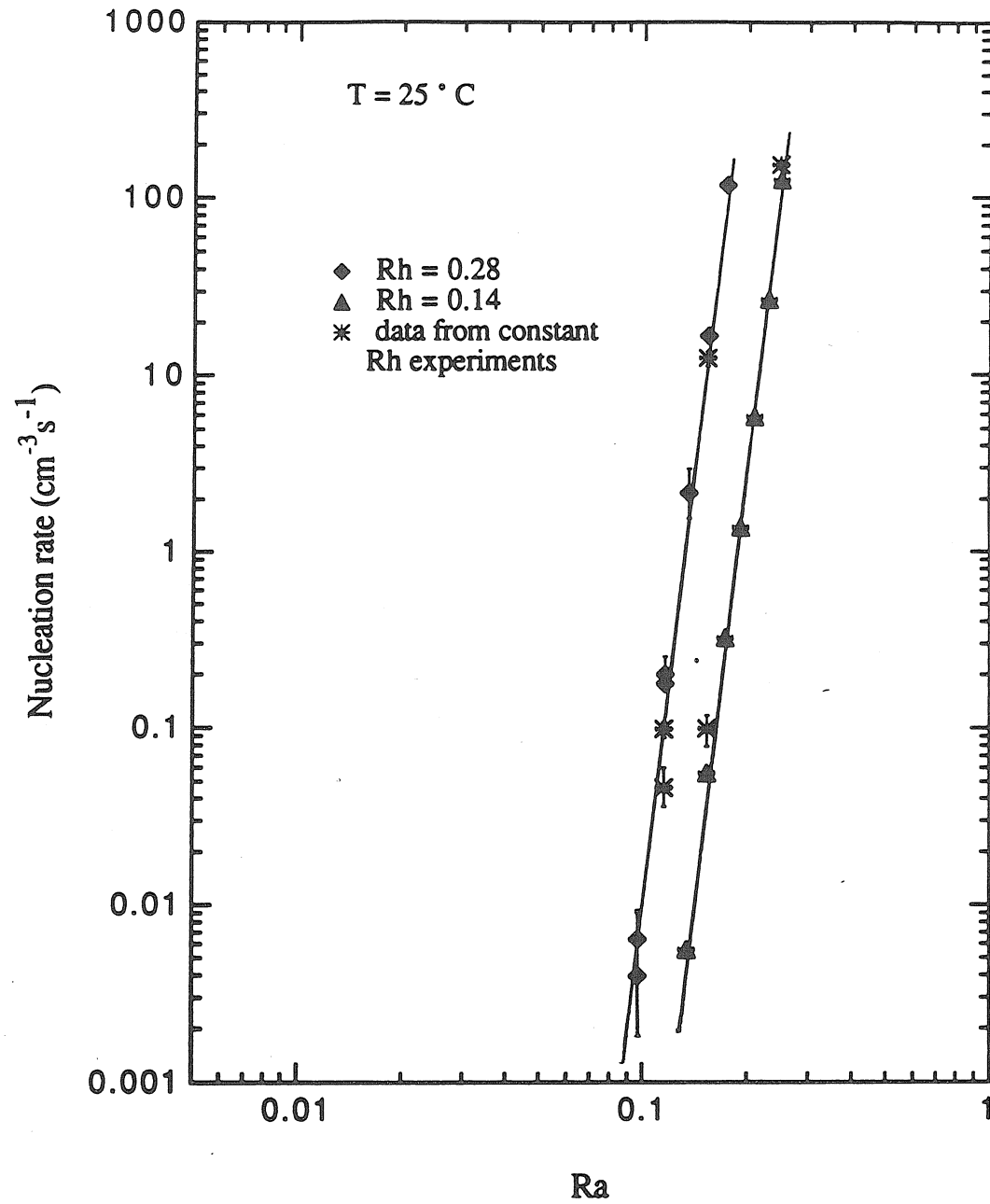
Figure 3 : Nucleation rates of H_2SO_4 - H_2O as a function of relative acidity at two different relative humidities and $T = 25\,°C$. The lines connect the data points only.
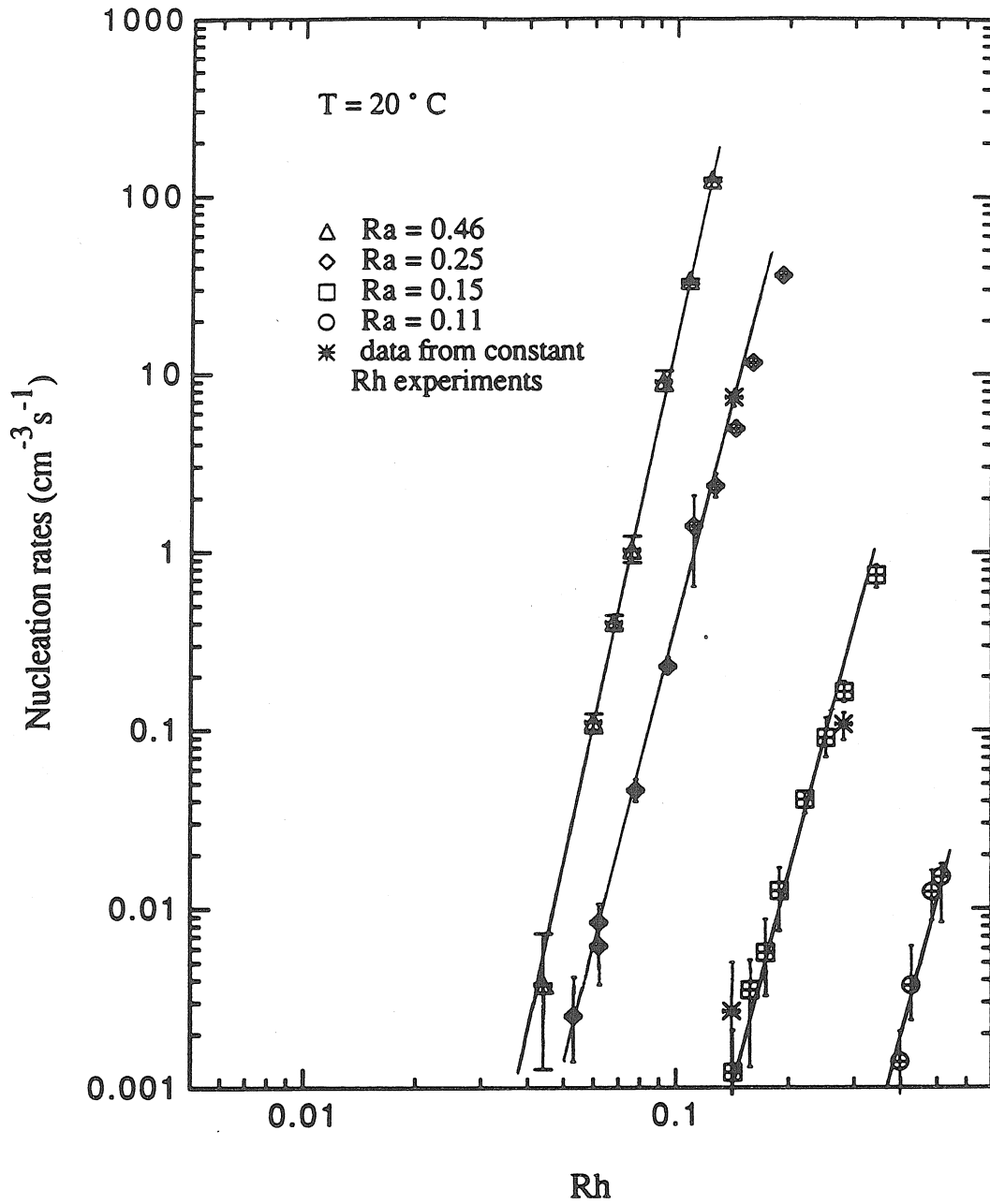
Figure 4 : Nucleation rates of H_2SO_4 - H_2O as a function of relative humidity at four different relative acidities and $T = 20 °C$. The lines connect the data points only.
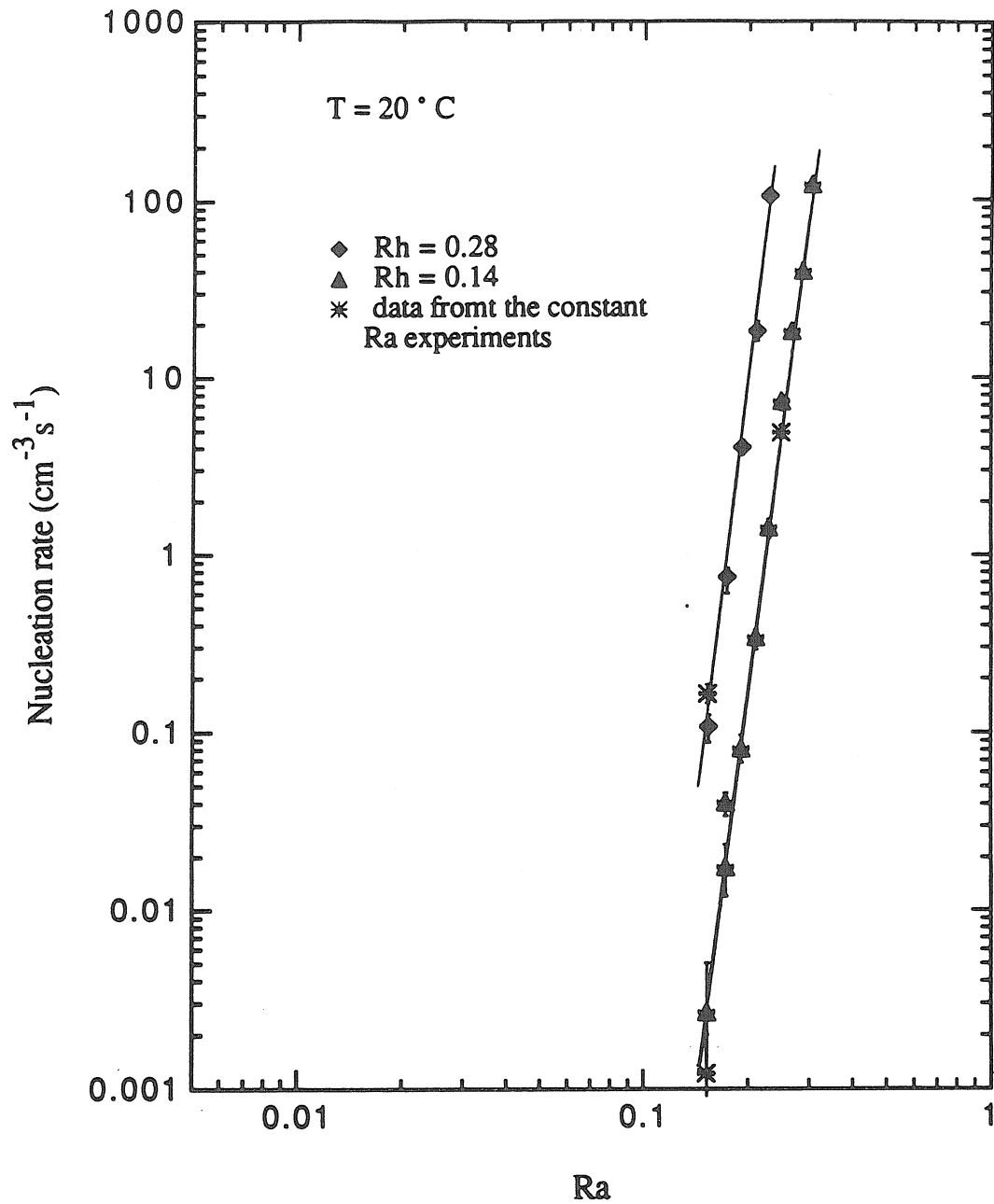
Figure 5 : Nucleation rates of H_2SO_4 - H_2O as a function of relative acidity at two different relative humidities and $T = 20$ ° C. The lines connect the data points only.
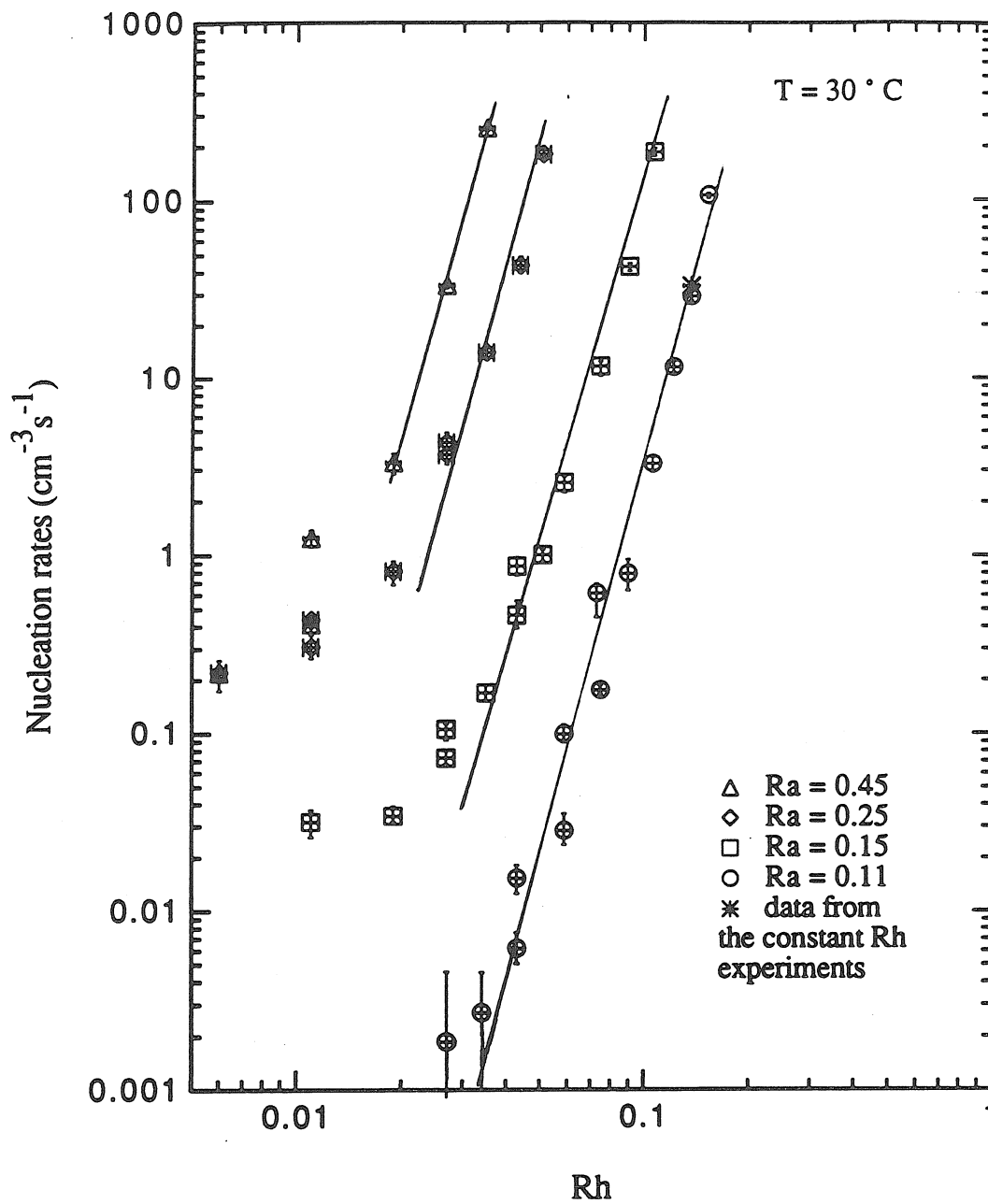
Figure 6 : Nucleation rates of H_2SO_4 - H_2O as a function of relative humidity at four different relative acidities and $T = 30$ ° C. The lines connect the data points only. Deviation from the straight line behavior at low Rh is due to flowmeter calibration inaccuracies.
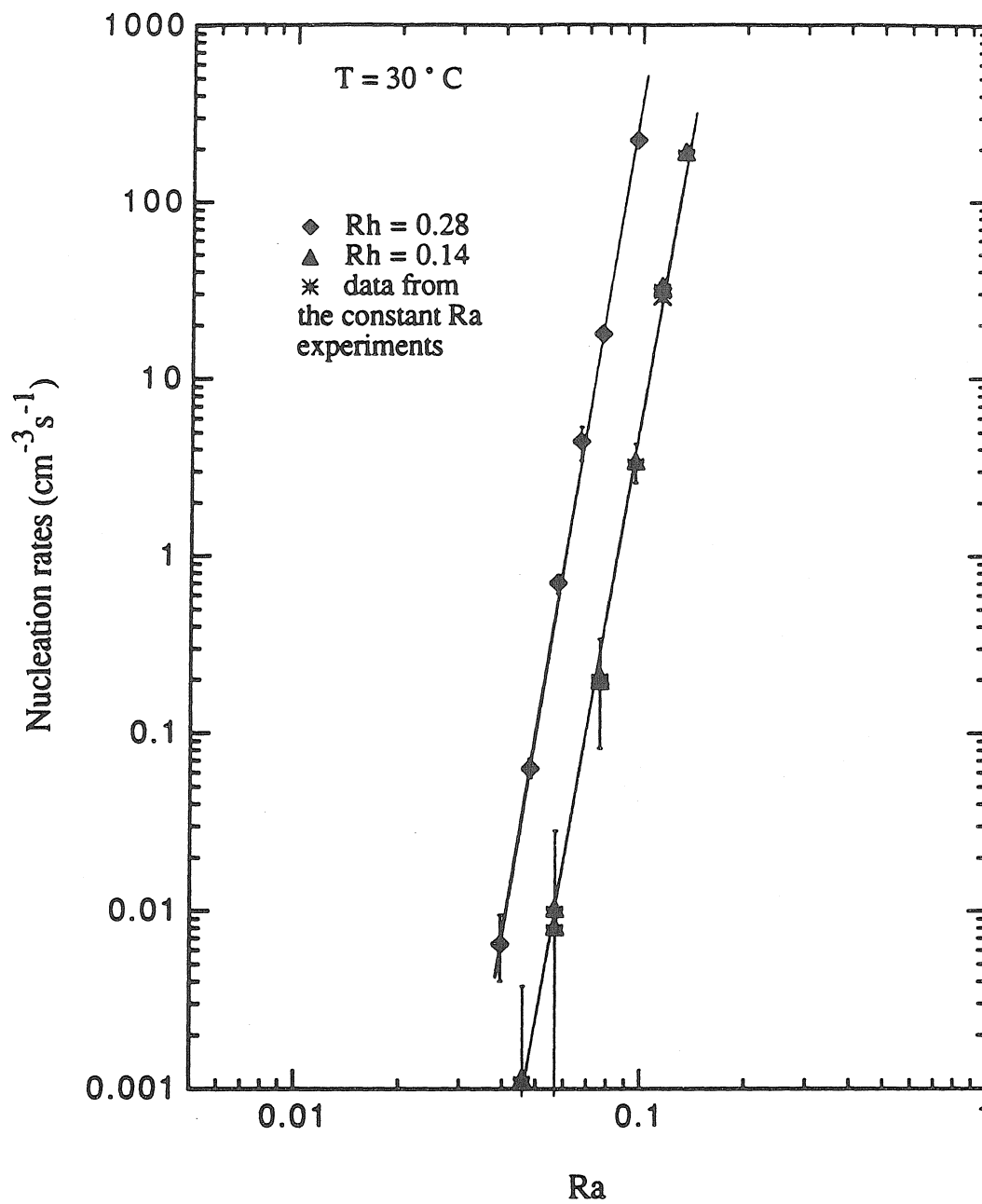
Figure 7 : Nucleation rates of H_2SO_4 - H_2O as a function of relative acidity at two different relative humidities and $T = 30$ ° C. The lines connect the data points only.
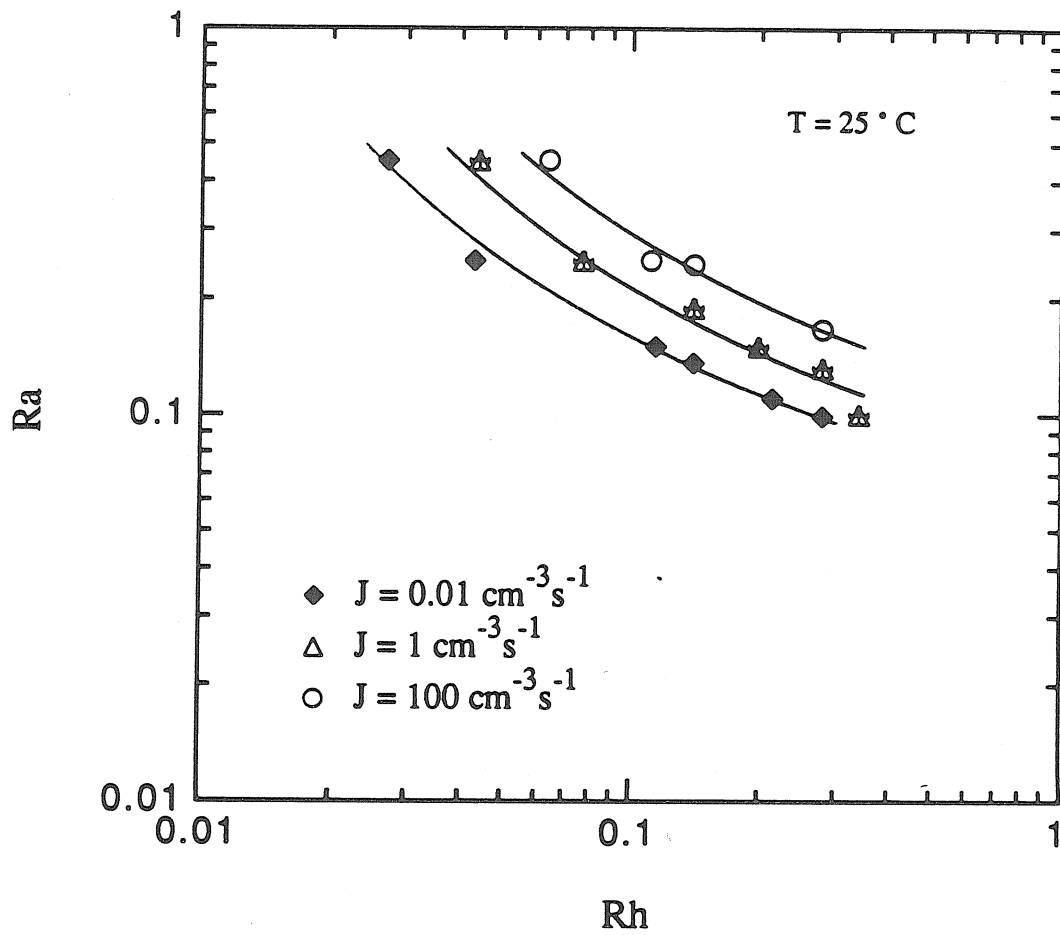
Figure 8 : The variation of nucleation rates with saturation levels for the H_2SO_4 - H_2O binary at J = 0.01, 1 and 100 cm^{-3}s^{-1} and T = 25° C.
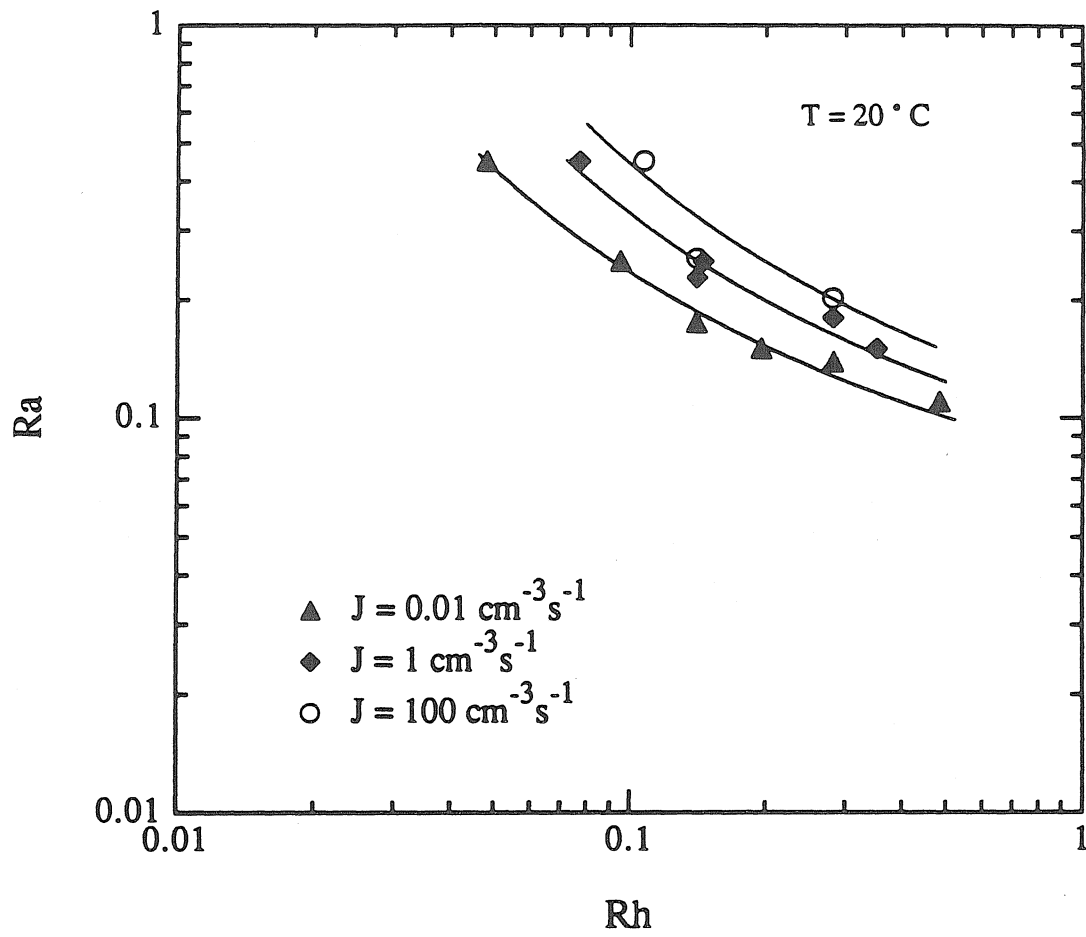
Figure 9 : The variation of nucleation rates with saturation levels for the H_2SO_4 - H_2O binary at J = 0.01, 1 and 100 cm^{-3}s^{-1} and T = 20° C.
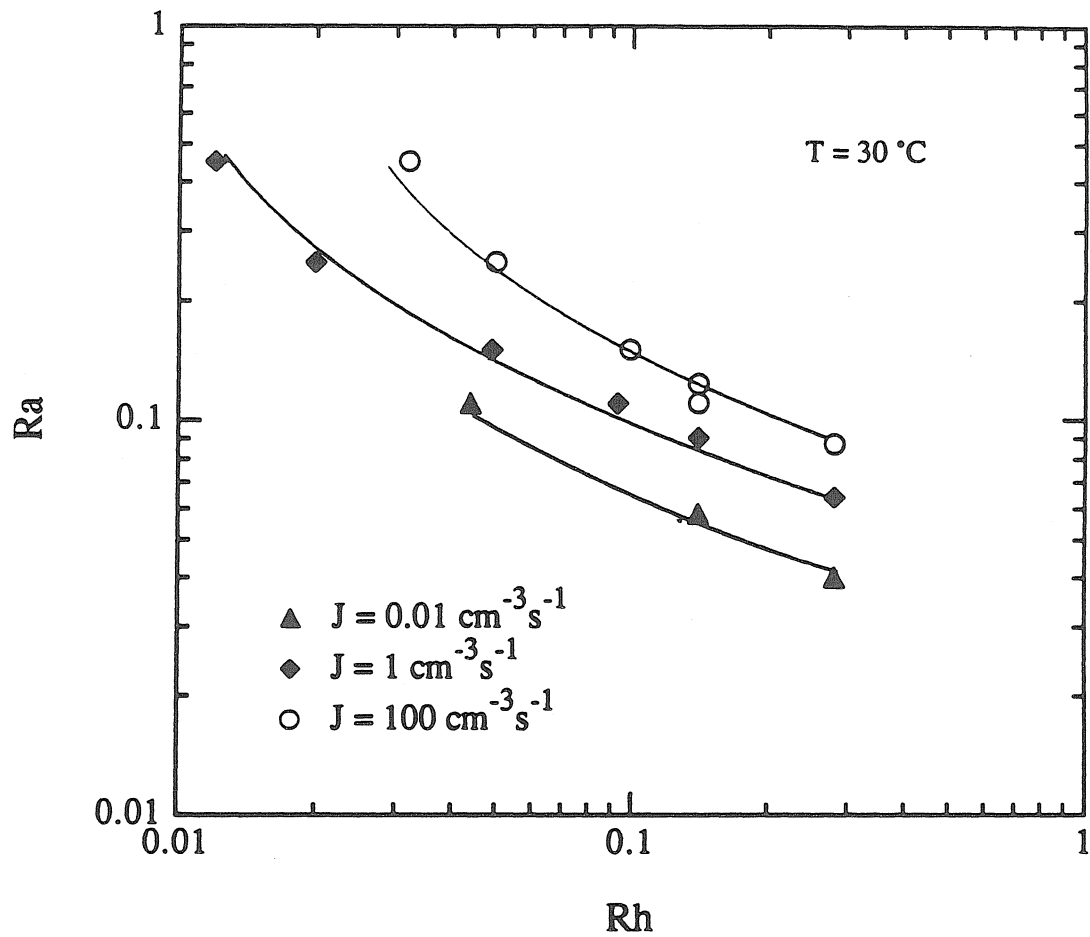
Figure 10 : The variation of nucleation rates with saturation levels for the H_2SO_4 - H_2O binary at J = 0.01, 1 and 100 $cm^{-3}s^{-1}$ and T = 30° C.
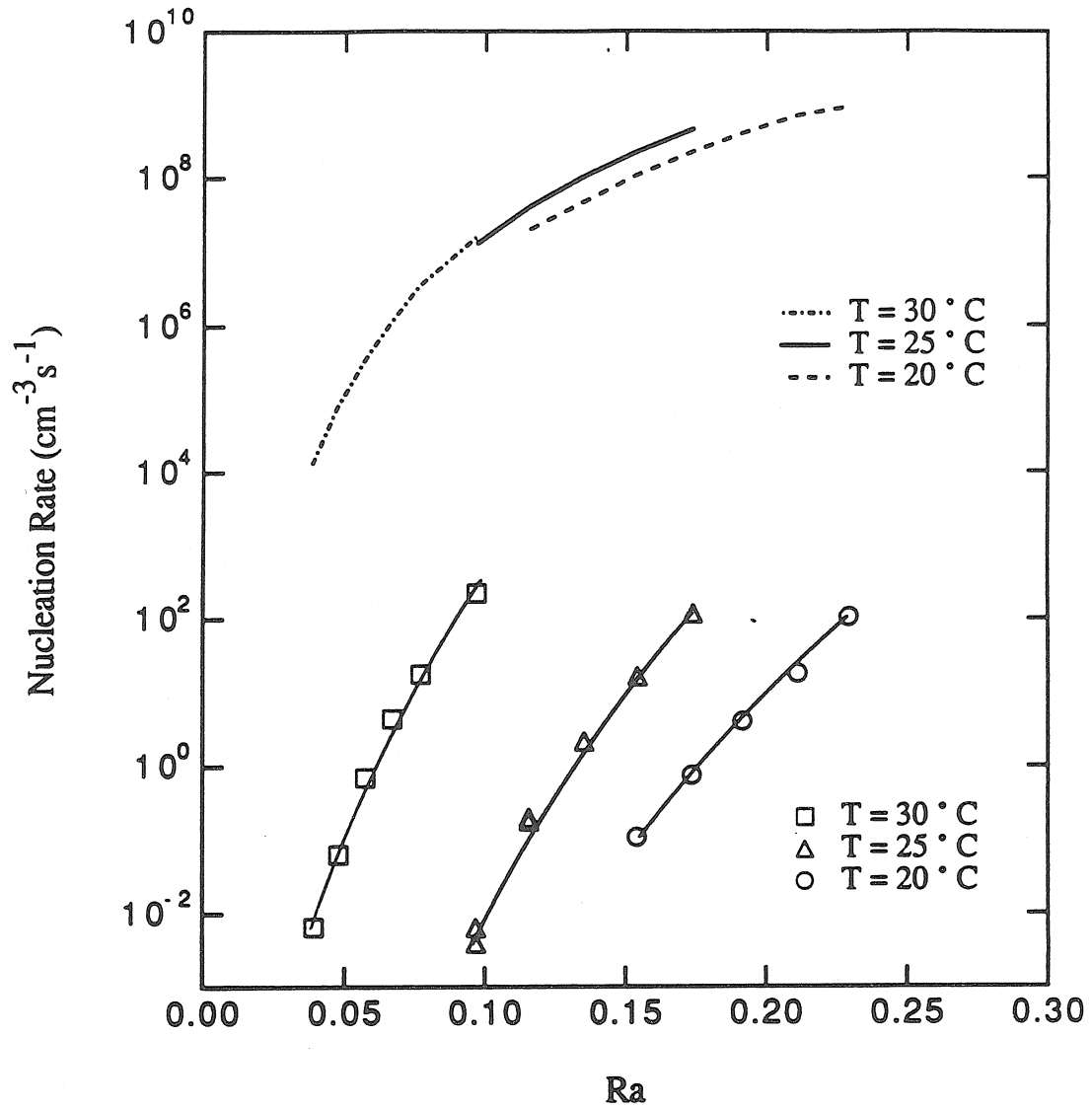
Figure 11 : The observed changes in nucleation rate with temperature are compared to those predicted by classical binary nucleation theory for Rh = 0.28 and T = 20, 25 and 30 ° C. The observed rates are far more sensitive to temperature than the calculated rates.
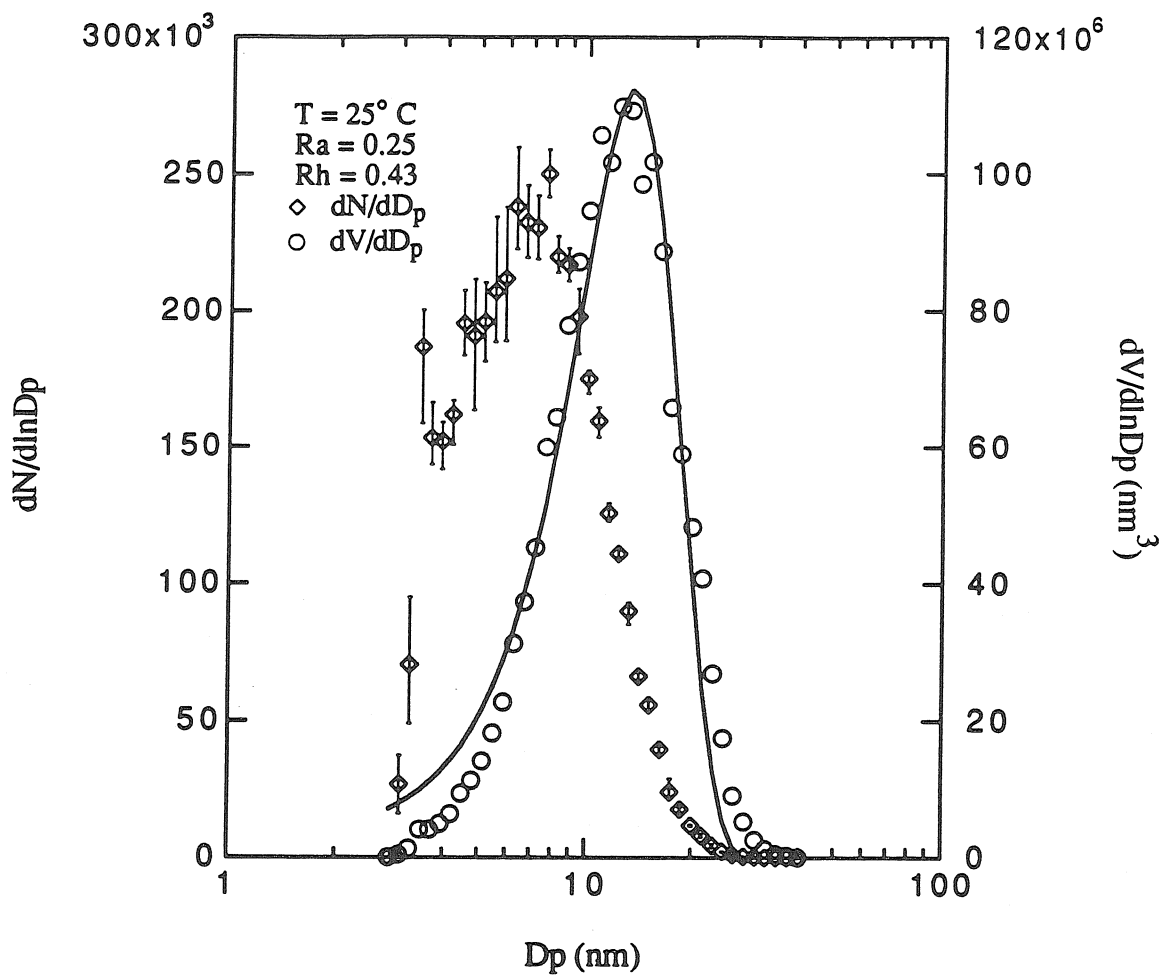
Figure 12 : A typical number and volume distribution for the H_2SO_4 - H_2O system. The solid line is a log normal fit to the volume data and illustrates that the produced aerosol is reasonably described in this manner.
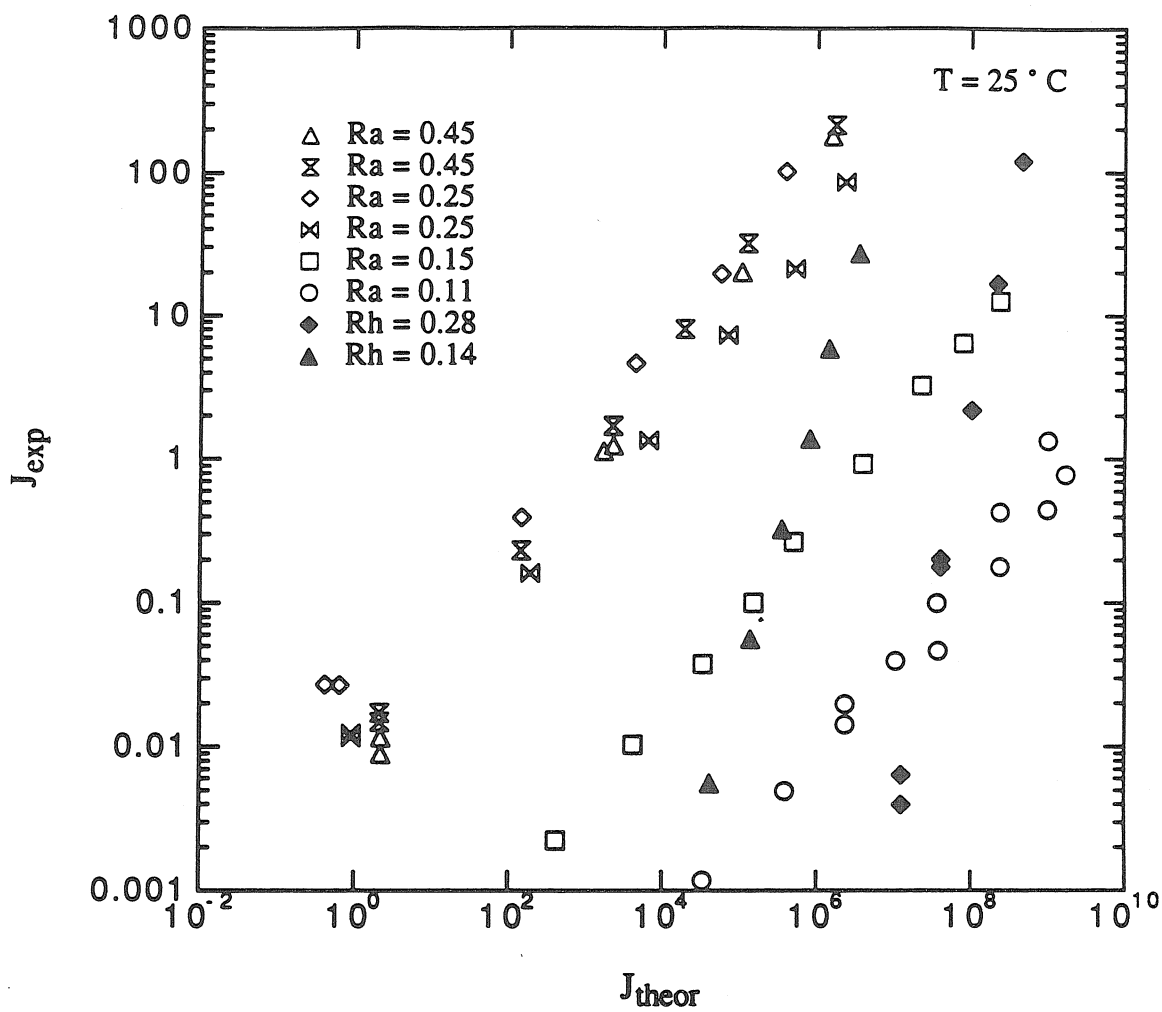
Figure 13 : A straight line correspondence between the experimental nucleation rates and the rates calculated by classical binary nucleation theory exists for each H_2SO_4 - H_2O data set at $T = 25 \, ^\circ C$.
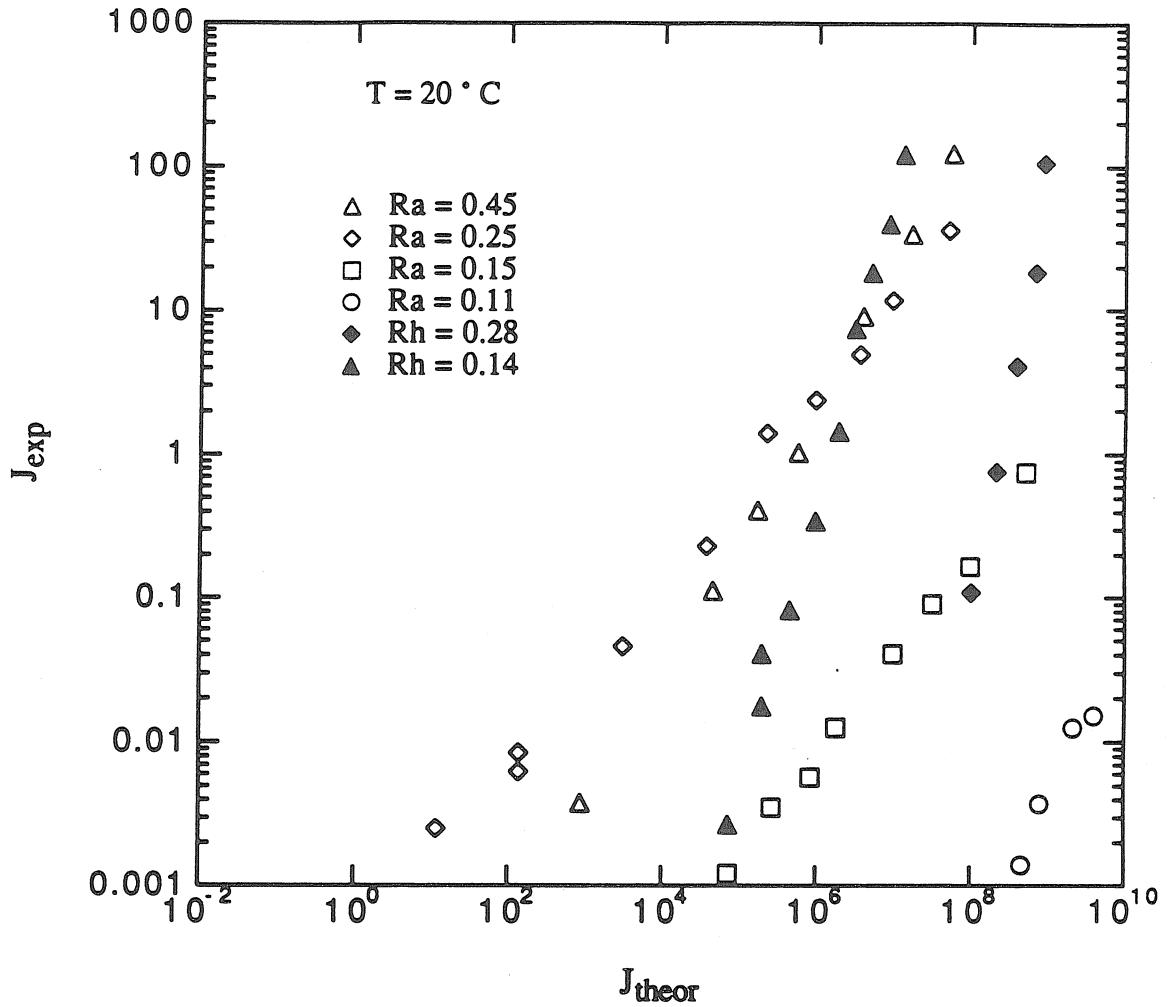
Figure 14 : A straight line correspondence between the experimental nucleation rates and the rates calculated by classical binary nucleation theory exists for each H_2SO_4 - H_2O data set at T =20 ˚ C.
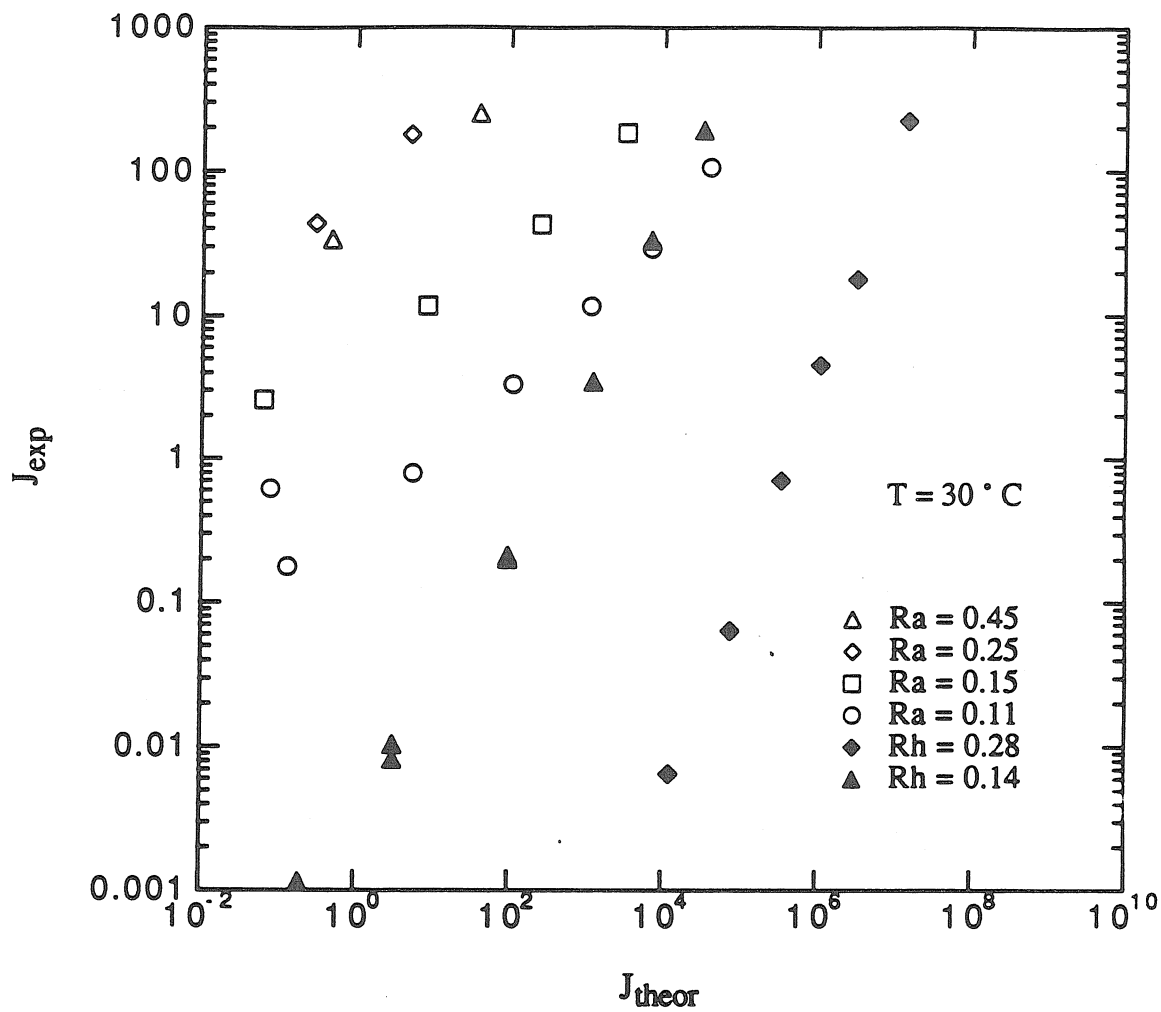
Figure 15 : A straight line correspondence between the experimental nucleation rates and the rates calculated by classical binary nucleation theory exists for each H_2SO_4 - H_2O data set at $T = 30\,^{\circ}$ C.
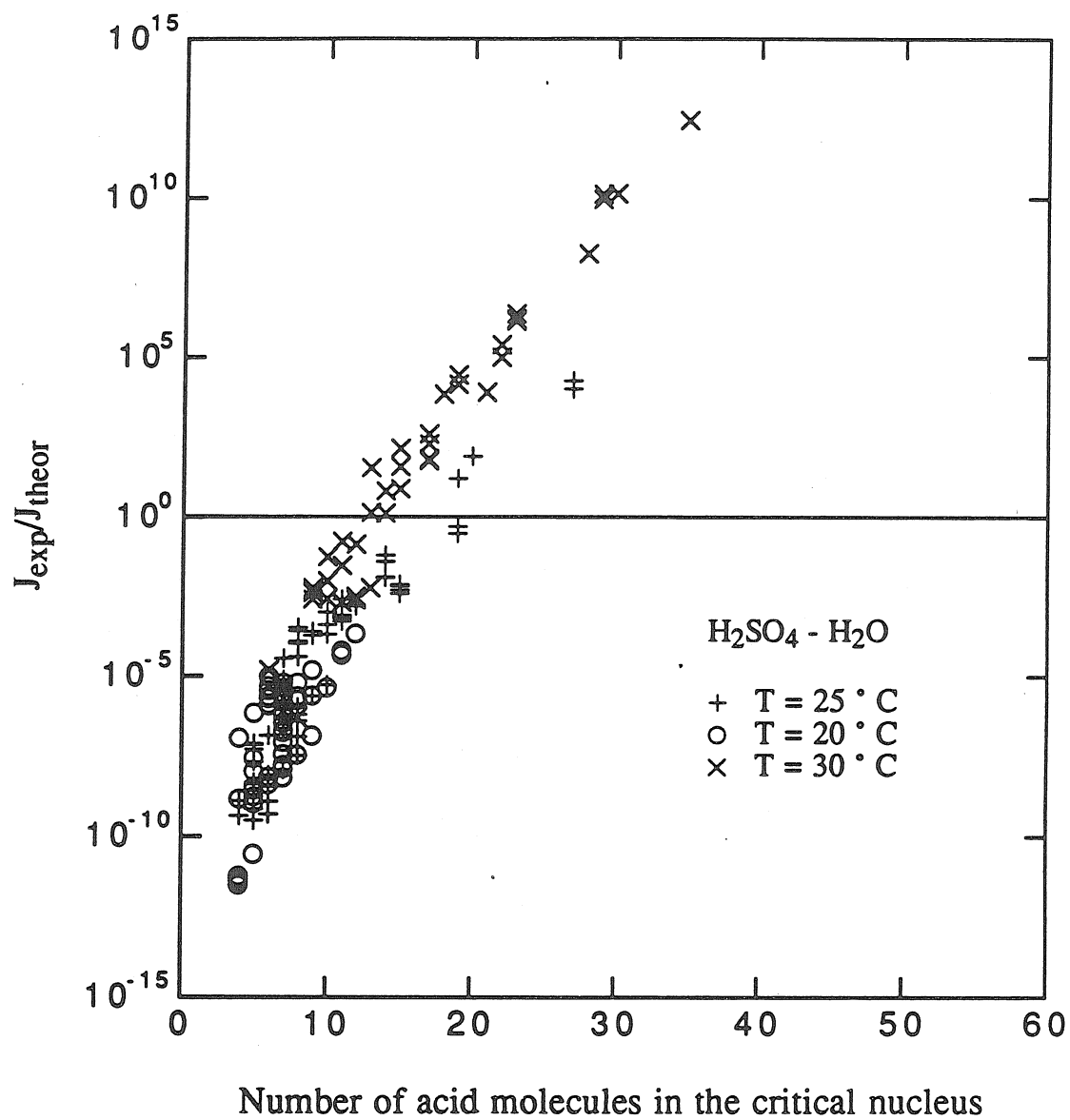
Figure 16 : Variation of the correction factor to classical binary nucleation theory with the number of acid molecules in the critical nucleus for the H_2SO_4 - H_2O system.
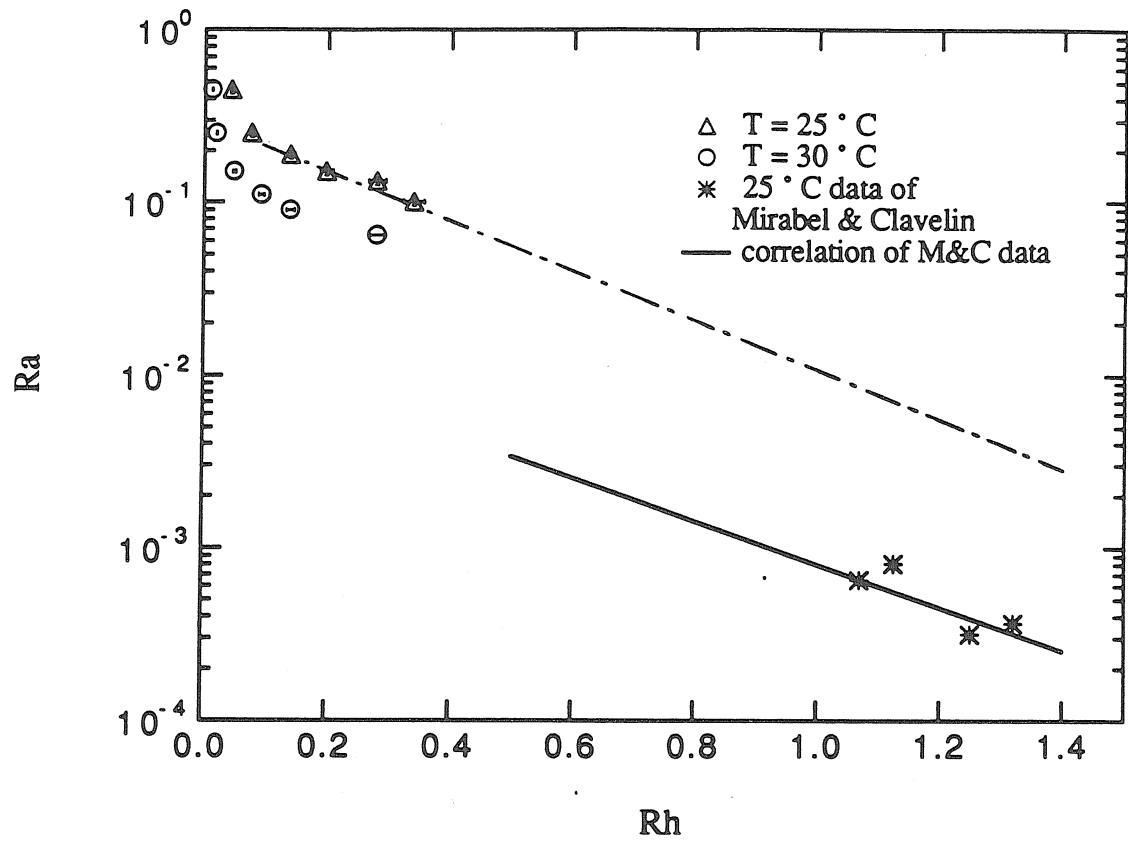
Figure 17 : Comparison of the results from the present work for $J = 1$ cm^{-3}s^{-1} to those of Mirabel and Clavelin[10].
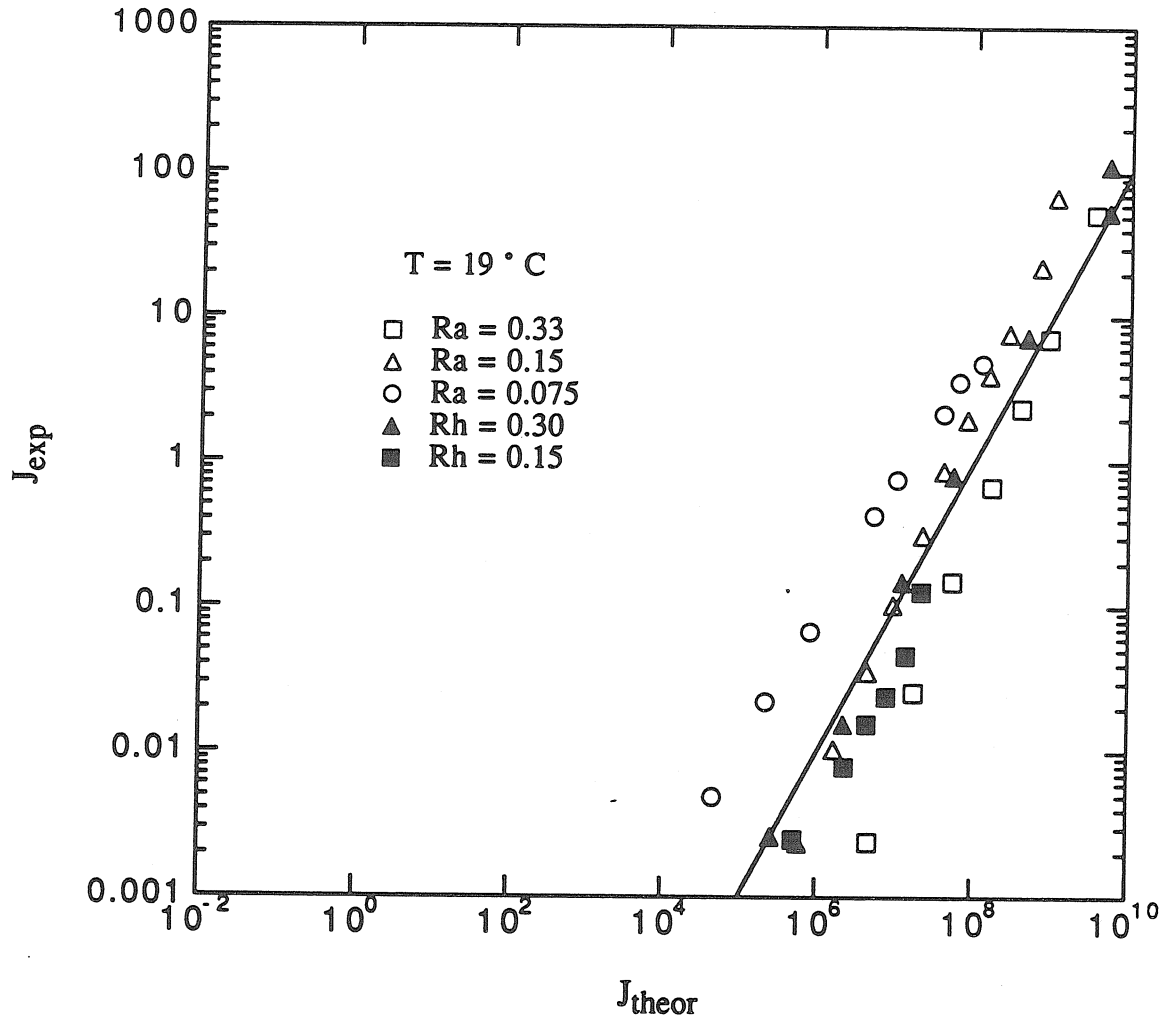
Figure 18 : The correspondence between the experimental nucleation rate and the theoretical rate for MSA- H_2O at 19 ° C. The data all lie close to the line $J_{exp}/J_{theor} = 10^{-8}$.
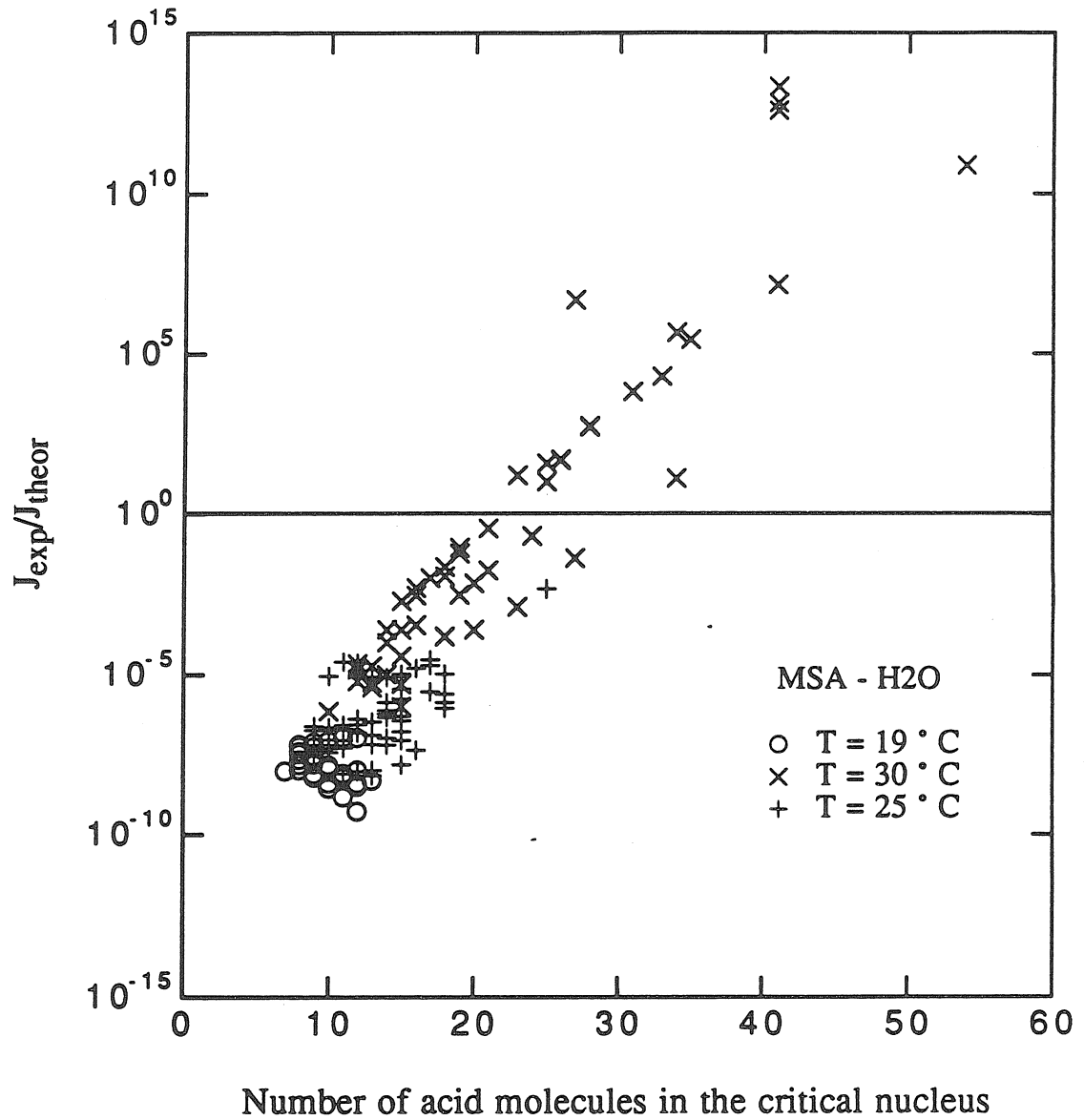
Figure 19 : Variation of the correction factor to classical binary nucleation theory with the number of acid molecules in the critical nucleus for the MSA - H_2O system.
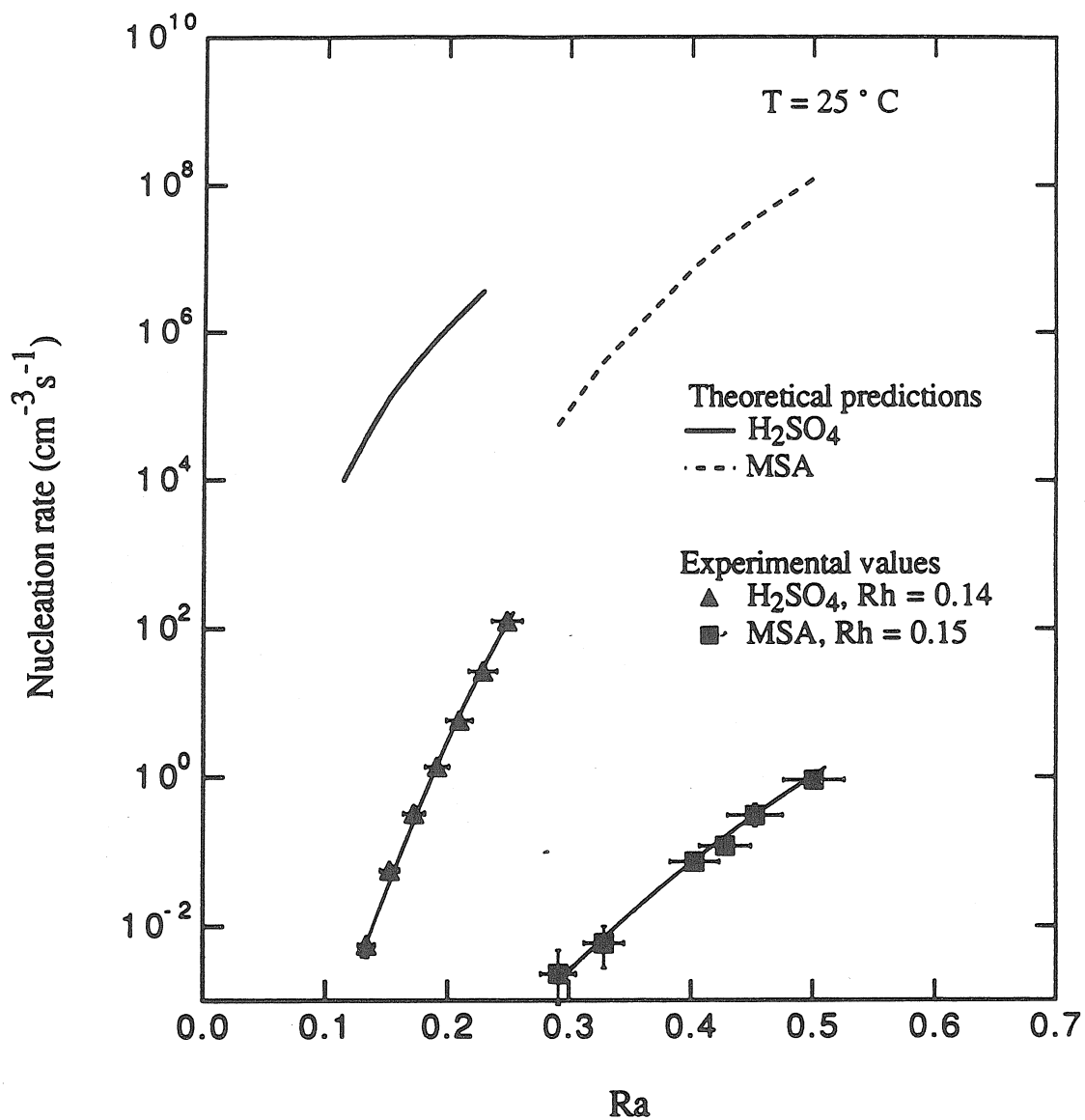
Figure 20 : Comparison of the observed and theoretical nucleation rates for the H_2SO_4 - H_2O system with those of the MSA- H_2O system at Rh = 0.15 and T = 25 ° C.

Appendix :

Supplementary Material to Chapter 3

The figures in this Appendix constitute the supplementary material deposited as AIP document no. PAPS JCPSA-94-6842-9 and listed as Reference 20 in the paper *Binary nucleation in acid-water systems. II. Sulfuric acid-water and a comparison with methanesulfonic acid-water.*, B. E. Wyslouzil, J. H. Seinfeld, R. C. Flagan and K. Okuyama, J. Chem. Phys. 94, 6842 (1991).

Binary Nucleation in Acid - Water Systems II. Sulfuric Acid - Water and a Comparison with Methanesulfonic Acid - Water

B.E. Wyslouzil, J.H. Seinfeld and R.C. Flagan,

Department of Chemical Engineering,

California Institute of Technology,

Pasadena California 91125

and

K. Okuyama

Department of Chemical Engineering,

Hiroshima University,

Saijo-cho, Higashi-Hiroshima,

Japan
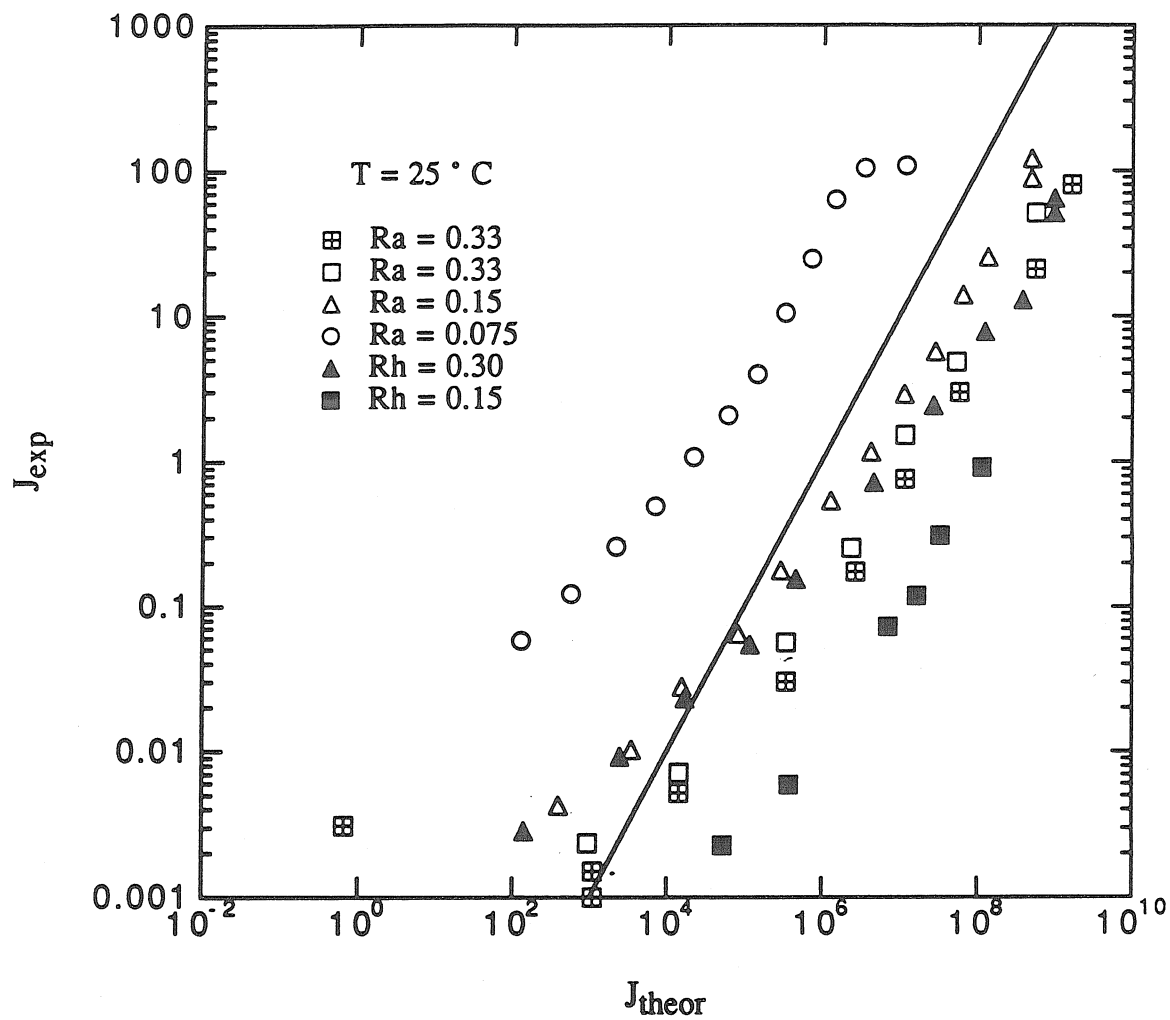
Figure 1 : The correspondence between experimental and theoretical nucleation rates for MSA- H_2O at 25 ° C. The data points lie near the line $J_{exp}/J_{theor} = 10^{-6}$.
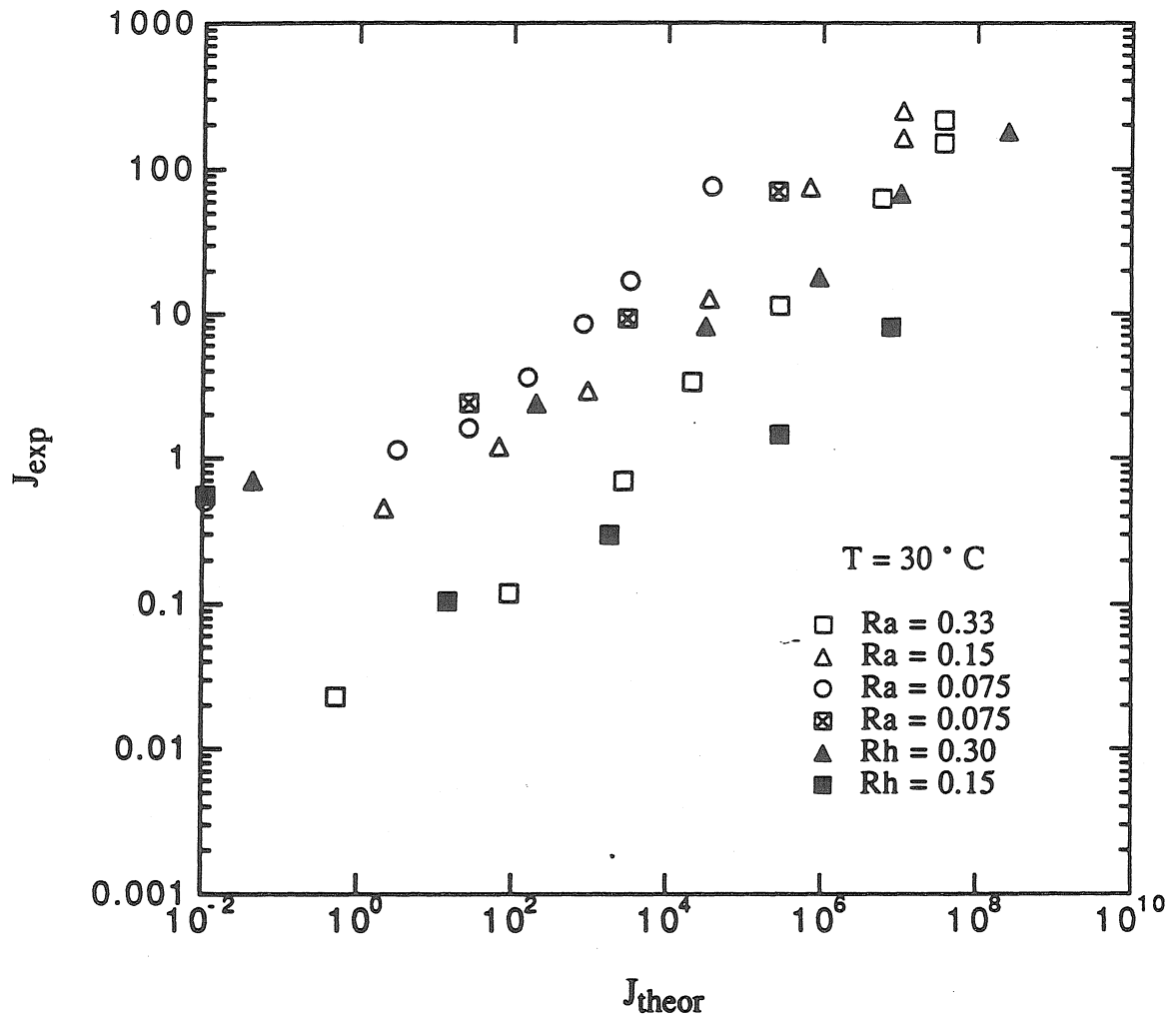
Figure 2 : The correspondence between the experimental and theoretical nucleation rates for MSA- H_2O at 30 ° C. The data are not clustered near any line J_{exp}/J_{theor} = constant.

CHAPTER 4

Nonisothermal Homogeneous Nucleation

B.E. Wyslouzil and J.H. Seinfeld,

Department of Chemical Engineering,

California Institute of Technology,

Pasadena, CA 91125

ABSTRACT

Classical homogeneous nucleation theory is extended to nonisothermal conditions through simultaneous cluster mass and energy balances. The transient nucleation of water vapor following a sudden increase in saturation ratio is studied by numerically solving the coupled mass and energy balance equations. The ultimate steady state nucleation rate, considering nonisothermal effects, is found to be lower than the corresponding isothermal rate, with the discrepancy increasing as the pressure of the background gas decreases. After the decay of the initial temperature transients, subcritical clusters in the vicinity of the critical cluster are found to have temperatures elevated with respect to that of the background gas.

I. INTRODUCTION

Classical homogeneous nucleation theory provides a simple physical model that describes the formation of a new phase from a supersaturated phase in the absence of foreign seed particles. In this model the new phase appears by the growth of clusters by monomer addition and, in the case of the gas to liquid phase transition, each cluster is assumed to behave as if it were an incompressible liquid drop with the physical properties of the bulk material. In addition all of the clusters and the monomer are assumed to be at the same temperature. Using these assumptions it is possible to solve for the steady state, isothermal rate of formation of stable particles of the new phase as a function of the bulk physical properties of the material, the temperature and the degree of supersaturation of the system.[1,2] By assuming isothermal conditions classical nucleation theory ignores any of the processes that could contribute to temperature differences between the old and the new phases, in particular any energy released or required by the phase transition. This, in turn, implies that the effect of nonisothermal conditions on the mass balances used to determine the rate of formation of the new phase is also ignored. The theory effectively separates the nucleation process from any potential effects that could influence the transfer of energy to and from the clusters, such as the amount and chemical nature of any background gas present.

That all of the clusters of a given size in a nucleating system will have the same temperature or energy is clearly an approximation. If the liquid drop model is adopted, the energy of the cluster is a well defined quantity equal to the product of the number of monomers in the cluster and the bulk energy per molecule of the new phase at the temperature of the cluster. In the gas to liquid phase transition for example, the latent heat that accompanies a condensing monomer brings more energy to the growing cluster than would be contributed by the addition of another liquid like monomer. Thus clusters that

have just been formed by the addition of a monomer will have on average more energy and be on average warmer than those which have just been formed by evaporation, with clusters at a whole range of temperatures in between depending on the number of collisions that have occurred with background gas molecules since a particular cluster last gained or lost a monomer. The warmer clusters will exhibit a higher evaporation rate than the cooler clusters and hence the average evaporation rate of clusters of a given size will depend on the relative populations of hot and cold clusters and their respective evaporation rates. The processes that lead to distributions in temperature within a given cluster size class exist whether the system on the whole is in a transient state or at steady state. However, at steady state a change in the relative rates of evaporation and condensation due to non-isothermal effects, over those predicted by the classical theory, will naturally alter the overall rate of formation of the new phase.

While there is the potential for a distribution of temperatures within a given cluster size, the average temperature of each cluster size will also be determined by a balance between the relative rates at which clusters are formed by condensation and evaporation versus the rate at which energy can be removed by collisions with non-accommodated monomers or inert background gas molecules. Again, this is true whether the total number of clusters of a given size is changing or not. Thus the clusters containing g monomers will be characterized by a temperature distribution function, $p_g(T_g)$, whose mean is $\overline{T_g}$. If the rate of energy transfer by collisions is very high because of a sufficient amount of background gas or a low mass accommodation of the nucleating species, it is reasonable to assume that T_g (dropping the overbar notation) will be very close to T_{amb}, the temperature of the ambient background gas. However the width of the distribution $p_g(T_g)$ will still be non-zero simply because there are distributions of energy in the colliding and condensing molecules themselves.

Both experimental and theoretical evidence exists demonstrating that the incorporation of a vapor monomer into a cluster has the potential to raise the temperature of the cluster significantly. During the nucleation and growth of iron clusters from the vapor phase in high temperature shock tube experiments, Kung and Bauer[3] used the ratio of emission intensities at two different wavelengths to estimate the nucleated particle temperatures and observed that the black body temperature of the clusters was significantly higher than that of the background gas. This positive temperature difference persisted as long as condensation dominated. In simulations of the addition of a monomer to water pentamer clusters, Plummer and Chen[4] found that at an initial temperature of 93 K the water monomer was incorporated and resulted in a hexamer with a final temperature of 174 or 184 K depending on the final configuration. As cluster size increases the effect that incorporating a monomer into a cluster has on the final temperature of the cluster should decrease because the total heat capacity of the cluster increases.

Aspects of non-isothermal homogeneous nucleation have been addressed previously by Kantrowitz,[5] Feder *et. al.,* [6] Salpeter,[7] Grinin and Kuni[8] and Ford and Clement.[9] Kantrowitz[5] used a simple energy balance to evaluate the average steady state temperature of the clusters assuming that all of the clusters are at the same elevated temperature, i.e. $T_g = T_{g+1} = T_{g+2} = ...$. From this he was able to predict an adjustment to the isothermal nucleation rate for small temperature differences. The assumption that all of the clusters are at the same temperature and that this is the temperature of the critical cluster does not consider the behavior of smaller clusters where the effect of monomer addition is more important. Moreover, since critical clusters result from the growth of smaller clusters, hindered growth of sub-critical clusters may affect the final concentration of stable clusters, slowing the nucleation process in a manner that is not apparent simply by focusing on clusters in the critical region. The analysis of non isothermal effects in nucleation by Feder *et. al.* [6] included the effect of fluctuations in the energy of the clusters on the steady state

nucleation rate. The authors found only a small change in the nucleation rate with respect to the isothermal theory, largely because the critical cluster is both in thermal and chemical equilibrium with the surrounding vapor. Consequently, when calculating the nucleation rate based on an analysis in the region of the critical nucleus, the concentration of critical clusters is unperturbed from that predicted by isothermal theory and the reduction in nucleation rate results solely from the nonisothermal diffusion coefficient. Again, the analysis is limited to the behavior of clusters in the critical region.

In the present work we wish to develop a theory of nonisothermal homogeneous nucleation. An energy balance applied to each cluster size, analogous to the mass balance, provides the most straightforward method of incorporating the strong coupling that exists between the mass and energy flows due to the evaporation rate coefficient. Because Feder et al.[6] showed that the effects of energy fluctuations within a cluster size class on the nucleation rate are rather small, these are ignored and only the average energy of all clusters of a given size are followed.

The objective of the current work is to demonstrate how the relative rates of mass and energy transfer combine to determine both the transient and steady state cluster concentrations, cluster temperature distributions, and mass and energy fluxes for both sub-critical and stable clusters. By simultaneously solving the differential equations governing the number and enthalpy evolution of the clusters as the supersaturation is suddenly increased from 1.0 to a constant higher value, both the transient and steady state behavior of the average cluster concentration and energy may be followed and compared with the isothermal results. The role of the mass accommodation coefficient as a factor in the energy transfer process, especially as the concentration of background gas decreases, is also investigated because it provides an alternate mechanism to change the relative rates of energy and mass transfer. The nature of energy transfer to the subcritical clusters is

discussed in terms of a model for energy transfer between excited state and background gas molecules from unimolecular reaction theory which in turn demonstrates how the chemical nature of both the nucleating species and the background gas can play a role in the homogeneous nucleation process. In order to compare the results of these nucleation rate calculations to previously published isothermal computations,[10,11] the vapor to liquid phase transition of water is studied.

II. CLUSTER MASS AND ENERGY BALANCES

A model for the formation of a new phase from a supersaturated parent phase should address the mechanism of incorporation of individual molecules into the emerging clusters, the redistribution of energy that is released or is required by the given phase transition. For the special case of the vapor to liquid phase transition the change in energy upon condensation, $\Delta h_{vap} = h_{vapor} - h_{liquid}$, is always positive, but in other processes, such as crystallization, $\Delta h_{phase1 \rightarrow phase2}$ can have either sign. Thus the incorporation or loss of a monomer from a cluster is always accompanied by a change in energy of the order of $q = \Delta h_{vap} - w$, where w is the work required to increase the area of the interface. Collisions with inert, background gas molecules or monomers that are not accommodated provide an alternative means of adding or removing energy from the cluster and will on average reduce the temperature differences between the new phase and the background gas resulting from the addition or loss of condensing molecules. Because the rate at which monomers condense or evaporate from the cluster may be a strong function of the temperature of a cluster, it is natural to try and understand how the simultaneous transfer of mass and energy affects the transient and final steady state rates with which this phase transition occurs.

Implicit in the formultion of the problem presented here is the assumption that all of the clusters of a given size are characterized by a mean temperature, T_g. This assumption will capture the essential physics of the strong coupling between the mass and energy fluxes that results from the temperature dependent evaporation rate coefficient. We also assume that the temperature of the background gas and the condensing monomer are characterized by a fixed ambient temperature, T_{amb}.

A. Cluster mass balance

To develop the cluster mass balance we assume that clusters of size g have concentration f_g and grow by the addition of monomer at a rate $\beta_g f_g$ or shrink by the loss of a monomer at a rate $\alpha_g f_g$, where β_g and α_g are the condensation and evaporation rate coefficients, respectively. The overall flux of clusters from $g-1$ to g is given by

$$I_g = \beta_{g-1} f_{g-1} - \alpha_g f_g. \tag{1}$$

As in classical nucleation theory only growth by loss or addition of monomers is considered. The evolution of the g-mer cluster concentration, f_g, is therefore given by

$$\frac{df_g}{dt} = I_{g-1} - I_g \tag{2}$$

The kinetic gas expression is used for the impingement rate of monomer onto the cluster containing g molecules, β_g, and is given by

$$\beta_g = A_g \frac{p}{(2\pi m k T_{amb})^{1/2}} \tag{3}$$

where A_g is the surface area of the g-mer, p is the partial pressure of the nucleating vapor, m is the molecular mass of the vapor, k is the Boltzmann constant and T_{amb} is the absolute ambient temperature. Assuming, as in classical nucleation theory, that each cluster behaves as if it were an incompressible liquid drop with the same physical properties as the bulk material, $A_g = 4\pi (3v_m/4\pi)^{2/3} g^{2/3}$, where v_m is the molecular volume.

The evaporation coefficient from clusters containing $g+1$ molecules, α_{g+1}, is a function only of the properties of the cluster itself and is calculated from the detailed balance condition of the equilibrium cluster distribution at the temperature T_g and saturation ratio S,

$$\alpha_{g+1} = \beta_g \frac{N_g^e}{N_{g+1}^e}$$

$$= \beta_g \exp\left(-\ln S + \frac{\sigma A_1}{kT_g}((g+1)^{2/3} - g^{2/3})\right)$$

$$= A_g \frac{p_{ve}(T_g)}{(2\pi mkT_{amb})^{1/2}} \exp\left(\frac{\sigma A_1}{kT_g}((g+1)^{2/3} - g^{2/3})\right) \tag{4}$$

where N_g^e, is the equilibrium cluster concentration of g-mers, σ is the surface tension, and A_1 is the surface area per molecule ($= 4\pi (3v_m/4\pi)^{2/3}$), and $p_{ve}(T_g)$ is the equilibrium vapor pressure over a flat surface at T_g.

Equations (1) - (4) are those that Abraham[10] and Courtney[11] first solved numerically in order to gain a better understanding of the transient kinetics and timelags involved as an isothermal system relaxes to the steady state.

B. Cluster energy balance

To estimate the transient flow of energy through the system of clusters as well as at the final steady state an energy balance including the effects of condensation, evaporation and heat transfer by impinging but non-condensing molecules has been derived by considering the relevant energy fluxes. The rate of change of the total enthalpy of the g - mers, $h_g f_g$, is governed by the following: 1) the rate at which energy enters the class of g-mers by the formation of new g-mers by condensation of a monomer onto g -1- mers or by of a monomer evaporation from g +1- mers, 2) the rate at which energy leaves the class of g-mers by the growth or evaporation of g-mers, and 3) the rate at which energy is removed from the g-mers by collisions with the background gas or non-condensing monomers. In addition, when the system is in equilibrium at $S = 1$, the clusters should all be characterized by the same temperature $T_{g-1} = T_g = T_{g+1} = T_{amb}$.

With the assumption of the liquid drop model for the cluster, the enthalpy of a single g - mer at its average temperature T_g is calculated as

$$h_g = h_g^o + g \, c_p \, (T_g - T_{ref}) \tag{5}$$

which simplifies when $h_g^o = 0$ at $T = T_{ref}$ and where c_p is the liquid heat capacity per molecule. This equation also defines the average temperature of a g -mer from the values of total enthalpy and cluster concentration as

$$T_g = T_{ref} + \frac{h_g f_g}{g \, c_p f_g} \tag{6}$$

The equilibrium constraint at $S = 1$ and $T = T_e$ determines the amount of energy removed from the class of g-mers each time a g-mer evaporates. If q_g is the energy released per monomer incorporated into a growing cluster of size g, the following balance must hold at equilibrium to maintain all of the clusters at the average temperature of the system T_e,

$$\beta_{g-1} f_{g-1} \left(h_{g-1}(T_e) + q_{g-1} \right) = \alpha_g f_g \left(h_g (T_e) + \Delta \right) \tag{7}$$

where $\Delta = q_{g-1} - h_1(T_e)$. Equation (7) also implies that every time a cluster of size g and temperature T_g evaporates the amount of energy lost to the class of g-mers is

$$\alpha_g f_g \left(h_g (T_g) + \Delta \right) = \alpha_g f_g \left(h_{g-1} (T_g) + q_{g-1} \right) \tag{8}$$

Thus the overall transient energy balance on the class of g-mers becomes

$$
\begin{aligned}
\frac{d(h_g f_g)}{dt} = \ & \beta_{g-1} f_{g-1} \left(h_{g-1} (T_{g-1}) + q_{g-1} \right) - \alpha_g f_g \left(h_{g-1} (T_g) + q_{g-1} \right) \\
& - \beta_g h_g f_g + \alpha_{g+1} f_{g+1} \left(h_g (T_{g+1}) \right) \\
& - Q_g
\end{aligned}
\tag{9}
$$

Clearly this energy balance satisfies the condition that at $S = 1$, $T_{g-1} = T_g = T_{g+1} = T_{amb}$.

A key quantity in the energy balance is q_g, the energy released per monomer incorporated into the growing cluster. In the liquid drop model this quantity is equal to the heat of condensation per molecule, $h_{vap}^{\infty} = \Delta H_{vap}^{\infty} / N_A$, where ΔH_{vap}^{∞} is the heat of vaporization of the bulk liquid and N_A is Avogadro's Number, less the amount of work

required to increase the surface of the cluster. The work term is given by the product of the surface tension and the incremental increase in area, $\sigma\dfrac{dA_g}{dg}$,

$$q_g = h_{vap}^\infty - \sigma\frac{dA_g}{dg}$$

$$= h_{vap}^\infty \left(1 - \frac{\sigma A_1}{h_{vap}^\infty} g^{-0.33}\right) \tag{10}$$

The heat of vaporization per molecule is quite similar for a range of materials commonly studied in nucleation experiments and at 298 K, h_{vap}^∞ for water is $\approx 7.3\times10^{-13}$ ergs/molecule ($\approx 20\,kT$), while the normal alcohols range from 6.2×10^{-13} ergs/molecule for methanol to 10.2×10^{-13} ergs/molecule for hexanol.[12] A typical value for $\dfrac{\sigma A_1}{h_{vap}^\infty}$ for water is approximately 0.5 for $T = 273$ to 323 K, decreasing only slightly as T increases, and thus for small g, q_g is reduced significantly over the value of h_{vap}^∞.

An alternate expression for the energy added per impinging molecule, q_g, is given by the empirical correlation developed by Freund and Bauer[13] who considered the normalized condensation energy per molecule $(\Delta E_g/g)/\Delta E^\infty$, where ΔE_g is the energy of the reaction $X_g \rightarrow gX$. Using five sets of theoretical data and one set of experimental data a least squares fitting of the data to the functional form $\Delta E_g/g = \Delta E^\infty(1 - ag^{-b})$ gave

$$\frac{\Delta E_g}{g} = \Delta E^\infty(1 - g^{-0.25}) \tag{11}$$

By assuming ΔE_g is approximately equal to ΔH_g (for water at 298 K $\Delta E^\infty \cong 0.95 \times \Delta H^\infty$) this gives

$$q_g = h_{vap}^\infty (1 - 0.75 \, g^{-0.25})$$ (12)

The similarity of the two equations both in form and in the magnitude of the coefficients suggests that the choice of which equation is used in the energy balances will not affect the general results although for a given set of conditions the final nucleation rates will differ. We will use the correlation proposed by Freund and Bauer because it is based on a large number of calculations for small clusters for which the liquid drop model implicit in Eqn. (10) is more difficult to justify.

A change in the temperature of a cluster from T_{amb} will necessarily alter the rate at which monomers leave the cluster. Applying Eqn. (4) at two different temperatures gives the following correction to the isothermal evaporation rate in terms of the cluster temperature T_g and the ambient temperature T_{amb} for small temperature differences or when σ is not a strong function of T,

$$\alpha_{g+1}(T_g) = \alpha_{g+1}(T_{amb}) \exp[(1 - \frac{T_{amb}}{T_g}) (\frac{h}{kT} - \frac{\sigma A_1}{kT} ((g+1)^{2/3} - g^{2/3})) + \frac{1}{2} \ln \frac{T_{amb}}{T_g}]$$ (13)

If σ is a strong function of temperature, Eqn. (13) should be modified to read

$$\alpha_{g+1}(T_g) = \alpha_{g+1}(T_{amb}) \exp[(1 - \frac{T_{amb}}{T_g}) \frac{h}{kT} +$$
$$(\frac{\sigma(T_{amb})}{T_{amb}} - \frac{\sigma(T_g)}{T_g}) \frac{A_1}{k} ((g+1)^{2/3} - g^{2/3}) + \frac{1}{2} \ln \frac{T_{amb}}{T_g}]$$ (14)

In the simulations that follow, Eqn. (14) was used to correct the evaporation rate for the difference in temperature between the clusters and the background gas.

C. Rate of energy transfer by non-accommodating molecules, Q_g

The energy removed from a cluster by molecules that impinge but are not incorporated into the growing cluster is given by Q_g. For clusters large enough to be treated as droplets, but still small compared to the mean free path of the gas, this term should reduce to the expression proposed by Kantrowitz from kinetic gas theory,

$$Q_g = A_g \, f_g \, (\beta_{gas} \, c'_{vgas} \, \alpha_{hgas} + (1 - \alpha_{mvap}) \, \beta_{vap} \, c'_{vvap} \, \alpha_{hvap}) \, (T_g - T_{amb}) \qquad (15)$$

where β_{gas}, c'_{vgas} and α_{hgas} are the impingement rate, heat capacity per molecule, and thermal accommodation coefficient of the noncondensing gas molecules, β_{vap}, c'_{vvap} and α_{hvap} are the impingement rate, heat capacity per molecule, and thermal accommodation coefficient of the vapor molecules, and α_{mvap} is the mass accommodation coefficient of the condensing vapor. Here $c'_v = c_v + kT/2$, where the additional energy $kT/2$ appears because the molecules found impinging onto the surface represent a subset of the gas molecules that have velocities directed only toward the cluster and thus averaging only over this subset gives a higher energy than averaging over a random set of molecules in the vapor phase[5,6].

Despite its convenient form, there are some difficulties in the straightforward application of Eqn. (15) to describe the energy transfer over the entire range of cluster sizes g. This equation assumes that the energy transfer between a gas molecule and a liquid-like cluster is independent of the relative sizes of the two species and is only of the order of $c_v \Delta T \approx 10^{-16} x \Delta T$ erg molecule^{-1} per collision. This assumption may not be appropriate for small g, where the molecular clusters and the impinging molecules are not terribly different in size. In this case it is reasonable to expect energy transfer to be similar to that which is observed experimentally[14,15] or predicted theoretically[16,17] during unimolecular

reactions. Here a single collision between a highly excited molecule and a background gas molecule can transfer an average energy on the order of $\langle \Delta E \rangle = 0.1 - 30$ kcal mol^{-1} ($= 7$ x10^{-15} - 2x10^{-12} erg/molecule) per collision.[18] The amount of energy transferred per collision depends mainly on the relative sizes (number of atoms in the molecule) of the excited molecule and background gas and on the absolute energy of the excited molecule, although the exact nature of the latter relationship is still rather controversial.[17]

These estimates of energy transfer demonstrate that if small clusters of the nucleating vapor are considered analogous to polyatomic molecules, then energy transfer by collisions with the background gas may be much higher than predicted by Eqn. (15) in its current form and furthermore the amount transferred should be a function of g. For clusters composed of strongly interacting fragments, such as ionic species, the assumption of a polyatomic molecule is a good one[5] and for water, or other highly hydrogen bonded molecular clusters, this assumption is probably still quite reasonable. Using the value for h_{vap}^{∞} for water from Table 1, each condensing water molecule brings in about 7x10^{-13} erg; thus, if each collision with a background gas molecule is capable of removing up to 10^{-13} to 10^{-12} erg,[18] temperature differences between the background gas and the smallest clusters should stay small at steady state even if the amount of background gas is reduced substantially below 1 atmosphere. To determine the true energy transfer between energetic water clusters and a cool background gas, calculations analogous to those performed by Bruehl and Schatz[17] for energy transfer from an excited CS_2 molecule to cool He gas molecules are required but such calculations are not presently available in the literature.

To predict the rate of energy transfer for small clusters, we will use some general results derived by Troe[16] for the probability, $P(E',E)$, of an excited molecule with initial energy E' having a final energy E after collision with a background gas molecule. These calculations assume that the excited molecule and the background gas form a collision

complex in which total momentum and angular momentum are conserved during the collision process and that the species do not have strong chemical interactions. The values of $P(E',E)$ depend on the number of atoms in the excited molecule, N_a, and the number of atoms in the background gas molecule, N_m, in the expected manner, that is, as N_a increases for fixed N_m the average energy transferred per collision with a background molecule decreases. Similarly for fixed N_a, the energy transfer per collision with a background molecule increases as N_m increases. Table 2 gives the values of the average energy transferred per collision as a function of N_a and N_m assuming that $<\Delta E/kT>$ is close to the peak in each of the probability transition curves. Figure 1 illustrates the variation of $<\Delta E/kT>$ as a function of the number of triatomic molecules in the cluster $g = N_a/3$ that has been extrapolated from the calculated data of Troe.[16] In addition, the dashed line represents the energy transfer predicted by Eqn. (15) per collision of a cluster with air when $c'_v = 4 \times 10^{-16}$ and assuming $\Delta T = 1K$.

To maintain the convenient functional form of Eqn. (15), that is $Q_g \propto (T_g - T_{amb})$, the functional form of $<\Delta E/kT>$ is used to define an effective energy transfer coefficient, $\phi(g)$ erg molecule^{-1} K^{-1}, for the impinging molecules striking small clusters,

$$\phi(g) \propto <\Delta E>$$
$$= C\, g^{-1.3} \propto \qquad (16)$$

where C is an undetermined constant referred to as the energy transfer parameter. The lack of information regarding energy transfer to small clusters makes it impossible to independently assign a value to C at this time. The expression for Q_g for small clusters then becomes

$$Q_g = A_g f_g \left(\beta_{gas} \, \phi_{gas}(g) + (1-\alpha_{mvap}) \, \beta_{vap} \, \phi_{vap}(g) \right) (T_g - T_{amb}) \tag{17}$$

where ϕ_{gas} and ϕ_{vap} are the energy transfer coefficients of the inert gas and non-accommodated vapor respectively. Inserting the appropriate expressions for ϕ_{gas} and ϕ_{vap} gives the more explicit functional dependence of Q_g on g for the small clusters,

$$Q_g = A_g f_g \left(\beta_{gas} \, C_{gas} \, g^{-1.3} + (1-\alpha_{mvap}) \, \beta_{vap} \, C_{vap} \, g^{-1.3} \right) (T_g - T_{amb}) \tag{18}$$

Although from Fig. 1 it is clear that for sufficiently large g Eqn. (18) should become independent of g to match the values of Eqn. (15) , these values of g are larger than the largest cluster size that will be considered in the simulations presented here. Therefore Eqn. (18) is the form of the energy transfer equation used in all of the simulations.

In the modelling of experimental results for the nucleation of iron vapor, Freund and Bauer[13] found it necessary to use an adjustable heat transfer coefficient $\theta = h^*(g+1)^{-1}$ to reproduce the observed time variation in the enthalpy of their system and commented that with the values of h^* found to provide the best fit, energy transfers for the smallest cluster were consistent with observations from unimolecular reaction theory. The functional form chosen here is very similar to that of Freund and Bauer[13], $g^{-1.3}$ versus $(g+1)^{-1}$, but by introducing the results from unimolecular reaction theory we have demonstrated the origin of this functional form and illustrated why it is appropriate. It is also clear that as numerical simulations become available that in essence combine the approaches of Bruehl and Schatz[17] and Plummer and Chen[4], a more realistic model of energy transfer between clusters and a non-condensing gas could be developed. This is certainly one avenue for incorporating the chemical nature of both the nucleating and inert species into the general formalism of nucleation theory.

III. NONISOTHERMAL NUCLEATION RATES

The strong coupling between the mass and energy equations should result in more complex behavior of the nucleating system than is observed under the assumption of isothermal nucleation, especially in the transient during the approach to steady state. To investigate this behavior Eqns. (1) and (9) are solved simultaneously for various levels of saturation and energy transfer rates. The model system investigated is the nucleation of liquid water vapor from the supersaturated vapor phase at 263.2 K, because the isothermal relaxation to steady state of this system has been studied previously[10,11] and physical properties of water are readily available.

Before solving the cluster concentration and energy equations simultaneously, the population equations were solved isothermally for various initial conditions and boundary values of g_{min} and g_{max}. In both the isothermal and nonisothermal simulations the smallest cluster considered, g_{min} is assumed to be at its equilibrium concentration and at the ambient temperature at the start of the simulation and to remain at these values throughout the simulation. In addition, the monomer concentration is assumed to remain constant and the monomer is at the ambient temperature. Rather than applying the Szilard boundary condition, $f_{gmax+1} = 0$, where g_{max} is the largest cluster, an extrapolated value for f_{gmax+1} is used, based on the values of f_{gmax} and f_{gmax-1}. This choice gives a slightly smoother transition for the right hand boundary condition and avoids some of the numerical stability problems associated with setting $f_{gmax+1} = 0$.

Results identical to those of Abraham[10] were obtained for identical initial conditions and physical property values. From the results in Fig. 2 it is clear that during the approach to steady state, mass fluxes through the subcritical clusters can exceed the final steady state flux by many orders of magnitude. This overshoot may be understood in light of the

following observations. As the saturation level, S, is suddenly increased from its initial value S_0 to a higher value S_1, the forward mass flux immediately increases by a factor of S_1/S_0, while the backward mass flux remains a function of the evaporation rate, which depends only on the properties of the cluster and not the saturation level, and the cluster concentration. Furthermore since the concentration of subcritical clusters at steady state, f_g, is close to its equilibrium value, N_g^e, the ratio of adjacent steady state cluster concentrations determined by S_0, f_g/f_{g+1}, is larger than the equivalent ratio at S_1 because $N_g^e/N_{g+1}^e \propto S^{-1}$. Finally, because clusters grow only by the addition of monomer, the number of clusters of size $g+1$ can only increase after the number of clusters of size g and f_g will reach its new steady state value before f_{g+1}. Thus there will be some time period for which f_g/f_{g+1} is larger than its final steady state ratio at S_1 and yet $f_g \cong f_g (S_1)$ leading to the observed overshoot. As f_g/f_{g+1} relaxes to its steady state value, so does the net mass flux. It is interesting to examine whether similar transient behavior is exhibited by the average energy of the clusters before they achieve their final steady state, how large these transients are and how they can affect the approach to steady state and the final steady state nucleation rate.

As illustrated in Fig. 2, setting the values of $g_{min} = 2$, $g_{max} = 200$ and f_g^o equal to the equilibrium distribution at $S_0 = 1$ from Abraham's values of $g_{min} = 10$, $g_{max} = 100$ and f_g^o $= 0$ for $g > g_{min}$, did not affect the steady state values of cluster concentration, nucleation rate (steady state current), J, or timelag, τ. Only the times at which the smaller cluster concentrations began to increase changed. This discrepancy occurs because Abraham assumed f_{10} was at its equilibrium value throughout the simulation, while with $g_{min} = 2$ our simulation requires a finite amount of time before f_{10} is essentially at its equilibrium value. The equations were not solved with $g_{min} = 1$ because of the large increase in computing time incurred from that for $g_{min} = 2$. Since the dimer concentration essentially reached its equilibrium value in the first timestep, $<10^{-10}$ s, setting $g_{min} = 2$ was justified.

Evolving 150 clusters was adequate except in cases where g^* was larger than about 90, in which case $g_{max} = 200$ was used. As expected, including a mass accommodation coefficient, $\alpha_{mvap} < 1$, simply reduced the final nucleation rate J to $J = \alpha_{mvap} J_0$ and increased the time required to reach steady state, τ, to $\tau = \tau_0/\alpha_{mvap}$.

The correct value of α_{mvap} for water is still a matter of controversy.[19] Based on the limited set of simulations with clusters containing both 5 and 20 molecules, Plummer and Chen[4] found that collision between a monomer and the cluster always resulted in the absorption of the monomer by the cluster. No scattering or evaporation events were observed and thus, at least for the temperature range investigated, ≤ 93 K, these simulations suggest that for water an accommodation coefficient close to one is a reasonable assumption. However the authors also note that at higher initial temperatures the increase in temperature due to incorporation of the monomer may lead to metastable structures and subsequent evaporation of a monomer. If this absorption - evaporation sequence occurs rapidly enough the net effect would be the same as an accommodation coefficient less than one that depends on the initial temperature of the cluster.

If the mass accommodation coefficient for the condensing vapor is assumed to be 1, the sole mechanism available for efficient cooling of clusters is collision with the inert background gas. Because the value of the energy transfer parameter C is not readily available and only appears in combination with the gas collision rate β_{gas}, the combination of $\beta_{gas}C$ will be varied as a single adjustable parameter in these simulations. Figure 3 illustrates the effects of varying the parameter $C^* = C \beta_{gas}$ from $C^* = C_0^* = 4 \times 10^{-11}$ erg cm^{-2} s^{-1} K^{-1} to $C^* = 0.0$ erg cm^{-2} s^{-1} K^{-1}, with the results of the isothermal nucleation calculations included for comparison. The effects of decreasing C^* becomes significant for $C^* \approx 0.001 \, C_0^*$, but even for $C^* = 0.0$, i.e. no background gas, the nucleation rate is decreased only by about 3 orders of magnitude. Varying the value of C^* can be interpreted

physically as varying the pressure of background gas available while maintaining the same saturation level of the nucleating species. Alternatively, if the amount of background gas is fixed, a decrease in C^* corresponds to a decrease in the efficiency of energy transfer from the clusters to the background gas when, for example, a monatomic gas has been substituted for a larger molecule.

Figure 4 illustrates the temperature distribution of the clusters as a function of time for a value of $C^* = 4 \times 10^{-11}$ erg cm^{-2} s^{-1} K^{-1} and for a sudden increase in S from 1 to 4.91. Clearly there is an energy transient that moves through the clusters as the new steady state cluster distribution is reached. The final temperature distribution, shown on an expanded scale in Fig. 5, is however very close to the ambient temperature $T_{amb} = 263.2$ K, with significant deviations only near and above the critical cluster size. The significantly higher temperatures predicted for final clusters should be ignored as this is simply an effect of the proximity to the boundary. If clusters of size g_{max+1} are underestimated slightly, the number of clusters of size g_{max} that are formed by evaporation events is too low compared to those formed by condensation events and the average temperature is too high. Increasing the number of clusters that are evolved, as indicated by the solid line in Fig. 5, clearly demonstrates that this sharp jump is not a physical phenomenon. The critical nucleus, g^* for these conditions is determined by searching for that value of g at which β_{g-1}/α_g changes from less than 1 to greater than 1. This corresponds to $g^*=74$, compared to $g^*=71$ under isothermal conditions and the increase in g^* is accompanied by a corresponding increase in the time required to reach steady state.

As expected, particles growing past the critical point increase in temperature. This agrees with the observations of Feder *et.al.*[6] However, in contrast to Feder *et.al.*[6] and Ford and Clement,[9] we predict that the clusters on either side of the critical cluster are on average warmer than the ambient temperature.

Looking at the time evolution of the temperature in particular cluster classes, Fig. 6, for the same conditions as in Figs. 4 and 5 and comparing these to the mass fluxes for the same clusters illustrated in Fig. 2, demonstrates that the peak in the temperature of a cluster class corresponds to the initial rapid increase in the concentration of that cluster class. (Although Fig. 2 is strictly the result of an isothermal calculation, the high value of C^* ensured that the cluster flux evolution in this case is very close to those in Fig. 2.) Physically this simply corresponds to the fact that suddenly far more clusters of that size are the result of condensation than evaporation and that the large mass flux is overwhelming the ability of the background gas to remove energy. It is interesting to observe the rather large transients in temperature that are predicted during the approach to steady state even when the value of C^* is high enough to predict minimal impact on the final nucleation rate.

The results in Figs. 2 to 6 present the following physical picture of nonisothermal nucleation. When q_g is positive, the nonisothermal nucleation rate is lower than the isothermal rate because the average temperature of the clusters in the critical region is higher than the ambient temperature and thus the evaporation rate is higher than in isothermal nucleation. As a consequence of the higher evaporation rates the size of the critical cluster, g^*, increases and hence the time required to reach steady state increases. This increase in time to reach steady state associated with an increase in g^* is analogous to that observed in isothermal nucleation as S decreases.

When the value of the mass accommodation coefficient, α_{mvap}, is varied in these calculations, competing effects are brought into play. As in isothermal nucleation, reducing α_{mvap} reduces the nucleation rate. However, in nonisothermal nucleation a lower value of α_{mvap} results in additional time available for energy transfer between incorporation of the

condensing species. The impinging but non-condensing molecules also provide additional energy transfer and overall the deviation from isothermal nucleation rates should decrease as α_{mvap} decreases . Depending on the relative energy transfer efficiencies, non-condensing vapor molecules may contribute proportionally more or less to the cooling than relative impingement rates would predict. For simplicity, in these simulations we have set $\phi_{gas}(g) = \phi_{vap}(g)$ and thus cooling rates due to the two species will be proportional to their relative impingement rates.

A set of simulations similar to those summarized in Fig.3 were conducted using a mass accommodation coefficient, $\alpha_{mvap} = 0.5$. In order to compare the two sets of results, the normalized nucleation rates, J/J_0, where J_0 is the isothermal nucleation rate, are presented in Fig. 7 as a function of the saturation level for $\alpha_{mvap} = 1.0$ (squares) and $\alpha_{mvap} = 0.5$ (crosses). In the discussion that follows the separate curves are interpreted as simulations corresponding physically to levels of background gas varying from p_0 to 0.0 with a constant value of the energy transfer parameter $C_{gas} = C_{vap} = C$. The effect of the mass accommodation coefficient is apparent when comparing the curves for $\alpha_{mvap} = 0.5$ and 1.0 at the highest background gas pressure p_0. As expected the deviation from the isothermal case is less for $\alpha_{mvap} = 0.5$ than for $\alpha_{mvap} = 1.0$ and this difference is best understood by realizing that normalizing Eqns. (1) and (9) by dividing by α_{mvap} results in an overall energy transfer coefficient proportional to

$$C* = \frac{\beta_{gas}\, C_{gas}\, g^{-1.3} + (1-\alpha_{mvap})\, \beta_{vap}\, C_{vap}\, g^{-1.3}}{\alpha_{mvap}} \qquad (19)$$

Thus at high levels of background gas where the contribution to cooling from non-accommodated molecules is insignificant we would expect the same degree of deviation from isothermal nucleation for $\alpha_{mvap} = 0.5$ and $p = 0.5p_0$ as for $\alpha_{mvap} = 1.0$ and a

background pressure of $p = p_0$ as these sets of conditions correspond to the same value of C^*. Figure 7 demonstrates that this is indeed the case. With the background gas removed the effect of cooling by the non-accommodating vapor molecules becomes important and the departure from the non-isothermal results is less severe for the case of $\alpha_{mvap} = 0.5$ simply because here the non-accommodated molecules are providing the only means of energy transfer. Simulations were done which considered the possibility of ratiative cooling of the particles, but for water at these temperatures this had no effect.

The effect of nonisothermal conditions on the steady state distribution of clusters is also interesting. Figure 8 compares the isothermal and nonisothermal cluster distributions for simulations in which $\alpha_{mvap} = 0.5$ and the background gas pressure $p_0 = 0.0$. The increase in the size of the critical nucleus for the nonisothermal case realtive to the isothermal calculation is clearly illustrated. Although for a given value of g the concentration of clusters is greater in the nonisothermal than in the isothermal case, the critical cluster concentration f_{g*} is lower under nonisothermal conditions and $J//J_0$ $= f_{g*}/f_{g*,0}$. The sharp drop in the cluster concetrations for the nonisothermal calculation at the largest clusters is again a consequence of the proximity to the boundary and reflects the extremely rapid increase in temperature observed in this region in Fig. 5.

Although the calculations presented here involve water as the model system, there is nothing in the general analysis that prevents this approach from being applied to other species. The key issues remain the uncertainty in using a single temperature and evaporation coefficient to characterize the behavior of a single cluster class and the need for a better understanding of energy transfer processes to small clusters. The two parameters that determine the importance of nonisothermal effects in gas-phase nucleation are the latent heat of vaporization and the rate of energy transfer for small clusters. The former is reasonably well characterized and does not vary greatly for the species that are of common

interest; the latter represents a poorly understood phenomenon that warrants further investigation.

IV. SUMMARY AND CONCLUSIONS

The phase transition as a monomer condenses onto or evaporates from a cluster is necessarily accompanied by a change in energy. In this paper cluster mass and energy balances were solved simultaneously to determine the effect including such an energy balance has on both the final nucleation rate and the approach to steady state. The energy balance assumed that the final temperature of the clusters in a given class were determined by a balance between the energy due to cluster growth and evaporation and energy transfer by collision with inert background gas molecules. The collisional energy transfer was described using a model based on energy transfer in unimolecular reaction theory.

The steady state nonisothermal nucleation rate is found to be a strong function of the degree of cooling; in all cases including an energy balance led to an increased average temperature of the clusters and a decreased final nucleation rate. During the approach to steady state, temperature transients much larger than the final steady state temperature deviation were observed and were associated with the onset of significant mass flux through a cluster class. The increased cluster temperatures and associated higher evaporation rates also led to an increase in g^* and hence an increase in the time required to establish steady state nucleation. The effect of a mass accommodation coefficient less than 1.0 reduces the deviation of the final nucleation rate from the isothermal rate both by providing extra time for temperature equilibration to occur by collision with background molecules between incorporation of vapor molecules and by providing additional energy transfer by molecules that impinge but are not incorporated. The latter effect is important

for low background gas pressures. This work also shows how the nature of the background gas can play a specific role in the nucleation process by changing the rate at which energy is transferred from the growing cluster.

ACKNOWLEDGEMENTS

REFERENCES

[1]F. F. Abraham, "Homogeneous Nucleation Theory", Academic Press, New York (1974).

[2]A. C. Zettlemoyer, "Nucleation", M. Dekker, New York (1969).

[3]Kung, R.T.V. and S.H. Bauer, "Shock Tube Research", 8th International Symposium, Chapman and Hall, London, 1971, paper No. 61

[4]Plummer, P.L.M. and T.S. Chen, J. Chem. Phys. **86**, 7149 (1987).

[5]A. Kantrowitz, J. Chem. Phys. **19**, 1097 (1951).

[6]J. Feder, K.C. Russel, J. Lothe and G.M. Pound, Adv. Phys. **5**, 111 (1966).

[7]E.E. Salpeter, J. Chem. Phys. **58**, 4331 (1973).

[8]A.P. Grinin and F.M. Kuni, Theor.-Math. **80**, 968 (1989).

[9]I. J. Ford and C. F. Clement, J. Phys. A. **22**, 4007 (1989).

[10]F.F. Abraham, J. Chem. Phys. **51**, 1632 (1969).

[11]W.G. Courtney, J. Chem. Phys. **36**, 2009 (1962).

[12]"Enthalpies of Vaporization of Organic Compounds", IUPAC, Chem data series #32

[13]Freund,H.J. and S.H.Bauer, J. Phys. Chem. 81,994 (1977).

[14]H. Hippler, J.Troe and H.J. Wendelken, J. Chem. Phys. 78, 6709 (1983).

[15]D.C. Tardy and B.S. Rabinovitch, J. Chem.Phys. 48, 1282 (1968).

[16]J.Troe, Ber. Buns. Ges. 77, 665 (1973).

[17]M.Bruehl and G. Schatz, J. Chem. Phys. 89, 770 (1988).

[18]see also Table 10.1 in P.J. Robinson and K.A. Holbrook, "Unimolecular Reactions", Wiley-Interscience, London (1972).

[19]H. K. Cammenga in "Current Topics in Material Science", E. Kaldis Ed., 5, 335, North-Holland, Washington, D.C. (1980).

Table 1 : Physical Properties of Water and Air

$c_{\text{vwater vapor}}$		4.66×10^{-16}	erg K^{-1} molecule^{-1}
$c_{\text{pwater liquid}}$		1.26×10^{-15}	erg K^{-1} molecule^{-1}
c_{vair}	3.46×10^{-16}	erg K^{-1} molecule^{-1}	
h_{vap}^{∞}	$9.29 \times 10^{-13} - 6.67 \times 10^{-16}T$	erg molecule^{-1}	
σ	$120.88 - 0.167\,(T - 273.15)$	dyne cm^{-1}	
ρ	1.0	g cm^{-3}	
m_{water}	2.99×10^{-23}	g molecule^{-1}	
m_{air}	4.81×10^{-23}	g molecule^{-1}	

Table 2 : Theoretical estimates of the average energy transferred between an excited molecule containing N_a atoms and a background gas molecule containing N_m atoms.[17]

N_a	N_m	$\dfrac{<\Delta E>}{kT}$
	1	2
		7
		11
		15
		20
	1	40
	15	
	8	
	3.5	
	2	
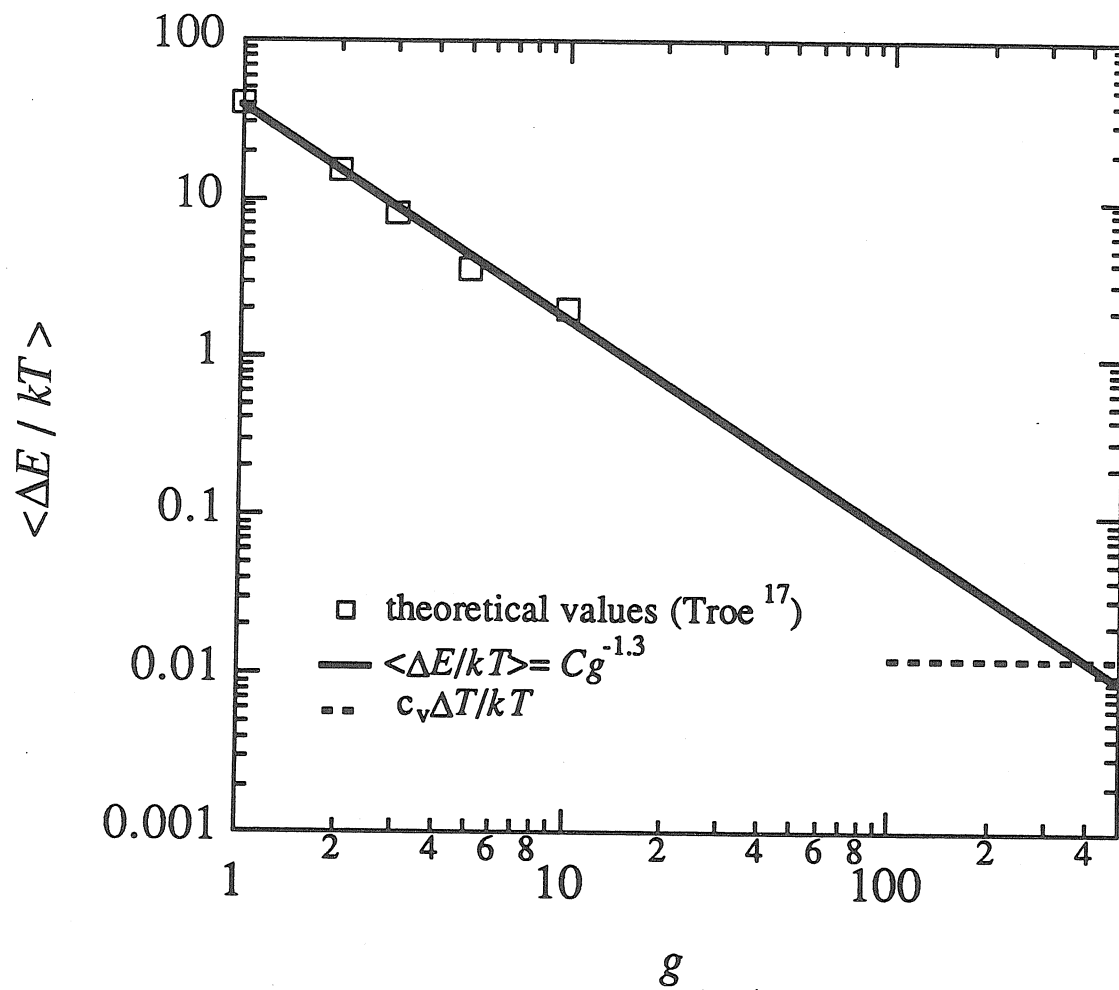
Figure 1 : Average energy transferred in a collision between a monatomic gas and a cluster containing g triatomic molecules. The squares are the results of simulations performed by Troe.[17]
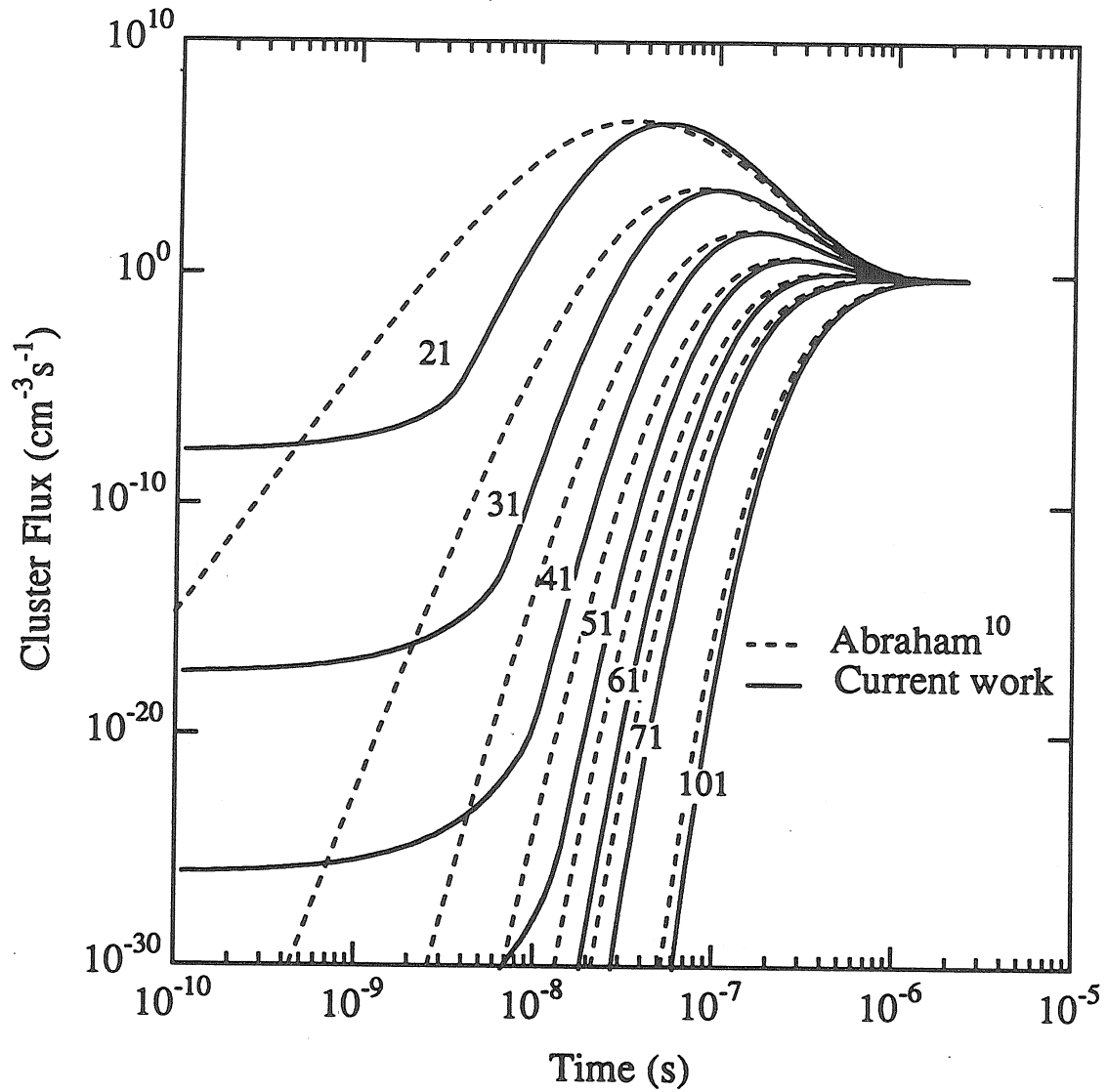
Figure 2 : The evolution of the cluster flux with time of selected clusters for water at $T_{amb} = 263.2$ K and in response to a sudden increase of S to $S = 4.91$. The final steady state is not affected by the choice of initial conditions, $S = 0$ or 1.0, or the number of clusters evolved. Isothermal conditions are assumed to hold.
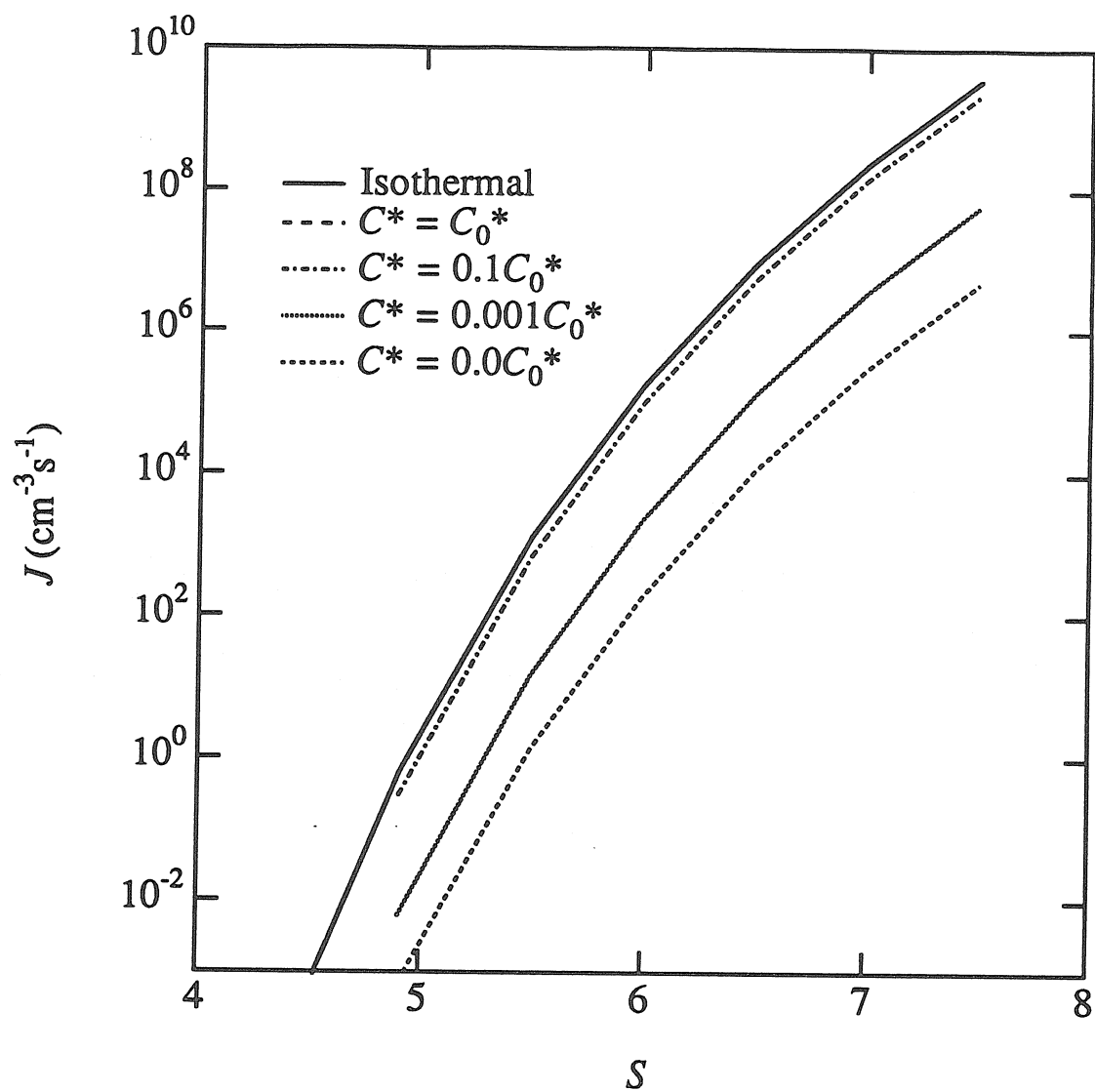
Figure 3 : Homogeneous nucleation rate of water at $T_{amb} = 263.2$ K as a function of the energy transfer parameter C^*.
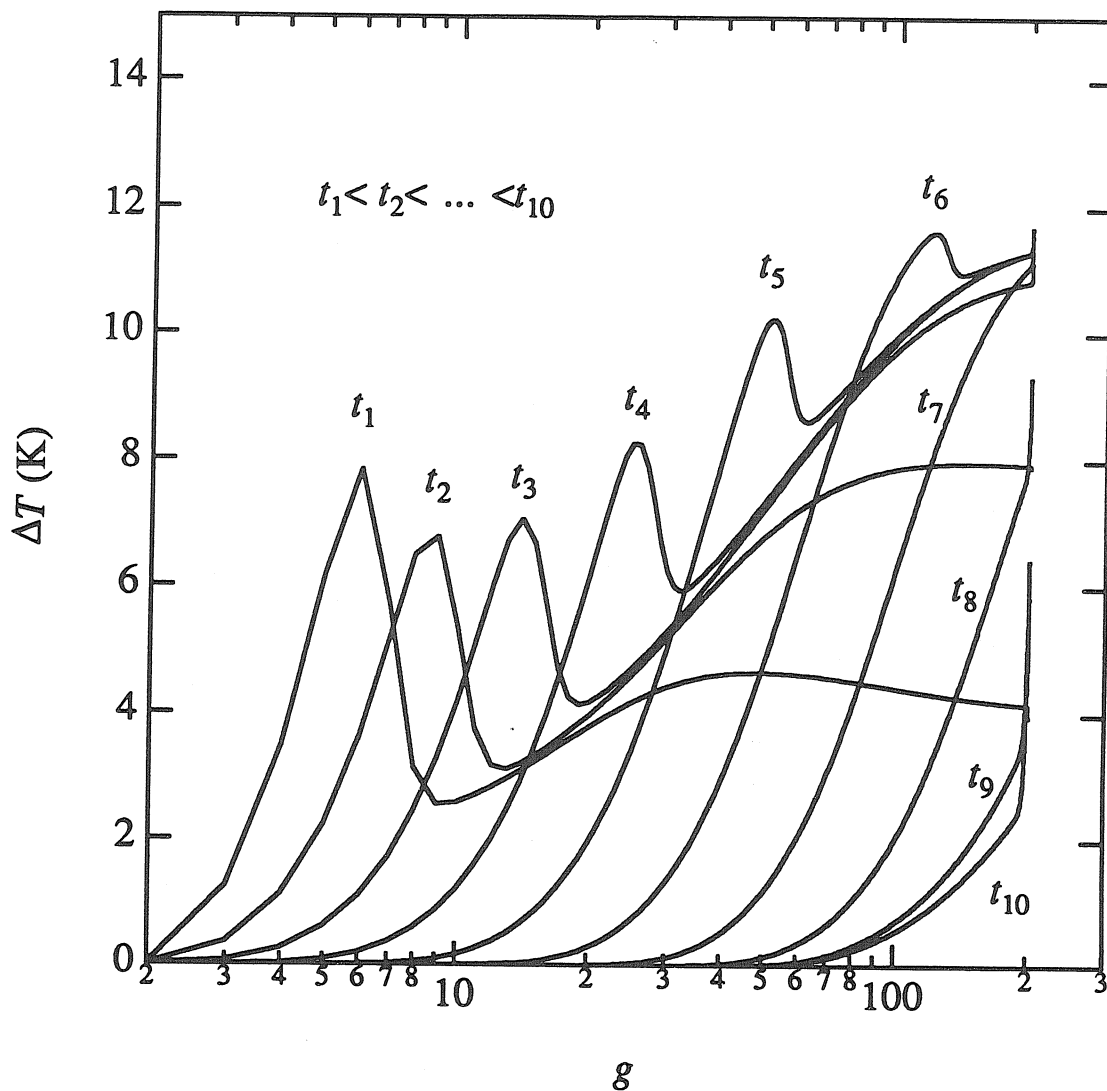
Figure 4 : Cluster temperature distribution as a function of time for water at

T_{amb} = 263.2 K with $C^* = C_0^*$ and in response to a sudden increase of S from 1 to 4.91.

The values of time are $t_1 = 2.8 \times 10^{-10}$ s , $t_2 = 7.6 \times 10^{-10}$ s, $t_3 = 2.1 \times 10^{-9}$ s,

$t_4 = 5.7 \times 10^{-9}$ s, $t_5 = 1.6 \times 10^{-8}$ s, $t_6 = 4.4 \times 10^{-8}$ s, $t_7 = 1.2 \times 10^{-7}$ s, $t_8 = 3.3 \times 10^{-7}$ s,

$t_9 = 9.1 \times 10^{-7}$ s, and $t_{10} = 2.5 \times 10^{-6}$ s.
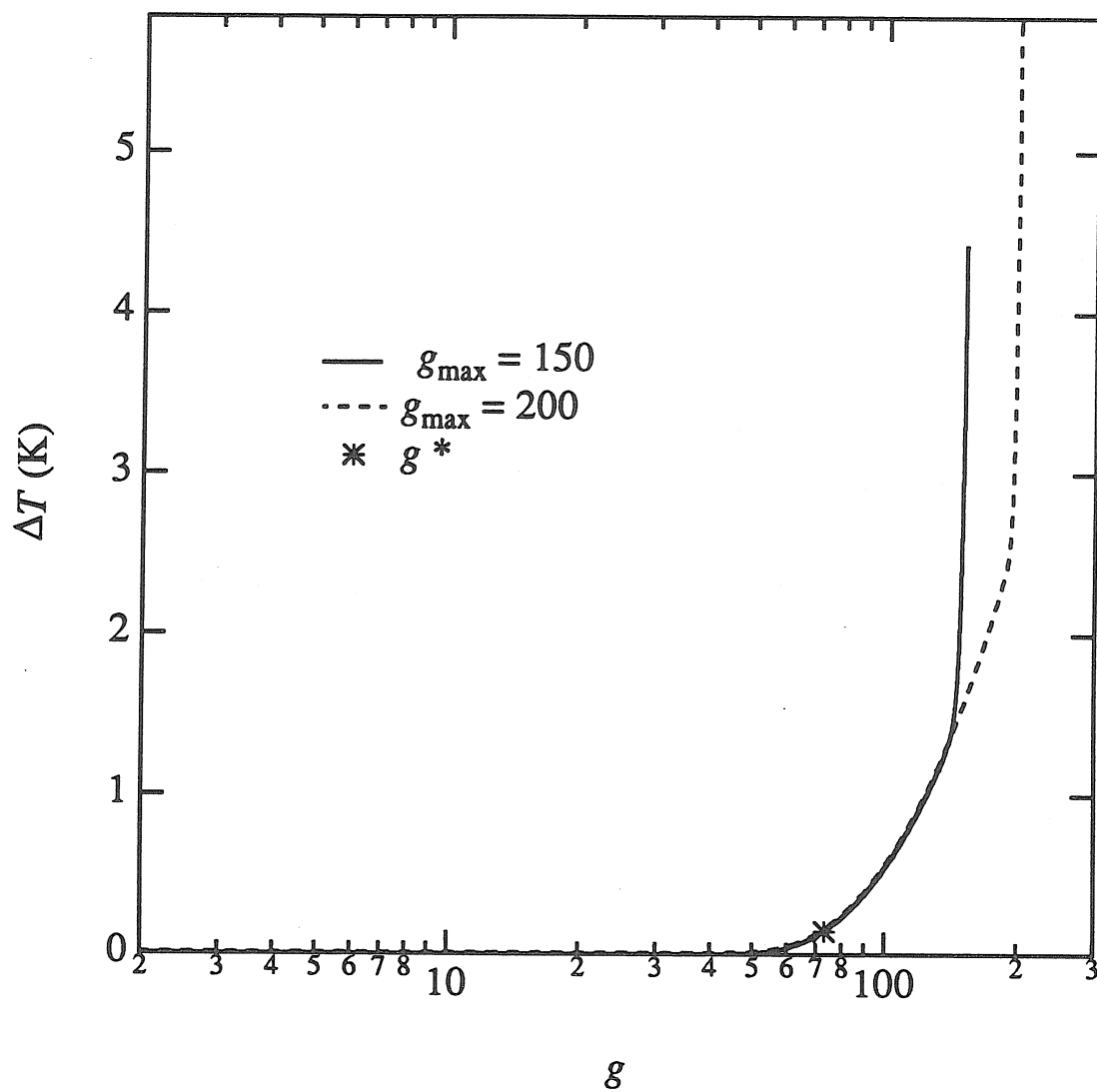
Figure 5 : The steady state cluster temperature distribution for $C^* = C_0^*$ and for $g_{max} = 150$ and 200.
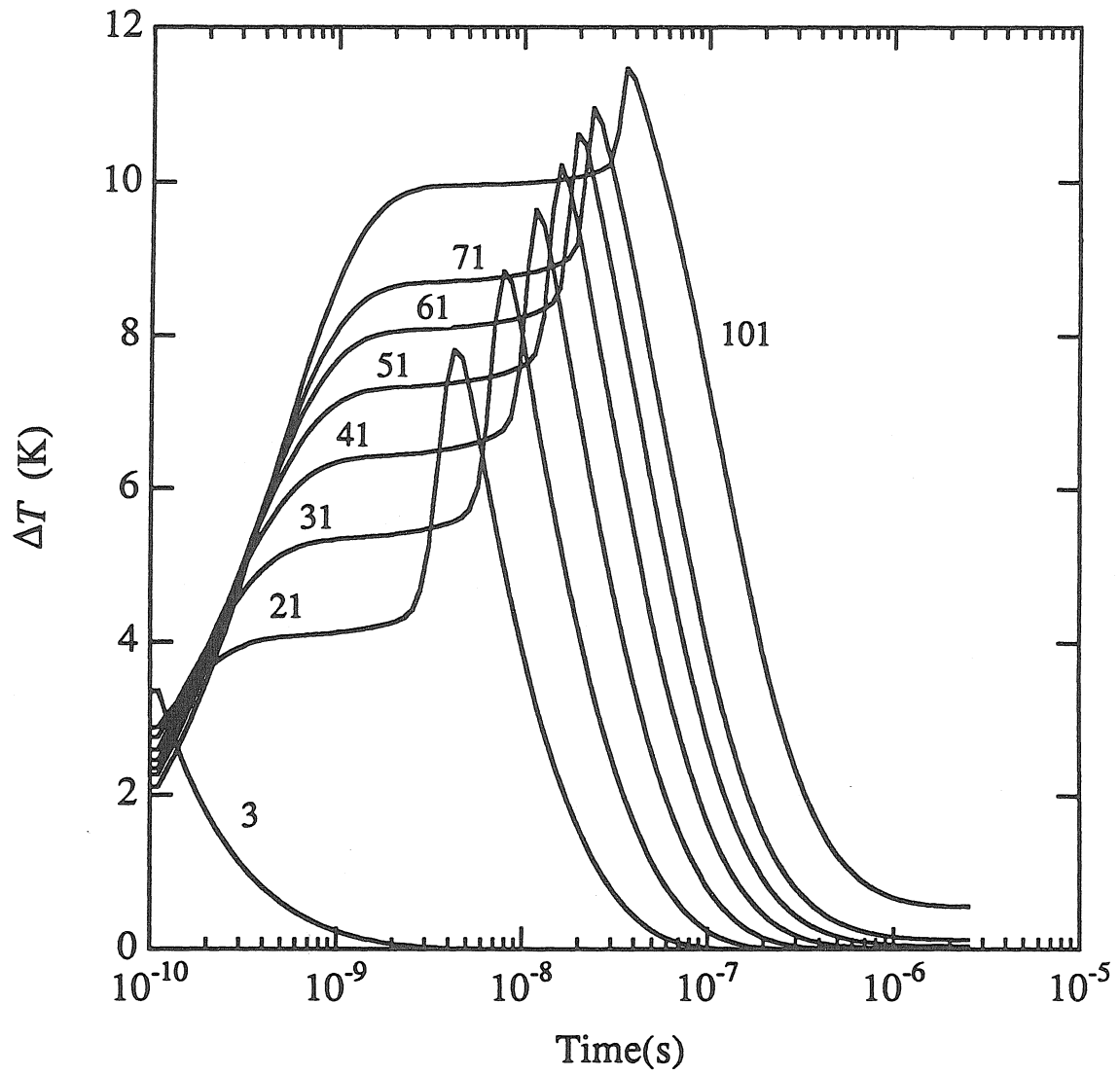
Figure 6 : Transient cluster temperature in the homogeneous nucleation of water at $T_{amb} =$ 263.2 K with $C^* = C_0^*$ and in response to a sudden increase of S from 1 to 4.91.
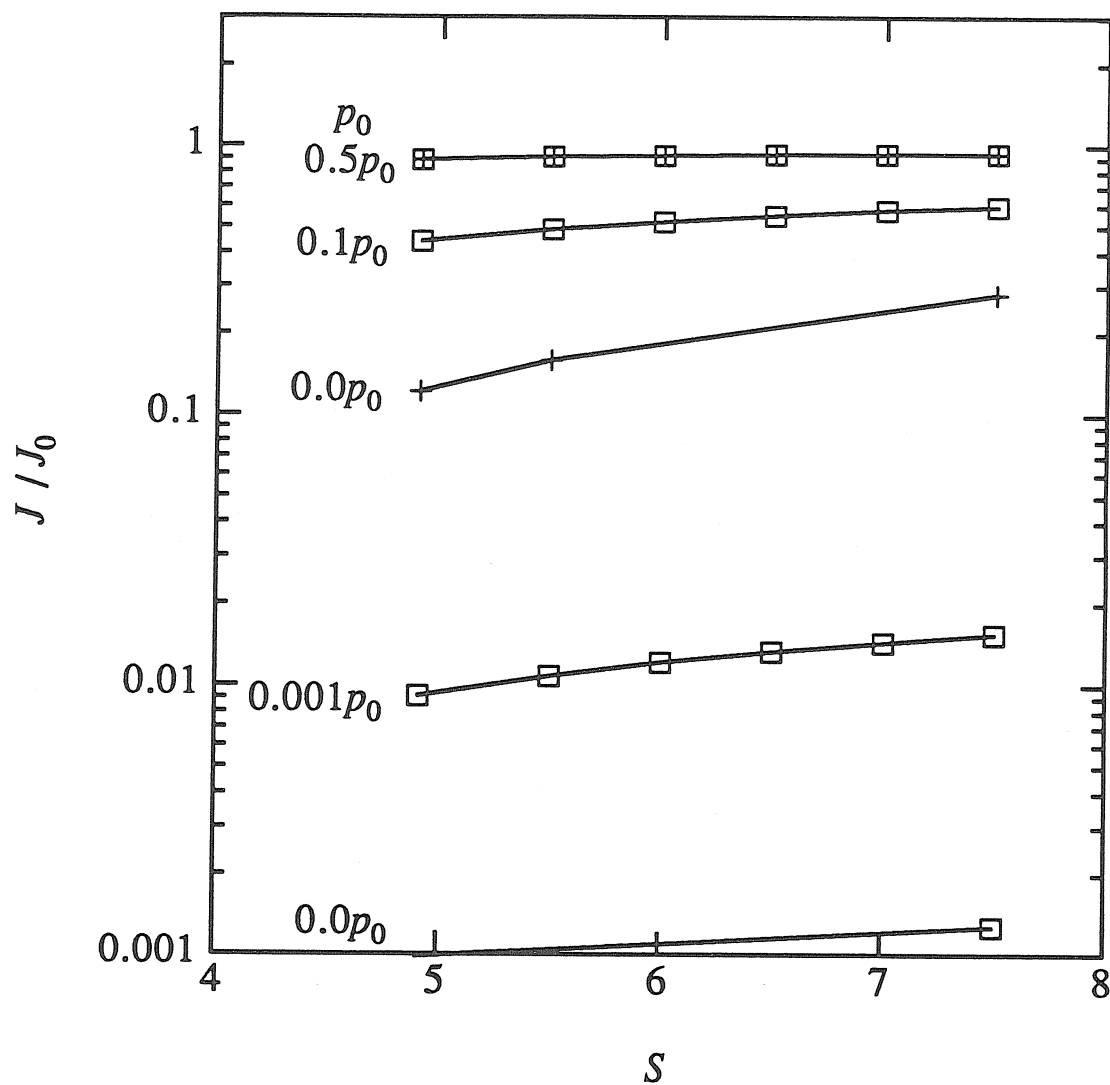
Figure 7 : Nonisothermal nucleation rates of water normalized with respect to the isothermal value, J/J_0, at $T_{amb} = 263.2$ as a function of the background gas pressure for $\alpha_{mvap} = 0.5$ and 1.0 and for fixed energy transfer parameter C.
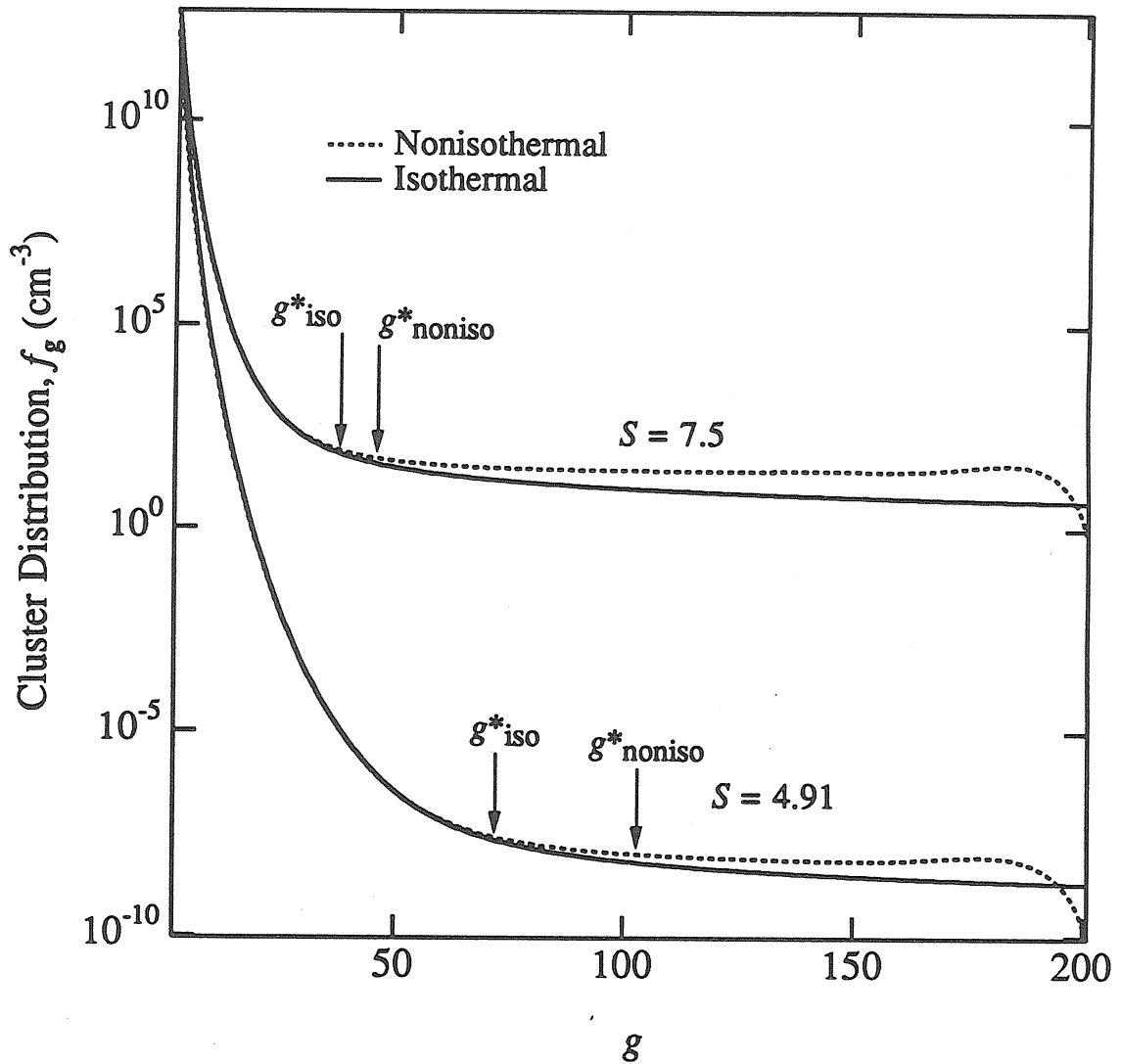
Figure 8 : Steady state cluster distributions for isothermal and non-isothermal nucleation at two saturation levels and $\alpha_{mvap} = 0.5$ illustrate the shift in the critical nucleus due to increased evaporation rates in the critical region.

CHAPTER 5

Summary and Conclusions

The highly non-ideal behavior of acid-water solutions permits formation of new particles from the vapor phase even when both components are subsaturated with respect to the pure species. Thus naturally occurring atmospheric acids, such as methanesulfonic acid (CH_3HSO_4) and sulfuric acid (H_2SO_4), may combine with the available water vapor to form new particles in the first step of the atmospheric gas-to-particle conversion process.

Using a fast mixing-type continuous flow device, the formation of new particles in the CH_3HSO_4 - H_2O and H_2SO_4 - H_2O systems was studied as a function of relative humidity (Rh), relative acidity (Ra), and at three different temperatures, $T = 20, 25$ and $30°$ C. Both the number concentration of particles produced and the particle size distributions were measured. At low particle production rates, nucleation rates were calculated as functions of Rh, Ra, and T and compared to the predictions of classical nucleation theory. As in single component homogeneous nucleation, the nucleation rate increased with an increase in temperature, but the temperature dependence was much stronger than that predicted by the theory. This work represents the first systematic study of the effect of temperature on binary nucleation rates.

The experimental observations from the CH_3HSO_4 - H_2O system were compared to an integral model that considered both nucleation and growth of the particles by condensation. To achieve good agreement between the particle number concentrations predicted by the theory and those observed in the experiments, correction factors to the nucleation rate ranging from 10^{-8} at $T = 19°$ C and 10^{-4} at

$T = 30$ ° C were incorporated into the model . The need for such a correction factor is not unusual in nucleation experiments where even in single component nucleation the ratio of experimental to theoretical nucleation rates, J_{expt}/J_{theor} varies from 10^{-11} to 10^7 depending on the substance and the temperature. The variation in the particle size distributions with changes in Ra, Rh and T agreed qualitatively with the predictions of the integral model.

For the H_2SO_4 - H_2O binary system, a comparison of the experimental and theoretical nucleation rates demonstrated that the ratio J_{expt}/J_{theor} is a strong function of the predicted number of acid molecules in the critical nucleus. Comparing the behavior of the two acid-water systems illustrated that classical nucleation theory is able to predict the major differences correctly: nucleation rates for H_2SO_4 were much higher than for CH_3HSO_4 at the same water vapor concentration and the particles produced in the H_2SO_4 experiments were much smaller than the particles produced with CH_3HSO_4. Thus classical nucleation theory does provide a basis for predicting trends and relative behavior of different systems, although it generally fails to predict accurately the exceedingly sensitive nucleation rates.

A critical issue in classical nucleation theory is the assumption that the phase transition occurs isothermally. To examine the validity of this assumption, the classical theory was extended to nonisothermal conditions through cluster mass and energy balances. By simultaneously solving the two sets of differential equations, the steady state nucleation rate was found to be a strong function of the degree of cooling. For the nucleation of water from the supersaturated vapor phase, including an energy balance reduced the final nucleation rate. Furthermore, temperature transients associated with the onset of significant mass flux through a cluster class were observed during the approach to steady state. Because the rate at which energy is

transferred from the growing clusters has a strong influence on both the transient and steady state behavior, this approach necessarily provides a specific role for the background gas in the nucleation process.

APPENDIX A

Instrumentation and Equipment Calibration

This appendix presents an overview of the principles of the aerosol measuring equipment used, the flow and temperature measurements systems and the relevant calibrations performed. For reference, Table 1 contains a list of the major pieces of equipment used in the experimental apparatus.

I. Particle Detection : The Condensation Nucleus Counters

The principle of the condensation nucleus counter (CNC) is to enlarge submicron particles by condensation of a working fluid to the point where they may be detected by simple light scattering techniques. Both CNCs in these experiments used butanol as the working fluid. The details of implementing this scheme will be explained with reference to Fig. 1, which is a schematic of the TSI - 3020 CNC.[1]

Sample aerosol is drawn into the 35 ° C saturator tube at 0.3 l min^{-1} using either the internal pump provided or an external vacuum pump. Butanol evaporates into the flowing stream from the reservoir and felt lining along the wall. The saturated sample then enters the 10 ° C condenser tube where the butanol vapor condenses onto the particles causing them to grow into ~12 µm droplets. The particles then pass through a 1.0 mm nozzle into the viewing volume where light from a lamp is scattered and collected by a photo detector. The output from the photo detector passes through a triggering circuit and a pulse counting circuit. Below 1000 particles cm^{-3}, individual

pulses are counted for a specified averaging time and the result is displayed on the front panel at the end of each averaging time. At higher concentrations the instrument switches to photometric mode where the d.c. voltage level of the light scattered by all the particles in the viewing volume is measured. A linearizing circuit converts this to concentration.

To correct the output from count mode for particle coincidence, the true number concentration N_a may be related to the observed number concentration N_i by

$$N_a = N_i \exp(N_a Q t) \tag{1}$$

where Q is the sample flowrate (5 cm^3 s^{-1}), t is the time spent in the sampling volume

(35 μs) and the approximation of $N_a = N_i$ is made in evaluating the exponential.[2]

Condensation nucleus counters begin to have limited efficiency as particle size drops below 30 nm. Figure 2 summarizes the efficiency data available in the literature for the 3020 CNC.[2-6] A similar curve, Fig. 3, was established for the TSI Model 3760 CNC by Wang and Flagan.[7]

The internal designs of the 3760 and 3020 CNC are very similar. The major differences are the flowrates (1.4 l min^{-1} vs 0.3 l min^{-1}), the light source (laser diode vs tungsten lamp) and the fact that the 3760 depends on a temperature difference between the saturator and condenser rather than setting each of these to predetermined values. The 3760 counts up to 10^4 particles cm^{-3} in single particle count mode, but does not have the option of photometric count mode. Particle

coincidence corrections are also required for this instrument but here $Q = 23.58$ cm^3/sec and $t = .25$ μs.[8]

The residence time of the aerosol in the 3020 CNC is estimated from the geometric data given in the manual.[1] For the saturator tube, the effective inner diameter, ID, accounting for the thickness of felt is 1.58 cm and the length is 11.4 cm. The residence time in the saturator is therefore $V_s/Q = 22.23/5.0 = 4.47$ s, where V_s is the saturator volume. Likewise the condenser tube has an ID of .46 cm and length of 8 cm, which gives a total volume of 1.35 cm^3 and residence time of 0.27 seconds. Total residence time in the CNC is therefore 4.8 seconds.

II. Particle Size Distributions : The Differential Mobility Analyzer and Scanning Electrical Mobility Spectrometer

The differential mobility analyzer (DMA) consists of the combination of an electrostatic classifier with a particle detection device. By varying the voltage applied to the classifier and recording the number of particles observed, a particle size distribution can be established. Condensation nucleus counters are convenient for use as particle detectors in this application because of their relatively fast response time. The use of appropriate software to control the voltage to the classifier and record the output of the CNC can greatly enhance the speed and versatility of this aerosol measuring device.

Both of the CNCs described in the previous section, were used as particle sensing devices. The 3760 CNC was used with the TSI model 3071 electrostatic classifier

which has a classifier tube length L^B = 44 cm. The 3020 CNC was used with a special electrostatic classifier, identical in design to the 3071 except with a classifier tube length of 10 cm for use with very fine aerosols.[9] In this section the operation of the electrostatic classifier is reviewed and the programs used to collect and invert the data are outlined.

A schematic of the electrostatic classifier is given in Fig. 4.[10] The classifier consists of two concentric cylinders with outer radius R and inner radius kR. The polydisperse aerosol and the clean sheath air enter the analyzer at the top and flow down the annular region in concentric laminar streams. A voltage, positive or negative, is applied to the inner cylinder while the outer cylinder is grounded. Particles of the opposite charge are attracted across the inner clean air stream to reach the central rod. Of all the particles entering the top of the analyzer, only a fraction will reach the central rod at just the right time to be swept out by that part of the flow leaving through the sample slit. In the absence of Brownian motion, the mean mobility of these particles is

$$Z_{pc} = \frac{q_c + 0.5(q_a - q_s)}{2\pi L^B V} \ln \frac{R}{kR} \qquad (2)$$

and the width of the mobility band is

$$\Delta Z_p = \frac{q_a + q_s}{4\pi L^B V} \ln \frac{R}{kR} \qquad (3)$$

where q_c, q_a and q_s are the clean sheath air, inlet aerosol and sample flowrates respectively and V is the voltage.

Both DMAs were operated using a recirculating air system, thus $q_a = q_s$ and the sheath air flowrate alone determines the mobility peak. Because of the importance of this variable, the flowmeter on the 3071 DMA was calibrated using a Precision Instruments wet test meter. Since the short DMA did not have an associated flowmeter, a simple capillary flowmeter was constructed for the sheath air flow and a calibration curve established. Figures 5 and 6 illustrate the calibration data and the best fit curves. From the graphs uncertainty in the sheath air flows is seen to be ± 3%.

Voltage control on 3071 DMA was checked by comparing the voltage read with a high voltage probe and the HP 34702A multimeter as the computer changed the voltage in accordance with a simple stepping program. For the short DMA the output voltage from the Fluke 412B high voltage power supply was also checked against the multimeter over the available range.

Because the particles generated in the experiments are not charged, the aerosol first flows through a TSI 3077 bipolar charger before entering the classifier. This charger uses Kr-85 source as a β- emitter to ionize gas molecules which collide with the particles to attain a charge equilibrium. The equilibrium distribution for the positive and negatively charged particles is assumed to equal that described by the Fuchs distribution.[11]

The standard method for operating the DMA is to set the voltage of the central cylinder and then wait until a steady signal is achieved. The voltage is then changed and another measurement is taken. This is the approach that was used with the short DMA. Even with computer control and a fast response CNC, particle size

distributions can take several minutes to complete. Recently Wang and Flagan[7] developed the necessary software to operate the DMA as a Scanning Electrical Mobility Analyzer (SEMS). By allowing the voltage to vary continuously with time and using a fast response detector, the 3760 CNC, they have shown that it is possible to get good size distribution data in as little as 30 seconds. Previously this was only possible if some of the channels were omitted. These programs were implemented for use with the 3071 DMA.

The first approximation to the size distribution for the SEMS is made with a simple data inversion program implemented as soon as the data has been collected. This inversion scheme assumes singly changed particles and that $n(D_p,j)$, $s(D_p,1)$ and $\Phi(D_p,1)$ are constant over the channel. Then

$$n(D_p,j) \cong \frac{s_j \frac{dZ_p}{dD_p}}{s(D_p,i)\ \Phi(D_p,1)\ \displaystyle\int_{Z_p-\Delta Z_p}^{Z_p+\Delta Z_p} \bar{\Omega}(Z_p,t_m,t_c)dZ_p} \tag{4}$$

Here D_p is the particle diameter, the subscript j refers to the jth channel, $n(D_p,j)$ is the number distribution, s_j is the instrument response, $s(D_p,j,i)$ is the detector response to a particle of size D_p and charge i, $\Phi(D_p,j,1)$ is the probability of a particle of size Dp acquiring a single positive charge, and $\bar{\Omega}(Zp,tm,tc)$ is the average transfer function over the measurement time and is given by

$$\bar{\Omega}(Z_p,t_m,t_c) = \frac{1}{tm} \int_{t_m}^{t_m+t_c} \Omega(Z_p,t)dt \tag{5}$$

where Ω is the trapezoidal transfer function described by the peak mobility and half width.

A more exact method of solving the particle size distribution using the complete instrument response function and accounting for multiple charging showed little difference in the the shape or height of the curves. The second method used was that of Wolfenbarger and Seinfeld[12]. Both data inversion schemes incorporated an estimate of the particle losses measured by Wang and Flagan[7] for the instrument combination used in these experiments, illustrated previously in Fig. 3.

The data from the short DMA were inverted using the simple transfer function as given by equations (4) and (5). Because the particles measured using the short DMA were all less than ~60 nm multiple charging is not a problem. Corrections were made to the data for loss of counting efficiency in the 3020 CNC using an estimate of the counting efficiency based only on the data of Bartz,[3] Keady et al,.[5] and Ahn and Liu[6] because these data include estimates of counting efficiencies for particles less than 4 nm, which we were also able to detect. Adachi et al.[10] showed that loss of particles due to Brownian diffusion is important at these small diameters and therefore the particle size distributions were also corrected for diffusional losses using their results for the 10 cm long column and a brass exit port. Figure 7 show the final combined efficiency for the short DMA based on the counting efficiency data fit and the diffusional loss equations of Adachi et al.[10]

III. Thermistor Placement and Calibration

Temperature measurements were made using AD590 series thermistor. Thermistors are ceramic semi-conductors which exhibit a large change in resistance with changes in temperature. By using these devices in a circuit similar to that shown in Fig. 8, it is easy to establish a very good linear relationship between temperature and voltage for the temperature range of interest. A 15 volt power supply was used to drive the thermistors and the two trim temperature circuit converted the output to a 0 to 5 volts over a ~ 0 to 50 ° C temperature range. The output voltage was read using the HP multimeter.

The thermistors were calibrated by placing them in the constant temperature bath close to a 0 - 50 ° C thermometer with 0.1 ° C scale divisions. The thermometer used in the calibrations could be read to the nearest 0.03 ° C and the voltmeter was read to 0.001 volts. Simple linear fits of temperature versus voltage were established and Table 2 summarizes all of the calibration results. From the calibration curves, the uncertainty in temperature is estimated as ± 0.05 ° C.

Thermistors were placed inside either 3/8" glass tubes (acid/water bubblers) or 1/4" O.D. machined stainless steel casings. A small quantity of heat sink compound ensured good thermal contact with the glass or metal. In the glass tubing configuration, the lead wires were further protected from moisture by 1/4" teflon tubing which is joined to the glass by a Swagelock reducing union. The stainless steel casings were designed to fit inside 1/4" teflon tees that were drilled so that the tip of the casing just protruded into the gas stream flowing past. Tygon tubing, sealed to the casing with silicone rubber, protected the leads from moisture. Figure 9,

reproduced from Kreidenweis,[13] illustrates schematically the two thermistor placements.

IV. Flowmeters

Figure 10 illustrates the simple flowmeters constructed using ~30 - 50 cm lengths of glass capillary tubing and 0-10 torr differential pressure transducers. The pressure inside the capillary tubes was kept at close to 30" Hg by regulating the pressure on the upstream side of the capillaries and placing the flow controlling needle valves on the downstream side. The volumetric flowrate was measured from 20-1000 cc min^{-1} as a function of differential pressure across the capillary using bubble flowmeters. The differential pressure transducers were read using the HP multimeter. The data were corrected to STP and calibration curves established by least squares fitting of a quadratic. Table 3 summarizes the results for the relevant calibrations. From the calibration data uncertainties in these flows is estimated as ± 3%.

REFERENCES

[1] TSI Model 3020 Condensation Nucleus Counter Instruction Manual, TSI P/N 1933020 (Revision A, October 1982)

[2] J. K. Agarwal and G. J. Sem, J. Aer. Sci., **11**, 343 (1980).

[3] H. Bartz, H. Fissan, C. Helsper, Y. Kousaka, K. Okuyama, N. Fukishima, P.B. Keady, S. Kerrigan, S.A. Fruin, P.H. McMurray, D.Y. Pui and M.R. Stolzenburg, J. Aerosol Sci., **16**, 443 (1985).

[4] H. Y. Wen and G. Kasper, J. Aer. Sci., **17**, 947 (1986).

[5] P.B. Keady, V.L. Denler, G.J. Sem, M.R. Stolzenburg and P.H. McMurray, in *Atmospheric Aerosols and Nucleation*, Wagner, P.E. and G. Vali Eds., 190 (Springer Verlag, 1988)

[6] K. H. Ahn and B.Y.H. Liu, J. Aerosol Sci., **21**, 263 (1990).

[7] S.C. Wang and R.C. Flagan, Aerosol Sci. Technol. **13**, 230 (1990).

[8] TSI Model 3760 Condensation Nucleus Counter Instruction Manual, TSI P/N 1933760 (1986)

[9] Y. Kousaka, K. Okuyama, M. Adachi and T. Mimura, J. Chem. Eng. Japan, **19**, 401 (1986).

[10] M. Adachi, K. Okuyama, Y. Kousaka, S.W. Moon and J.H. Seinfeld, Aerosol Sci. Techn., **12**, 225 (1990).

[11] N.A. Fuchs, Geophis. Pura Appl., **56**, 185 (1963)

[12]J.K. Wolfenbarger and J. H. Seinfeld, J. Aer. Sci., **21**, 227 (1990).

[13]S. M. Kreidenweis, Experimental and Theoretical Studies of Binary Nucleation and Condensation, PhD Thesis, California Institute of Technology (1988).

Table 1 : List of Equipment Used in Experiments

Particle Detection :

    direct measurement : TSI Model 3020 condensation nucleus counter

    after DMA :   TSI Model 3760 condensation nucleus counter (MSA expts.)

                          TSI Model 3020 condensation nucleus counter (H_2SO_4 expts.)

Particle Size Distribution :

    TSI Model 3071 differential mobility analyzer (MSA experiments)

    short body differential mobility analyzer (H_2SO_4 experiments)

Flowmeter pressure transducers :

    Baratron 223BD-00010AAB : 0-10 torr

Pressure Gauges :

    Dwyer Magnehelic gages :   water bubbler : 0-40 " H_2O

                                   acid bubbler : 0-5 psig

                                   short DMA sheath air : 0-3 psig

    Wallace and Tiernan : flow control assembly :   FA145 0-90 " Hg

Temperature :

    Analogue Devices AD5903F thermistors

Multimeter :

    Hewlett Packard Model 34702A

Constant temperature recirculating refrigeration bath :

    Neslab Model RTE-8DD

Table 2 : Thermistor Calibrations, T is temperature in $°C$ and V is the measured voltage.

Thermistor	Formula
T_1	$T_1 = 9.8346V + 1.9994$
T_2	$T_2 = 9.7614V + 0.82185$
T_3	$T_3 = 10.225V + 0.67312$
T_5	$T_5 = 9.9907V - 0.52799$
T_6	$T_6 = 10.104V - 1.6984$
T_p	$T_p = 10.039V - 39.834$

Table 3 : Flowmeter calibrations, F is flowrate in $l\ min^{-1}$ and V is the measured voltage.

Flow	Formula
Dry air, F_d	$F_d = 0.041288\ V^3 - 0.19171\ V^2 + 1.01713\ V - 0.0014707$
Acidic air, F_a	$F_a = 0.16002\ V^3 - 0.58897\ V^2 + 1.7883\ V - 0.010301$
Humid air, F_h	$F_d = -0.0036044\ V^3 - 0.18264\ V^2 + 1.1616\ V - 0.0054522$
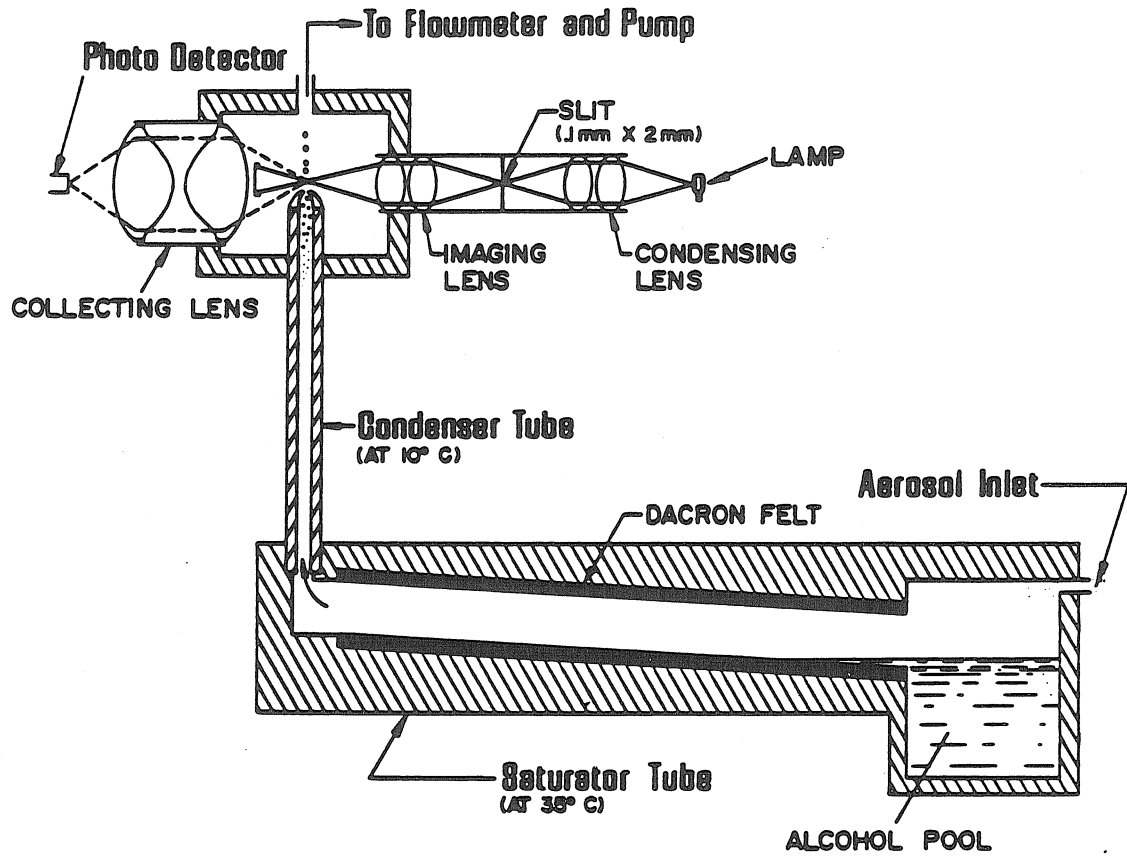
Figure 1. : Schematic of the TSI 3020 condensation nucleus counter.
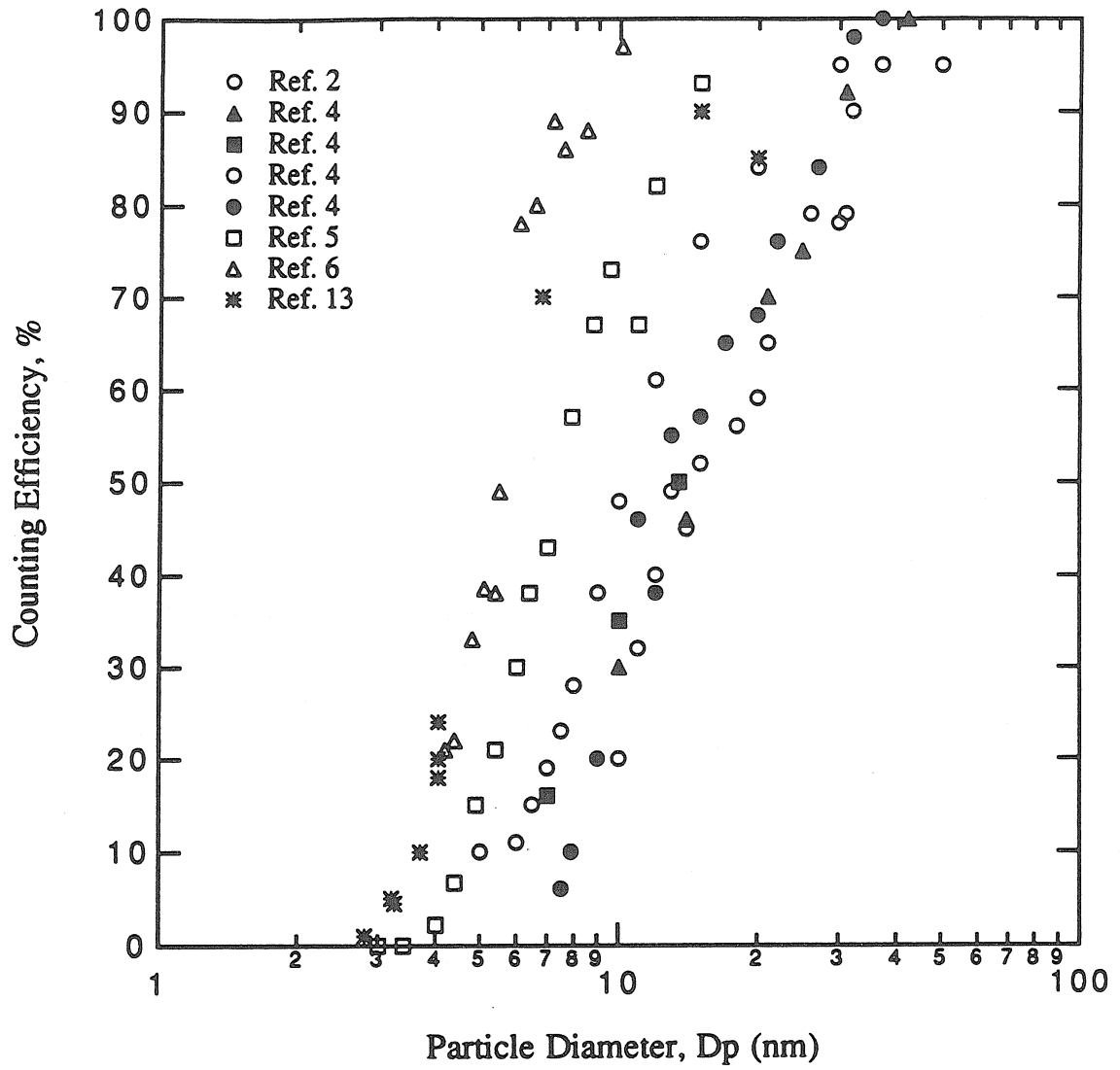
Figure 2 : Detection efficiency of the TSI 3020 condensation nucleus counter.
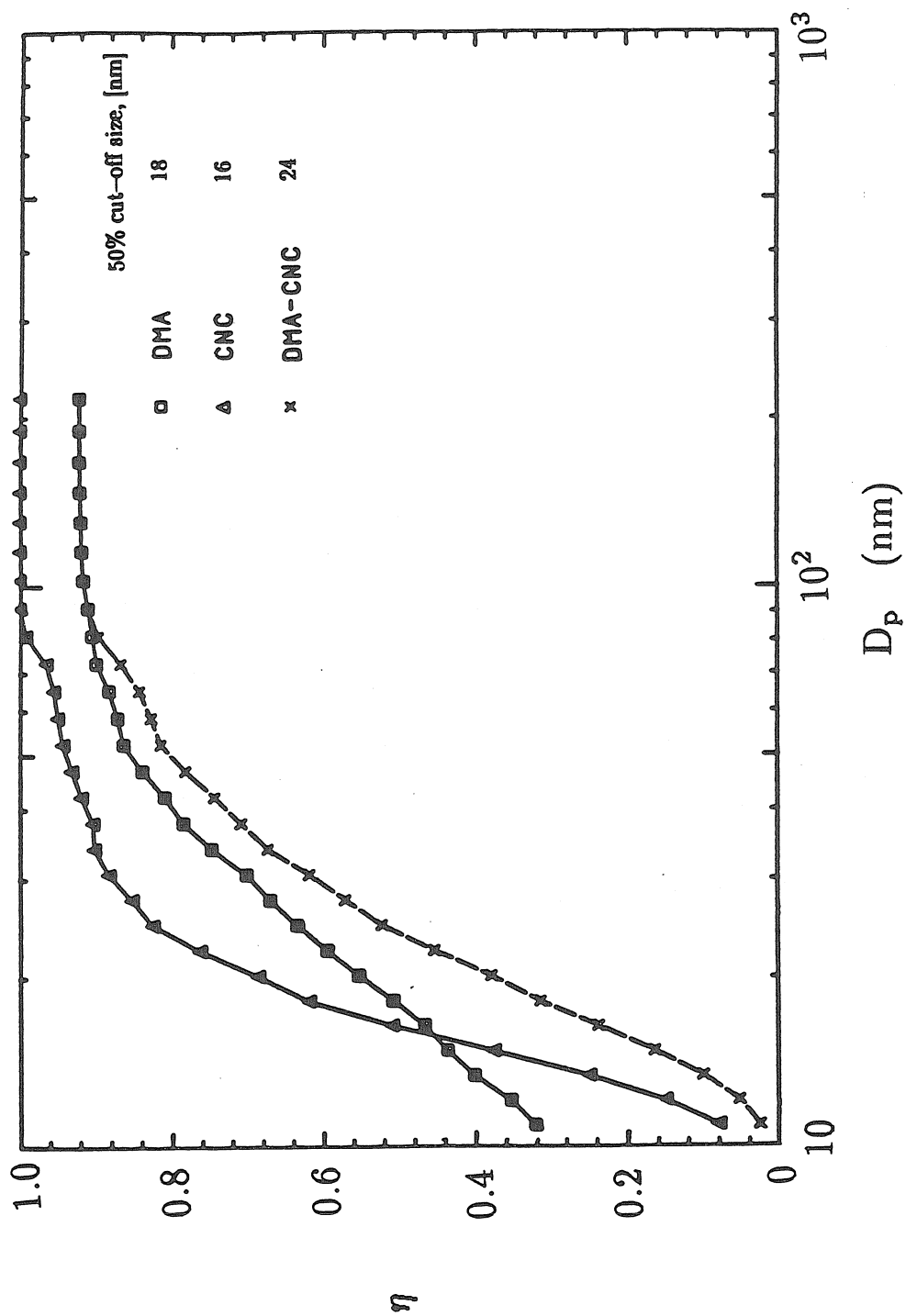
Figure 3 : Particle detection efficiency for the TSI 3760 condensation nucleus counter alone and combined with the TSI 3071 differential mobility analyzer.
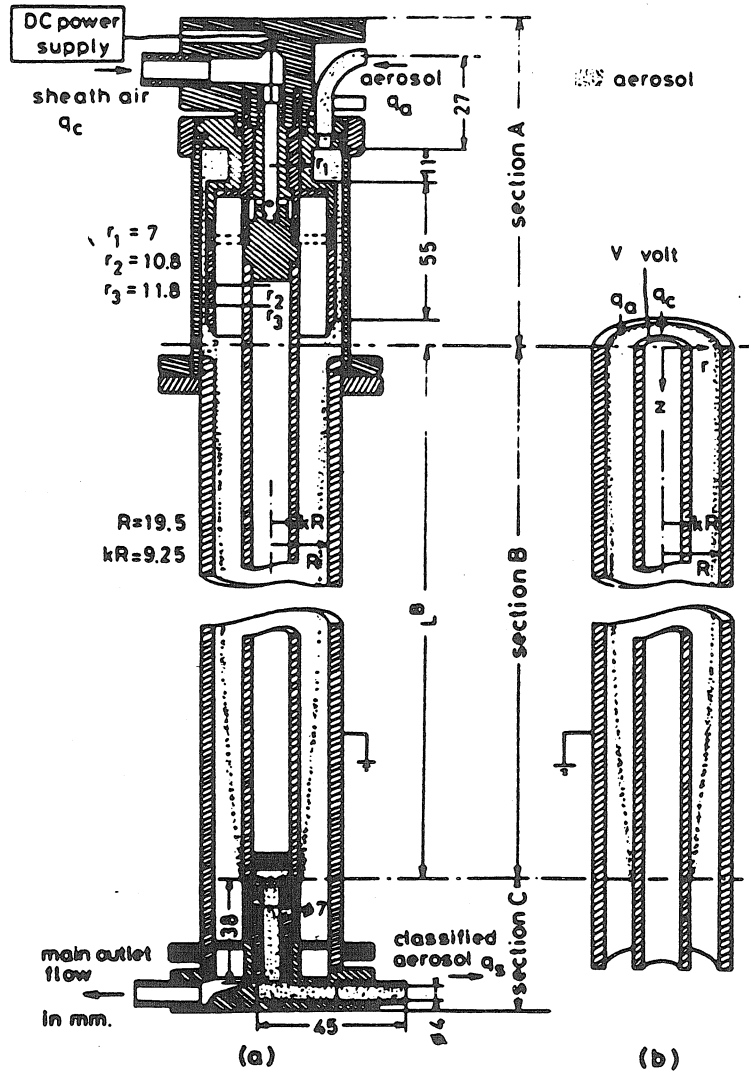
Figure 4 : Schematic of the differential mobility analyzer.
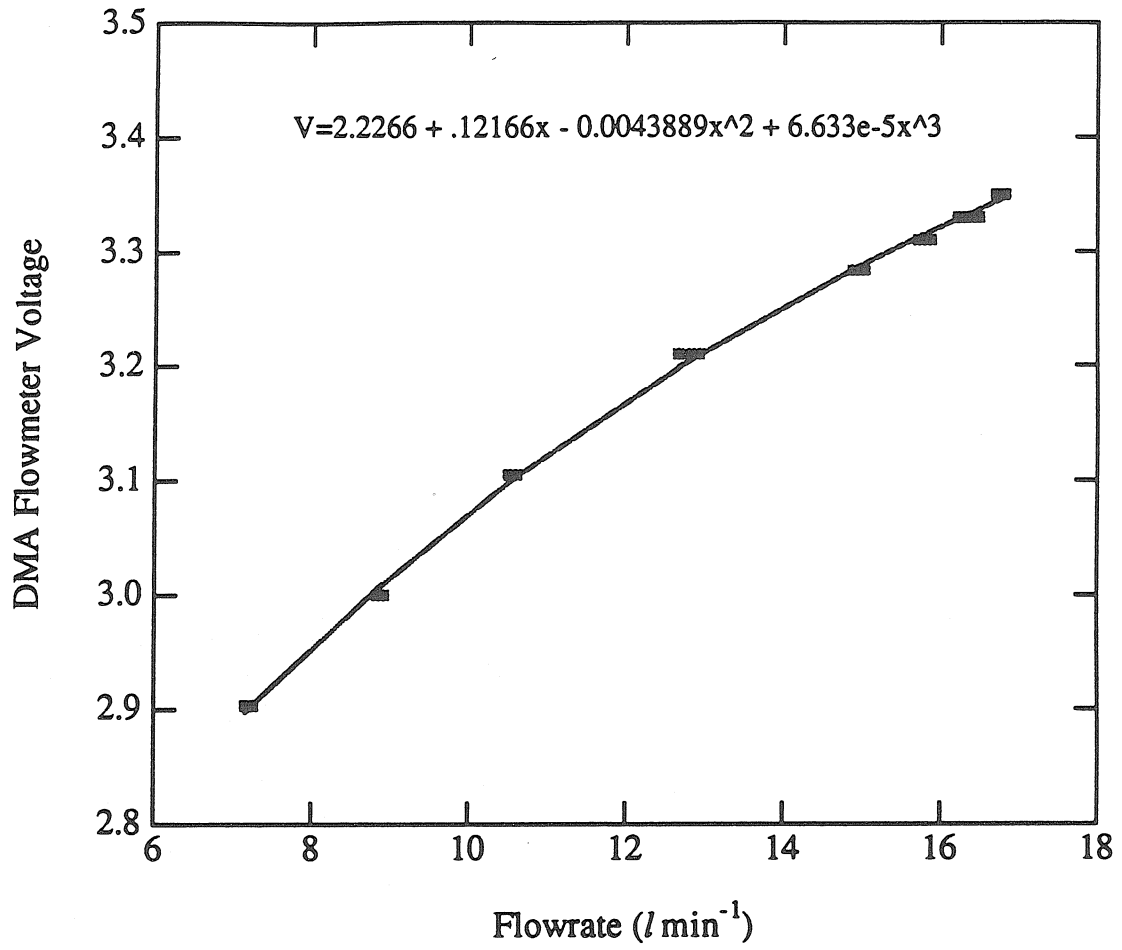
Figure 5 : Sheath air calibration for the 3071 differential mobility analyzer.
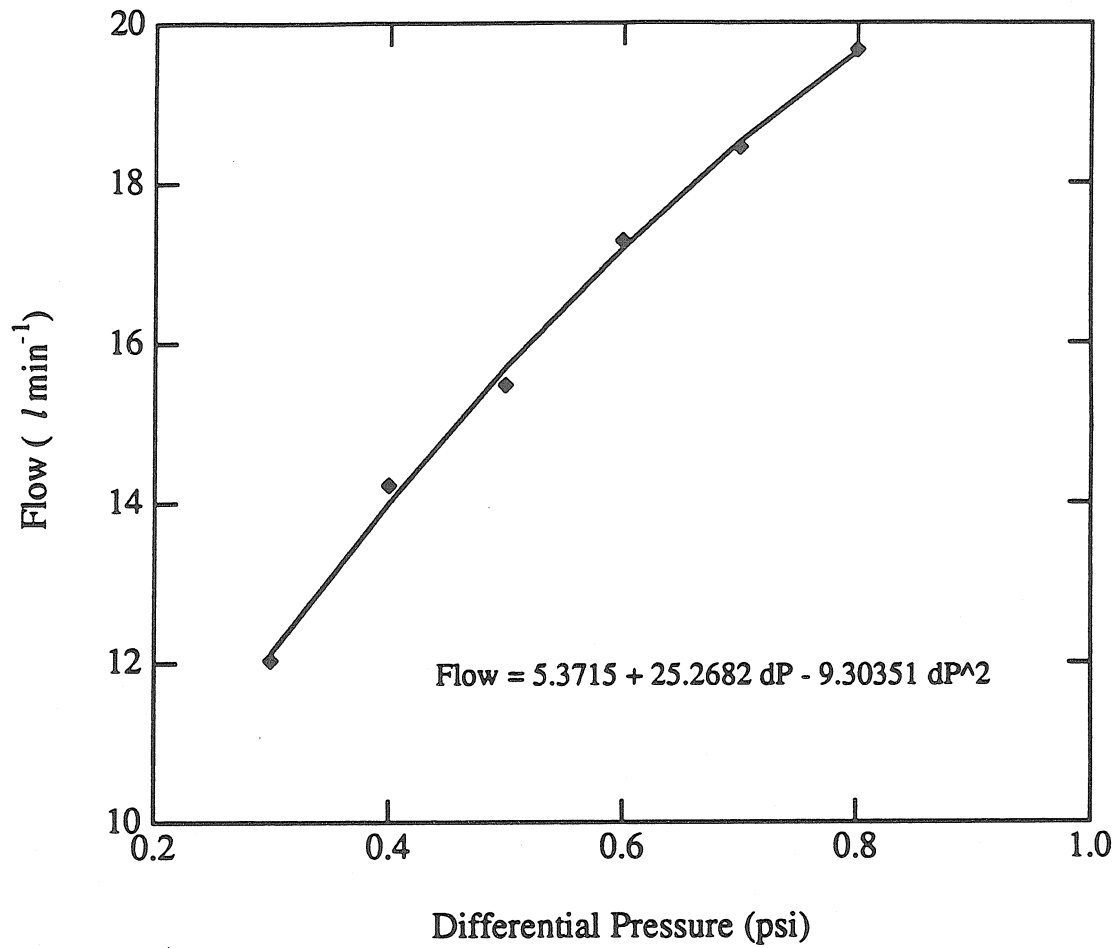
Figure 6 : Sheath air calibration for the short body (L^B = 10 cm) differential mobility analyzer.
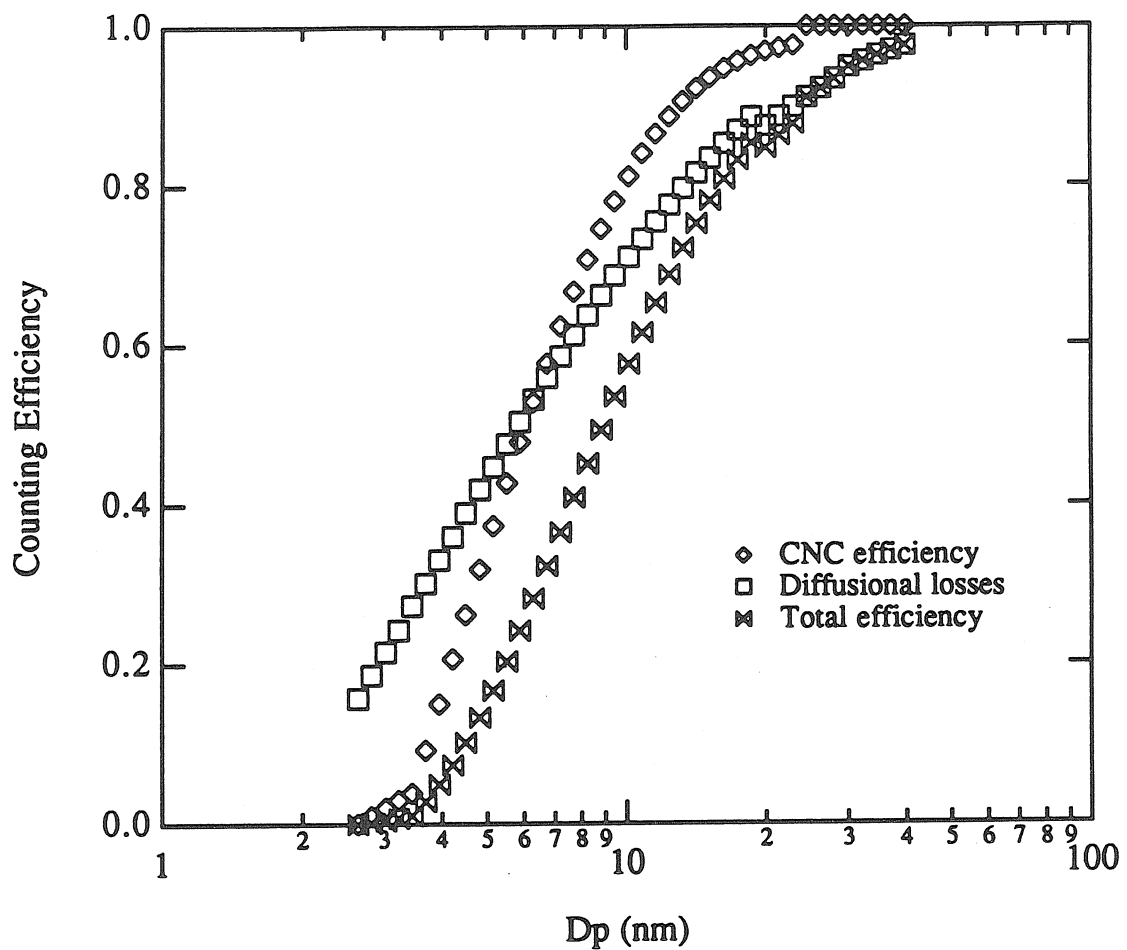
Figure 7 : Combined detection efficiency for the 3020 condensation nucleus counter and the short body differential mobility analyzer.

Figure 8 : Linearizing circuit for the AD590 series thermistor.

TEFLON FITTING

GLASS TUBING

TEFLON TUBING

THERMISTOR

HEAT SINK COMPOUND

TYGON TUBING

SILICONE RUBBER SEALANT

STAINLESS STEEL CASING

TEFLON FITTING

THERMISTOR

HEAT SINK COMPOUND
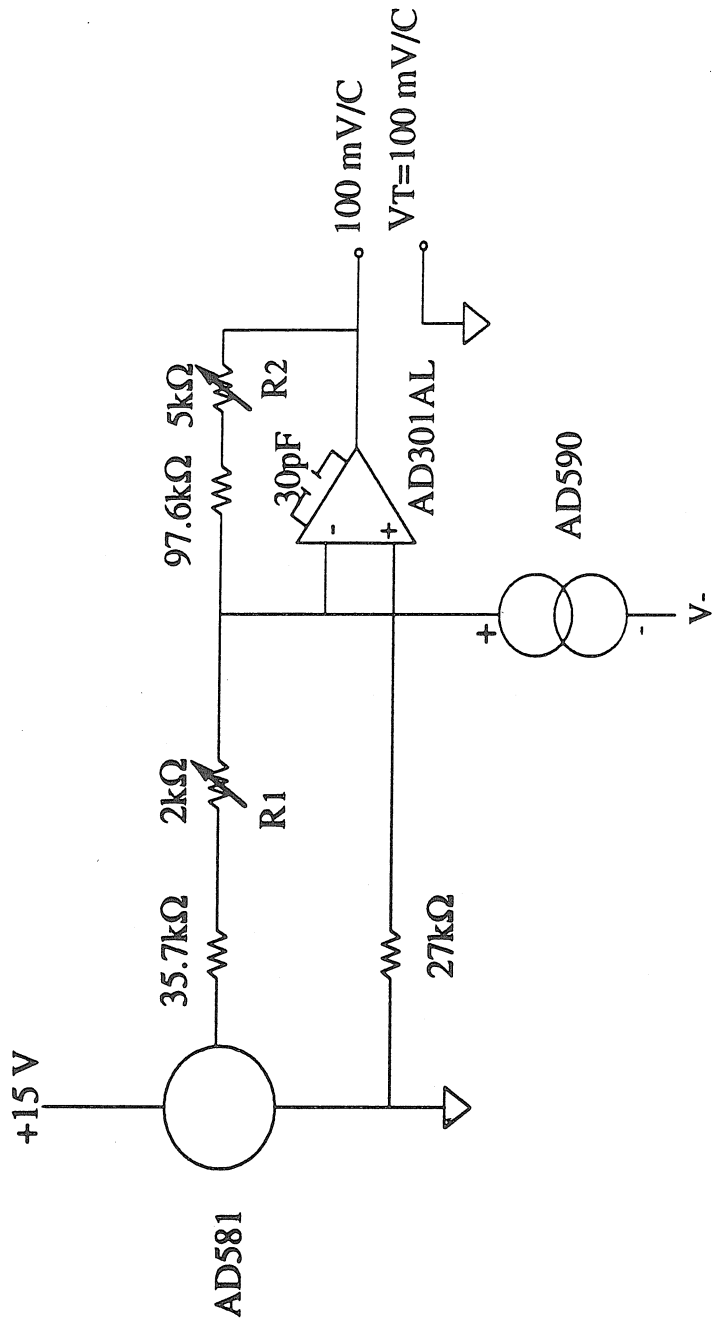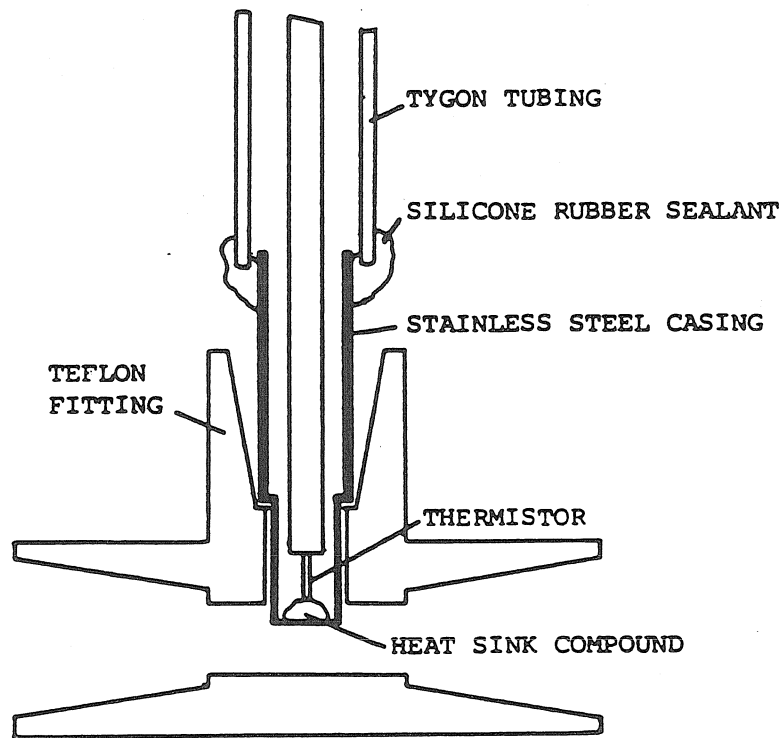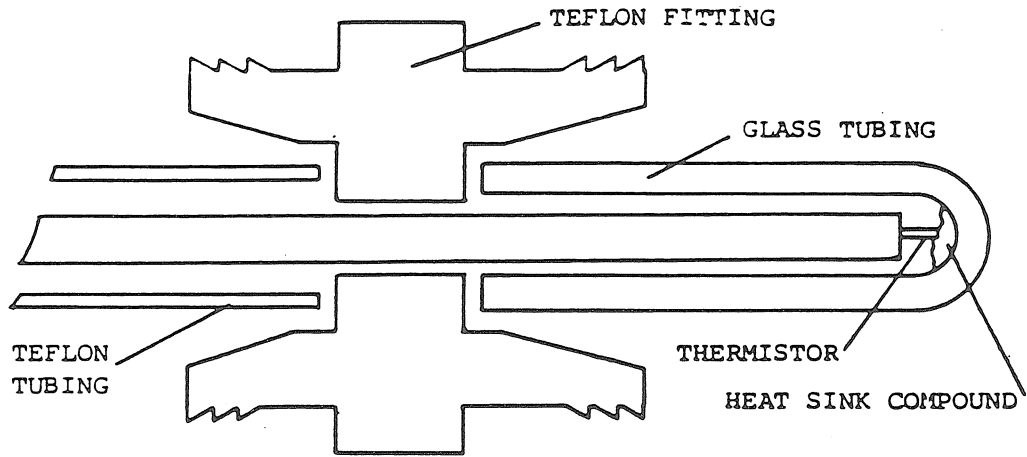
Figure 9 : Schematic diagram of the thermistor placement.
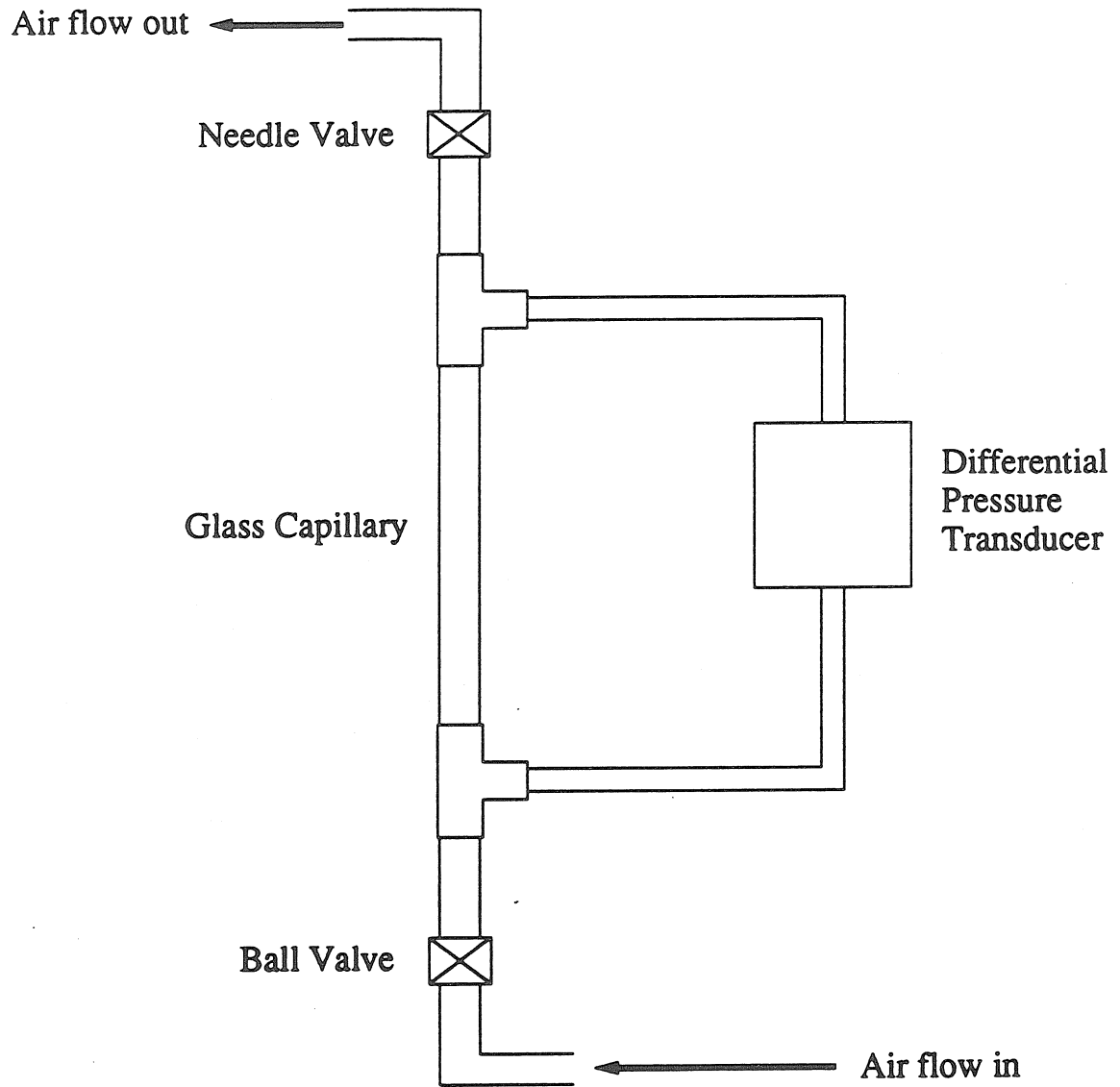
Figure 10 : Schematic of the capillary flowmeters.

APPENDIX B

Estimation of Uncertainty and Error
in the Experimental Results

I. Total Number Concentration Experiments

The sources of uncertainty in the measurement of total number concentration as a function of saturation level include uncertainties in the measured values of temperature, pressure, flowrate which affect the calculated values of relative humidity, Rh, relative acidity, Ra, and residence time. In addition there are uncertainties related to particle detection, vapor and particle losses, and hydrodynamic uncertainties associated with the initial mixing of the humid and acidic streams and subsequent flow through the mixer and reaction chamber.

A. Relative Humidity

The uncertainty in the calculated value of relative humidity is a function of the uncertainties in the temperature, pressure and flowrates. The relative humidity after mixing is

$$Rh = \frac{p_l \, Y_w \, F_h}{p_w(T_m) \, [(1+Y_w)F_h + F_d + F_a]} \tag{1}$$

where F_h, F_d and F_a are the humid, dry and acidic flows, p_l is the absolute pressure in the laboratory, $p_w(T_m)$ is the saturation vapor pressure of water at the temperature inside the

mixer and T_m is equal to the temperature in the nucleation and growth tube. The uncertainty in Rh is therefore given by

$$\frac{dRh}{Rh} = \frac{dY_w}{Y_w} + \frac{dF_t}{F_t} + \frac{dF_h}{F_h} + \frac{dp_l}{p_l} + \frac{dp_w(T_m)}{p_w(T_m)} \tag{2}$$

Y_w, the ratio of the moles of water to the moles of dry air is

$$Y_w = \frac{p_w(T_{wb})}{p_{wb} - p_w(T_{wb})} \tag{3}$$

Here $p_w(T_{wb})$ is the saturation vapor pressure of water at the temperature inside the water bubbler and p_{wb} is the measured pressure inside the water bubbler. The variation of Y_w is therefore given by

$$\frac{dY_w}{Y_w} = \frac{dp_{wb}}{p_{wb}} + \frac{dp_w(T_{wb})}{p_w(T_{wb})} \tag{4}$$

The least significant error is due to the uncertainty in the laboratory pressure since this value may be read to 0.1 mm Hg on an average reading of 760 mm Hg. Thus the pressure is known to better than $0.1/760 = 10^{-4}$. The uncertainty in the temperature readings is related to the calibration procedure and uncertainty in the voltage measurement. Based on the calibration results of the thermistors a reasonable estimate of the uncertainty in the temperature readings is 0.05 ° C.

The uncertainty in the saturation vapor pressure of water may be related to the uncertainty in the temperature measurement, T, by assuming that the vapor pressure may be expressed as

$$\ln p_w(T) = \frac{A}{T} + B \tag{5}$$

therefore

$$\frac{dp_w(T)}{p_w} = \frac{-A}{T^2}dT \tag{6}$$

$A \cong - 5216$ for water on the interval $20\degree C < T < 30\degree C$, therefore at $25\degree C$
$\frac{dp_w(T)}{p_w} \cong 2.9 \times 10^{-3}$.

Inside the water bubbler the total pressure is the sum of the gauge, p_{wbg} plus lab pressures and therefore

$$\frac{dp_{wb}}{p_{wb}} = \frac{d(p_{wbg} + p_l)}{p_{wbg} + p_l} \tag{7}$$

The pressure gauge could be read to the nearest 0.4 mm Hg, thus the uncertainty was less than $0.5/760 = 6 \times 10^{-4}$.

The use of differential pressure transducers and capillary flow meters has greatly improved the reliability of the flow measurements over the earlier experiments.[1] Reading errors associated with differential pressure gages are eliminated, especially at the low flow rates. Placing the flow controlling needle valves at the downstream side of the capillaries and maintaining the pressure in the capillaries constant also improves reproducibility. Based on the calibration results presented in Appendix A, the error in both the total flow and the humid flow is estimated at 3%.

The major source of error is due to uncertainties in the flow. The total uncertainty in the relative humidity may thus be expressed as

$$\frac{(\sigma Rh)^2}{Rh^2} \cong \frac{(dF_h)^2}{F_h^2} + \frac{(dF_t)^2}{F_t^2} + 2\frac{(dp_w(T))^2}{p_w^2(T)} + \frac{(dp_{wb})^2}{p_{wb}^2} \tag{8}$$

$$\frac{\sigma Rh}{Rh} \cong (0.03^2 + 0.03^2 + 2(2.9 \times 10^{-3})^2 + (6 \times 10^{-4})^2)^{1/2} = 0.043 \tag{9}$$

Thus a reasonable estimate of the total uncertainty in the relative humidity is 5%.

B. Relative Acidity

Approximately 300 g of acid were used during each test, providing a height of more than 10 cm through which the fine air bubbles had to rise and which should provide adequate time and surface area for equilibration between the two phases. Combined with the extremely short distance between the top of the filter and the center of the mixer, the assumption of a saturated acid stream should be a reasonable one. The relative acidity after mixing is given by

$$Ra = \frac{p_l \, p_a(T_{ab}) \, F_a}{p_{ab} \, p_a(T_m) \, [(1+Y_w)F_h + F_d + F_a]} \tag{10}$$

where p_{ab}, $p_a(T_{ab})$ and $p_a(T_m)$ are the actual acid bubbler pressure, the saturation vapor pressure of the acid at the temperature in the acid bubbler and the saturation vapor pressure of acid at the temperature of the mixer. Furthermore the ratio of moles of acid to moles of air, Y_a, is approximately equal to zero because the vapor pressure of the acid at 25 ° C is approximately 1 ppm. The uncertainty for relative acidity then becomes

$$\frac{dRa}{Ra} = \frac{dp_{ab}}{p_{ab}} + \frac{dF_a}{F_a} + \frac{dF_t}{F_t} + \frac{dp_a(T_m)}{p_a(T_m)^2} \tag{11}$$

where the variation in vapor pressure of methanesulfonic acid with temperature has recently been measured by Tang and Munkelwitz[2] who give the following correlation with $\ln p_a(T)$ in atmospheres.

$$\ln p_a(T) = 22.81669 - \frac{9030.18}{T} \tag{12}$$

The uncertainty due to reading error on the acid bubbler pressure is approximately 2.6 mm Hg on a total pressure of 760+50 mm Hg, which is a relative error of 3.2×10^{-3}. A $0.05\,^\circ C$ uncertainty in the temperature of the acid bubbler at $25\,^\circ C$ gives a relative error in the saturation vapor pressure of 5×10^{-3}. The uncertainty in the flow rate through the acid bubbler is also estimated at 0.03 thus the relative acidity is again found to depend mostly on the flow rates. This gives

$$\frac{(\sigma Ra)^2}{Ra^2} \cong \frac{(dF_a)^2}{F_a^2} + \frac{(dF_t)^2}{F_t^2} + \frac{(dp_a(T_m))^2}{p_a^2(T_m)} + \frac{(dp_{ab})^2}{p_{ab}^2} \tag{13}$$

and

$$\frac{\sigma Rh}{Rh} \cong (0.03^2 + 0.03^2 + (3.2 \times 10^{-3})^2 + (5 \times 10^{-3})^2)^{1/2} = 0.043 \tag{14}$$

Again a reasonable estimate of the uncertainty in the relative acidity is 5%.

C. Acid Purity

In addition to the questions of the initial purity of the acid used in the experiments, which has been addressed in the body of the thesis, it is important to consider contamination of the acid by absorption of water from the dry air stream during an experiment. The dry air stream contains less that 11 ppm of water. An additional air drying column between the air bottle and the equipment protects against a potentially contaminated bottle. Flow rates through the acid bubbler are always less that $1 \ l \ min^{-1}$, thus less than 0.003 moles of water will be absorbed in 5 days of continuous running, which is a negligible amount. A constant flow of air out of the bubbler also minimizes diffusion of water vapor from the humid stream back on to the acid filters or into the bubbler itself. Leak testing of the apparatus before beginning an experiment at pressures roughly five times higher than encountered during an experiment minimized the chance of leakage of water from the bath into the apparatus during a test.

D. CNC Response

Condensation nucleus counters have limited counting efficiencies when particles become smaller than about 30 nm.[3-7] Generally the smallest particles are formed when nucleation rates are highest. From the particle size distributions measured during the MSA experiments it is clear that the peaks of the distribution are well above the particle diameter where limited counting efficiency becomes important, and that the total number of particles is dominated by the peak of the distribution. In the H_2SO_4 experiments, although the peak is within the range for which counting efficiency and diffusion losses are important, the fact that the peak is still observed after correcting the particle size distributions for these effects implies that most of the particles produced are counted. Because it is not possible to

measure particle size distributions at low nucleation rates it is not possible to correct the measured number concentrations using the counting efficiency correlation established in Appendix A. Thus this uncertainty still exists in the final nucleation rates but it its probably still less than the factor of 3 to 4 that was the overall repeatability of the experiments.

The length of time spent in the CNC (4.8 s) is small compared to the total residence time in the reactor, thus if nucleation continues in the CNC the total number of particles will still be dominated by those formed in the reactor. Furthermore, because it was possible to obtain very low number concentrations during each experiment, the potential problem of nucleation between the working fluid of the CNC and the experimental gases does not appear to be an issue.

Coincidence error in total particle count mode was corrected to give the actual particle count, N_a, in terms of the indicated particle count, N_i, using

$$N_a = N_i \exp(N_a Q t) \tag{15}$$

where Q is the sample flowrate (5 cm^3/s), t is the time spent in the sampling volume (35 µs) and the approximation of $N_a = N_i$ is made in evaluating the exponential.

The effect of statistical error must also be addressed at low particle counts where the relative error is given by

$$\frac{\sigma_r}{N} = \frac{1}{\sqrt{N}} = \frac{1}{\sqrt{N Q t_{av}}} \tag{16}$$

and where t_{av} is the time over which the counts are averaged. With the value of t_{av} for $N<10$ equal to 20 seconds and Q given as above,

$$\frac{\sigma_T}{N} = \frac{1}{10\sqrt{N}} = 0.3 \tag{17}$$

when N is 0.1. So much of the variation observed at low particle counts may simply be statistical in nature. Overall, the total number of particles measured should be close to the number of particles formed by binary nucleation.

E. Loss of Vapor and Particles to Surfaces

The loss of vapor and particles to the walls of the apparatus will affect the total number of particles observed in several ways. Particles formed and subsequently deposited on the walls cannot be counted by the particle detector. Of greater concern however is the strong reduction in nucleation rate that will occur if vapor losses are significant during transport of the air streams from the saturators to the mixer, in the mixer itself or along the length of the reactor at low nucleation rates. Vapor loss will also reduce the final size to which particles can grow and can therefore increase the number of particles lost by diffusional deposition because of the strong dependence of particle diffusivity on particle diameter.

A simple way to estimate both vapor and particle loss from a flowing gas stream in laminar flow in a circular tube is to model it as a Graetz problem. The solution to this problem given by Brown[8] was used here. This model assumes the walls act as perfect sinks for the vapors and particles, and will act as an upper bound to the losses actually incurred. Flows in the equipment give rise to Reynolds numbers in the range from 300

(1.0 l min^{-1} in .48 mm ID tubing) to 30 (1 l min^{-1} flow in the 51 mm dia ID reactor), thus the assumption of laminar flow is a good one.

The variation of average particle concentration with dimensionless distance is given by

$$\frac{n_{av}}{n_0} = 8 \sum_{n=0}^{\infty} \frac{G_n}{\lambda_n^2} \exp(-\lambda_n^2 x_1) \tag{18}$$

where G_n and λ_n are the coefficients and eigenvalues of the series solution and x_1 is the dimensionless distance. For vapor losses

$$x_1 = \frac{2x}{a^2} \frac{D_A}{U} \tag{19}$$

where D_A is the vapor diffusivity in air, U is the average velocity of the gas stream, a is the tube diameter and x is the axial distance. At 25 ° C D_A is estimated at 0.118 cm^2 s^{-1} for MSA and at 0.22 cm^2 s^{-1} for water. Likewise, for particle losses,

$$x_1 = \frac{2x}{a^2} \frac{D}{U} \tag{20}$$

where D is now the particle diffusivity and is calculated using the Stokes-Einstein relationship. Values of D were taken from those tabulated in Friedlander.[9]

Particles will be lost only downstream of the mixer and will be removed from the gas stream more slowly than vapor molecules because of their lower diffusivities. Figure 1 shows the predicted losses for 1, 5 and 10 nm particles as a function of dimensionless length along the reactor. Even for particles as small as 1 nm, which are on the order of the

critical nuclei, losses amount to only about 50% by the end of the reactor. This loss decreases rapidly as the size of particle increases. Thus particle losses due to diffusional deposition should not greatly impact the final number of particles observed by the CNC, if we consider that overall repeatability of the experiments is at best a factor 3 to 4. Losses due to impaction of larger particles on surfaces at bends have not been considered here.

Vapor losses along the reactor are potentially far more significant and because of the highly nonlinear dependence of nucleation rate on saturation levels, are expected to have a much greater influence on the number of particles produced than particle loss itself. The vapor losses predicted by the Graetz solution for water and MSA are shown in Fig. 2. However, it must be noted that condensation on the walls of the reactor was never observed during the experiments. This implies that the walls are not acting as perfect sinks, rather they are coming to some level of equilibrium with both the acid and water vapors in the gas stream. As demonstrated in Chapter 2, the fact that experiment 16.13 agreed so well with experiment 16.01 despite the three day interval between the two tests, would favour the argument that this equilibrium has already been established by the time experiment 16.01 was conducted.

The loss of water vapor from the humid gas stream as it travels from the bubbler to the mixer may be analyzed by first considering the amount of water required to cover the entire surface with a monolayer of water. Assuming 30 cm of 0.51 cm ID tubing, this corresponds to a surface area of ~6 cm^2. A monolayer coverage by water corresponds to 2×10^{-9} moles of water. As in the relative humidity calculations, the ratio of moles of water to moles of air exiting the water bubbler is given by $Y_w \cong p_w(T_{wb}) / p_{lab} \cong 0.03$ at 25 ° C. Even at a flow rate as low as 0.01 lpm, $\sim 2 \times 10^{-5}$ moles of water min^{-1} are therefore available to provide the initial monolayer coverage. Since condensation was not observed while running these experiments, the walls cannot be continuously absorbing significant

amount of vapor from the passing gas stream and so the the relative humidities, as calculated previously, should be good estimates of the actual relative humidities.

F. Losses Due to Coagulation of the Aerosol

There are two extreme cases that should be considered that could lead to significant particle losses by coagulation in the experimental system. These correspond to high particle concentrations and large values of coagulation coefficient. The case of a high initial particle concentration would result from extremely rapid nucleation at the entrance of the reactor. Relatively large coagulation coefficients could occur when nucleation is significant along the length of the reactor thereby leading to a highly polydisperse system. It is best to look at these cases by referring to Fig. 3 where the change in the aerosol number concentration has been plotted as a function of initial particle concentration and coagulation coefficient. This graph was generated by plotting the solution of the coagulation equation assuming a constant value of the coagulation coefficient given by

$$\frac{N(t)}{N_0} = \frac{1}{1 + \dfrac{t\, K\, N_0}{2}} \tag{21}$$

where N_0 is the initial number concentration, $N(t)$ is the number concentration after time t and K is the coagulation coefficient.

In the case of high initial concentrations, nucleation rate calculations show that a typical critical nucleus contains about 10 - 20 acid molecules and has a diameter of roughly 1.5 nm. Values of K given by Flagan and Seinfeld[11] for particles of this size are on the order of 10^{-9} cm^3 s^{-1}. Thus from Fig. 3, coagulation could be important if the initial

concentration is higher than 10^8 cm^{-3}. The worst case scenario in the experiments occurs at Ra = 0.65 where the number of acid molecules in the gas phase is about 10^{13} cm^{-3}. If all of the acid is immediately converted into particles in the absence of condensation, there could be as many as ~10^{12} particles cm^{-3} initially. Coagulation alone would reduce the number to about 10^8 cm^{-3} after 22 s, which represents a significant change. However it is unlikely that nucleation rates that high can be described by classical steady state nucleation theory and problems regarding relative times scales of mixing and nucleation in the experiment are most likely of greater concern than coagulation.

For constant nucleation along the length of the reactor, coagulation coefficients between large (~250 nm) particles and particles of the size of the critical nucleus are on the order of 10^{-6} cm^{-3} s^{-1}. However, for continued nucleation, the total number of particles must be low (< ~10^4 cm^{-3}) and from Fig. 3 it is clear that coagulation is not of concern here.

G. Time Scales in the Mixer

The residence time in the mixer, τ_{rm}, is approximately 60 ms since the volume in the mixing chamber is ~1.0 cm^3 and the total flow through the mixer is 1.0 l min^{-1}. This time scale is of interest because it shows that τ_{rm} / τ_{rr} is small (τ_{rr} is the residence time of the reactor $\cong$ 18 sec) and thus the number of particles that may form in the mixer rather than in the reactor is very small. As well, by comparing τ_{rm} to the time scale of mixing τ_m, the degree of mixing in the stream entering the reactor can be estimated.

During the experiments, mixing is assumed to occur instantaneously, with nucleation and condensation proceeding from initial saturation levels determined by the mixed stream.

There is however a finite amount of time associated with mixing that may be estimated based on Taylor microscale arguments. The characteristic mixing time, τ_m, should depend on the kinetic energy available from the high velocity gas stream entering the chamber through the eight 0.5 mm ports, KE, the amount of vapor present in the chamber M, and some characteristic length scale L_c over which mixing takes place. A simple expression for τ_m combining these quantities is[11]

$$\tau_m = \left(\frac{ML_c^2}{KE}\right)^{1/3} \tag{22}$$

where $KE = \frac{1}{2}\rho Q u^2$, ρ is the density of the incoming humid air stream and Q is the volumetric flow rate. The values of τ_m estimated using this expression and the corresponding values of τ_m/τ_{rm} are given in Table 1. Generally τ_m is on the order of 10 ms, with the ratio of residence to mixing times ranging from 5 to 10. A more extensive set of calculations completed by Kreidenweis[11] showed that the average nucleation rate was not perturbed greatly by some incompleteness in mixing.

II. Particle Size Experiments

The sources of uncertainty in the particle size measurements are associated with uncertainty in the mobility of the particle band produced by the DMA, which depends on the flowrates and voltage control of the DMA, the counting efficiency of the CNC, particle losses in the lines and data inversion.

A. Particle Mobility

The aerosol stream at the sample outlet of the DMA contains particles with mobilities characterized by a central peak mobility value Z_{pc} and a mobility bandwidth ΔZ_p. In the absence of multiple charging or agglomeration, mobility correspond directly to a single particle diameter. When the Brownian motion of the particles is negligible, these quantities are given by

$$Z_{pc} = \frac{q_c + 0.5(q_a - q_s)}{2\pi L^B V} \ln \frac{R}{kR} \tag{23}$$

and

$$\Delta Z_p = \frac{q_a + q_s}{4\pi L^B V} \ln \frac{R}{kR} \tag{24}$$

where q_c, q_a and q_s are the clean sheath air, inlet aerosol and sample flowrates respectively, L^B is the length of the DMA classifier tube, V is the voltage and R/kR is the ratio of the outer to inner diameters inside the classifier tube.

In the recirculating sheath air system, $q_a = q_s$, thus the error associated with assigning the mobility of a given fraction of particles is given by

$$\frac{dZ_{pc}}{Z_{pc}} = \frac{dq_c}{q_c} + \frac{dV}{V} + \frac{d\Lambda}{\Lambda} \tag{25}$$

where

$$\Lambda = \frac{\ln \frac{R}{kR}}{4\pi L^B} \tag{26}$$

contains the error due to uncertainties in the geometric parameters. The uncertainty is estimated from the tolerance values given in Table 2 which have been taken from the instrument drawings for the 3071 DMA.[12] A conservative estimate of the uncertainty

$d\Lambda/\Lambda = 0.012$.

Voltage readings were checked on the 3071 DMA while it ran in stepping mode, and the difference between the voltage requested by the controlling program and the voltage actually measured ranged from -4% to +1% for voltages higher than 100. Below 100 volts the uncertainties in the voltage appear to be as high as 10-15%. Apart from this extreme, which generally only represents 3 or 4 points in the distribution, in general a worst case uncertainty is estimated as 4%. For the voltage supply used with the short column DMA, agreement with the multimeter was within 1% for voltages required in the experiments.

A calibration of the sheath air flow rates assured the the flow was known to within 3%. This gives and overall uncertainty in particle mobility as

$$\left(\frac{\sigma Zpc}{Zpc}\right)^2 = (.012^2 + .04^2 + .03^2)^{1/2} = .051 \tag{27}$$

or 5% for the 3071 DMA and about 4% for the short column DMA.

B. Particle Detection

The relative uncertainty in the number concentration for the 3071 DMA- 3076 CNC combination was shown by Wang and Flagan[13] to be

$$\frac{\sqrt{V}}{N} \cong \frac{1}{\sqrt{\frac{dN(D_p)}{d\log D_p} \Delta \log D_p \, q_a \, t_c \, p(1-p)}} \tag{28}$$

in the absence of counting error. Here t_c is the counting time and p is the probability that a particle entering the analyzer will be detected. Using the values of p established by Wang and Flagan[13], and a counting time of 0.5 seconds, Fig. 4 illustrates the number concentration corresponding to a signal to noise ratio $\sqrt{V}/N \cong 1$ superimposed on a size distribution with the lowest total number concentration investigated with this instrument. This curve represents the detection limit for the SEMS as used in the MSA particle size experiments. All of the features of interest in these particle size distributions are therefore clearly distinguishable from the background noise.

C. Data Inversion

The sensitivity of the size distributions to the type of inversion scheme is investigated by examining two different inversion methods. Size distributions were first calculated while the data were collected using the simple inversion scheme outlined in Appendix A. This program assumes each particle carries only a single positive charge and does not address the issue that significant numbers of particles on the order of 100 nm and larger may be multiply charged. Figure 5 illustrates the results of inverting the raw data using (a) the simple inversion scheme and (b) the methods and programs developed by Wolfenbarger

and Seinfeld.[14] The latter program (Micron) uses the method of constrained regularization to produce a smooth aerosol distribution. It accounts for the probability of multiple charging and also uses the positive charging probability distribution. Above 50 nm, the value of $dN/d\ln Dp$ is somewhat lower than the first inversion scheme because the contribution due to multiply charged particles has been removed. The shape of the number distribution is otherwise unchanged and the peak in the mass distribution has not been shifted significantly. However, to check more carefully, all of the distributions with mass peaks within the range of the instrument were reinverted using Micron and the mass distributions were recalculated and compared to the distributions calculated using the simple program. From the inverted data graphs it is possible to measure the diameter corresponding to the peak of a distribution to within about 5%. Thus the total uncertainty in the diameter corresponding to the peak of a distribution should be about

$(0.05^2 + 0.05^2)^{1/2} = 0.07$, or 7%.

REFERENCES

[1]S. Kreidenweis, R. Flagan, J. Seinfeld and K. Okuyama, J. Aer. Sci. 20, 585 (1989).

[2]I.N. Tang and H.R.Munkelwitz, J. Coll. Inter. Sci. 141, 109 (1991).

[3]J. K. Agarwal and G. J. Sem, J. Aer. Sci., 11, 343 (1980).

[4]H. Bartz, H. Fissan, C. Helsper, Y. Kousaka, K. Okuyama, N. Fukishima, P.B. Keady, S. Kerrigan, S.A. Fruin, P.H. McMurray, D.Y. Pui and M.R. Stolzenburg, J. Aerosol Sci., 16, 443 (1985).

[5]H. Y. Wen and G. Kasper, J. Aer. Sci., 17, 947 (1986).

[6]P.B. Keady, V.L. Denler, G.J. Sem, M.R. Stolzenburg and P.H. McMurray, in *Atmospheric Aerosols and Nucleation*, Wagner, P.E. and G. Vali Eds., 190 (Springer Verlag, 1988)

[7]K. H. Ahn and B.Y.H. Liu, J. Aerosol Sci., 21, 263 (1990).

[8]G.M. Brown, AIChE J. 6, 179 (1960).

[9]S. K. Friedlander, *Smoke, Dust and Haze : Fundamentals of Aerosol Behavior*, (J. Wiley and Sons, New York, 1977)

[10]R. C. Flagan and J. H. Seinfeld, *Fundamentals of Air Pollution Engineering*,

(Prentice Hall, New Jersey, 1988)

[11]S. M. Kreidenweis, Experimental and Theoretical Studies of Binary Nucleation and Condensation, PhD Thesis, California Institute of Technology (1988).

[12]TSI Model 3071 Electrostatic Classifier Instruction Manual, TSI P/N1933071 (Revised March 1977)

[13]S.C. Wang and R.C. Flagan, Aerosol Sci. Technol. 13, 230 (1990).

[14]J.K. Wolfenbarger and J. H. Seinfeld, J. Aer. Sci., 21, 227 (1990).

Table 1 : Mixing time and the ratio of mixing to residence time in the mixer as functions of the humid air flow.

F_h (cm^3 min^{-1})	F_h (cm^3 s^{-1})	τ_m (ms)	τ_m/τ_{rm} (ms)
200	3.33	23.4	2.6
300	5.00	15.8	3.8
400	6.67	11.9	5.0
500	8.33	9.48	6.3
600	10.0	7.90	7.6
700	11.7	6.77	8.9
800	13.3	5.93	10

Table 2 : Values of tolerance in the dimensions of the TSI Model 3071 DMA.

Dimension	Nominal Value (cm)	Tolerance (cm)
L^B	44.44	+ 0.000 - 0.013
R	1.956	+ 0.006 - 0.000
kR	0.936	+ 0.001 - 0.000
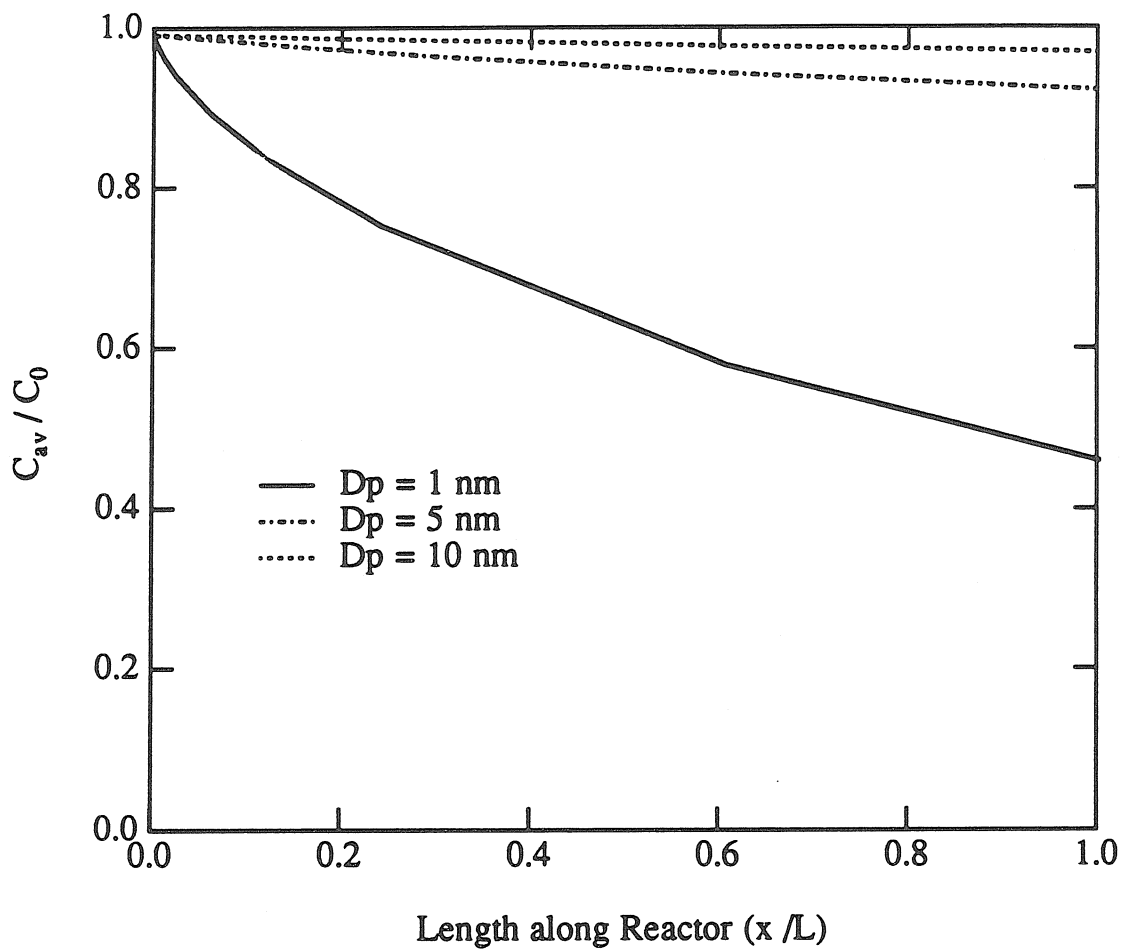
Figure 1 : Particle loss along the length of the reactor for 1, 5 and 10 nm particles.
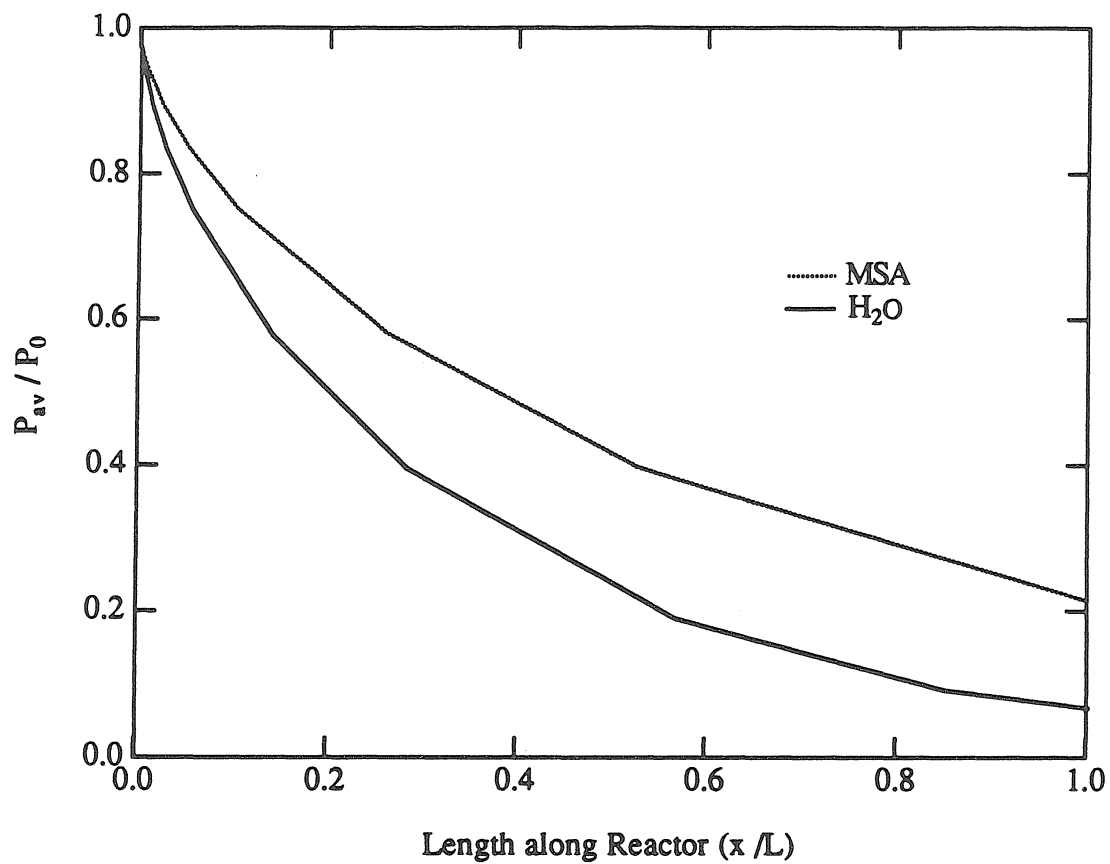
Figure 2 : Vapor losses along the length of the reactor for water and methanesulfonic acid.
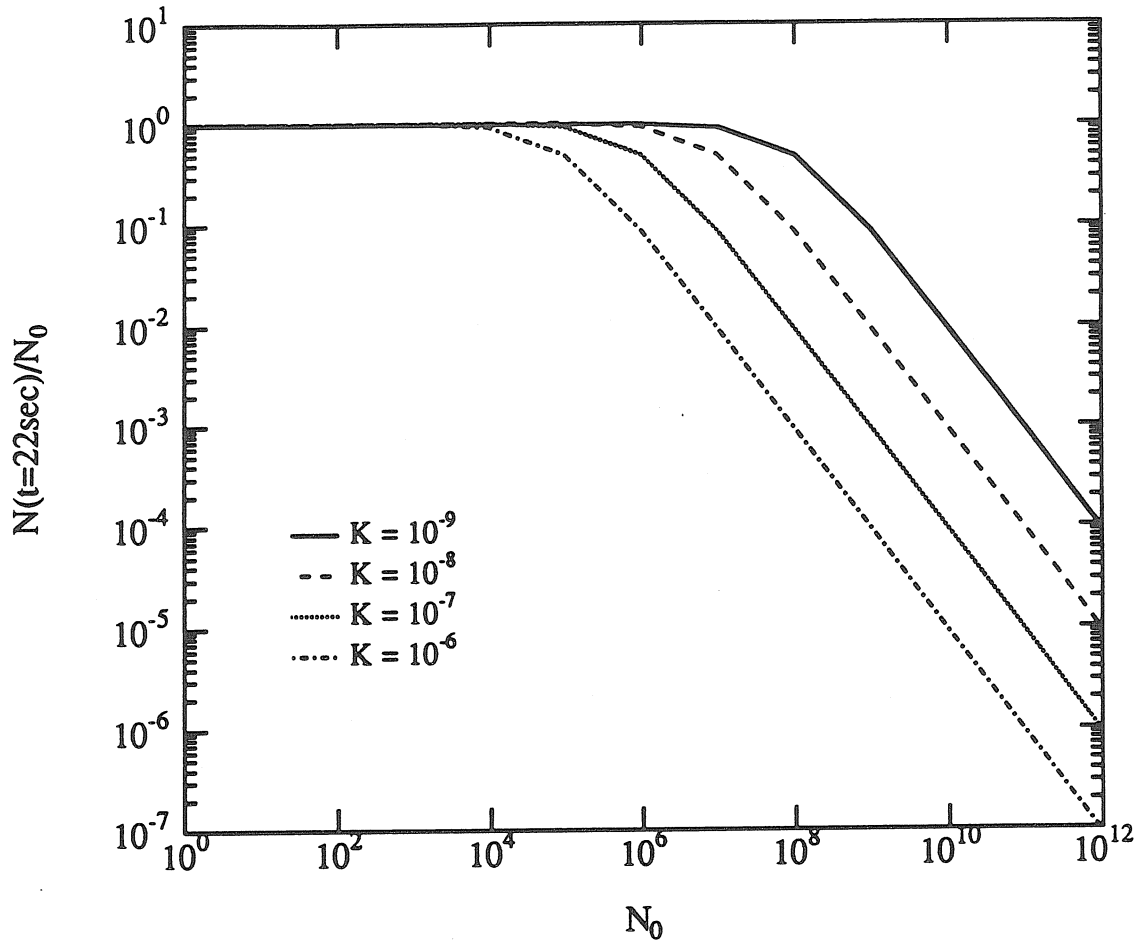
Figure 3 : Change in the particle concentration after 22 s of coagulation as a function of the initial concentration and the coagulation coefficient.
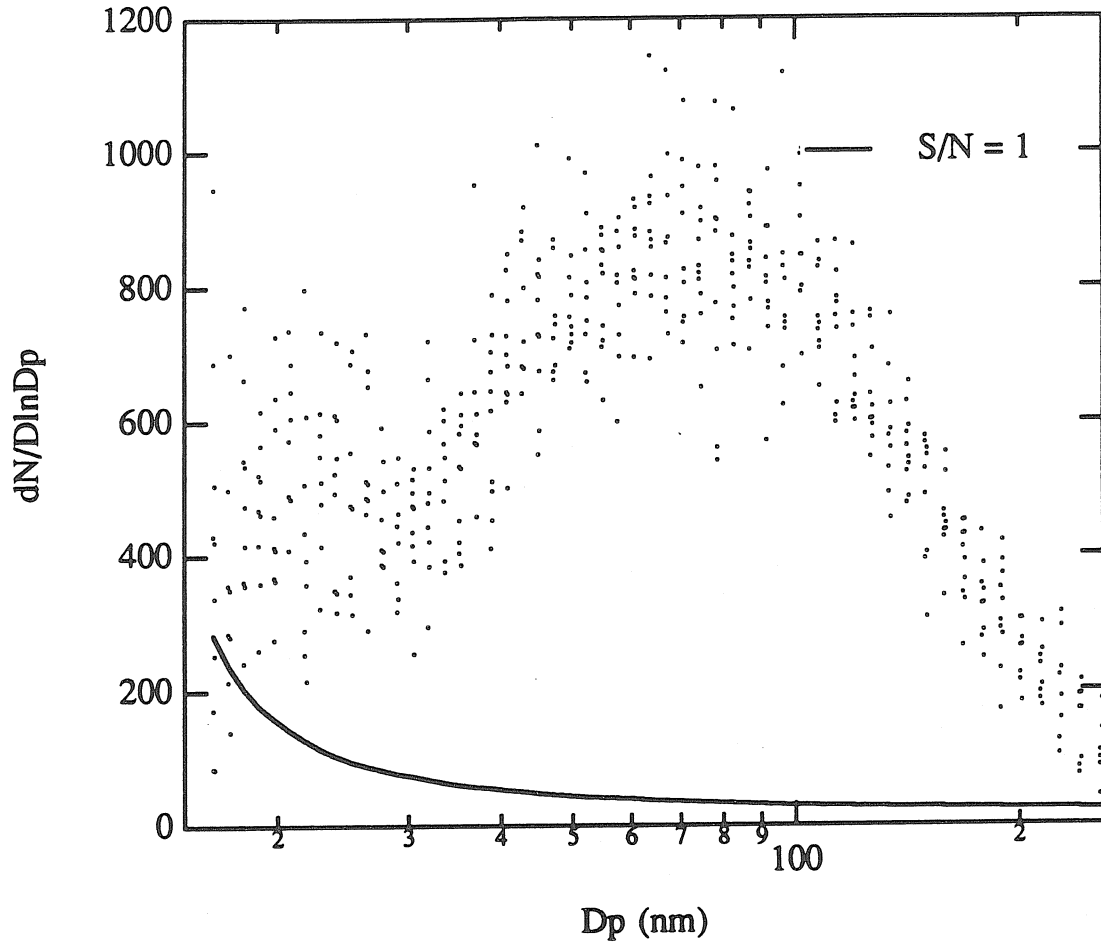
Figure 4 : A typical size distribution is compared to the line showing a signal to noise ratio of 1.
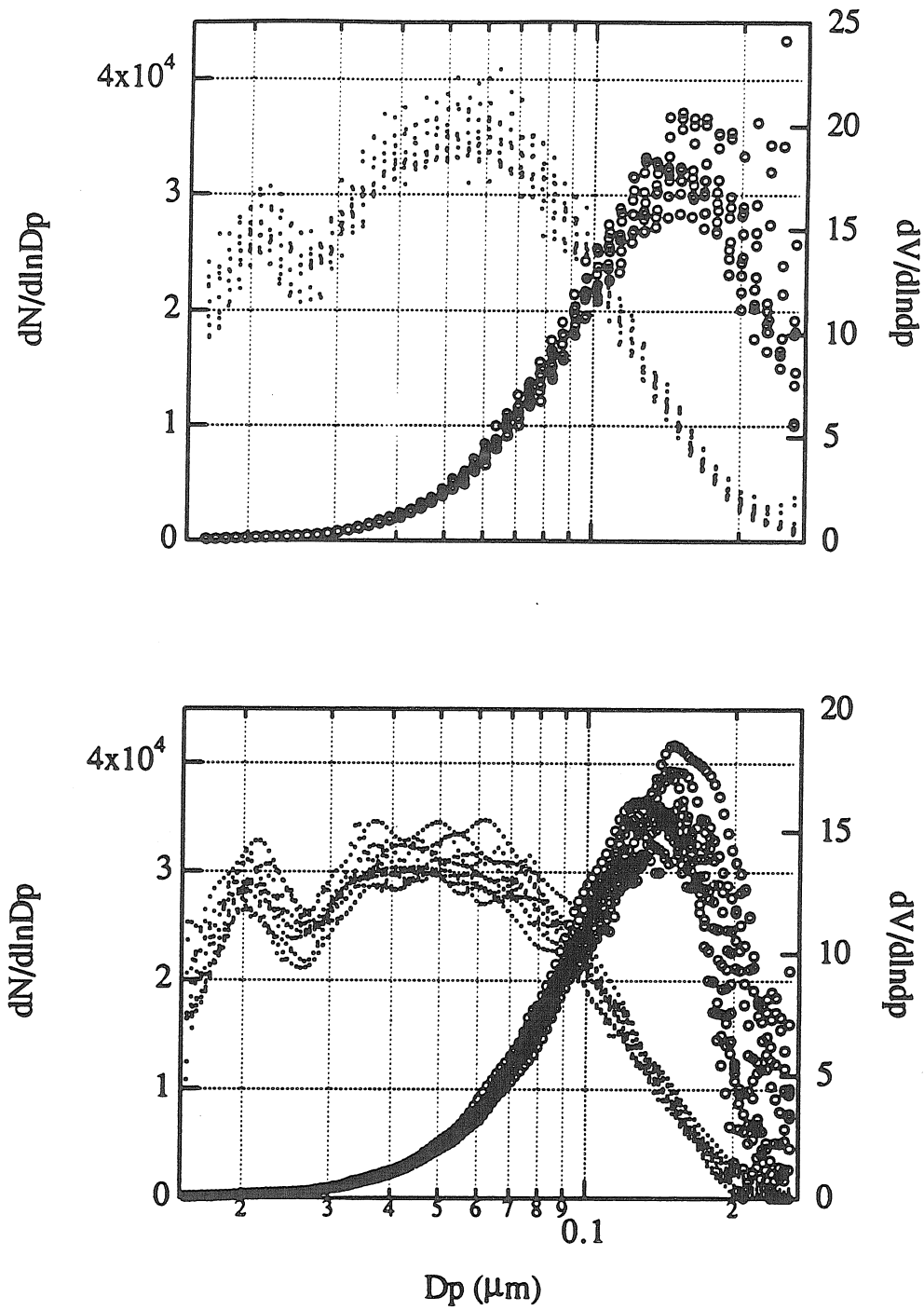
Figure 5 : A comparison of the number a volume distributions calculated using a) the simple inversion program and b) the Micron inversion program. The experimental conditions are Ra = 0.66, Rh = 0.075, and T = 30 °C.

APPENDIX C

Programs and Data

This appendix contains the following :

1) a copy of the program used to reduce the data from the number concentration experiments

2) the raw and reduced data from the number concentration experiments for both MSA and H_2SO_4.

There are two tables for each experiment. The first table contains the raw data consisting of the voltages measured for the thermistors and the differential pressure transducers, the pressures in the water and acid bubblers, the average of the observed CNC readings, the extremes observed in the CNC readings once stable operating conditions had been achieved, and an estimate of the standard deviation of the measurements. The second table contains the reduced data consisting of the temperatures, the flowrates in l min^{-1}, the relative humidity and relative acidity, and the average and extreme CNC values that have been corrected for coincidence error.

I. Data analysis program

```
c program lab3.for to analyze the laboratory data
c that includes reducing all of the raw cnc data
c
c
        real max,mean,min,num,s,s2,xsum,x2sum
        character*20 date
c
c first read in the exp ID:
c
        read(22,*) exptno
        read(22,10) date
 10     format(20a)
c
        read(22,*) time, plab
c
        write(20,35) exptno,date
        write(21,35) exptno,date
 35     format(///,8x,'Expt.#: ',f8.2,4x,'Date: ',20a,/)
c
        write(20,40) time,plab
        write(21,40) time,plab
 40     format(8x,'Time started: ',f6.2,4x,'Plab: ',f8.1,' mm Hg',/)
c
        read(22,*)t1,t2,t3,t5,t6
        write(20,50)t1,t2,t3,t5,t6
c
        call therm(t1,t2,t3,t5,t6)
        write(21,60)t1,t2,t3,t5,t6
c
 50     format(8x,'Thermistor readings (VDC) : (1,2,3,5,6) ',/,12x,'Room',
     1  4x,'Bath',4x,'WBub',3x,'Humid',4x,'ABub',//,8x,5f8.3,/)
 60     format(8x,'Temperatures (C) : (1,2,3,5,6) ',/,12x,'Room',4x,
     1  'Bath',4x,'WBub',3x,'Humid',4x,'ABub',//,8x,5f8.2,/)
c
        write(20,70)
        write(21,80)
 70     format(/,5x,'fd',6x,'fa',6x,'fh',5x,'Pwb',5x,'Pab',6x,'CNC',12x,
     1  'range',12x,'s',/)
 80     format(/,5x,'fd',6x,'fa',6x,'fh',4x,'ftot',6x,'rh',6x,'ra',6x,
     1  'CNC',7x, '-       /       +',/)
c
c loop to read in flows, pressures and cnc data
c
        do 1000 j=1,1000
c
        read(22,*)fd
        if (fd.lt.0.0) goto 200
        read(22,*)fa,fh,pwbi,pabp
        write(*,*)fd,fa,fh,pwbi,pabp
c
        pwb = (pwbi*1.86015) + plab
        pab = (pabp*760./14.7) + plab
c
c Section to read in the CNC data and compute the mean, standard
c deviation and extremes.
c
        min = 1.0e10
        max = 0.0
        xsum = 0.0
        x2sum = 0.0
```

```
        mean = 0.0
        s2 = 0.0
        s = 0.0
        num = 0.0
c
        do 2000 k = 1,1000
c
        read(22,*)val
c
        if (val.lt.0.0) goto 210
c
        xsum = xsum + val
        x2sum = x2sum + val*val
        if (val .lt. min) min = val
        if (val .gt. max) max = val
        num = num + 1.0
c
 2000   continue
c
 210    continue
        mean = xsum/num
        s2 = (x2sum - xsum*xsum/num)/(num-1.0)
        s = s2**0.5
        scale = -1.0*val
        cnc = mean*scale
        min = min*scale
        max = max*scale
        s = s*scale
c
        write(20,90)fd,fa,fh,pwb,pab,cnc,min,max,s
 90     format(3f8.3,2f8.1,4e10.3)
c
c Now data has been read into raw data file, compute the rest
c
c First the flows
c
        call flow(fd,fa,fh)
c Saturation water Pressure inside the bubbler
c
        call pwat(t3,pw3)
        call pacid(t6,pa6)
c
c Saturation water pressure at the mixer inlet
c
        call pwat(t2,pwm)
        call pacid(t2,pam)
c
c
c Ready to compute the realtive humidity
c
        y = pw3/(pwb-pw3)
        ftot = ((1.+y)*fh)+fd+fa
        rh = plab*y*fh/(pwm*ftot)
        ra = plab*pa6*fa/(pab*pam*ftot)
        ra = plab*fa/(pab*ftot)
c
c Correct CNC reading less than 1000 for coincidence error:
c
        if(cnc.lt.1000.0) cnc = cnc*exp(cnc*5.*35.0e-6)
```

```
            if(cnc.lt.1000.0) min = min*exp(min*5.*35.0e-6)
            if(cnc.lt.1000.0) max = max*exp(max*5.*35.0e-6)
            devn = cnc - min
            devp = max - cnc
c
c write out data
c
            write(21,160)fd,fa,fh,ftot,rh,ra,cnc,devn,devp
c
  160       format(4f8.3,3x,f5.3,3x,f5.3,1x,3e10.3)
c
c
 1000 continue
c
  200       continue
c
            read(22,*)time
            write(20,220) time
            write(21,230) time
  220       format(//,8x,'Time finished: ',f6.2)
  230       format(//,8x,'Time finished: ',f6.2)
c
            read(22,*)t1,t2,t3,t5,t6
            write(20,240) t1,t2,t3,t5,t6
            call therm(t1,t2,t3,t5,t6)
            write(21,250) t1,t2,t3,t5,t6
  240       format(//,8x,'Thermistor readings (VDC): (1,2,3,5,6)',//,8x,5f8.3)
  250       format(//,8x,'Temperatures (C): (1,2,3,5,6) ',//,8x,5f8.2)
c
            stop
            end
c
c Subroutine to compute water vapor pressure: use interpolation
c and the correlation from Seifeld
c
            subroutine pwat(t,pw)
c
            tr = 1 - (373.15/(t+273.15))
            pw = 1013.25*exp(13.3185*tr - 1.976*tr**2 - 0.6445*tr**3
     1         - 0.1299*tr**4)
            pw = pw/1013.25 * 760.0
c
            return
            end
c
c
c Subroutine to compute acid vapour pressure: use corrlation developed
c by kreidenweis.
c
            subroutine pacid(t,pa)
c
            tk = 273.15 + t
            plog = (-8006.48/tk) + 2.14237*(alog(tk)) + 7.45208
            pa = exp(plog)
c
            return
            end
c
c
c Subroutine to compute temperatures from thermistor calibration
```

```
c curves.
c
        subroutine therm(t1,t2,t3,t5,t6)
c
        t1 = 9.8346*t1 + 1.9994
        t2 = 9.7614*t2 + .82185
c
        t3 = 10.225*t3 + 0.67312
c
        t5 = 9.9907*t5 - 0.52799
c
        t6 = 10.014*t6 - 1.6984
c
        tp = 10.039*tp - 39.834
c
        return
        end
c
c
c Subroutine to compute the flows from the flow calibration curves.
c
        subroutine flow(fd,fa,fh)
c
        fd = 0.041288*(fd**3) - 0.19171*(fd**2) + 1.0713*fd
     1       - .0014707
c
        fa = 0.16002*(fa**3) - 0.58897*(fa**2) + 1.7883*fa
     1       - 0.010301
c
        fh = -0.0036044*(fh**3) - 0.18264*(fh**2) + 1.1616*fh
     1       - 0.0054522
c
        return
        end
```

II. The raw and reduced data for the methanesulfonic acid-water experiments.

Expt.#:   16.01   Date: Jan. 16,1990
Time started: 20.50   Plab: 734.7 mm Hg

Thermistor readings (VDC) : (1,2,3,5,6)
```
    Room     Bath     WBub    Humid     ABub
    2.154    2.500    2.415   2.641     2.729
```

fd	fa	fh	Pwb	Pab	CNC		range		s
.622	.201	.076	741.2	744.0	.617E-01	.300E-01	.120E+00		.259E-01
.582	.200	.105	741.4	744.0	.200E-01	.100E-01	.300E-01		.141E-01
.205	.200	.421	754.8	744.0	.714E+05	.665E+05	.757E+05		.332E+04
.321	.200	.315	750.0	744.0	.236E+05	.228E+05	.245E+05		.525E+03
.355	.200	.286	749.2	744.0	.113E+05	.109E+05	.115E+05		.159E+03
.389	.201	.255	748.1	744.0	.520E+04	.499E+04	.542E+04		.125E+03
.425	.201	.225	746.8	744.0	.159E+04	.154E+04	.166E+04		.392E+02
.445	.201	.210	746.2	744.0	.391E+03	.374E+03	.411E+03		.976E+01
.480	.201	.180	744.9	744.0	.589E+02	.547E+02	.685E+02		.324E+01
.501	.201	.165	744.4	744.0	.151E+02	.128E+02	.183E+02		.132E+01
.519	.201	.150	744.0	744.0	.347E+01	.313E+01	.385E+01		.241E+00
.541	.201	.135	743.1	744.0	.601E+00	.430E+00	.710E+00		.955E-01
.560	.201	.119	742.5	744.0	.104E+00	.400E-01	.150E+00		.387E-01
.581	.201	.105	742.1	744.0	.300E-01	.000E+00	.600E-01		.220E-01

Time finished: 22.15

Thermistor readings (VDC): (1,2,3,5,6)
```
    2.143    2.487    2.401   2.627    2.715
```

Expt.#:   16.01   Date: Jan. 16,1990
Time started: 20.50   Plab: 734.7 mm Hg

Temperatures (C) : (1,2,3,5,6)
```
    Room     Bath     WBub    Humid     ABub
    23.18    25.23    25.37   25.86     25.63
```

fd	fa	fh	ftot	rh	ra	CNC	-	/	+
.601	.327	.082	1.012	.084	.332	.617E-01	.317E-01	.583E-01	
.565	.325	.114	1.009	.117	.331	.200E-01	.100E-01	.100E-01	
.210	.325	.451	1.001	.457	.333	.714E+05	.492E+04	.428E+04	
.324	.325	.342	1.003	.348	.333	.236E+05	.847E+03	.853E+03	
.357	.325	.312	1.004	.317	.333	.113E+05	.356E+03	.244E+03	
.389	.327	.279	1.004	.284	.334	.520E+04	.213E+03	.218E+03	
.422	.327	.247	1.004	.252	.334	.159E+04	.486E+02	.714E+02	
.441	.327	.230	1.006	.235	.334	.419E+03	.196E+02	.227E+02	
.473	.327	.198	1.004	.202	.334	.595E+02	.426E+01	.984E+01	
.492	.327	.181	1.006	.185	.333	.152E+02	.233E+01	.320E+01	
.509	.327	.165	1.006	.169	.334	.347E+01	.340E+00	.380E+00	
.529	.327	.148	1.008	.151	.333	.601E+00	.171E+00	.109E+00	
.546	.327	.130	1.007	.133	.333	.104E+00	.643E-01	.457E-01	
.564	.327	.114	1.009	.117	.332	.300E-01	.300E-01	.300E-01	

Time finished: 22.15

Temperatures (C): (1,2,3,5,6)
```
    23.07    25.10    25.22   25.72    25.49
```

Expt.#:   16.02   Date: Jan. 17, 1990
Time started: 8.00   Plab: 734.7 mm Hg

Thermistor readings (VDC) : (1,2,3,5,6)
         Room   Bath   WBub   Humid   ABub
         2.093   2.948   2.844   3.073   3.166

fd	fa	fh	Pwb	Pab	CNC		range		s
.200	.200	.421	755.2	746.1	.473E+06	.463E+06	.481E+06		.582E+04
.200	.200	.421	755.2	746.1	.420E+06	.402E+06	.437E+06		.111E+05
.316	.200	.315	751.1	746.1	.922E+05	.901E+05	.940E+05		.111E+04
.316	.200	.315	751.1	746.1	.980E+05	.940E+05	.102E+06		.293E+04
.352	.200	.285	750.0	746.1	.568E+05	.528E+05	.606E+05		.214E+04
.352	.200	.285	750.0	746.1	.576E+05	.568E+05	.588E+05		.688E+03
.386	.200	.255	747.7	746.1	.357E+05	.343E+05	.370E+05		.905E+03
.422	.200	.225	747.3	746.1	.224E+05	.217E+05	.234E+05		.467E+03
.422	.200	.225	747.3	746.1	.210E+05	.205E+05	.224E+05		.570E+03
.459	.200	.195	746.0	746.1	.101E+05	.990E+04	.104E+05		.154E+03
.499	.199	.166	744.4	746.1	.430E+04	.418E+04	.444E+04		.684E+02
.499	.199	.166	744.4	746.1	.299E+04	.291E+04	.308E+04		.586E+02
.518	.199	.149	744.0	746.1	.125E+04	.114E+04	.140E+04		.819E+02
.538	.199	.135	743.6	746.1	.218E+03	.197E+03	.254E+03		.168E+02
.588	.200	.120	743.1	746.1	.655E+02	.562E+02	.806E+02		.820E+01
.580	.200	.105	742.5	746.1	.139E+02	.101E+02	.181E+02		.223E+01
.600	.200	.090	742.0	746.1	.238E+01	.173E+01	.288E+01		.393E+00
.621	.200	.075	741.2	746.1	.455E+00	.240E+00	.650E+00		.119E+00
.642	.200	.060	740.7	746.1	.105E+00	.400E-01	.190E+00		.424E-01

Time finished: 10.30

Thermistor readings (VDC): (1,2,3,5,6)
        2.131   2.966   2.869   3.091   3.183

Expt.#:   16.02   Date: Jan. 17, 1990
Time started: 8.00   Plab: 734.7 mm Hg

Temperatures (C) : (1,2,3,5,6)
         Room   Bath   WBub   Humid   ABub
         22.58   29.60   29.75   30.17   30.01

fd	fa	fh	ftot	rh	ra	CNC	-	/	+
.205	.325	.451	1.001	.461	.332	.473E+06	.104E+05		.762E+04
.205	.325	.451	1.001	.461	.332	.420E+06	.184E+05		.166E+05
.319	.325	.342	1.001	.352	.332	.922E+05	.211E+04		.179E+04
.319	.325	.342	1.001	.352	.332	.980E+05	.400E+04		.400E+04
.354	.325	.311	1.003	.320	.332	.568E+05	.396E+04		.384E+04
.354	.325	.311	1.003	.320	.332	.576E+05	.820E+03		.118E+04
.386	.325	.279	1.002	.288	.332	.357E+05	.142E+04		.128E+04
.420	.325	.247	1.002	.255	.332	.224E+05	.725E+03		.975E+03
.420	.325	.247	1.002	.255	.332	.210E+05	.530E+03		.137E+04
.454	.325	.214	1.002	.222	.332	.101E+05	.200E+03		.300E+03
.491	.324	.182	1.004	.189	.330	.430E+04	.121E+03		.139E+03
.491	.324	.182	1.004	.189	.330	.299E+04	.790E+02		.910E+02
.508	.324	.164	1.002	.170	.330	.125E+04	.111E+03		.149E+03
.526	.324	.148	1.004	.153	.330	.226E+03	.226E+02		.391E+02
.571	.325	.131	1.033	.132	.322	.662E+02	.947E+01		.155E+02
.563	.325	.114	1.008	.118	.330	.139E+02	.380E+01		.424E+01
.581	.325	.098	1.008	.101	.330	.238E+01	.654E+00		.497E+00
.600	.325	.081	1.009	.083	.330	.455E+00	.215E+00		.195E+00
.618	.325	.064	1.010	.066	.329	.105E+00	.654E-01		.846E-01

Time finished: 10.30

Temperatures (C): (1,2,3,5,6)
        22.96   29.77   30.01   30.35   30.18

```
Expt.#:     16.03    Date: Jan. 17, 1990
Time started: 11.45    Plab:    734.7 mm Hg

Thermistor readings (VDC) : (1,2,3,5,6)
     Room    Bath    WBub    Humid    ABub
     2.131   2.966   2.869   3.091    3.183
```

fd	fa	fh	Pwb	Pab	CNC		range	s
.382	.09?	.420	755.5	740.9	.434E+05	.428E+05	.438E+05	.369E+03
.180	.09?	.640	766.0	740.9	.114E+06	.108E+06	.121E+06	.474E+04
.180	.092	.640	766.0	740.9	.122E+06	.118E+06	.127E+06	.247E+04
.253	.092	.580	763.0	740.9	.105E+06	.101E+06	.110E+06	.243E+04
.286	.092	.520	761.3	740.9	.836E+05	.790E+05	.855E+05	.237E+04
.286	.092	.520	761.3	740.9	.833E+05	.812E+05	.863E+05	.169E+04
.320	.092	.479	758.7	740.9	.667E+05	.642E+05	.701E+05	.145E+04
.382	.092	.420	756.8	740.9	.470E+05	.467E+05	.473E+05	.242E+03
.382	.092	.420	756.8	740.9	.436E+05	.431E+05	.442E+05	.329E+03
.452	.092	.360	753.7	740.9	.267E+05	.251E+05	.280E+05	.732E+03
.525	.092	.299	751.4	740.9	.105E+05	.100E+05	.108E+05	.260E+03
.562	.092	.270	750.5	740.9	.497E+04	.488E+04	.506E+04	.645E+02
.562	.092	.270	750.5	740.9	.326E+04	.318E+04	.334E+04	.550E+02
.603	.092	.240	749.2	740.9	.149E+04	.128E+04	.169E+04	.123E+03
.644	.092	.210	747.7	740.9	.241E+03	.202E+03	.301E+03	.266E+02
.684	.092	.181	746.8	740.9	.571E+02	.484E+02	.678E+02	.616E+01
.706	.092	.166	746.2	740.9	.237E+02	.191E+02	.298E+02	.289E+01
.727	.092	.150	745.5	740.9	.902E+01	.719E+01	.106E+02	.119E+01
.749	.092	.135	744.4	740.9	.296E+01	.215E+01	.365E+01	.463E+00
.771	.092	.120	744.0	740.9	.109E+01	.930E+00	.128E+01	.895E-01
.794	.092	.105	743.8	740.9	.301E+00	.370E-01	.470E+00	.122E+00
.818	.092	.089	743.6	740.9	.990E-01	.500E-01	.150E+00	.321E-01
.840	.092	.075	742.5	740.9	.409E-01	.100E-01	.900E-01	.251E-01

```
Time finished:  13.35


Thermistor readings (VDC): (1,2,3,5,6)
     2.210   2.974   2.871   3.098    3.193
```

Expt.#:   16.03   Date: Jan. 17, 1990
Time started: 11.45   Plab: 734.7 mm Hg

Temperatures (C) : (1,2,3,5,6)
　　　Room   Bath   WBub   Humid   ABub
　　　22.96   29.77   30.01   30.35   30.18

fd	fa	fh	ftot	rh	ra	CNC	-	/	+
.382	.149	.450	1.001	.462	.154	.434E+05	.571E+03		.429E+03
.185	.149	.662	1.026	.655	.150	.114E+06	.645E+04		.655E+04
.185	.149	.662	1.026	.655	.150	.122E+06	.442E+04		.458E+04
.258	.149	.606	1.040	.594	.148	.105E+06	.429E+04		.471E+04
.290	.149	.549	1.012	.553	.152	.836E+05	.455E+04		.195E+04
.290	.149	.549	1.012	.553	.152	.833E+05	.212E+04		.298E+04
.323	.149	.509	1.003	.519	.153	.667E+05	.254E+04		.336E+04
.382	.149	.450	1.001	.462	.154	.470E+05	.309E+03		.291E+03
.382	.149	.450	1.001	.462	.154	.436E+05	.544E+03		.556E+03
.447	.149	.389	1.003	.400	.153	.267E+05	.160E+04		.130E+04
.514	.149	.325	1.003	.336	.153	.105E+05	.473E+03		.327E+03
.547	.149	.295	1.005	.304	.153	.497E+04	.889E+02		.911E+02
.547	.149	.295	1.005	.304	.153	.326E+04	.825E+02		.775E+02
.584	.149	.263	1.008	.271	.153	.149E+04	.209E+03		.201E+03
.620	.149	.230	1.010	.237	.152	.251E+03	.420E+02		.660E+02
.655	.149	.199	1.012	.205	.152	.577E+02	.888E+01		.109E+02
.674	.149	.182	1.014	.187	.152	.238E+02	.459E+01		.620E+01
.692	.149	.165	1.013	.170	.152	.903E+01	.183E+01		.159E+01
.711	.149	.148	1.015	.152	.152	.296E+01	.806E+00		.695E+00
.729	.149	.131	1.016	.135	.151	.109E+01	.158E+00		.192E+00
.749	.149	.114	1.018	.118	.151	.301E+00	.264E+00		.169E+00
.769	.149	.096	1.019	.099	.151	.990E-01	.490E-01		.510E-01
.788	.149	.081	1.021	.083	.151	.409E-01	.309E-01		.491E-01

Time finished: 13.35

Temperatures (C): (1,2,3,5,6)
　　　23.73   29.85   30.03   30.42   30.28

Expt.#:   16.04   Date: Jan. 17, 1990
Time started: 14.20   Plab: 734.7 mm Hg

Thermistor readings (VDC) : (1,2,3,5,6)
     Room   Bath   WBub   Humid   ABub
     2.160   2.975   2.876   3.100   3.191

fd	fa	fh	Pwb	Pab	CNC		range		s
.256	.048	.640	765.4	738.8	.512E+05	.497E+05	.538E+05		.148E+04
.256	.048	.640	765.4	738.8	.585E+05	.572E+05	.595E+05		.789E+03
.471	.048	.420	757.0	738.8	.105E+05	.102E+05	.109E+05		.256E+03
.471	.048	.420	757.0	738.8	.745E+04	.718E+04	.791E+04		.188E+03
.361	.048	.520	760.7	738.8	.275E+05	.268E+05	.284E+05		.480E+03
.472	.048	.420	756.6	738.8	.799E+04	.769E+04	.853E+04		.259E+03
.574	.048	.330	753.3	738.8	.150E+04	.144E+04	.169E+04		.694E+02
.613	.048	.300	751.8	738.8	.315E+03	.273E+03	.355E+03		.203E+02
.632	.048	.286	751.4	738.8	.162E+03	.141E+03	.178E+03		.111E+02
.652	.048	.270	750.5	738.8	.701E+02	.641E+02	.782E+02		.360E+01
.674	.048	.255	750.0	738.8	.318E+02	.279E+02	.363E+02		.253E+01
.693	.048	.240	749.6	738.8	.226E+02	.185E+02	.261E+02		.262E+01
.736	.048	.210	748.5	738.8	.996E+01	.760E+01	.115E+02		.943E+00
.758	.048	.194	747.3	738.8	.442E+01	.375E+01	.555E+01		.620E+00
.779	.048	.180	746.6	738.8	.184E+01	.167E+01	.207E+01		.144E+00
.801	.048	.165	746.2	738.8	.103E+01	.810E+00	.121E+01		.144E+00
.823	.048	.150	746.0	738.8	.500E+00	.390E+00	.600E+00		.729E-01
.847	.048	.136	745.7	738.8	.188E+00	.150E+00	.260E+00		.449E-01
.869	.048	.120	744.4	738.8	.886E-01	.700E-01	.110E+00		.186E-01

Time finished: 16.20

Thermistor readings (VDC): (1,2,3,5,6)
     2.180   2.977   2.874   3.103   3.196

Expt.#:   16.04   Date: Jan. 17, 1990
Time started: 14.20   Plab: 734.7 mm Hg

Temperatures (C) : (1,2,3,5,6)
     Room   Bath   WBub   Humid   ABub
     23.24   29.86   30.08   30.44   30.26

fd	fa	fh	ftot	rh	ra	CNC	-	/	+
.261	.074	.662	1.026	.655	.075	.512E+05	.146E+04	.264E+04
.261	.074	.662	1.026	.655	.075	.585E+05	.128E+04	.102E+04
.465	.074	.450	1.009	.458	.076	.105E+05	.337E+03	.363E+03
.465	.074	.450	1.009	.458	.076	.745E+04	.273E+03	.457E+03
.362	.074	.549	1.009	.555	.076	.275E+05	.744E+03	.856E+03
.466	.074	.450	1.010	.457	.076	.799E+04	.305E+03	.535E+03
.558	.074	.358	1.006	.367	.076	.150E+04	.607E+02	.189E+03
.593	.074	.326	1.008	.335	.076	.333E+03	.462E+02	.452E+02
.609	.074	.312	1.009	.319	.076	.167E+03	.226E+02	.166E+02
.627	.074	.295	1.009	.302	.076	.710E+02	.614E+01	.832E+01
.646	.074	.279	1.012	.286	.076	.320E+02	.398E+01	.452E+01
.663	.074	.263	1.011	.269	.076	.227E+02	.414E+01	.352E+01
.700	.074	.230	1.014	.236	.075	.997E+01	.236E+01	.155E+01
.718	.074	.213	1.015	.218	.075	.443E+01	.673E+00	.113E+01
.736	.074	.198	1.017	.202	.075	.184E+01	.165E+00	.235E+00
.755	.074	.181	1.018	.185	.075	.104E+01	.225E+00	.175E+00
.773	.074	.165	1.020	.168	.075	.500E+00	.110E+00	.100E+00
.793	.074	.149	1.023	.152	.075	.188E+00	.380E-01	.720E-01
.812	.074	.131	1.023	.134	.075	.886E-01	.186E-01	.214E-01

Time finished: 16.20

Temperatures (C): (1,2,3,5,6)
     23.44   29.88   30.06   30.47   30.31

Expt.#:   16.05   Date: Jan. 17, 1990
Time started: 15.20   Plab: 734.7 mm Hg

Thermistor readings (VDC) : (1,2,3,5,6)
     Room   Bath   WBub   Humid   ABub
     2.133   2.977   2.878   3.101   3.193

fd	fa	fh	Pwb	Pab	CNC	range		s
.040	.421	.270	747.7	756.4	.379E+06	.377E+06	.380E+06	.102E+04
.040	.421	.270	747.7	756.4	.473E+06	.446E+06	.516E+06	.221E+05
.185	.315	.269	747.7	752.3	.637E+05	.580E+05	.712E+05	.463E+04
.185	.315	.269	747.7	752.3	.998E+05	.875E+05	.127E+06	.135E+05
.288	.248	.269	748.1	750.2	.467E+05	.455E+05	.475E+05	.538E+03
.288	.248	.269	748.1	750.2	.473E+05	.465E+05	.493E+05	.101E+04
.368	.201	.269	748.3	746.1	.243E+05	.225E+05	.274E+05	.135E+04
.368	.201	.269	748.3	746.1	.170E+05	.167E+05	.172E+05	.196E+03
.451	.154	.269	748.7	745.0	.932E+04	.902E+04	.971E+04	.195E+03
.451	.154	.269	748.7	745.0	.751E+04	.731E+04	.771E+04	.155E+03
.506	.122	.269	749.2	742.5	.359E+04	.344E+04	.369E+04	.827E+02
.563	.092	.269	749.6	740.9	.134E+04	.129E+04	.137E+04	.235E+02
.593	.078	.269	749.6	740.9	.335E+03	.316E+03	.352E+03	.110E+02
.623	.063	.269	749.8	739.9	.158E+03	.149E+03	.166E+03	.519E+01
.652	.048	.269	750.0	738.8	.469E+02	.430E+02	.521E+02	.271E+01
.682	.034	.269	750.0	738.3	.140E+02	.116E+02	.162E+02	.128E+01

Time finished: 19.00

Thermistor readings (VDC): (1,2,3,5,6)
     2.211   2.981   2.875   3.106   3.199

Expt.#:   16.05   Date: Jan. 17, 1990
Time started: 15.20   Plab: 734.7 mm Hg

Temperatures (C) : (1,2,3,5,6)
     Room   Bath   WBub   Humid   ABub
     22.98   29.88   30.10   30.45   30.28

fd	fa	fh	ftot	rh	ra	CNC	-	/	+
.041	.650	.295	.999	.307	.656	.379E+06	.156E+04		.144E+04
.041	.650	.295	.999	.307	.656	.473E+06	.267E+05		.433E+05
.190	.500	.294	.997	.306	.508	.637E+05	.572E+04		.748E+04
.190	.500	.294	.997	.306	.508	.998E+05	.123E+05		.272E+05
.292	.399	.294	.998	.306	.407	.467E+05	.124E+04		.760E+03
.292	.399	.294	.998	.306	.407	.473E+05	.757E+03		.204E+04
.369	.327	.294	1.002	.304	.333	.243E+05	.176E+04		.314E+04
.369	.327	.294	1.002	.304	.333	.170E+05	.289E+03		.211E+03
.446	.252	.294	1.005	.303	.256	.932E+04	.304E+03		.386E+03
.446	.252	.294	1.005	.303	.256	.751E+04	.203E+03		.197E+03
.497	.199	.294	1.003	.304	.204	.359E+04	.153E+03		.967E+02
.548	.149	.294	1.004	.303	.153	.134E+04	.482E+02		.318E+02
.575	.126	.294	1.008	.302	.128	.355E+03	.210E+02		.194E+02
.602	.100	.294	1.008	.302	.102	.162E+03	.897E+01		.899E+01
.627	.074	.294	1.008	.302	.076	.473E+02	.393E+01		.533E+01
.653	.050	.294	1.010	.301	.051	.140E+02	.238E+01		.225E+01

Time finished: 19.00

Temperatures (C): (1,2,3,5,6)
     23.74   29.92   30.07   30.50   30.34

Expt.#:   16.06   Date: Jan. 17, 1990
Time started: 19.40   Plab: 734.7 mm Hg

Thermistor readings (VDC) : (1,2,3,5,6)
       Room   Bath   WBub   Humid   ABub
       2.142   2.979   2.881   3.105   3.196

fd	fa	fh	Pwb	Pab	CNC		range		s
.188	.421	.135	742.0	758.0	.232E+03	.207E+03	.252E+03		.141E+02
.343	.315	.135	742.1	752.8	.506E+03	.448E+03	.546E+03		.286E+02
.451	.248	.135	742.3	750.2	.156E+03	.126E+03	.187E+03		.169E+02
.538	.200	.135	742.7	747.1	.286E+02	.244E+02	.358E+02		.334E+01
.624	.153	.135	743.1	744.0	.595E+01	.434E+01	.756E+01		.122E+01
.686	.122	.135	743.8	743.0	.208E+01	.172E+01	.246E+01		.261E+00
.749	.092	.135	744.0	741.4	.105E+01	.910E+00	.117E+01		.112E+00
.845	.048	.135	744.4	738.8	.176E+00	.130E+00	.220E+00		.316E-01

Time finished: 20.30

Thermistor readings (VDC): (1,2,3,5,6)
       2.142   2.979   2.881   3.105   3.196

Expt.#:   16.06   Date: Jan. 17, 1990
Time started: 19.40   Plab: 734.7 mm Hg

Temperatures (C) : (1,2,3,5,6)
       Room   Bath   WBub   Humid   ABub
       23.07   29.90   30.13   30.49   30.31

fd	fa	fh	ftot	rh	ra	CNC	-	/	+
.193	.650	.148	.998	.156	.656	.242E+03	.272E+02		.215E+02
.345	.500	.148	.999	.155	.507	.552E+03	.678E+02		.484E+02
.446	.399	.148	1.001	.155	.406	.160E+03	.311E+02		.333E+02
.526	.325	.148	1.006	.154	.330	.288E+02	.426E+01		.726E+01
.602	.250	.148	1.007	.154	.255	.596E+01	.162E+01		.161E+01
.657	.199	.148	1.011	.153	.203	.208E+01	.355E+00		.385E+00
.711	.149	.148	1.015	.153	.152	.105E+01	.144E+00		.116E+00
.792	.074	.148	1.021	.152	.075	.176E+00	.463E-01		.438E-01

Time finished: 20.30

Temperatures (C): (1,2,3,5,6)
       23.07   29.90   30.13   30.49   30.31

Expt.#:   16.07   Date: Jan. 17, 1990
Time started: 20.30   Plab: 734.7 mm Hg

Thermistor readings (VDC) : (1,2,3,5,6)
      Room   Bath   WBub   Humid   ABub
      2.142   2.979   2.881   3.105   3.196

fd	fa	fh	Pwb	Pab	CNC	range		s
.256	.048	.640	766.1	738.8	.393E+05	.383E+05	.404E+05	.814E+03
.322	.048	.580	763.5	738.8	.271E+05	.259E+05	.281E+05	.646E+03
.395	.048	.480	759.3	738.8	.112E+05	.110E+05	.114E+05	.150E+03
.464	.048	.420	757.0	738.8	.427E+04	.404E+04	.458E+04	.167E+03
.537	.048	.360	754.8	738.8	.139E+04	.129E+04	.147E+04	.480E+02
.614	.048	.300	752.4	738.8	.178E+03	.157E+03	.202E+03	.154E+02
.674	.048	.255	750.0	738.8	.471E+02	.357E+02	.547E+02	.515E+01
.735	.048	.210	748.3	738.8	.110E+02	.760E+01	.132E+02	.164E+01
.800	.048	.165	746.6	738.8	.224E+01	.174E+01	.292E+01	.396E+00
.846	.048	.135	745.7	738.8	.471E+00	.360E+00	.700E+00	.955E-01

Time finished: 21.00

Thermistor readings (VDC): (1,2,3,5,6)
      2.159   2.980   2.876   3.105   3.199

Expt.#:   16.07   Date: Jan. 17, 1990
Time started: 20.30   Plab: 734.7 mm Hg

Temperatures (C) : (1,2,3,5,6)
      Room   Bath   WBub   Humid   ABub
      23.07   29.90   30.13   30.49   30.31

fd	fa	fh	ftot	rh	ra	CNC	-	/	+
.261	.074	.662	1.026	.654	.075	.393E+05	.104E+04		.106E+04
.325	.074	.606	1.032	.598	.074	.271E+05	.116E+04		.104E+04
.394	.074	.510	1.001	.521	.077	.112E+05	.208E+03		.192E+03
.458	.074	.450	1.002	.461	.076	.427E+04	.232E+03		.308E+03
.525	.074	.389	1.005	.398	.076	.139E+04	.992E+02		.808E+02
.594	.074	.326	1.009	.334	.076	.183E+03	.220E+02		.259E+02
.646	.074	.279	1.012	.286	.076	.475E+02	.115E+02		.776E+01
.699	.074	.230	1.014	.236	.076	.110E+02	.343E+01		.219E+01
.754	.074	.181	1.018	.186	.075	.224E+01	.497E+00		.683E+00
.793	.074	.148	1.022	.151	.075	.471E+00	.111E+00		.229E+00

Time finished: 21.00

Temperatures (C): (1,2,3,5,6)
      23.23   29.91   30.08   30.49   30.34

Expt.#:   16.08   Date: Jan. 18, 1990
Time started: 10.00   Plab: 734.5 mm Hg

Thermistor readings (VDC) : (1,2,3,5,6)
      Room   Bath   WBub   Humid   ABub
      2.067   1.856   1.790 2.010   2.093

fd	fa	fh	Pwb	Pab	· CNC		range	s
.210	.200	.420	754.0	747.9	.406E+05	.395E+05	.435E+05	.161E+04
.323	.200	.315	749.8	747.9	.298E+04	.286E+04	.308E+04	.753E+02
.272	.200	.360	751.2	747.9	.851E+04	.824E+04	.897E+04	.241E+03
.272	.200	.360	751.2	747.9	.780E+04	.761E+04	.800E+04	.151E+03
.210	.201	.420	753.1	747.9	.308E+05	.301E+05	.317E+05	.600E+03
.210	.201	.420	753.1	747.9	.319E+05	.315E+05	.325E+05	.264E+03
.306	.201	.330	749.9	747.9	.553E+04	.539E+04	.567E+04	.827E+02
.340	.201	.300	749.4	747.9	.267E+04	.231E+04	.288E+04	.176E+03
.375	.201	.270	747.9	747.9	.103E+04	.980E+03	.107E+04	.305E+02
.410	.201	.240	747.1	747.9	.139E+03	.131E+03	.145E+03	.398E+01
.429	.200	.225	746.4	747.9	.470E+02	.382E+02	.561E+02	.527E+01
.447	.200	.210	746.0	747.9	.135E+02	.115E+02	.166E+02	.130E+01
.465	.200	.194	745.3	747.9	.301E+01	.223E+01	.390E+01	.549E+00
.484	.200	.180	744.5	747.9	.512E+00	.350E+00	.680E+00	.993E-01
.503	.200	.165	744.0	747.9	.483E-01	.200E-01	.800E-01	.223E-01

Time finished: 12.00

Thermistor readings (VDC): (1,2,3,5,6)
      2.119   1.851   1.780   2.005   2.090

Expt.#:   16.08   Date: Jan. 18, 1990
Time started: 10.00   Plab: 734.5 mm Hg

Temperatures (C) : (1,2,3,5,6)
      Room   Bath   WBub   Humid   ABub
      22.33   18.94   18.98 19.55   19.26

fd	fa	fh	ftot	rh	ra	CNC	-	/	+
.215	.325	.450	1.000	.449	.330	.406E+05	.110E+04		.290E+04
.326	.325	.342	1.001	.343	.329	.298E+04	.117E+03		.103E+03
.277	.325	.389	.999	.390	.330	.851E+04	.274E+03		.456E+03
.277	.325	.389	.999	.390	.330	.780E+04	.193E+03		.197E+03
.215	.327	.450	1.002	.449	.331	.308E+05	.664E+03		.936E+03
.215	.327	.450	1.002	.449	.331	.319E+05	.360E+03		.640E+03
.310	.327	.358	1.002	.358	.331	.553E+04	.136E+03		.144E+03
.342	.327	.326	1.003	.327·	.330	.267E+04·	.360E+03		.210E+03
.375	.327	.295	1.004	.296	.330	.103E+04	.474E+02		.426E+02
.408	.327	.263	1.004	.264	.330	.142E+03	.791E+01		.678E+01
.426	.325	.247	1.003	.248	.329	.474E+02	.893E+01		.927E+01
.443	.325	.230	1.003	.232	.329	.135E+02	.198E+01		.315E+01
.459	.325	.213	1.002	.215	.329	.301E+01	.779E+00		.893E+00
.477	.325	.198	1.004	.199	.328	.512E+00	.162E+00		.168E+00
.494	.325	.181	1.005	.183 ʌ	.328	.483E-01	.283E-01		.317E-01

Time finished: 12.00

Temperatures (C): (1,2,3,5,6)
      22.84   18.89   18.87   19.50   19.23

Expt.#:   16.09   Date: Jan. 18, 1990
Time started: 12.30   Plab: 734.5 mm Hg

Thermistor readings (VDC) : (1,2,3,5,6)
         Room   Bath   WBub   Humid   ABub
         2.119   1.851   1.780   2.005   2.090

fd	fa	fh	Pwb	Pab	CNC		range		s
.393	.092	.420	754.0	741.7	.173E+03	.153E+03	.192E+03		.101E+02
.324	.092	.480	756.8	741.7	.654E+03	.627E+03	.679E+03		.173E+02
.295	.093	.521	758.5	741.7	.199E+04	.190E+04	.211E+04		.633E+02
.295	.093	.521	758.5	741.7	.233E+04	.225E+04	.244E+04		.581E+02
.252	.092	.580	760.9	741.7	.448E+04	.411E+04	.482E+04		.226E+03
.252	.092	.580	760.9	741.7	.593E+04	.553E+04	.628E+04		.225E+03
.185	.092	.640	762.8	741.7	.117E+05	.114E+05	.120E+05		.168E+03
.185	.092	.640	763.0	741.7	.173E+05	.159E+05	.186E+05		.993E+03
.393	.093	.420	755.0	741.7	.135E+04	.910E+03	.167E+04		.317E+03
.410	.093	.405	754.6	741.7	.411E+03	.375E+03	.446E+03		.240E+02
.444	.093	.375	753.1	741.7	.150E+03	.140E+03	.158E+03		.495E+01
.461	.093	.360	752.7	741.7	.784E+02	.674E+02	.852E+02		.452E+01
.479	.093	.345	752.7	741.7	.392E+02	.329E+02	.474E+02		.318E+01
.497	.093	.330	751.6	741.7	.173E+02	.148E+02	.200E+02		.146E+01
.515	.093	.316	751.2	741.7	.629E+01	.528E+01	.709E+01		.548E+00
.533	.093	.299	750.9	741.7	.206E+01	.189E+01	.250E+01		.160E+00
.551	.093	.285	749.8	741.7	.712E+00	.500E+00	.910E+00		.144E+00
.571	.093	.270	749.4	741.7	.210E+00	.110E+00	.250E+00		.463E-01
.591	.092	.255	749.0	741.7	.475E-01	.200E-01	.700E-01		.171E-01
.183	.092	.640	763.3	741.7	.927E+04	.906E+04	.941E+04		.115E+03
.252	.092	.580	761.5	741.7	.426E+04	.411E+04	.444E+04		.980E+02
.295	.092	.520	759.1	741.7	.256E+04	.244E+04	.264E+04		.682E+02
.324	.092	.480	757.6	741.7	.165E+04	.161E+04	.170E+04		.247E+02
.393	.092	.420	755.0	741.7	.341E+03	.321E+03	.363E+03		.106E+02
.183	.092	.640	763.3	741.7	.101E+05	.940E+04	.107E+05		.470E+03

Time finished: 14.30

Thermistor readings (VDC): (1,2,3,5,6)
         2.113   1.851   1.780   2.006   2.091

Expt.#:   16.09   Date: Jan. 18, 1990
Time started: 12.30   Plab: 734.5 mm Hg

Temperatures (C) : (1,2,3,5,6)
        Room   Bath   WBub   Humid   ABub
        22.84   18.89   18.87   19.50   19.23

fd	fa	fh	ftot	rh	ra	CNC	- / +
.392	.149	.450	1.002	.447	.153	.178E+03	.212E+02 .202E+02
.327	.149	.510	.997	.506	.154	.733E+03	.332E+02 .317E+02
.299	.151	.550	1.012	.537	.153	.199E+04	.889E+02 .121E+03
.299	.151	.550	1.012	.537	.153	.233E+04	.844E+02 .106E+03
.257	.149	.606	1.026	.582	.149	.448E+04	.369E+03 .341E+03
.257	.149	.606	1.026	.582	.149	.593E+04	.397E+03 .353E+03
.190	.149	.662	1.016	.640	.151	.117E+05	.308E+03 .292E+03
.190	.149	.662	1.016	.640	.151	.173E+05	.138E+04 .132E+04
.392	.151	.450	1.003	.445	.154	.135E+04	.438E+03 .322E+03
.408	.151	.435	1.004	.430	.154	.442E+03	.411E+02 .407E+02
.440	.151	.404	1.004	.401	.154	.154E+03	.101E+02 .884E+01
.456	.151	.389	1.004	.386	.154	.795E+02	.113E+02 .700E+01
.472	.151	.373	1.005	.370	.154	.395E+02	.640E+01 .831E+01
.489	.151	.358	1.006	.355	.154	.174E+02	.252E+01 .271E+01
.505	.151	.343	1.007	.340	.154	.630E+01	.101E+01 .800E+00
.521	.151	.325	1.005	.323	.154	.206E+01	.167E+00 .444E+00
.538	.151	.311	1.006	.309	.154	.713E+00	.213E+00 .198E+00
.555	.151	.295	1.008	.293	.154	.210E+00	.100E+00 .400E-01
.573	.149	.279	1.008	.277	.152	.475E-01	.275E-01 .225E-01
.188	.149	.662	1.014	.641	.151	.927E+04	.213E+03 .137E+03
.257	.149	.606	1.026	.582	.149	.426E+04	.153E+03 .177E+03
.299	.149	.549	1.009	.537	.152	.256E+04	.122E+03 .784E+02
.327	.149	.510	.997	.506	.154	.165E+04	.443E+02 .457E+02
.392	.149	.450	1.002	.446	.153	.362E+03	.221E+02 .251E+02
.188	.149	.662	1.014	.641	.151	.101E+05	.740E+03 .560E+03

Time finished: 14.30

Temperatures (C): (1,2,3,5,6)
        22.78   18.89   18.87   19.51   19.24

Expt.#:   16.10   Date: Jan. 18, 1990
Time started: 14.30   Plab: 734.5 mm Hg

Thermistor readings (VDC) : (1,2,3,5,6)
      Room   Bath   WBub   Humid   ABub
      2.113   1.851   1.780   2.006   2.091

fd	fa	fh	Pwb	Pab	CNC		range	s
.268	.048	.640	763.5	738.6	.191E+03	.480E-01	.247E+03	.541E+02
.327	.048	.580	762.2	738.6	.935E+02	.740E+02	.111E+03	.101E+02
.348	.048	.550	760.9	738.6	.700E+02	.636E+02	.740E+02	.283E+01
.363	.048	.520	759.1	738.6	.429E+02	.362E+02	.484E+02	.369E+01
.404	.048	.480	757.9	738.6	.150E+02	.125E+02	.177E+02	.139E+01
.420	.048	.451	756.8	738.6	.842E+01	.714E+01	.913E+01	.581E+00
.476	.048	.420	755.7	738.6	.133E+01	.104E+01	.171E+01	.187E+00
.510	.048	.390	754.6	738.6	.440E+00	.280E+00	.700E+00	.123E+00
.546	.048	.360	753.5	738.6	.969E-01	.500E-01	.140E+00	.278E-01

Time finished: 15.30

Thermistor readings (VDC): (1,2,3,5,6)
      2.141   1.847   1.778   2.003   2.088

Expt.#:   16.10   Date: Jan. 18, 1990
Time started: 14.30   Plab: 734.5 mm Hg

Temperatures (C) : (1,2,3,5,6)
      Room   Bath   WBub   Humid   ABub
      22.78   18.89   18.87   19.51   19.24

fd	fa	fh	ftot	rh	ra	CNC	-	/	+
.273	.074	.662	1.024	.635	.075	.197E+03	.197E+03	.608E+02
.330	.074	.606	1.023	.583·	.075	.951E+02	.201E+02	.181E+02
.350	.074	.578	1.014	.561	.075	.709E+02	.659E+01	.406E+01
.364	.074	.549	.999	.543	.077	.432E+02	.675E+01	.564E+01
.403	.074	.510	.998	.505	.077	.150E+02	.250E+01	.273E+01
.418	.074	.481	.983	.485	.078	.843E+01	.128E+01	.716E+00
.469	.074	.450	1.004	.445	.076	.133E+01	.293E+00	.377E+00
.501	.074	.420	1.004	.416	.076	.440E+00	.160E+00	.260E+00
.533	.074	.389	1.005	.385	.076	.969E-01	.469E-01	.431E-01

Time finished: 15.30

Temperatures (C): (1,2,3,5,6)
      23.06   18.85   18.85   19.48   19.21

Expt.#:   16.11   Date: Jan. 18, 1990
Time started: 17.45   Plab: 734.5 mm Hg

Thermistor readings (VDC) : (1,2,3,5,6)
    Room   Bath   WBub   Humid   ABub
    2.114   1.845   1.778   2.000   2.083

fd	fa	fh	Pwb	Pab	CNC	range		s
.048	.421	.270	746.6	759.3	.208E+06	.202E+06	.212E+06	.297E+04
.048	.421	.270	746.6	759.3	.232E+06	.221E+06	.246E+06	.728E-04
.194	.315	.270	747.3	754.1	.240E+05	.229E+05	.260E+05	.103E+04
.194	.315	.270	747.3	754.1	.262E+05	.256E+05	.271E+05	.543E+03
.296	.248	.270	747.1	751.0	.122E+05	.118E+05	.128E+05	.297E+03
.296	.248	.270	747.3	751.0	.809E+04	.786E+04	.841E+04	.155E+03
.375	.200	.270	747.5	746.9	.224E+04	.219E+04	.230E+04	.375E+02
.375	.200	.270	747.5	746.9	.915E+03	.894E+03	.947E+03	.169E+02
.458	.153	.270	748.1	744.8	.141E+03	.127E+03	.157E+03	.799E+01
.512	.122	.271	748.3	743.8	.159E+02	.120E+02	.207E+02	.213E+01
.542	.107	.271	748.5	742.8	.298E+01	.252E+01	.352E+01	.282E+00
.571	.092	.270	748.6	741.7	.311E+00	.210E+00	.380E+00	.568E-01
.599	.078	.270	749.0	740.7	.525E-01	.100E-01	.100E+00	.255E-01
.048	.421	.270	746.6	759.3	.168E+06	.165E+06	.171E+06	.219E+04

Time finished: 19.30

Thermistor readings (VDC): (1,2,3,5,6)
    2.143   1.852   1.782   2.007   2.092

Expt.#:   16.11   Date: Jan. 18, 1990
Time started: 17.45   Plab: 734.5 mm Hg

Temperatures (C) : (1,2,3,5,6)
    Room   Bath   WBub   Humid   ABub
    22.79   18.83   18.85   19.45   19.16

fd	fa	fh	ftot	rh	ra	CNC	-	/	+
.050	.650	.295	1.001	.297	.649	.208E+06	.567E+04		.433E+04
.050	.650	.295	1.001	.297	.649	.232E+06	.106E+05		.144E+05
.199	.500	.295	1.000	.296	.503	.240E+05	.111E+04		.199E+04
.199	.500	.295	1.000	.296	.503	.262E+05	.600E+03		.900E+03
.300	.399	.295	1.001	.296	.404	.122E+05	.395E+03		.605E+03
.300	.399	.295	1.001	.296	.404	.809E+04	.228E+03		.322E+03
.375	.325	.295	1.002	.296	.330·	.224E+04	.494E+02		.606E+02
.375	.325	.295	1.002	.296	.330·	.107E+04	.180E+03		-.127E+03
.453	.250	.295	1.004	.295	.254	.144E+03	.144E+02		.171E+02
.502	.199	.296	1.004	.296	.203	.160E+02	.395E+01		.480E+01
.529	.175	.296	1.006	.295	.177	.298E+01	.457E+00		.544E+00
.555	.149	.295	1.006	.294	.152	.311E+00	.101E+00		.686E-01
.580	.126	.295	1.007	.294	.128·	.525E-01	.425E-01		.475E-01
.050	.650	.295	1.001	.297	.649	.168E+06	.260E+04		.340E+04

Time finished: 19.30

Temperatures (C): (1,2,3,5,6)
    23.07   18.90   18.89   19.52   19.25

Expt.#:   16.12   Date: Jan. 18, 1990
Time started: 19.45   Plab: 734.5 mm Hg

Thermistor readings (VDC) : (1,2,3;5,6)
       Room   Bath   WBub   Humid   ABub
       2.143   1.852   1.782   2.007   2.092

fd	fa	fh	Pwb	Pab	CNC		range	s
.193	.421	.135	741.6	759.3	.347E+01	.317E+01	.397E+01	.243E+00
.347	.315	.135	740.8	754.1	.605E+01	.469E+01	.791E+01	.117E+01
.371	.302	.135	741.9	753.6	.255E+01	.234E+01	.293E+01	.222E+00
.390	.288	.135	741.9	753.1	.920E+00	.690E+00	.118E+01	.147E+00
.413	.275	.135	741.9	752.1	.484E+00	.380E+00	.540E+00	.498E-01
.435	.262	.135	741.9	751.0	.311E+00	.250E+00	.370E+00	.404E-01
.457	.248	.135	741.9	750.5	.158E+00	.800E-01	.240E+00	.461E-01
.502	.222	.135	742.1	750.0	.500E-01	.200E-01	.100E+00	.245E-01

Time finished: 21.00

Thermistor readings (VDC): (1,2,3,5,6)
       2.125   1.851   1.783   2.006   2.091

Expt.#:   16.12   Date: Jan. 18, 1990
Time started: 19.45   Plab: 734.5 mm Hg

Temperatures (C) : (1,2,3,5,6)
       Room   Bath   WBub   Humid   ABub
       23.07   18.90   18.89   19.52   19.25

fd	fa	fh	ftot	rh	ra	CNC	-	/	+
.198	.650	.148	1.000	.150	.652	.347E+01	.301E+00		.500E+00
.349	.500	.148	1.000	.150	.504,	.605E+01	.136E+01		.187E+01
.372	.480	.148	1.004	.149	.483	.255E+01	.214E+00		.377E+00
.390	.460	.148	1.001	.150	.464	.920E+00	.230E+00		.260E+00
.411	.440	.148	1.003	.149	.444	.484E+00	.104E+00		.563E-01
.432	.421	.148	1.004	.149	.425	.311E+00	.611E-01		.589E-01
.452	.399	.148	1.003	.149	.404	.158E+00	.780E-01		.820E-01
.493	.359	.148	1.004	.149	.363	.500E-01	.300E-01		.500E-01

Time finished: 21.00

Temperatures (C): (1,2,3,5,6)
       22.90   18.89   18.90   19.51   19.24

Expt.#:   16.13   Date: Jan. 19,1990
Time started: 8.00   Plab: 734.2 mm Hg

Thermistor readings (VDC) : (1,2,3,5,6)
       Room   Bath   WBub   Humid   ABub
       2.057   2.431   2.346 2.570   2.657

fd	fa	fh	Pwb	Pab	CNC		range	s
.205	.200	.421	753.2	750.7	.237E+06	.229E+06	.252E+06	.630E+04
.205	.200	.421	753.2	750.7	.200E+06	.184E+06	.226E+06	.105E+05
.320	.201	.315	749.5	750.7	.383E+05	.351E+05	.395E+05	.938E+03
.320	.201	.315	749.5	750.7	.294E+05	.291E+05	.299E+05	.255E+03
.372	.201	.270	748.0	750.7	.123E+05	.117E+05	.134E+05	.474E+03
.372	.201	.270	748.0	750.7	.933E+04	.900E+04	.970E+04	.232E+03
.408	.200	.240	746.8	750.7	.427E+04	.404E+04	.465E+04	.201E+03
.408	.200	.240	746.8	750.7	.313E+04	.297E+04	.330E+04	.972E+02
.444	.201	.210	745.7	750.7	.102E+04	.920E+03	.118E+04	.903E+02
.482	.201	.179	744.4	750.7	.941E+02	.790E+02	.112E+03	.621E+01
.501	.201	.165	743.9	750.7	.302E+02	.230E+02	.377E+02	.354E+01
.521	.201	.150	743.3	750.7	.503E+01	.409E+01	.674E+01	.807E+00
.540	.201	.135	743.1	750.7	.112E+01	.980E+00	.137E+01	.152E+00
.560	.201	.120	742.4	750.7	.142E+00	.500E-01	.220E+00	.443E-01
.581	.200	.104	742.0	750.7	.469E-01	.300E-01	.800E-01	.160E-01
.205	.201	.421	753.7	750.7	.119E+06	.990E+05	.131E+06	.146E+05

Time finished: 9.30

Thermistor readings (VDC): (1,2,3,5,6)
       2.087   2.445   2.359   2.585   2.672

Expt.#:   16.13   Date: Jan. 19,1990
Time started: 8.00   Plab: 734.2 mm Hg

Temperatures (C) : (1,2,3,5,6)
       Room   Bath   WBub   Humid   ABub
       22.23   24.55   24.66 25.15   24.91

fd	fa	fh	ftot	rb	ra	CNC	-	/	+
.210	.325	.451	1.001	.456	.329	.237E+06	.810E+04		.149E+05
.210	.325	.451	1.001	.456	.329	.200E+06	.158E+05		.262E+05
.323	.327	.342	1.003	.347	.330	.383E+05	.317E+04		.123E+04
.323	.327	.342	1.003	.347	.330	.294E+05	.344E+03		.456E+03
.373	.327	.295	1.004	.300	.330	.123E+05	.621E+03		.108E+04
.373	.327	.295	1.004	.300	.330	.933E+04	.331E+03		.369E+03
.407	.325	.263	1.003	.268	.328	.427E+04	.234E+03		.376E+03
.407	.325	.263	1.003	.268	.328	.313E+04	.161E+03		.169E+03
.440	.327	.230	1.004	.235	.329	.102E+04	.104E+03		.156E+03
.475	.327	.197	1.005	.201	.329	.956E+02	.155E+02		.186E+02
.492	.327	.181	1.006	.185	.329	.303E+02	.722E+01		.764E+01
.510	.327	.165	1.007	.168	.328	.503E+01	.939E+00		.172E+01
.528	.327	.148	1.007	.151	.328	.112E+01	.140E+00		.250E+00
.546	.327	.131	1.008	.134	.328	.143E+00	.925E-01		.775E-01
.564	.325	.113	1.006	.116	.327	.469E-01	.169E-01		.331E-01
.210	.327	.451	1.002	.455	.330	.119E+06	.197E+05		.123E+05

Time finished: 9.30

Temperatures (C): (1,2,3,5,6)
       22.52   24.69   24.79   25.30   25.06

Expt.#: 16.14 Date: Jan. 19, 1990
Time started: 10.00 Plab: 734.2 mm Hg

Thermistor readings (VDC) : (1,2,3,5,6)

Room	Bath	WBub	Humid	ABub
2.087	2.445	2.359	2.585	2.672

fd	fa	fh	Pwb	Pab	CNC	range		s
.181	.092	.639	764.0	742.5	.488E+05	.475E+05	.500E+05	.692E+03
.181	.092	.639	764.0	742.5	.622E+05	.591E+05	.654E+05	.199E+04
.248	.092	.580	761.2	742.5	.520E+05	.509E+05	.535E+05	.689E+03
.248	.092	.580	761.2	742.5	.478E+05	.470E+05	.485E+05	.434E+03
.291	.092	.520	759.5	742.5	.400E+05	.388E+05	.411E+05	.765E+03
.291	.092	.520	759.5	742.5	.363E+05	.357E+05	.369E+05	.333E+03
.320	.092	.480	758.0	742.5	.271E+05	.259E+05	.283E+05	.620E+03
.320	.092	.480	758.0	742.5	.226E+05	.220E+05	.230E+05	.335E+03
.387	.092	.420	755.2	742.5	.103E+05	.100E+05	.107E+05	.179E+03
.387	.092	.420	755.2	742.5	.765E+04	.723E+04	.839E+04	.347E+03
.457	.092	.360	752.8	742.5	.241E+04	.236E+04	.256E+04	.507E+02
.457	.092	.360	752.8	742.5	.177E+04	.167E+04	.189E+04	.705E+02
.493	.092	.330	751.9	742.5	.466E+03	.418E+03	.545E+03	.451E+02
.511	.092	.315	750.9	742.5	.266E+03	.238E+03	.294E+03	.199E+02
.530	.092	.300	750.6	742.5	.111E+03	.103E+03	.118E+03	.419E+01
.548	.092	.285	750.0	742.5	.573E+02	.479E+02	.636E+02	.373E+01
.568	.092	.270	749.5	742.5	.232E+02	.197E+02	.259E+02	.175E+01
.587	.092	.254	748.7	742.5	.107E+02	.839E+01	.134E+02	.146E+01
.606	.092	.240	748.2	742.5	.355E+01	.288E+01	.438E+01	.389E+00
.626	.092	.225	747.6	742.5	.129E+01	.920E+00	.159E+01	.179E+00
.648	.092	.209	747.0	742.5	.551E+00	.460E+00	.640E+00	.624E-01
.667	.092	.195	746.5	742.5	.206E+00	.150E+00	.290E+00	.443E-01
.687	.092	.179	745.7	742.5	.847E-01	.300E-01	.130E+00	.280E-01
.181	.092	.640	764.0	742.5	.349E+05	.326E+05	.381E+05	.291E+04

Time finished: 12.00

Thermistor readings (VDC): (1,2,3,5,6)
2.116 2.462 2.375 2.602 2.691

Expt.#:   16.14   Date: Jan. 19, 1990
Time started: 10.00   Plab: 734.2 mm Hg

Temperatures (C) : (1,2,3,5,6)
       Room   Bath   WBub   Humid   ABub
       22.52   24.69   24.79   25.30   25.06

fd	fa	fh	ftot	rh	ra	CNC	-	/	+
.186	.149	.661	1.018	.648	.150	.488E+05	.128E+04		.122E+04
.186	.149	.661	1.018	.648	.150	.622E+05	.305E+04		.325E+04
.253	.149	.606	1.028	.591	.149	.520E+05	.111E+04		.149E+04
.253	.149	.606	1.028	.591	.149	.478E+05	.763E+03		.737E+03
.295	.149	.549	1.011	.545	.152	.400E+05	.124E+04		.106E+04
.295	.149	.549	1.011	.545	.152	.363E+05	.555E+03		.645E+03
.323	.149	.510	.998	.513	.153	.271E+05	.123E+04		.117E+04
.323	.149	.510	.998	.513	.153	.226E+05	.571E+03		.429E+03
.387	.149	.450	1.001	.454	.153	.103E+05	.274E+03		.426E+03
.387	.149	.450	1.001	.454	.153	.765E+04	.418E+03		.742E+03
.452	.149	.389	1.003	.393	.153	.241E+04	.486E+02		.151E+03
.452	.149	.389	1.003	.393	.153	.177E+04	.995E+02		.121E+03
.485	.149	.358	1.004	.362	.153	.505E+03	.554E+02		.944E+02
.501	.149	.342	1.004	.346	.153	.279E+03	.305E+02		.309E+02
.519	.149	.326	1.005	.330	.152	.113E+03	.807E+01		.752E+01
.535	.149	.311	1.005	.314	.152	.579E+02	.962E+01		.639E+01
.553	.149	.295	1.006	.298	.152	.233E+02	.355E+01		.270E+01
.570	.149	.278	1.006	.281	.152	.107E+02	.232E+01		.271E+01
.587	.149	.263	1.007	.266	.152	.355E+01	.673E+00		.829E+00
.604	.149	.247	1.008	.250	.152	.129E+01	.375E+00		.296E+00
.623	.149	.229	1.010	.232	.152	.551E+00	.908E-01		.892E-01
.640	.149	.214	1.010	.217	.152	.206E+00	.562E-01		.839E-01
.657	.149	.197	1.010	.199	.152	.847E-01	.547E-01		.453E-01
.186	.149	.662	1.019	.648	.150	.349E+05	.232E+04		.318E+04

Time finished: 12.00

Temperatures (C): (1,2,3,5,6)
     22.81   24.85   24.96   25.47   25.25

Expt.#:   16.15   Date: Jan. 19, 1990
Time started: 12.30   Plab: 734.2 mm Hg

Thermistor readings (VDC) : (1,2,3,5,6)
Room   Bath   WBub   Humid   ABub
2.116   2.462   2.375   2.602   2.691

fd	fa	fh	Pwb	Pab	CNC		range		s
.263	.048	640	764.3	740.9	.540E+04	.509E+04	.570E+04	.199E+03
.263	.048	.640	764.3	740.9	.617E+04	.585E+04	.661E+04	.265E+03
.291	.048	.610	763.6	740.9	.471E+04	.447E+04	.515E+04	.227E+03
.291	.048	.610	763.6	740.9	.477E+04	.432E+04	.511E+04	.227E+03
.321	.048	.580	762.1	740.9	.328E+04	.311E+04	.343E+04	.929E+02
.321	.048	.580	762.1	740.9	.307E+04	.289E+04	.328E+04	.107E+03
.344	.048	.551	761.2	740.9	.215E+04	.208E+04	.225E+04	47.E+02
.344	.048	.551	761.2	740.9	.207E+04	.201E+04	.216E+0.	.+02
.370	.048	.519	760.1	740.9	.126E+04	.120E+04	.131E+04	.-2
.400	.048	.480	758.4	740.9	.454E+03	.428E+03	.491E+03	
.435	.048	.450	756.9	740.9	.201E+03	.182E+03	.226E+03	.114E+02
.470	.048	.420	756.1	740.9	.775E+02	.699E+02	.842E+02	.407E+01
.487	.048	.405	755.2	740.9	.408E+02	.346E+02	.459E+02	.259E+01
.505	.048	.390	754.7	740.9	.215E+02	.190E+02	.247E+02	.179E+01
.523	.048	.375	754.3	740.9	.982E+01	.870E+01	.115E+02	.926E+00
.542	.048	.360	753.2	740.9	.514E+01	.414E+01	.602E+01	.622E+00
.559	.048	.345	753.0	740.9	.244E+01	.199E+01	.301E+01	.288E+00
.579	.048	.330	752.4	740.9	.115E+01	.820E+00	.131E+01	.148E+00
.598	.048	.314	751.9	740.9	.530E+00	.410E+00	.630E+00	.662E-01
.617	.048	.300	751.3	740.9	.276E+00	.190E+00	.410E+00	.702E-01
.637	.048	.285	750.8	740.9	.132E+00	.700E-01	.210E+00	.419E-01
.657	.048	.270	750.0	740.9	.783E-01	.500E-01	.140E+00	.272E-01
.263	.048	.640	764.3	740.9	.242E+04	.229E+04	.265E+04	.123E+03

Time finished: 15.00

Thermistor readings (VDC): (1,2,3,5,6)
2.155   2.469   2.382   2.608   2.699

```
Expt.#:     16.15     Date: Jan. 19, 1990
Time started:  12.30     Plab:      734.2 mm Hg

Temperatures (C) :  (1,2,3,5,6)
         Room    Bath    WBub    Humid    ABub
         22.81   24.85   24.96   25.47    25.25
```

fd	fa	fh	ftot	rh	ra	CNC	- /	+
.268	.074	.662	1.025	.644	.075	.540E+04	.307E+03	.303E+03
.268	.074	.662	1.025	.644	.075	.617E+04	.325E+03	.435E+03
.295	.074	.634	1.024	.619	.075	.471E+04	.238E+03	.442E+03
.295	.074	.634	1.024	.619	.075	.477E+04	.448E+03	.342E+03
.324	.074	.606	1.024	.592	.075	.328E+04	.167E+03	.153E+03
.324	.074	.606	1.024	.592	.075	.307E+04	.179E+03	.211E+03
.346	.074	.579	1.017	.570	.075	.215E+04	.713E+02	.987E+02
.346	.074	.579	1.017	.570	.075	.207E+04	.620E+02	.880E+02
.371	.074	.548	1.010	.544	.076	.126E+04	.607E+02	.493E+02
.399	.074	.510	.999	.513	.076	.491E+03	.302E+02	.436E+02
.432	.074	.480	1.001	.483	.076	.209E+03	.206E+02	.266E+02
.464	.074	.450	1.003	.453	.076	.785E+02	.779E+01	.690E+01
.480	.074	.435	1.003	.438	.076	.411E+02	.627E+01	.519E+01
.496	.074	.420	1.003	.423	.076	.215E+02	.248E+01	.26E+01
.512	.074	.404	1.004	.407	.076	.984E+01	.112E+01	.169E+01
.529	.074	.389	1.005	.392	.076	.514E+01	.100E+01	.883E+00
.545	.074	.373	1.004	.377	.076	.244E+01	.453E+00	.568E+00
.563	.074	.358	1.006	.361	.076	.115E+01	.328E+00	.162E+00
.579	.074	.341	1.006	.344	.076	.530E+00	.120E+00	.100E+00
.596	.074	.326	1.008	.329	.076	.276E+00	.862E-01	.134E+00
.614	.074	.311	1.009	.313	.076	.132E+00	.621E-01	.779E-01
.631	.074	.295	1.010	.297	.076	.783E-01	.283E-01	.617E-01
.268	.074	.662	1.025	.644	.075	.242E+04	.131E+03	.229E+03

```
Time finished:  15.00


Temperatures (C):  (1,2,3,5,6)
    23.19   24.92   25.03   25.53    25.33
```

Expt.#:   16.16   Date: Jan. 19, 1990
Time started: 16.00   Plab: 734.2 mm Hg

Thermistor readings (VDC) : (1,2,3,5,6)
       Room   Bath   WBub   Humid   ABub
       2.155   2.469   2.382   2.608   2.699

fd	fa	fh	Pwb	Pab	CNC		range		s
.044	.422	.270	746.8	760.1	.315E+06	.247E+06	.374E+06	.434E+05
.044	.422	.270	746.8	760.1	.321E+06	.303E+06	.355E+06	.125E+05
.190	.315	.270	746.8	755.9	.676E+05	.642E+05	.693E+05	.113E+04
.190	.315	.270	746.8	755.9	.866E+05	.731E+05	.950E+05	.395E+04
.242	.248	.270	747.2	752.8	.329E+05	.320E+05	.356E+05	.110E+04
.242	.248	.270	747.2	752.8	.292E+05	.273E+05	.312E+05	.127E+04
.372	.200	.269	747.6	750.7	.878E+04	.834E+04	.919E+04	.259E+03
.372	.200	.269	747.6	750.7	.438E+04	.430E+04	.446E+04	.519E+02
.455	.153	.270	748.0	747.6	.128E+04	.122E+04	.134E+04	.329E+02
.455	.153	.270	748.0	747.6	.102E+04	.990E+03	.105E+04	.208E+02
.510	.122	.270	748.3	745.6	.152E+03	.140E+03	.164E+03	.711E+01
.480	.139	.270	748.2	746.6	.246E+03	.233E+03	.258E+03	.795E+01
.538	.107	.270	748.7	744.5	.479E+02	.420E+02	.561E+02	.381E+01
.567	.092	.270	749.1	743.5	.143E+02	.113E+02	.188E+02	.161E+01
.598	.078	.270	749.1	742.5	.307E+01	.225E+01	.374E+01	.485E+00
.612	.071	.270	749.5	742.0	.108E+01	.930E+00	.122E+01	.933E-01
.628	.063	.270	749.5	741.4	.461E+00	.310E+00	.540E+00	.718E-01
.642	.056	.270	749.5	740.9	.184E+00	.900E-01	.260E+00	.546E-01
.657	.048	.270	749.5	740.4	.569E-01	.100E-01	.100E+00	.266E-01
.044	.421	.270	746.8	762.6	.296E+06	.291E+06	.303E+06	.383E+04

Time finished: 17.30

Thermistor readings (VDC): (1,2,3,5,6)
       2.138   2.473   2.384   2.617   2.701

Expt.#:   16.16   Date: Jan. 19, 1990
Time started: 16.00   Plab: 734.2 mm Hg

Temperatures (C) : (1,2,3,5,6)
       Room   Bath   WBub   Humid   ABub
       23.19   24.92   25.03   25.53   25.33

fd	fa	fh	ftot	rh	ra	CNC	− /		+
.045	.652	.295	1.001	.301	.654	.315E+06	.675E+05	.595E+05
.045	.652	.295	1.001	.301	.654	.321E+06	.175E+05	.345E+05
.195	.500	.295	1.000	.301	.505	.676E+05	.340E+04	.170E+04
.195	.500	.295	1.000	.301	.505	.866E+05	.750E+04	.840E+04
.247	.399	.295	.951	.317	.426	.329E+05	.918E+03	.268E+04
.247	.399	.295	.951	.317	.426	.292E+05	.185E+04	.205E+04
.373	.325	.294	1.001	.300	.330	.878E+04	.437E+03	.413E+03
.373	.325	.294	1.001	.300	.330	.438E+04	.809E+02	.791E+02
.450	.250	.295	1.005	.299	.254	.128E+04	.567E+02	.633E+02
.450	.250	.295	1.005	.299	.254	.102E+04	.310E+02	.290E+02
.501	.199	.295	1.004	.299	.203	.156E+03	.125E+02	.128E+02
.473	.227	.295	1.005	.299	.231	.257E+03	.139E+02	.133E+02
.526	.175	.295	1.005	.299	.178	.483E+02	.595E+01	.839E+01
.552	.149	.295	1.006	.299	.153	.143E+02	.298E+01	.456E+01
.579	.126	.295	1.010	.297	.128	.308E+01	.825E+00	.666E+00
.592	.114	.295	1.010	.297	.116	.108E+01	.154E+00	.136E+00
.606	.100	.295	1.010	.297	.102	.461E+00	.151E+00	.793E-01
.618	.088	.295	1.011	.297	.090	.184E+00	.936E-01	.764E-01
.631	.074	.295	1.010	.297	.076	.569E-01	.469E-01	.431E-01
.045	.650	.295	1.000	.301	.651	.296E+06	.522E+04	.678E+04

Time finished: 17.30

Temperatures (C): (1,2,3,5,6)
       23.03   24.96   25.05   25.62   25.35

Expt.#:   16.17   Date: Jan. 19, 1990
Time started: 17.30   Plab: 734.2 mm Hg

Thermistor readings (VDC) : (1,2,3,5,6)
        Room   Bath   WBub   Humid   ABub
        2.138   2.473   2.384   2.617   2.701

fd	fa	fh	Pwb	Pab	CNC		range	s
.192	.421	.135	741.3	762.6	.110E+02	.890E+01	.129E+02	.116E+01
.243	.385	.135	741.5	761.1	.977E+01	.850E+01	.115E+02	.812E+00
.294	.350	.135	741.6	760.1	.166E+02	.142E+02	.187E+02	.130E+01
.347	.315	.135	741.6	759.0	.181E+02	.162E+02	.212E+02	.139E+01
.400	.281	.135	755.9	755.9	.615E+01	.455E+01	.844E+01	.131E+01
.427	.265	.135	742.0	754.9	.236E+01	.209E+01	.266E+01	.183E+00
.455	.248	.135	742.0	753.8	.145E+01	.123E+01	.186E+01	.159E+00
.539	.200	.135	742.6	750.7	.117E+00	.600E-01	.190E+00	.381E-01
.584	.177	.135	742.6	749.7	.455E-01	.200E-01	.900E-01	.221E-01

Time finished: 18.30

Thermistor readings (VDC): (1,2,3,5,6)
        2.125   2.471   2.384   2.615   2.698

Expt.#:   16.17   Date: Jan. 19, 1990
Time started: 17.30   Plab: 734.2 mm Hg

Temperatures (C) : (1,2,3,5,6)
        Room   Bath   WBub   Humid   ABub
        23.03   24.96   25.05   25.62   25.35

fd	fa	fh	ftot	rh	ra	CNC	-	/	+
.197	.650	.148	1.001	.152	.650	.110E+02	.213E+01		.188E+01
.248	.600	.148	1.001	.152	.600	.979E+01	.128E+01		.173E+01
.298	.550	.148	1.001	.152	.551	.167E+02	.244E+01		.208E+01
.349	.500	.148	1.001	.152	.501	.181E+02	.190E+01		.313E+01
.399	.449	.148	1.001	.152	.453	.615E+01	.160E+01		.230E+01
.424	.425	.148	1.002	.152	.428	.236E+01	.274E+00		.297E+00
.450	.399	.148	1.003	.152	.403	.145E+01	.218E+00		.412E+00
.527	.325	.148	1.005	.151	.329	.118E+00	.575E-01		.725E-01
.567	.289	.148	1.009	.151	.291	.455E-01	.255E-01		.445E-01

Time finished: 18.30

Temperatures (C): (1,2,3,5,6)
        22.90   24.94   25.05   25.60   25.32

II. The raw and reduced data for the sulfuric acid-water experiments.

```
Expt.#:     20.09    Date: Mar.17, 1990
Time started: 20.00    Plab:    736.4 mm Hg

Thermistor readings (VDC) : (1,2,3,5,6)
        Room    Bath    WBub    Humid    ABub
        2.333   2.490   2.316   2.667    2.692
```

fd	fa	fh	Pwb	Pab	CNC	range		s
0.352	0.385	0.045	740.1	764.3	0.224E+02	0.198E+02	0.247E+02	0.140E+01
0.371	0.385	0.030	739.2	764.3	0.232E+00	0.160E+00	0.290E+00	0.454E-01
0.390	0.385	0.015	739.2	764.3	0.333E-02	0.000E+00	0.100E-01	0.577E-02
0.381	0.385	0.022	739.2	764.3	0.160E-01	0.000E+00	0.300E-01	0.114E-01
0.371	0.385	0.030	739.0	764.3	0.178E+00	0.130E+00	0.200E+00	0.295E-01
0.352	0.385	0.045	739.4	764.3	0.245E+02	0.222E+02	0.266E+02	0.175E+01
0.333	0.385	0.060	739.7	764.3	0.371E+03	0.360E+03	0.387E+03	0.832E+01
0.315	0.385	0.075	740.1	764.3	0.354E+04	0.347E+04	0.374E+04	0.935E+02
0.296	0.385	0.090	740.9	764.3	0.119E+05	0.117E+05	0.122E+05	0.170E+03
0.278	0.385	0.105	741.2	764.3	0.328E+05	0.325E+05	0.329E+05	0.165E+03
0.242	0.385	0.135	742.4	764.3	0.796E+05	0.788E+05	0.803E+05	0.596E+03
0.208	0.385	0.165	743.7	764.3	0.122E+06	0.121E+06	0.124E+06	0.107E+04
0.157	0.385	0.210	745.7	764.3	0.198E+06	0.196E+06	0.201E+06	0.168E+04
0.092	0.385	0.270	747.9	764.3	0.273E+06	0.270E+06	0.275E+06	0.175E+04

```
Time finished:   21.30


Thermistor readings (VDC): (1,2,3,5,6)
        2.333   2.490   2.316   2.667    2.692



Expt.#:     20.09    Date: Mar.17, 1990
Time started: 20.00    Plab:    736.4 mm Hg

Temperatures (C) : (1,2,3,5,6)
        Room    Bath    WBub    Humid    ABub
        24.94   25.13   24.35   26.12    25.26
```

fd	fa	fh	ftot	rh	ra	CNC	–	/	+
0.354	0.600	0.046	1.002	0.045	0.577	0.225E+02	0.263E+01	0.230E+01	
0.372	0.600	0.029	1.002	0.029	0.577	0.232E+00	0.717E-01	0.583E-01	
0.390	0.600	0.012	1.002	0.012	0.577	0.333E-02	0.333E-02	0.667E-02	
0.381	0.600	0.020	1.002	0.020	0.577	0.160E-01	0.160E-01	0.140E-01	
0.372	0.600	0.029	1.002	0.029	0.577	0.178E+00	0.480E-01	0.220E-01	
0.354	0.600	0.046	1.002	0.046	0.577	0.246E+02	0.235E+01	0.209E+01	
0.336	0.600	0.064	1.001	0.062	0.577	0.396E+03	0.123E+02	0.184E+02	
0.318	0.600	0.081	1.001	0.079	0.577	0.354E+04	0.700E+02	0.200E+03	
0.300	0.600	0.098	1.001	0.096	0.577	0.119E+05	0.209E+03	0.291E+03	
0.282	0.600	0.114	1.001	0.112	0.578	0.328E+05	0.280E+03	0.120E+03	
0.247	0.600	0.148	1.000	0.145	0.578	0.796E+05	0.788E+03	0.713E+03	
0.213	0.600	0.181	1.000	0.177	0.578	0.122E+06	0.857E+03	0.214E+04	
0.162	0.600	0.230	1.000	0.224	0.578	0.198E+06	0.238E+04	0.262E+04	
0.095	0.600	0.295	1.000	0.286	0.578	0.273E+06	0.267E+04	0.233E+04	

```
Time finished:   21.30


Temperatures (C): (1,2,3,5,6)
        24.94   25.13   24.35   26.12    25.26
```

Expt.#:   20.10   Date: Mar.18, 1990
Time started: 7.30   Plab: 736.1 mm Hg

Thermistor readings (VDC) : (1,2,3,5,6)
        Room   Bath   WBub   Humid   ABub
        2.316   2.447   2.305   2.657   2.663

fd	fa	fh	Pwb	Pab	CNC	range		s
0.352	0.385	0.045	739.8	766.1	0.332E+02	0.313E+02	0.355E+02	0.144E+01
0.371	0.385	0.030	739.1	766.1	0.340E+00	0.280E+00	0.440E+00	0.646E-01
0.390	0.385	0.015	738.7	766.1	0.571E-02	0.000E+00	0.200E-01	0.787E-02
0.381	0.385	0.022	738.3	766.1	0.256E-01	0.100E-01	0.400E-01	0.113E-01
0.371	0.385	0.030	738.5	766.1	0.294E+00	0.150E+00	0.370E+00	0.689E-01
0.361	0.385	0.038	738.7	766.1	0.458E+01	0.378E+01	0.532E+01	0.561E+00
0.352	0.385	0.045	739.1	766.1	0.334E+02	0.297E+02	0.370E+02	0.217E+01
0.343	0.385	0.052	739.4	766.1	0.156E+03	0.144E+03	0.169E+03	0.736E+01
0.333	0.385	0.060	739.8	766.1	0.573E+03	0.554E+03	0.591E+03	0.100E+02
0.315	0.385	0.075	740.2	766.1	0.427E+04	0.411E+04	0.445E+04	0.101E+03
0.296	0.385	0.090	740.4	766.1	0.181E+05	0.176E+05	0.188E+05	0.373E+03
0.278	0.385	0.105	741.1	766.1	0.412E+05	0.407E+05	0.414E+05	0.237E+03
0.260	0.385	0.120	741.9	766.1	0.690E+05	0.600E+05	0.706E+05	0.318E+04
0.225	0.385	0.150	742.8	766.1	0.129E+06	0.127E+06	0.130E+06	0.917E+03
0.157	0.385	0.210	745.4	766.1	0.238E+06	0.236E+06	0.239E+06	0.967E+03
0.092	0.385	0.270	747.6	766.1	0.297E+06	0.295E+06	0.299E+06	0.116E+04

Time finished: 8.50

Thermistor readings (VDC): (1,2,3,5,6)
        2.328   2.488   2.308   2.669   2.678

Expt.#:   20.10   Date: Mar.18, 1990
Time started: 7.30   Plab: 736.1 mm Hg

Temperatures (C) : (1,2,3,5,6)
        Room   Bath   WBub   Humid   ABub
        24.78   24.71   24.24   26.02   24.97

fd	fa	fh	ftot	rh	ra	CNC	-	/	+
0.354	0.600	0.046	1.002	0.046	0.576	0.334E+02	0.190E+01	0.235E+01
0.372	0.600	0.029	1.002	0.029	0.575	0.340E+00	0.600E-01	0.100E+00
0.390	0.600	0.012	1.002	0.012	0.575	0.571E-02	0.571E-02	0.143E-01
0.381	0.600	0.020	1.002	0.020	0.575	0.256E-01	0.156E-01	0.144E-01
0.372	0.600	0.029	1.002	0.029	0.575	0.294E+00	0.144E+00	0.763E-01
0.362	0.600	0.038	1.002	0.038	0.575	0.459E+01	0.805E+00	0.738E+00
0.354	0.600	0.046	1.002	0.046	0.576	0.336E+02	0.370E+01	0.369E+01
0.345	0.600	0.054	1.001	0.054	0.576	0.160E+03	0.126E+02	0.138E+02
0.336	0.600	0.064	1.001	0.063	0.576	0.634E+03	0.231E+02	0.219E+02
0.318	0.600	0.081	1.001	0.080	0.576	0.427E+04	0.158E+03	0.182E+03
0.300	0.600	0.098	1.001	0.097	0.576	0.181E+05	0.520E+03	0.680E+03
0.282	0.600	0.114	1.001	0.114	0.576	0.412E+05	0.454E+03	0.246E+03
0.265	0.600	0.131	1.000	0.131	0.576	0.690E+05	0.899E+04	0.161E+04
0.230	0.600	0.165	1.000	0.164	0.576	0.129E+06	0.220E+04	0.800E+03
0.162	0.600	0.230	1.000	0.228	0.577	0.238E+06	0.178E+04	0.122E+04
0.095	0.600	0.295	1.000	0.291	0.577	0.297E+06	0.233E+04	0.167E+04

Time finished: 8.50

Temperatures (C): (1,2,3,5,6)
        24.89   25.11   24.27   26.14   25.12

Expt.#:   20.11   Date: Mar.18, 1990
Time started: 10.00   Plab: 736.1 mm Hg

Thermistor readings (VDC) : (1,2,3,5,6)
      Room   Bath   WBub   Humid   ABub
      2.318   2.476   2.310   2.657   2.671

fd	fa	fh	Pwb	Pab	CNC	range		s
0.664	0.200	0.044	740.2	755.7	0.539E+00	0.490E+00	0.660E+00	0.576E-01
0.686	0.200	0.030	740.0	755.7	0.350E-01	0.200E-01	0.800E-01	0.193E-01
0.665	0.200	0.045	740.4	755.7	0.532E+00	0.370E+00	0.620E+00	0.904E-01
0.643	0.200	0.060	740.8	755.7	0.781E+01	0.722E+01	0.868E+01	0.460E+00
0.622	0.200	0.075	741.7	755.7	0.903E+02	0.836E+02	0.997E+02	0.523E+01
0.601	0.200	0.090	742.1	755.7	0.364E+03	0.390E+01	0.426E+03	0.120E+03
0.581	0.200	0.105	742.6	755.7	0.202E+04	0.186E+04	0.217E+04	0.104E+03
0.560	0.200	0.120	743.4	755.7	0.395E+04	0.382E+04	0.416E+04	0.101E+03
0.540	0.200	0.135^	743.9	755.7	0.694E+04	0.663E+04	0.730E+04	0.246E+03
0.540	0.200	0.135'	743.9	755.7	0.777E+04	0.723E+04	0.824E+04	0.358E+03
0.501	0.200	0.165	745.4	755.7	0.192E+05	0.179E+05	0.203E+05	0.780E+03
0.444	0.200	0.210'	7:.9	755.7	0.391E+05	0.379E+05	0.401E+05	0.730E+03
0.372	0.200	0.270^	7 .5	755.7	0.709E+05	0.677E+05	0.719E+05	0.144E+04
0.372	0.200	0.270'	749.5	755.7	0.528E+05	0.508E+05	0.546E+05	0.129E+04
0.286	0.200	0.345	752.5	755.7	0.957E+05	0.927E+05	0.979E+05	0.196E+04
0.205	0.200	0.420'	755.6	755.7	0.121E+06	0.117E+06	0.125E+06	0.293E+04
0.205	0.200	0.420	755.6	755.7	0.103E+06	0.100E+06	0.108E+06	0.286E+04

Time finished: 13.50

Thermistor readings (VDC): (1,2,3,5,6)
      2.337   2.502   2.315   2.671   2.707

Expt.#:   20.11   Date: Mar.18, 1990
Time started: 10.00   Plab: 736.1 mm Hg

Temperatures (C) : (1,2,3,5,6)
      Room   Bath   WBub   Humid   ABub
      24.80   24.99   24.29   26.02   25.05

fd	fa	fh	ftot	rh	ra	CNC	-	/	+
0.637	0.325	0.045	1.009	0.044	0.314	0.539E+00	0.486E-01	0.121E+00	
0.657	0.325	0.029	1.012	0.028	0.313	0.350E-01	0.150E-01	0.450E-01	
0.638	0.325	0.046	1.011	0.045	0.313	0.532E+00	0.162E+00	0.884E-01	
0.619	0.325	0.064	1.010	0.062	0.314	0.782E+01	0.589E+00	0.875E+00	
0.601	0.325	0.081	1.009	0.078	0.314	0.918E+02	0.695E+01	0.968E+01	
0.582	0.325	0.098	1.008	0.095	0.314	0.388E+03	0.385E+03	0.705E+02	
0.564	0.325	0.114	1.008	0.111	0.314	0.202E+04	0.162E+03	0.148E+03	
0.546	0.325	0.131	1.006	0.128	0.315	0.395E+04	0.131E+03	0.209E+03	
0.528	0.325	0.148	1.005	0.144	0.315	0.694E+04	0.310E+03	0.360E+03	
0.528	0.325	0.148	1.005	0.144	0.315	0.777E+04	0.544E+03	0.466E+03	
0.492	0.325	0.181	1.004	0.176	0.315	0.192E+05	0.134E+04	0.106E+04	
0.440	0.325	0.230	1.003	0.224	0.316	0.391E+05	0.122E+04	0.975E+03	
0.373	0.325	0.295	1.002	0.286	0.316	0.709E+05	0.317E+04	0.103E+04	
0.373	0.325	0.295	1.002	0.286	0.316	0.528E+05	0.202E+04	0.178E+04	
0.290	0.325	0.373	1.000	0.361	0.317	0.957E+05	0.301E+04	0.219E+04	
0.210	0.325	0.450	0.999	0.434	0.317	0.121E+06	0.450E+04	0.350E+04	
0.210	0.325	0.450	0.999	0.434	0.317	0.103E+06	0.317E+04	0.483E+04	

Time finished: 13.50

Temperatures (C): (1,2,3,5,6)
      24.98   25.24   24.34   26.16   25.41

Expt.#:   20.12   Date: Mar.18, 1990
Time started: 14.50   Plab: 736.1 mm Hg

Thermistor readings (VDC) : (1,2,3,5,6)
        Room   Bath   WBub   Humid   ABub
        2.312   2.477   2.308   2.649   2.676

fd	fa	fh	Pwb	Pab	CNC	range		s
0.754	0.122	0.090	743.5	749.5	0.443E-01	0.100E-01	0.800E-01	0.282E-01
0.732	0.122	0.105	743.9	749.5	0.206E+00	0.140E+00	0.280E+00	0.532E-01
0.710	0.122	0.121	744.5	749.5	0.743E+00	0.570E+00	0.890E+00	0.114E+00
0.689	0.122	0.135	745.2	749.5	0.199E+01	0.162E+01	0.233E+01	0.246E+00
0.668	0.122	0.150	745.4	749.5	0.529E+01	0.468E+01	0.588E+01	0.444E+00
0.647	0.122	0.180	746.3	749.5	0.182E+02	0.166E+02	0.197E+02	0.949E+00
0.587	0.122	0.210	747.6	749.5	0.637E+02	0.544E+02	0.703E+02	0.397E+01
0.548	0.122	0.240	748.9	749.5	0.124E+03	0.112E+03	0.134E+03	0.687E+01
0.510	0.122	0.270	750.2	749.5	0.239E+03	0.218E+03	0.257E+03	0.110E+02
0.455	0.122	0.315	751.9	749.5	0.548E+03	0.492E+03	0.609E+03	0.322E+02
0.402	0.122	0.360	753.8	749.5	0.176E+04	0.171E+04	0.183E+04	0.436E+02
0.334	0.122	0.420·	756.4	749.5	0.335E+04	0.319E+04	0.345E+04	0.877E+02
0.334	0.122	0.420·	756.4	749.5	0.281E+04	0.260E+04	0.368E+04	0.388E+03
0.271	0.122	0.480	758.8	749.5	0.389E+04	0.350E+04	0.415E+04	0.218E+03
0.207	0.122	0.540	761.8	749.5	0.722E+04	0.710E+04	0.735E+04	0.101E+03
0.141	0.122	0.600	764.0	749.5	0.842E+04	0.796E+04	0.876E+04	0.310E+03

Time finished: 16.50

Thermistor readings (VDC): (1,2,3,5,6)
        2.322   2.485   2.298   2.656   2.692

Expt.#:   20.12   Date: Mar.18, 1990
Time started: 14.50   Plab: 736.1 mm Hg

Temperatures (C) : (1,2,3,5,6)
        Room   Bath   WBub   Humid   ABub
        24.74   25.00   24.27   25.94   25.10

fd	fa	fh	ftot	rh	ra	CNC	-	/	+
0.715	0.199	0.098	1.015	0.094	0.193	0.443E-01	0.343E-01	0.357E-01	
0.696	0.199	0.114	1.014	0.110	0.193	0.206E+00	0.657E-01	0.743E-01	
0.677	0.199	0.132	1.013	0.128	0.193	0.743E+00	0.173E+00	0.148E+00	
0.659	0.199	0.148	1.011	0.143	0.194	0.199E+01	0.373E+00	0.338E+00	
0.641	0.199	0.165	1.010	0.159	0.194	0.529E+01	0.609E+00	0.594E+00	
0.623	0.199	0.198	1.026	0.188	0.191	0.183E+02	0.162E+01	0.150E+01	
0.570	0.199	0.230	1.007	0.223	0.195	0.644E+02	0.946E+01	0.679E+01	
0.535	0.199	0.263	1.005	0.254	0.195	0.127E+03	0.129E+02	0.101E+02	
0.501	0.199	0.295	1.004	0.284	0.195	0.249E+03	0.227E+02	0.196E+02	
0.450	0.199	0.342	1.002	0.330	0.195	0.603E+03	0.663E+02	0.749E+02	
0.401	0.199	0.389	1.001	0.374	0.196	0.176E+04	0.500E+02	0.700E+02	
0.336	0.199	0.450	1.000	0.432·	0.196	0.335E+04	0.160E+03	0.100E+03	
0.336	0.199	0.450	1.000	0.432·	0.196	0.281E+04	0.214E+03	0.866E+03	
0.276	0.199	0.510	1.000	0.488	0.196	0.389E+04	0.390E+03	0.260E+03	
0.212	0.199	0.568	0.997	0.543	0.196	0.722E+04	0.123E+03	0.127E+03	
0.146	0.199	0.625	0.989	0.601	0.198	0.842E+04	0.460E+03	0.340E+03	

Time finished: 16.50

Temperatures (C): (1,2,3,5,6)
        24.84   25.08   24.17   26.01   25.26

Expt.#:   20.13   Date: Mar.18, 1990
Time started: 17.30   Plab: 736.1 mm Hg

Thermistor readings (VDC) : (1,2,3,5,6)
```
         Room     Bath    WBub    Humid    ABub
         2.309    2.477   2.290   2.644    2.673
```

fd	fa	fh	Pwb	Pab	CNC		range		s
0.389	0.092	0.420	756.9	747.5	0.154E+02	0.139E+02	0.173E+02	0.1?	?-01
0.422	0.092	0.390	756.2	747.5	0.880E+01	0.817E+01	0.951E+01	0.5?	?-00
0.493	0.092	0.330	753.6	747.5	0.352E+01	0.275E+01	0.404E+01	0.527E+00	
0.567	0.092	0.270	751.9	747.5	0.923E+00	0.740E+00	0.117E+01	0.185E+00	
0.646	0.092	0.210	749.7	747.5	0.283E+00	0.220E+00	0.420E+00	0.734E-01	
0.730	0.092	0.150	747.3	747.5	0.233E-01	0.000E+00	0.400E-01	0.163E-01	
0.688	0.092	0.181	747.6	747.5	0.971E-01	0.500E-01	0.140E+00	0.287E-01	
0.646	0.092	0.210	748.2	747.5	0.393E+00	0.320E+00	0.450E+00	0.441E-01	
0.606	0.092	0.240	749.5	747.5	0.780E+00	0.650E+00	0.910E+00	0.771E-01	
0.568	0.092	0.270	750.6	747.5	0.197E+01	0.178E+01	0.213E+01	0.159E+00	
0.493	0.092	0.330	753.2	747.5	0.847E+01	0.749E+01	0.972E+01	0.895E+00	
0.422	0.092	0.390	755.4	747.5	0.263E+02	0.245E+02	0.288E+02	0.163E+01	
0.388	0.092	0.420	756.6	747.5	0.334E+02	0.293E+02	0.390E+02	0.322E+01	
0.319	0.092	0.480	759.0	747.5	0.772E+02	0.722E+02	0.841E+02	0.379E+01	
0.291	0.092	0.520	760.7	747.5	0.863E+02	0.782E+02	0.989E+02	0.623E+01	
0.249	0.092	0.580	763.8	747.5	0.779E+02	0.726E+02	0.813E+02	0.238E+01	
0.181	0.092	0.640	765.9	747.5	0.145E+03	0.140E+03	0.152E+03	0.364E+01	
0.141	0.092	0.680	767.7	747.5	0.179E+03	0.157E+03	0.194E+03	0.118E+02	

Time finished: 19.00

Thermistor readings (VDC): (1,2,3,5,6)
```
         2.326    2.481   2.291   2.359    2.685
```

Expt.#:   20.13   Date: Mar.18, 1990
Time started: 17.30   Plab: 736.1 mm Hg

Temperatures (C) : (1,2,3,5,6)
```
         Room     Bath    WBub    Humid    ABub
         24.71    25.00   24.09   25.89    25.07
```

fd	fa	fh	ftot	rh	ra	CNC	-	/	+
0.389	0.149	0.450	1.002	0.426	0.147	0.154E+02	0.146E+01	0.196E+01	
0.420	0.149	0.420	1.001	0.398	0.147	0.882E+01	0.634E+00	0.711E+00	
0.485	0.149	0.358	1.003	0.340	0.147	0.353E+01	0.776E+00	0.516E+00	
0.552	0.149	0.295	1.005	0.280	0.146	0.923E+00	0.183E+00	0.247E+00	
0.622	0.149	0.230	1.009	0.219	0.146	0.283E+00	0.633E-01	0.137E+00	
0.694	0.149	0.165	1.014	0.156	0.145	0.233E-01	0.233E-01	0.167E-01	
0.658	0.149	0.199	1.013	0.189	0.145	0.971E-01	0.471E-01	0.429E-01	
0.622	0.149	0.230	1.009	0.219	0.146	0.393E+00	0.733E-01	0.567E-01	
0.587	0.149	0.263	1.007	0.250	0.146	0.780E+00	0.130E+00	0.130E+00	
0.553	0.149	0.295	1.006	0.281	0.146	0.197E+01	0.188E+00	0.162E+00	
0.485	0.149	0.358	1.003	0.340	0.147	0.848E+01	0.984E+00	0.125E+01	
0.420	0.149	0.420	1.001	0.398	0.147	0.264E+02	0.184E+01	0.250E+01	
0.388	0.149	0.450	1.001	0.427	0.147	0.336E+02	0.418E+01	0.564E+01	
0.322	0.149	0.510	0.997	0.484	0.148	0.783E+02	0.517E+01	0.706E+01	
0.295	0.149	0.549	1.010	0.513	0.146	0.876E+02	0.832E+01	0.130E+02	
0.254	0.149	0.606	1.028	0.554	0.143	0.790E+02	0.544E+01	0.350E+01	
0.186	0.149	0.662	1.018	0.610	0.144	0.148E+03	0.478E+01	0.785E+01	
0.146	0.149	0.699	1.015	0.644	0.145	0.185E+03	0.235E+02	0.158E+02	

Time finished: 19.00

Temperatures (C): (1,2,3,5,6)
```
         24.87    25.04   24.10   23.04    25.19
```

Expt.#:   20.14   Date: Mar.18,1990
Time started: 21.00   Plab: 736.1 mm Hg

Thermistor readings (VDC) : (1,2,3,5,6)
     Room   Bath   WBub   Humid   ABub
     2.306   2.471   2.291   2.637   2.665

fd	fa	fh	Pwb	Pab	CNC		range		s
0.751	0.092	0.135	751.0	747.5	0.000E+00	0.000E+00	0.000E+00	0.000E+00	
0.720	0.107	0.135	745.2	748.0	0.111E+00	0.800E-01	0.130E+00	0.227E-01	
0.689	0.122	0.135	745.4	748.5	0.111E+01	0.910E+00	0.121E+01	0.105E+00	
0.659	0.138	0.135	745.4	750.1	0.645E+01	0.527E+01	0.783E+01	0.759E+00	
0.628	0.153	0.135	745.4	751.1	0.272E+02	0.251E+02	0.314E+02	0.196E+01	
0.599	0.168	0.135	745.0	752.6	0.114E+03	0.109E+03	0.125E+03	0.456E+01	
0.569	0.184	0.135	745.0	753.7	0.489E+03	0.454E+03	0.543E+03	0.249E+02	
0.540	0.201	0.135	745.0	754.7	0.251E+04	0.227E+04	0.277E+04	0.162E+03	
0.512	0.216	0.135	744.7	755.7	0.572E+04	0.533E+04	0.597E+04	0.213E+03	
0.456	0.248	0.135	744.5	757.8	0.190E+05	0.175E+05	0.208E+05	0.893E+03	
0.400	0.281	0.135	743.9	759.4	0.461E+05	0.447E+05	0.477E+05	0.873E+03	
0.347	0.314	0.135	743.9	760.9	0.734E+05	0.717E+05	0.768E+05	0.176E+04	
0.294	0.350	0.135	743.5	762.0	0.795E+05	0.776E+05	0.809E+05	0.128E+04	
0.242	0.385	0.135	743.2	763.0	0.762E+05	0.743E+05	0.793E+05	0.154E+04	

Time finished: 22.45

Thermistor readings (VDC): (1,2,3,5,6)
     2.331   2.487   2.303   2.662   2.688

Expt.#:   20.14   Date: Mar.18,1990
Time started: 21.00   Plab: 736.1 mm Hg

Temperatures (C) : (1,2,3,5,6)
     Room   Bath   WBub   Humid   ABub
     24.68   24.94   24.10   25.82   24.99

fd	fa	fh	ftot	rh	ra	CNC	-	/	+
0.712	0.149	0.148	1.014	0.140	0.145	0.000E+00	0.000E+00	0.000E+00	
0.686	0.175	0.148	1.013	0.142	0.170	0.111E+00	0.314E-01	0.186E-01	
0.659	0.199	0.148	1.011	0.142	0.194	0.111E+01	0.201E+00	0.986E-01	
0.633	0.226	0.148	1.011	0.142	0.219	0.646E+01	0.118E+01	0.139E+01	
0.606	0.250	0.148	1.009	0.142	0.243	0.273E+02	0.214E+01	0.422E+01	
0.580	0.274	0.148	1.007	0.142	0.266	0.116E+03	0.528E+01	0.114E+02	
0.554	0.300	0.148	1.006	0.143	0.291	0.533E+03	0.414E+02	0.642E+02	
0.528	0.327	0.148	1.007	0.142	0.316	0.251E+04	0.240E+03	0.260E+03	
0.502	0.350	0.148	1.005	0.143	0.339	0.572E+04	0.393E+03	0.247E+03	
0.451	0.399	0.148	1.003	0.143	0.387	0.190E+05	0.147E+04	0.183E+04	
0.399	0.449	0.148	1.001	0.143	0.435	0.461E+05	0.136E+04	0.164E+04	
0.349	0.498	0.148	1.000	0.144	0.482	0.734E+05	0.175E+04	0.335E+04	
0.298	0.550	0.148	1.001	0.144	0.531	0.795E+05	0.187E+04	0.143E+04	
0.247	0.600	0.148	1.000	0.144	0.579	0.762E+05	0.195E+04	0.305E+04	

Time finished: 22.45

Temperatures (C): (1,2,3,5,6)
     24.92   25.10   24.22   26.07   25.22

Expt.#:   20.15   Date: Mar.18, 1990
Time started: 23.00   Plab: 736.1 mm Hg

Thermistor readings (VDC) : (1,2,3,5,6)
         Room   Bath   WBub   Humid   ABub
         2.331   2.487   2.303   2.662   2.688

fd	fa	fh	Pwb	Pab	CNC	range		s
0.567	0.092	0.270	750.8	745.4	0.400E+01	0.347E+01	0.494E+01	0.511E+00
0.597	0.078	0.270	750.6	743.9	0.127E+00	0.800E-01	0.180E+00	0.427E-01
0.612	0.070	0.270	742.8	742.8	0.250E-02	0.000E+00	0.100E-01	0.500E-02
0.597	0.078	0.270	750.8	743.9	0.786E-01	0.400E-01	0.1⁻ ⁼+00	0.434E-01
0.567	0.092	0.270	750.8	745.4	0.355E+01	0.337E+01	0.3. ⁼+01	0.148E+00
0.538	0.107	0.270	750.8	745.4	0.428E+02	0.318E+02	0.572E+02	0.798E+01
0.510	0.122	0.270	750.6	746.4	0.314E+03	0.288E+03	0.342E+03	0.179E+02
0.482	0.138	0.270	750.6	747.5	0.235E+04	0.223E+04	0.250E+04	0.743E+02
0.454	0.154	0.270	750.6	749.0	0.578E+04	0.543E+04	0.606E+04	0.177E+03
0.399	0.184	0.270	750.2	751.6	0.297E+05	0.283E+05	0.314E+05	0.972E+03
0.372	0.201	0.270	750.1	752.6	0.473E+05	0.462E+05	0.482E+05	0.660E+03
0.292	0.248	0.270	749.5	755.7	0.131E+06	0.128E+06	0.135E+06	0.228E+04
0.241	0.281	0.270	749.5	756.8	0.216E+06	0.210E+06	0.224E+06	0.505E+04
0.140	0.350	0.270	749.1	759.9	0.331E+06	0.325E+06	0.336E+06	0.354E+04
0.092	0.385	0.270	748.7	762.0	0.328E+06	0.325E+06	0.333E+06	0.297E+04

Time finished: 0.00

Thermistor readings (VDC): (1,2,3,5,6)
      2.343   2.498   2.316   2.677   2.701

Expt.#:   20.15   Date: Mar.18, 1990
Time started: 23.00   Plab: 736.1 mm Hg

Temperatures (C) : (1,2,3,5,6)
         Room   Bath   WBub   Humid   ABub
         2·.92   25.10   24.22   26.07   25.22

fd	fa	fh	ftot	rh	ra	CNC	-	/	+
0.552	0.149	0.295	1.005	0.2⁻⁻	0.147	0.400E+01	0.526E+00	0.946E+00	
0.579	0.126	0.295	1.008	0.⁻	0.123	0.127E+00	0.467E-01	0.533E-01	
0.592	0.112	0.295	1.008	0.⁻	0.110	0.250E-02	0.250E-02	0.750E-02	
0.579	0.126	0.295	1.008	0.281	0.123	0.786E-01	0.386E-01	0.914E-01	
0.552	0.149	0.295	1.005	0.281	0.147	0.355E+01	0.176E+00	0.225E+00	
0.526	0.175	0.295	1.004	0.282	0.172	0.431E+02	0.111E+02	0.147E+02	
0.501	0.199	0.295	1.004	0.282	0.196	0.332E+03	0.287E+02	0.315E+02	
0.475	0.226	0.295	1.005	0.282	0.221	0.235E+04	0.116E+03	0.154E+03	
0.449	0.252	0.295	1.005	0.281	0.246	0.578E+04	0.353E+03	0.277E+03	
0.398	0.300	0.295	1.002	0.282	0.293	0.297E+05	0.137E+04	0.173E+04	
0.373	0.327	0.295	1.003	0.282	0.318	0.473E+05	0.111E+04	0.891E+03	
0.296	0.399	0.295	0.999	0.283	0.389	0.131E+06	0.322E+04	0.378E+04	
0.246	0.449	0.295	0.999	0.283	0.437	0.216E+06	0.556E+04	0.844E+04	
0.145	0.550	0.295	0.999	0.284	0.534	0.331E+06	0.571E+04	0.529E+04	
0.095	0.600	0.295	1.000	0.284	0.580	0.328E+06	0.325E+04	⁻.475E+04	

Time finished: 0.00

Temperatures (C): (1,2,3,5,6)
      25.04   25.21   24.35   26.22   25.35

Expt.#:   20.16   Date: Mar.19, 1990
Time started: 7.30   Plab: 736.4 mm Hg

Thermistor readings (VDC) : (1,2,3,5,6)
        Room   Bath   WBub   Humid   ABub
        1.862   1.987   1.794   2.222   2.162

fd	fa	fh	Pwb	Pab	CNC	range		s
0.352	0.385	0.045	740.1	764.8	0.756E-01	0.300E-01	0.140E+00	0.384E-01
0.334	0.385	0.060	740.3	764.8	0.222E+01	0.196E+01	0.245E+01	0.187E+00
0.325	0.385	0.068	740.5	764.8	0.806E+01	0.750E+01	0.877E+01	0.414E+00
0.315	0.385	0.075	740.5	764.8	0.205E+02	0.177E+02	0.240E+02	0.151E+01
0.297	0.385	0.090	740.9	764.8	0.175E+03	0.157E+03	0.198E+03	0.158E+02
0.279	0.385	0.105	741.4	764.8	0.604E+03	0.583E+03	0.614E+03	0.869E+01
0.261	0.385	0.120	742.0	764.8	0.247E+04	0.242E+04	0.254E+04	0.430E+02
0.244	0.385	0.135	742.5	764.8	0.604E+04	0.581E+04	0.627E+04	0.186E+03
0.209	0.385	0.165	743.8	764.8	0.227E+05	0.213E+05	0.234E+05	0.694E+03
0.159	0.385	0.210	745.7	764.8	0.522E+05	0.506E+05	0.550E+05	0.130E+04
0.094	0.385	0.270·	747.9	764.8	0.102E+06	0.980E+05	0.104E+06	0.244E+04
0.094	0.385	0.270'	747.9	764.8	0.847E+05	0.838E+05	0.860E+05	0.838E+03
0.033	0.385	0.330	750.9	764.8	0.107E+06	0.103E+06	0.111E+06	0.331E+04

Time finished: 9.30

Thermistor readings (VDC): (1,2,3,5,6)
        1.899   1.962   1.811   2.251   2.196

Expt.#:   20.16   Date: Mar.19, 1990
Time started: 7.30   Plab: 736.4 mm Hg

Temperatures (C) : (1,2,3,5,6)
        Room   Bath   WBub   Humid   ABub
        20.31   20.22   19.02   21.67   19.95

fd	fa	fh	ftot	rh	ra	CNC	-	/	+
0.354	0.600	0.046	1.001	0.044 ·	0.577	0.756E-01	0.456E-01	0.644E-01	
0.336	0.600	0.064	1.002	0.060	0.577	0.222E+01	0.262E+00	0.229E+00	
0.328	0.600	0.073	1.002	0.068	0.576	0.807E+01	0.563E+00	0.711E+00	
0.318	0.600	0.081	1.001	0.076	0.577	0.205E+02	0.278E+01	0.357E+01	
0.301	0.600	0.098	1.001	0.092	0.577	0.180E+03	0.186E+02	0.250E+02	
0.283	0.600	0.114	1.001	0.108	0.577	0.671E+03	0.253E+02	0.127E+02	
0.266	0.600	0.131	1.000	0.124 '	0.578	0.247E+04	0.544E+02	0.656E+02	
0.249	0.600	0.148	1.001	0.139	0.577	0.604E+04	0.227E+03	0.233E+03	
0.214	0.600	0.181	1.000	0.170	0.578	0.227E+05	0.139E+04	0.710E+03	
0.164	0.600	0.230	1.000	0.216	0.578	0.522E+05	0.158E+04	0.282E+04	
0.098	0.600	0.295	0.999	0.276	0.578	0.102E+06	0.378E+04	0.222E+04	
0.098	0.600	0.295	0.999	0.276	0.578	0.847E+05	0.886E+03	0.131E+04	
0.034	0.600	0.358	1.000	0.333	0.578	0.107E+06	0.417E+04	0.383E+04	

Time finished: 9.30

Temperatures (C): (1,2,3,5,6)
        20.68   19.97   19.19   21.96   20.29

Expt.#:   20.17   Date: Mar.19, 1990
Time started: 10.10   Plab: 736.4 mm Hg

Thermistor readings (VDC) : (1,2,3,5,6)
        Room   Bath   WBub   Humid   ABub
        1.879   1.944   1.812   2.233   2.208

fd	fa	fh	Pwb	Pab	CNC		range		s
0.665	0.200	0.045	741.1	755.0	0.000E+00	0.000E+00	0.000E+00	0.000E+00	
0.644	0.200	0.060	741.2	755.0	0.168E+00	0.120E+00	0.210E+00	0.392E-01	
0.655	0.200	0.052	741.2	755.0	0.500E-01	0.300E-01	0.800E-01	0.163E-01	
0.644	0.200	0.060	741.2	755.0	0.124E+00	0.800E-01	0.170E+00	0.341E-01	
0.623	0.200	0.075	742.0	755.0	0.914E+00	0.800E+00	0.104E+01	0.102E+00	
0.602	0.200	0.090	742.4	755.0	0.455E+01	0.418E+01	0.506E+01	0.327E+00	
0.582	0.200	0.105	742.9	755.0	0.277E+02	0.141E+02	0.147E+03	0.396E+02	
0.562	0.200	0.120	743.5	755.0	0.466E+02	0.408E+02	0.537E+02	0.397E+01	
0.542	0.200	0.135	744.2	755.0	0.962E+02	0.900E+02	0.105E+03	0.525E+01	
0.522	0.200	0.150	744.6	755.0	0.222E+03	0.207E+03	0.236E+03	0.100E+02	
0.484	0.200	0.180	745.7	755.0	0.640E+03	0.611E+03	0.675E+03	0.215E+02	
0.428	0.201	0.225	747.6	755.0	0.301E+04	0.289E+04	0.316E+04	0.946E+02	
0.374	0.200	0.270	749.4	755.0	0.518E+04	0.472E+04	0.541E+04	0.216E+03	
0.306	0.200	0.330	751.7	755.0	0.121E+05	0.114E+05	0.128E+05	0.460E+03	
0.209	0.200	0.420·	755.4	755.0	0.227E+05	0.217E+05	0.234E+05	0.587E+03	
0.209	0.200	0.420·	755.4	755.0	0.183E+05	0.173E+05	0.192E+05	0.589E+03	

Time finished: 12.15

Thermistor readings (VDC): (1,2,3,5,6)
        1.888   1.957   1.805   2.244   2.217

Expt.#:   20.17   Date: Mar.19, 1990
Time started: 10.10   Plab: 736.4 mm Hg

Temperatures (C) : (1,2,3,5,6)
        Room   Bath   WBub   Humid   ABub
        20.48   19.80   19.20   21.78   20.41

fd	fa	fh	ftot	rh	ra	CNC	-	/	+
0.638	0.325	0.046	1.011	0.045·	0.314	0.000E-)0	0.000E+00	0.000E+00	
0.620	0.325	0.064	1.010	0.062	0.314	0.168E-)0	0.483E-01	0.417E-01	
0.630	0.325	0.054	1.010	0.053	0.314	0.500E-01	0.200E-01	0.300E-01	
0.620	0.325	0.064	1.010	0.062	0.314	0.124E+00	0.443E-01	0.457E-01	
0.602	0.325	0.081	1.009	0.078	0.314	0.914E+00	0.114E+00	0.126E+00	
0.583	0.325	0.098	1.008	0.095	0.315	0.456E+01	0.372E+00	0.509E+00	
0.565	0.325	0.114	1.007	0.111	0.315	0.279E+02	0.137E+02	0.123E+03	
0.547	0.325	0.131	1.007	0.127	0.315	0.470E+02	0.591E+01	0.72ⁱ5E+01	
0.529	0.325	0.148	1.006	0.144	0.315	0.978E+02	0.639E+01	0.913E+01	
0.511	0.325	0.165	1.005	0.160	0.316	0.231E+03	0.163E+02	0.151E+02	
0.477	0.325	0.198	1.004	0.192·	0.316	0.716E+03	0.365E+02	0.432E+02	
0.425	0.327	0.247	1.004	0.238	0.317	0.301E+04	0.117E+03	0.153E+03	
0.375	0.325	0.295	1.001	0.285	0.317	0.518E+04	0.457E+03	0.233E+03	
0.310	0.325	0.358	1.001	0.345	0.317	0.121E+05	0.660E+03	0.740E+03	
0.214	0.325	0.450	1.000	0.432	0.317	0.227E+05	0.103E+04	0.673E+03	
0.214	0.325	0.450	1.000	0.432	0.317	0.183E+05	0.967E+03	0.933E+03	

Time finished: 12.15

Temperatures (C): (1,2,3,5,6)
        20.57   19.92   19.13   21.89   20.50

Expt.#:   20.18   Date: Mar.19, 1990
Time started: 14.00   Plab: 736.4 mm Hg

Thermistor readings (VDC) : (1,2,3,5,6)
        Room   Bath   WBub   Humid   ABub
        1.864   1.937   1.796   2.220   2.193

fd	fa	fh	Pwb	Pab	CNC	range		s
0.733	0.122	0.105	744.2	748.8	0.667E-02	0.000E+00	0.200E-01	0.115E-01
0.712	0.122	0.120	744.2	748.8	0.114E-01	0.000E+00	0.300E-01	0.107E-01
0.691	0.122	0.135	745.3	748.8	0.243E-01	0.000E+00	0.400E-01	0.140E-01
0.670	0.122	0.150	745.7	748.8	0.700E-01	0.300E-01	0.100E+00	0.271E-01
0.649	0.122	0.165	746.1	748.8	0.114E+00	0.700E-01	0.170E+00	0.324E-01
0.629	0.122	0.180	746.8	748.8	0.251E+00	0.160E+00	0.330E+00	0.557E-01
0.589	0.122	0.210	747.9	748.8	0.811E+00	0.690E+00	0.880E+00	0.671E-01
0.550	0.122	0.240	749.0	748.8	0.181E+01	0.144E+01	0.229E+01	0.272E+00
0.513	0.122	0.270	750.5	748.8	0.328E+01	0.290E+01	0.370E+01	0.239E+00
0.440	0.122	0.330	752.8	748.8	0.148E+02	0.128E+02	0.167E+02	0.132E+01
0.426	0.122	0.390	755.4	748.8	0.860E+01	0.823E+01	0.896E+01	0.313E+00
0.392	0.122	0.420	756.5	748.8	0.129E+02	0.120E+02	0.141E+02	0.818E+00
0.331	0.122	0.480	759.1	748.8	0.299E+02	0.275E+02	0.322E+02	0.170E+01
0.268	0.122	0.540	761.1	748.8	0.408E+02	0.352E+02	0.466E+02	0.311E+01
0.209	0.122	0.600	764.3	748.8	0.593E+02	0.533E+02	0.668E+02	0.370E+01

Time finished: 15.40

Thermistor readings (VDC): (1,2,3,5,6)
        1.880   1.948   1.792   2.236   2.207

Expt.#:   20.18   Date: Mar.19, 1990
Time started: 14.00   Plab: 736.4 mm Hg

Temperatures (C) : (1,2,3,5,6)
        Room   Bath   WBub   Humid   ABub
        20.33   19.73   19.04   21.65   20.26

fd	fa	fh	ftot	rh	ra	CNC	-	/	+
0.697	0.199	0.114	1.014	0.109	0.193	0.667E-02	0.667E-02	0.133E-01	
0.679	0.199	0.131	1.013	0.126	0.194	0.114E-01	0.114E-01	0.186E-01	
0.661	0.199	0.148	1.012	0.142	0.194	0.243E-01	0.243E-01	0.157E-01	
0.643	0.199	0.165	1.010	0.158	0.194	0.700E-01	0.400E-01	0.300E-01	
0.624	0.199	0.181	1.009	0.174	0.194	0.114E+00	0.444E-01	0.556E-01	
0.607	0.199	0.198	1.008	0.189	0.194	0.251E+00	0.913E-01	0.788E-01	
0.571	0.199	0.230	1.006	0.221	0.195	0.811E+00	0.121E+00	0.688E-01	
0.537	0.199	0.263	1.005	0.252	0.195	0.181E+01	0.366E+00	0.484E+00	
0.503	0.199	0.295	1.004	0.282	0.195	0.328E+01	0.378E+00	0.423E+00	
0.436	0.199	0.358	1.002	0.342	0.196	0.149E+02	0.204E+01	0.188E+01	
0.423	0.199	0.420	1.052	0.381	0.186	0.861E+01	0.367E+00	0.365E+00	
0.392	0.199	0.450	1.051	0.408	0.187	0.129E+02	0.854E+00	0.126E+01	
0.334	0.199	0.510	1.054	0.459	0.186	0.300E+02	0.241E+01	0.234E+01	
0.273	0.199	0.568	1.053	0.511	0.186	0.411E+02	0.570E+01	0.586E+01	
0.214	0.199	0.625	1.053	0.560	0.186	0.599E+02	0.609E+01	0.769E+01	

Time finished: 15.40

Temperatures (C): (1,2,3,5,6)
        20.49   19.84   19.00   21.81   20.40

Expt.#:   20.19   Date: Mar.19, 1990
Time started: 17.00   Plab: 736.4 mm Hg

Thermistor readings (VDC) : (1,2,3,5,6)
        Room   Bath   WBub   Humid   ABub
        1.876   1.938   1.790   2.224   2.196

fd	fa	fh	Pwb	Pab	CNC		range		s
0.426	0.093	0.389	755.9	746.2	0.278E-01	0.100E-01	0.400E-01		0.109E-01
0.392	0.093	0.420	757.2	746.2	0.744E-01	0.500E-01	0.120E+00		0.230E-01
0.323	0.093	0.480	759.1	746.2	0.249E+00	0.180E+00	0.320E+00		0.500E-01
0.291	0.093	0.520	761.3	746.2	0.300E+00	0.180E+00	0.350E+00		0.571E-01
0.251	0.092	0.580	763.4	746.2	0.236E+00	0.180E+00	0.310E+00		0.493E-01
0.181	0.092	0.640	766.5	746.2	0.539E+00	0.440E+00	0.600E+00		0.598E-01
0.142	0.092	0.680	767.7	746.2	0.744E+00	0.610E+00	0.930E+00		0.113E+00

Time finished: 17.30

Thermistor readings (VDC): (1,2,3,5,6)
        1.871   1.943   1.789   2.228   2.201

Expt.#:   20.19   Date: Mar.19, 1990
Time started: 17.00   Plab: 736.4 mm Hg

Temperatures (C) : (1,2,3,5,6)
        Room   Bath   WBub   Humid   ABub
        20.45   19.74   18.98   21.69   20.29

fd	fa	fh	ftot	rh	ra	CNC	-	/	+
0.423	0.151	0.419	1.002	0.397	0.149	0.278E-01	0.178E-01	0.122E-01	
0.392	0.151	0.450	1.002	0.425	0.149	0.744E-01	0.244E-01	0.456E-01	
0.326	0.151	0.510	0.998	0.483	0.149	0.249E+00	0.688E-01	0.713E-01	
0.295	0.151	0.549	1.007	0.514	0.148	0.300E+00	0.120E+00	0.500E-01	
0.256	0.149	0.606	1.025	0.556	0.144	0.236E+00	0.557E-01	0.743E-01	
0.186	0.149	0.662	1.013	0.612	0.146	0.539E+00	0.986E-01	0.614E-01	
0.147	0.149	0.699	1.010	0.647	0.146	0.745E+00	0.134E+00	0.186E+00	

Time finished: 17.30

Temperatures (C): (1,2,3,5,6)
        20.40   19.79   18.97   21.73   20.34

Expt.#:   20.20   Date: Mar.19, 1990
Time started: 18.45   Plab: 736.4 mm Hg

Thermistor readings (VDC) : (1,2,3,5,6)
        Room   Bath   WBub   Humid   ABub
        1.865   1.936   1.792   2.222   2.193

fd	fa	fh	Pwb	Pab	CNC		range		s
0.660	0.138	0.135	744.8	749.3	0.810E+00	0.680E+00	0.910E+00		0.988E-01
0.691	0.122	0.135	745.3	748.3	0.533E-01	0.100E-01	0.100E+00		0.316E-01
0.660	0.138	0.135	745.3	749.3	0.351E+00	0.240E+00	0.470E+00		0.685E-01
0.630	0.153	0.135	745.3	750.9	0.163E+01	0.136E+01	0.192E+01		0.181E+00
0.600	0.168	0.135	744.8	751.9	0.682E-01	0.581E+01	0.750E+01		0.484E+00
0.571	0.184	0.135	745.0	752.9	0.285E-02	0.247E+02	0.317E+02		0.260E+01
0.540	0.200	0.135	744.8	754.5	0.144E+03	0.128E+03	0.153E+03		0.717E+01
0.513	0.216	0.135	744.6	756.0	0.342E+03	0.322E+03	0.370E+03		0.145E+02
0.485	0.233	0.135	744.6	757.1	0.700E+03	0.638E+03	0.762E+03		0.362E+02
0.457	0.248	0.135	744.4	758.1	0.243E+04	0.231E+04	0.257E+04		0.737E+02
0.402	0.281	0.135	744.2	759.7	0.836E+04	0.787E+04	0.946E+04		0.468E+03
0.348	0.345	0.135	743.8	761.2	0.171E+05	0.147E+05	0.185E+05		0.132E+04
0.295	0.350	0.135	743.7	762.3	0.220E+05	0.213E+05	0.226E+05		0.453E+03
0.244	0.385	0.135	743.5	764.3	0.116E+05	0.114E+05	0.119E+05		0.170E+03

Time finished: 20.20

Thermistor readings (VDC): (1,2,3,5,6)
        1.880   1.947   1.793   2.230   2.187

Expt.#:   20.20   Date: Mar.19, 1990
Time started: 18.45   Plab: 736.4 mm Hg

Temperatures (C) : (1,2,3,5,6)
        Room   Bath   WBub   Humid   ABub
        20.34   19.72   19.00   21.67   20.26

fd	fa	fh	ftot	rh	ra	CNC	- /	+
0.634	0.226	0.148	1.011	0.142	0.219	0.810E+00	0.130E+00	0.100E+00
0.661	0.199	0.148	1.012	0.141	0.194	0.533E-01	0.433E-01	0.467E-01
0.634	0.226	0.148	1.011	0.141	0.219	0.351E+00	0.111E+00	0.119E+00
0.608	0.250	0.148	1.009	0.142	0.243	0.163E+01	0.268E+00	0.293E+00
0.581	0.274	0.148	1.007	0.142	0.267	0.683E+01	0.101E+01	0.684E+00
0.555	0.300	0.148	1.007	0.142	0.291	0.286E+02	0.380E+01	0.327E+01
0.528	0.325	0.148	1.004	0.142	0.316	0.147E+03	0.162E+02	0.100E+02
0.503	0.350	0.148	1.005	0.142	0.339	0.363E+03	0.221E+02	0.320E+02
0.478	0.376	0.148	1.006	0.142	0.364	0.791E+03	0.774E+02	0.799E+02
0.452	0.399	0.148	1.003	0.143	0.387	0.243E+04	0.115E+03	0.145E+03
0.401	0.449	0.148	1.002	0.143	0.435	0.836E+04	0.492E+03	0.110E+04
0.350	0.543	0.148	1.044	0.137	0.503	0.171E+05	0.238E+04	0.142E+04
0.299	0.550	0.148	1.001	0.143	0.531	0.220E+05	0.660E+03	0.640E+03
0.249	0.600	0.148	1.001	0.143	0.578	0.116E+05	0.200E+03	0.300E+03

Time finished: 20.20

Temperatures (C): (1,2,3,5,6)
        20.49   19.83   19.01   21.75   20.20

Expt.#:   20.21   Date: Mar.19, 1990
Time started: 21.15   Plab: 736.4 mm Hg

Thermistor readings (VDC) : (1,2,3,5,6)
        Room   Bath   WBub   Humid   ABub
        1.870   1.936   1.789   2.226   2.195

fd	fa	fh	Pwb	Pab	CNC		range		s
0.570	0.092	0.270	751.3	746.2	0.100E-01	0.000E+00	0.200E-01		0.707E-02
0.513	0.122	0.270	751.1	747.8	0.216E+01	0.176E+01	0.250E+01		0.228E+00
0.484	0.138	0.270	750.9	749.3	0.149E+02	0.120E+02	0.167E+02		0.114E+01
0.457	0.153	0.270	750.5	750.9	0.797E+02	0.721E+02	0.872E+02		0.458E+01
0.429	0.169	0.270	750.4	752.9	0.343E+03	0.304E+03	0.385E+03		0.218E+02
0.402	0.184	0.270	750.2	753.5	0.210E+04	0.202E+04	0.223E+04		0.566E+02
0.372	0.200	0.270	750.0	754.5	0.536E+04	0.229E+04	0.609E+04		0.775E+03
0.348	0.216	0.270	750.0	755.5	0.112E+05	0.108E+05	0.116E+05		0.275E+03
0.321	0.232	0.270	749.8	756.0	0.208E+05	0.204E+05	0.214E+05		0.295E+03
0.295	0.248	0.270	749.4	757.1	0.324E+05	0.301E+05	0.348E+05		0.138E+04
0.243	0.281	0.270	749.2	758.6	0.599E+05	0.584E+05	0.626E+05		0.147E+04
0.193	0.315	0.270	748.9	760.7	0.935E+05	0.907E+05	0.983E+05		0.258E+04
0.143	0.350	0.270	748.7	762.8	0.111E+06	0.107E+06	0.116E+06		0.331E+04
0.094	0.385	0.270	748.5	764.3	0.126E+06	0.121E+06	0.132E+06		0.362E+04

Time finished: 22.20

Thermistor readings (VDC): (1,2,3,5,6)
        1.878   1.944   1.792   2.232   2.189

Expt.#:   20.21   Date: Mar.19, 1990
Time started: 21.15   Plab: 736.4 mm Hg

Temperatures (C) : (1,2,3,5,6)
        Room   Bath   WBub   Humid   ABub
        20.39   19.72   18.97   21.71   20.28

fd	fa	fh	ftot	rh	ra	CNC	-	/	+
0.555	0.149	0.295	1.005	0.280	0.147.	0.100E-01	0.100E-01	0.100E-01	
0.503	0.199	0.295	1.004	0.281	0.196	0.216E+01	0.400E+00	0.340E+00	
0.477	0.226	0.295	1.004	0.281	0.221	0.150E+02	0.295E+01	0.177E+01	
0.452	0.250	0.295	1.004	0.281	0.244	0.808E+02	0.776E+01	0.777E+01	
0.426	0.276	0.295	1.003	0.281	0.269	0.364E+03	0.433E+02	0.479E+02	
0.401	0.300	0.295	1.002	0.282	0.292,	0.210E+04	0.842E+02	0.126E+03	
0.373	0.325	0.295	0.999	0.283	0.318	0.536E+04	0.307E+04	0.726E+03	
0.350	0.350	0.295	1.001	0.282	0.341	0.112E+05	0.430E+03	0.370E+03	
0.324	0.375	0.295	1.000	0.282	0.365	0.208E+05	0.450E+03	0.550E+03	
0.299	0.399	0.295	1.000	0.283	0.389	0.324E+05	0.228E+04	0.242E+04	
0.248	0.449	0.295	0.999	0.283	0.437	0.599E+05	0.149E+04	0.271E+04	
0.198	0.500	0.295	0.999	0.283	0.484	0.935E+05	0.278E+04	0.482E+04	
0.148	0.550	0.295	1.000	0.283	0.531	0.111E+06	0.410E+04	0.490E+04	
0.098	0.600	0.295	0.999	0.283	0.579	0.126E+06	0.494E+04	0.606E+04	

Time finished: 22.20

Temperatures (C): (1,2,3,5,6)
        20.47   19.80   19.00   21.77   20.22

```
Expt.#:      20.22     Date: Mar.20, 1990
Time started:  10.00     Plab:     736.0 mm Hg

Thermistor readings (VDC) : (1,2,3,5,6)
       Room     Bath    WBub   Humid    ABub
       2.732    2.937   2.657  3.055    3.069
```

fd	fa	fh	Pwb	Pab	CNC	range		s
0.390	0.385	0.015	738.2	773.2	0.249E+02	0.222E+02	0.275E+02	0.169E+01
0.396	0.385	0.010	738.2	773.2	0.437E+01	0.346E+01	0.514E+01	0.620E+00
0.390	0.385	0.015	738.2	773.2	0.821E+01	0.738E+01	0.897E+01	0.581E+00
0.381	0.385	0.022	738.4	773.2	0.654E+02	0.566E+02	0.736E+02	0.521E+01
0.371	0.385	0.030	738.4	773.2	0.606E+03	0.588E+03	0.638E+03	0.170E+02
0.361	0.385	0.037	738.8	773.2	0.505E+04	0.486E+04	0.517E+04	0.776E+02
0.351	0.385	0.045	739.0	773.2	0.211E+05	0.201E+05	0.218E+05	0.587E+03
0.343	0.385	0.052	739.2	773.2	0.447E+05	0.436E+05	0.452E+05	0.430E+03
0.332	0.385	0.060	739.3	773.2	0.783E+05	0.778E+05	0.789E+05	0.316E+03
0.314	0.385	0.075	739.9	773.2	0.157E+06	0.149E+06	0.168E+06	0.491E+04
0.295	0.385	0.090	741.2	773.2	0.292E+06	0.291E+06	0.294E+06	0.103E+04
0.277	0.385	0.105	741.4	773.2	0.359E+06	0.357E+06	0.362E+06	0.148E+04
0.241	0.385	0.135	742.3	773.2	0.451E+06	0.407E+06	0.484E+06	0.288E+05
0.208	0.385	0.164	743.8	773.2	0.590E+06	0.581E+06	0.601E+06	0.696E+04
0.154	0.385	0.210	745.3	773.2	0.685E+06	0.682E+06	0.688E+06	0.198E+04
0.089	0.385	0.270	748.1	773.2	0.799E+06	0.794E+06	0.803E+06	0.238E+04

```
Time finished:  12.30


Thermistor readings (VDC): (1,2,3,5,6)
       2.807    3.026   2.712   3.131   3.144
```

```
Expt.#:      20.22     Date: Mar.20, 1990
Time started:  10.00     Plab:     736.0 mm Hg

Temperatures (C) : (1,2,3,5,6)
       Room     Bath    WBub   Humid    ABub
       28.87    29.49   27.84  29.99    29.03
```

fd	fa	fh	ftot	rh	ra	CNC	-	/	+
0.390	0.600	0.012	1.002	0.011	0.570	0.250E+02	0.267E+01		0.267E+01
0.395	0.600	0.006	1.002	0.006	0.570	0.437E+01	0.906E+00		0.776E+00
0.390	0.600	0.012	1.002	0.011	0.570	0.822E+01	0.830E+00		0.765E+00
0.381	0.600	0.020	1.002	0.019	0.570	0.661E+02	0.894E+01		0.845E+01
0.372	0.600	0.029	1.002	0.027	0.570	0.673E+03	0.215E+02		0.401E+02
0.362	0.600	0.037	1.001	0.035	0.571	0.505E+04	0.186E+03		0.124E+03
0.353	0.600	0.046	1.001	0.044	0.571	0.211E+05	0.100E+04		0.700E+03
0.345	0.600	0.054	1.002	0.051	0.570	0.447E+05	0.111E+04		0.493E+03
0.335	0.600	0.064	1.001	0.060	0.571	0.783E+05	0.533E+03		0.567E+03
0.317	0.600	0.081	1.001	0.076	0.570	0.157E+06	0.753E+04		0.115E+05
0.299	0.600	0.098	1.000	0.092	0.571	0.292E+06	0.133E+04		0.167E+04
0.281	0.600	0.114	1.000	0.107	0.571	0.359E+06	0.175E+04		0.325E+04
0.246	0.600	0.148	1.000	0.139	0.571	0.451E+06	0.438E+05		0.332E+05
0.213	0.600	0.180	1.001	0.168	0.571	0.590E+06	0.878E+04		0.112E+05
0.159	0.600	0.230	0.999	0.215	0.572	0.685E+06	0.325E+04		0.275E+04
0.092	0.600	0.295	0.999	0.274	0.572	0.799E+06	0.500E+04		0.400E+04

```
Time finished:  12.30


Temperatures (C): (1,2,3,5,6)
       29.61    30.36   28.40   30.75   29.79
```

Expt.#:   20.23   Date: Mar.20, 1990
Time started: 14.00   Plab: 736.0 mm Hg

Thermistor readings (VDC) : (1,2,3,5,6)
      Room   Bath   WBub   Humid   ABub
      2.761   2.968   2.705   3.071   3.084

fd	fa	fh	Pwb	Pab	CNC	range		s
0.686	0.200	0.030	740.5	759.8	0.849E+02	0.770E+02	0.959E+02	0.559E+01
0.708	0.200	0.015	740.1	759.8	0.869E+01	0.731E+01	0.930E+01	0.670E+00
0.717	0.200	0.010	739.9	759.8	0.440E+01	0.399E+01	0.482E+01	0.307E+00
0.708	0.200	0.015	740.1	759.8	0.610E+01	0.527E+01	0.711E+01	0.625E+00
0.697	0.200	0.022	740.1	759.8	0.162E+02	0.136E+02	0.184E+02	0.175E+01
0.686	0.200	0.030	740.3	759.8	0.725E+02	0.640E+02	0.795E+02	0.392E+01
0.675	0.200	0.037	740.5	759.8	0.268E+03	0.251E+03	0.290E+03	0.119E+02
0.664	0.200	0.045	740.5	759.8	0.759E+03	0.695E+03	0.840E+03	0.394E+02
0.653	0.200	0.052	740.8	759.8	0.359E+04	0.340E+04	0.381E+04	0.115E+03
0.642	0.200	0.060	741.0	759.8	0.739E+04	0.700E+04	0.784E+04	0.221E+03
0.621	0.200	0.075	742.0	759.8	0.288E+05	0.277E+05	0.306E+05	0.898E+03
0.621	0.200	0.090	742.3	759.8	0.373E+06	0.453E+05	0.462E+07	0.122E+07
0.559	0.200	0.120	743.4	759.8	0.141E+06	0.136E+06	0.145E+06	0.311E+04
0.538	0.200	0.135	743.8	759.8	0.172E+06	0.160E+06	0.189E+06	0.875E+04
0.499	0.200	0.165	745.3	759.8	0.241E+06	0.235E+06	0.248E+06	0.382E+04
0.441	0.201	0.210	747.2	759.8	0.314E+06	0.310E+06	0.319E+06	0.308E+04
0.368	0.201	0.270	749.4	759.8	0.349E+06	0.335E+06	0.361E+06	0.956E+04
0.298	0.200	0.330	751.8	759.8	0.385E+06	0.379E+06	0.389E+06	0.337E+04
0.200	0.200	0.420	756.1	759.8	0.443E+06	0.426E+06	0.463E+06	0.116E+05

Time finished: 17.00

Thermistor readings (VDC): (1,2,3,5,6)
      2.823   3.040   2.723   3.146   3.163

Expt.#:   20.23   Date: Mar.20, 1990
Time started: 14.00   Plab: 736.0 mm Hg

Temperatures (C) : (1,2,3,5,6)
      Room   Bath   WBub   Humid   ABub
      29.15   29.79   28.33   30.15   29.18

fd	fa	fh	ftot	rh	ra	CNC	-	/	+
0.657	0.325	0.029	1.012	0.027	0.311	0.862E+02	0.816E+01	0.113E+02
0.676	0.325	0.012	1.013	0.011	0.311	0.871E+01	0.139E+01	0.607E+00
0.683	0.325	0.006	1.015	0.006	0.310	0.440E+01	0.407E+00	0.424E+00
0.676	0.325	0.012	1.013	0.011	0.311	0.611E+01	0.834E+00	0.101E+01
0.666	0.325	0.020	1.012	0.019	0.311	0.163E+02	0.263E+01	0.219E+01
0.657	0.325	0.029	1.012	0.027	0.311	0.735E+02	0.873E+01	0.716E+01
0.647	0.325	0.037	1.011	0.035	0.312	0.281E+03	0.187E+02	0.241E+02
0.637	0.325	0.046	1.011	0.044	0.312	0.867E+03	0.819E+02	0.106E+03
0.628	0.325	0.054	1.010	0.051	0.312	0.359E+04	0.186E+03	0.224E+03
0.618	0.325	0.064	1.009	0.060	0.312	0.739E+04	0.392E+03	0.448E+03
0.600	0.325	0.081	1.009	0.076	0.312	0.288E+05	0.112E+04	0.178E+04
0.600	0.325	0.098	1.026	0.090	0.307	0.373E+06	0.328E+06	0.425E+07
0.545	0.325	0.131	1.006	0.123	0.313	0.141E+06	0.464E+04	0.436E+04
0.526	0.325	0.148	1.005	0.139	0.313	0.172E+06	0.121E+05	0.169E+05
0.491	0.325	0.181	1.004	0.170	0.314	0.241E+06	0.582E+04	0.718E+04
0.437	0.327	0.230	1.004	0.216	0.315	0.314E+06	0.425E+04	0.475E+04
0.369	0.327	0.295	1.002	0.276	0.316	0.349E+06	0.144E+05	0.116E+05
0.302	0.325	0.358	0.999	0.335	0.315	0.385E+06	0.575E+04	0.425E+04
0.205	0.325	0.450	0.998	0.419	0.315	0.443E+06	0.169E+05	0.201E+05

Time finished: 17.00

Temperatures (C): (1,2,3,5,6)
      29.76   30.50   28.52   30.90   29.98

Expt.#:   20.24   Date: Mar.20, 1990
Time started: 18.30   Plab: 736.0 mm Hg

Thermistor readings (VDC) : (1,2,3,5,6)
      Room   Bath   WBub   Humid   AEub
      2.788   2.990   2.723   3.100   3.113

fd	fa	fh	Pwb	Pab	CNC	range		s
0.821	0.122	0.045	742.0	752.5	0.173E+02	0.153E+02	0.193E+02	0.128E+01
0.845	0.122	0.030	741.6	752.5	0.211E+01	0.184E+01	0.227E+01	0.157E+00
0.869	0.122	0.015	741.2	752.5	0.633E+00	0.520E+00	0.740E+00	0.848E-01
0.857	0.122	0.022	741.2	752.5	0.680E+00	0.630E+00	0.770E+00	0.518E-01
0.845	0.122	0.030	741.4	752.5	0.145E+01	0.133E+01	0.160E+01	0.846E-01
0.833	0.122	0.037	741.6	752.5	0.338E+01	0.303E+01	0.374E+01	0.204E+00
0.821	0.122	0.045	741.8	752.5	0.922E+01	0.779E+01	0.111E+02	0.109E-01
0.810	0.122	0.052	742.0	752.5	0.200E+02	0.184E+02	0.214E+02	0.101E-01
0.798	0.122	0.060	742.1	752.5	0.507E+02	0.448E+02	0.546E+02	0.271E+01
0.775	0.122	0.075	742.5	752.5	0.225E+03	0.200E+03	0.239E+03	0.110E+02
0.753	0.122	0.090	743.8	752.5	0.745E+03	0.708E+03	0.773E+03	0.172E+02
0.730	0.122	0.105	744.0	752.5	0.368E+04	0.349E+04	0.385E+04	0.112E+03
0.708	0.122	0.120	744.4	752.5	0.735E+04	0.665E+04	0.802E+04	0.462E+03
0.667	0.122	0.150	745.5	752.5	0.207E+05	0.201E+05	0.214E+05	0.423E+03
0.604	0.122	0.195	747.3	752.5	0.474E+05	0.462E+05	0.489E+05	0.847E+03
0.544	0.122	0.240	749.4	752.5	0.787E+05	0.763E+05	0.814E+05	0.173E+04
0.508	0.122	0.270	750.3	752.5	0.913E+05	0.895E+05	0.940E+05	0.149E+04
0.432	0.122	0.330	753.1	752.5	0.123E+06	0.121E+06	0.125E+06	0.125E+04
0.329	0.122	0.420	756.5	752.5	0.151E+06	0.145E+06	0.155E+06	0.283E+04
0.251	0.122	0.480	758.9	752.5	0.176E+06	0.172E+06	0.180E+06	0.245E+04

Time finished: 20.15

Thermistor readings (VDC): (1,2,3,5,6)
      2.815   3.026   2.719   3.133   3.150

Expt.#:   20.24   Date: Mar.20, 1990
Time started: 18.30   Plab: 736.0 mm Hg

Temperatures (C) : (1,2,3,5,6)
      Room   Bath   WBub   Humid   ABub
      29.42   30.01   28.52   30.44   29.48

fd	fa	fh	ftot	rh	ra	CNC	−	/	+
0.772	0.199	0.046	1.019	0.043	0.191	0.173E+02	0.199E+01	0.203E+01	
0.792	0.199	0.029	1.022	0.027	0.191	0.211E+01	0.273E+00	0.158E+00	
0.812	0.199	0.012	1.024	0.011	0.191	0.633E+00	0.113E+00	0.107E+00	
0.802	0.199	0.020	1.022	0.019	0.191	0.680E+00	0.500E-01	0.900E-01	
0.792	0.199	0.029	1.022	0.027	0.191	0.145E+01	0.121E+00	0.149E+00	
0.782	0.199	0.037	1.020	0.035	0.191	0.338E+01	0.346E+00	0.365E+00	
0.772	0.199	0.046	1.019	0.043	0.191	0.924E+01	0.144E+01	0.188E+01	
0.762	0.199	0.054	1.019	0.051	0.191	0.201E+02	0.163E+01	0.139E+01	
0.752	0.199	0.064	1.018	0.059	0.192	0.511E+02	0.597E+01	0.400E+01	
0.733	0.199	0.081	1.016	0.075	0.192	0.234E+03	0.272E+02	0.148E+02	
0.714	0.199	0.098	1.015	0.091	0.192	0.848E+03	0.470E+02	0.366E+02	
0.694	0.199	0.114	1.013	0.107	0.193	0.368E+04	0.187E+03	0.173E+03	
0.676	0.199	0.131	1.012	0.123	0.193	0.735E+04	0.697E+03	0.673E+03	
0.640	0.199	0.165	1.011	0.154	0.193	0.207E+05	0.564E+03	0.736E+03	
0.585	0.199	0.214	1.007	0.200	0.194	0.474E+05	0.123E+04	0.147E+04	
0.531	0.199	0.263	1.004	0.245	0.194	0.787E+05	0.237E+04	0.273E+04	
0.499	0.199	0.295	1.005	0.275	0.194	0.913E+05	0.182E+04	0.268E+04	
0.429	0.199	0.358	1.001	0.334	0.195	0.123E+06	0.218E+04	0.182E+04	
0.332	0.199	0.450	0.999	0.418	0.195	0.151E+06	0.600E+04	0.400E+04	
0.256	0.199	0.510	0.985	0.479	0.198	0.176E+06	0.400E+04	0.400E+04	

Time finished: 20.15

Temperatures (C): (1,2,3,5,6)
      29.68   30.36   28.47   30.77   29.85

Expt.#:   20.25   Date: Mar.20. 1990
Time started: 21.15   Plab: 736.0 mm Hg

Thermistor readings (VDC) : (1,2,3,5,6)
          Room   Bath   WBub   Humid   ABub
          2.793   2.996   2.725   3.105   3.116

fd	fa	fh	Pwb	Pab	CNC		range	s
0.841	0.092	0.074	743.4	748.9	0.121E+02	0.890E+01	0.137E+02	0.139E+01
0.864	0.092	0.060	743.1	748.9	0.198E+01	0.178E+01	0.224E+01	0.164E+00
0.888	0.092	0.045	742.9	748.9	0.305E+00	0.250E+00	0.360E+00	0.373E-01
0.912	0.092	0.030	742.5	748.9	0.370E-01	0.000E+00	0.900E-01	0.327E-01
0.901	0.092	0.037	742.1	748.9	0.538E-01	0.200E-01	0.900E-01	0.256E-01
0.888	0.092	0.045	742.5	748.9	0.123E+00	0.100E+00	0.150E+00	0.198E-01
0.864	0.092	0.060	742.7	748.9	0.564E+00	0.470E+00	0.700E+00	0.693E-01
0.840	0.092	0.075	742.9	748.9	0.351E+01	0.333E+01	0.374E+01	0.152E+00
0.817	0.092	0.090	743.8	748.9	0.157E+02	0.126E+02	0.188E+02	0.173E+01
0.794	0.092	0.105	744.2	748.9	0.645E+02	0.581E+02	0.706E+02	0.298E+01
0.771	0.092	0.120	744.9	748.9	0.221E+03	0.206E+03	0.239E+03	0.919E+01
0.749	0.092	0.135	745.7	748.9	0.526E+03	0.498E+03	0.554E+03	0.181E+02
0.727	0.092	0.150	746.0	748.9	0.212E+04	0.205E+04	0.218E+04	0.411E+02
0.706	0.092	0.165	746.6	748.9	0.319E+04	0.312E+04	0.326E+04	0.481E+02
0.643	0.092	0.210	748.3	748.9	0.853E+04	0.829E+04	0.874E+04	0.126E+03
0.563	0.092	0.270	751.3	748.9	0.189E+05	0.183E+05	0.197E+05	0.389E+03
0.488	0.092	0.330	753.5	748.9	0.343E+05	0.336E+05	0.352E+05	0.566E+03
0.382	0.092	0.420	756.8	748.9	0.489E+05	0.476E+05	0.505E+05	0.105E+04

Time finished: 23.00

Thermistor readings (VDC): (1,2,3,5,6)
        2.778   2.991   2.706   3.097   3.109

Expt.#:   20.25   Date: Mar.20. 1990
Time started: 21.15   Plab: 736.0 mm Hg

Temperatures (C) : (1,2,3,5,6)
          Room   Bath   WBub   Humid   ABub
          29.47   30.07   28.54   30.49   29.51

fd	fa	fh	ftot	rh	ra	CNC	-	/	+
0.788	0.149	0.080	1.021	0.073	0.144	0.122E+02	0.326E+01	0.156E+01
0.808	0.149	0.064	1.023	0.059	0.143	0.198E+01	0.203E+00	0.258E+00
0.828	0.149	0.046	1.025	0.043	0.143	0.305E+00	0.550E-01	0.550E-01
0.847	0.149	0.029	1.027	0.027	0.143	0.370E-01	0.370E-01	0.530E-01
0.838	0.149	0.037	1.027	0.034	0.143	0.538E-01	0.338E-01	0.363E-01
0.828	0.149	0.046	1.025	0.043	0.143	0.123E+00	0.225E-01	0.275E-01
0.808	0.149	0.064	1.023	0.059	0.143	0.565E+00	0.945E-01	0.136E+00
0.788	0.149	0.081	1.021	0.075	0.144	0.351E+01	0.178E+00	0.233E+00
0.768	0.149	0.098	1.019	0.090	0.144	0.157E+02	0.308E+01	0.315E+01
0.749	0.149	0.114	1.017	0.106	0.144	0.653E+02	0.658E+01	0.620E+01
0.729	0.149	0.131	1.015	0.122	0.145	0.230E+03	0.163E+02	0.193E+02
0.711	0.149	0.148	1.014	0.137	0.145	0.577E+03	0.332E+02	0.339E+02
0.692	0.149	0.165	1.013	0.153	0.145	0.212E+04	0.711E+02	0.589E+02
0.674	0.149	0.181	1.012	0.168	0.145	0.319E+04	0.711E+02	0.689E+02
0.619	0.149	0.230	1.008	0.214	0.146	0.853E+04	0.235E+03	0.215E+03
0.548	0.149	0.295	1.004	0.274	0.146	0.189E+05	0.609E+03	0.791E+03
0.480	0.149	0.358	1.002	0.332	0.146	0.343E+05	0.656E+03	0.944E+03
0.382	0.149	0.450	0.999	0.417	0.147	0.489E+05	0.134E+04	0.156E+04

Time finished: 23.00

Temperatures (C): (1,2,3,5,6)
        29.32   30.02   28.34   30.41   29.44

Expt.#:   20.26   Date: Mar.21, 1990
Time started: 0.00   Plab: 736.0 mm Hg

Thermistor readings (VDC) : (1,2,3,5,6)
       Room   Bath   WBub   Humid   ABub
       2.784   2.987   2.710   3.094   3.104

fd	fa	fh	Pwb	Pab	CNC	range		s
0.813	0.063	0.135	746.2	746.3	0.397E+01	0.347E+01	0.443E+01	0.323E+00
0.846	0.048	0.135	746.2	744.8	0.163E+00	0.110E+00	0.260E+00	0.532E-01
0.863	0.040	0.135	746.4	744.3	0.229E-01	0.100E-01	0.300E-01	0.756E-02
0.846	0.048	0.135	746.2	744.8	0.207E+00	0.170E+00	0.240E+00	0.258E-01
0.813	0.063	0.135	746.2	746.3	0.419E+01	0.370E+01	0.463E+01	0.389E+00
0.781	0.078	0.135	746.0	747.9	0.679E+02	0.608E+02	0.741E+02	0.396E+01
0.749	0.092	0.135	745.9	748.9	0.597E+03	0.565E+03	0.624E+03	0.202E+02
0.718	0.107	0.135	745.9	750.0	0.385E+04	0.373E+04	0.399E+04	0.723E+02
0.687	0.122	0.135	745.7	751.5	0.896E+04	0.827E+04	0.968E+04	0.421E+03
0.656	0.138	0.135	745.5	752.5	0.169E+05	0.165E+05	0.173E+05	0.220E+03
0.596	0.168	0.135	745.3	754.6	0.502E+05	0.483E+05	0.525E+05	0.140E+04
0.538	0.199	0.135	744.9	757.7	0.123E+06	0.120E+06	0.125E+06	0.215E+04
0.453	0.248	0.135	744.4	760.3	0.266E+06	0.256E+06	0.275E+06	0.577E+04
0.345	0.316	0.135	743.8	763.4	0.126E+07	0.400E+06	0.530E+07	0.185E+07
0.241	0.385	0.135	743.4	766.0	0.246E+08	0.385E+06	0.339E+09	0.904E+08

Time finished: 1.00

Thermistor readings (VDC): (1,2,3,5,6)
       2.795   3.009   2.712   3.113   3.124

Expt.#:   20.26   Date: Mar.21, 1990
Time started: 0.00   Plab: 736.0 mm Hg

Temperatures (C) : (1,2,3,5,6)
       Room   Bath   WBub   Humid   ABub
       29.38   29.98   28.38   30.38   29.39

fd	fa	fh	ftot	rh	ra	CNC	- /	+
0.765	0.100	0.148	1.019	0.136	0.097	0.397E+01	0.502E+00	0.459E+00
0.793	0.074	0.148	1.021	0.136	0.072	0.163E+00	0.533E-01	0.967E-01
0.807	0.060	0.148	1.021	0.136	0.058	0.229E-01	0.129E-01	0.714E-02
0.793	0.074	0.148	1.021	0.136	0.072	0.207E+00	0.367E-01	0.333E-01
0.765	0.100	0.148	1.019	0.136	0.097	0.420E+01	0.495E+00	0.436E+00
0.738	0.126	0.148	1.018	0.136	0.122	0.688E+02	0.731E+01	0.631E+01
0.711	0.149	0.148	1.014	0.137	0.145	0.663E+03	0.395E+02	0.328E+02
0.684	0.175	0.148	1.013	0.137	0.169	0.385E+04	0.124E+03	0.136E+03
0.657	0.199	0.148	1.011	0.137	0.193	0.896E+04	0.692E+03	0.718E+03
0.630	0.226	0.148	1.010	0.137	0.219	0.169E+05	0.380E+03	0.420E+03
0.578	0.274	0.148	1.006	0.138	0.266	0.502E+05	0.194E+04	0.226E+04
0.526	0.324	0.148	1.003	0.138	0.313	0.123E+06	0.289E+04	0.211E+04
0.448	0.399	0.148	1.002	0.139	0.386	0.266E+06	0.970E+04	0.930E+04
0.347	0.501	0.148	1.002	0.139	0.482	0.126E+07	0.863E+06	0.404E+07
0.246	0.600	0.148	1.000	0.139	0.576	0.246E+08	0.242E+08	0.314E+09

Time finished: 1.00

Temperatures (C): (1,2,3,5,6)
       29.49   30.19   28.40   30.57   29.59

Expt.#:   20.27   Date: Mar.21, 1990
Time started: 2.00   Plab: 736.0 mm Hg

Thermistor readings (VDC) : (1,2,3,5,6)
        Room   Bath   WBub   Humid   ABub
        2.801   3.005   2.711   3.120   3.127

fd	fa	fh	Pwb	Pab	CNC		range	s
0.683	0.035	0.270	752.4	743.2	0.129E+00	0.800E-01	0.190E+00	0.376E-01
0.673	0.041	0.270	752.2	743.8	0.126E+01	0.112E+01	0.143E+01	0.105E+00
0.652	0.048	0.271	752.2	744.8	0.139E+02	0.121E+02	0.154E+02	0.106E+01
0.635	0.055	0.270	752.0	745.3	0.877E+02	0.700E+01	0.106E+03	0.252E+02
0.622	0.063	0.270	751.8	745.8	0.335E+03	0.309E+03	0.351E+03	0.140E+02
0.593	0.078	0.270	751.6	746.3	0.447E+04	0.438E+04	0.453E+04	0.518E+02
0.563	0.092	0.270	751.4	747.9	0.172E+05	0.162E+05	0.180E+05	0.551E+03
0.534	0.107	0.270	751.3	748.9	0.367E+05	0.352E+05	0.384E+05	0.920E+03
0.506	0.122	0.270	751.1	750.0	0.647E+05	0.635E+05	0.676E+05	0.129E+04
0.449	0.153	0.270	750.9	752.5	0.134E+06	0.132E+06	0.137E+06	0.140E+04
0.368	0.200	0.270	750.3	755.1	0.324E+06	0.314E+06	0.329E+06	0.459E+04
0.289	0.248	0.270	749.8	758.2	0.530E+06	0.516E+06	0.545E+06	0.105E+05
0.187	0.316	0.270	749.4	761.9	0.789E+06	0.779E+06	0.793E+06	0.451E+04
0.089	0.385	0.270	749.0	764.4	0.812E+06	0.804E+06	0.826E+06	0.709E+04

Time finished: 2.30

Thermistor readings (VDC): (1,2,3,5,6)
        2.806   3.017   2.715   3.126   3.135

Expt.#:   20.27   Date: Mar.21, 1990
Time started: 2.00   Plab: 736.0 mm Hg

Temperatures (C) : (1,2,3,5,6)
        Room   Bath   WBub   Humid   ABub
        29.55   30.15   28.39   30.64   29.62

fd	fa	fh	ftot	rh	ra	CNC	- /	+
0.654	0.052	0.295	1.012	0.268	0.050	0.129E+00	0.488E-01	0.613E-01
0.645	0.062	0.295	1.014	0.267	0.061	0.126E+01	0.143E+00	0.168E+00
0.627	0.074	0.296	1.009	0.270	0.073	0.140E+02	0.183E+01	0.148E+01
0.612	0.086	0.295	1.005	0.270	0.085	0.891E+02	0.821E+02	0.189E+02
0.601	0.100	0.295	1.007	0.269	0.098	0.355E+03	0.286E+02	0.185E+02
0.575	0.126	0.295	1.007	0.269	0.123	0.447E+04	0.944E+02	0.556E+02
0.548	0.149	0.295	1.004	0.270	0.146	0.172E+05	0.959E+03	0.841E+03
0.522	0.175	0.295	1.003	0.270	0.171	0.367E+05	0.149E+04	0.171E+04
0.497	0.199	0.295	1.003	0.271	0.195	0.647E+05	0.124E+04	0.286E+04
0.445	0.250	0.295	1.001	0.271	0.244	0.134E+06	0.220E+04	0.280E+04
0.369	0.325	0.295	1.001	0.272	0.317	0.324E+06	0.980E+04	0.520E+04
0.293	0.399	0.295	0.999	0.272	0.388	0.530E+06	0.142E+05	0.148E+05
0.192	0.501	0.295	1.000	0.272	0.484	0.789E+06	0.101E+05	0.388E+04
0.092	0.600	0.295	0.999	0.272	0.578	0.812E+06	0.845E+04	0.135E+05

Time finished: 2.30

Temperatures (C): (1,2,3,5,6)
        29.60   30.27   28.43   30.70   29.70

Expt.#:   20.28   Date: Mar.21, 1990
Time started: 10.00   Plab: 736.0 mm Hg

Thermistor readings (VDC) : (1,2,3,5,6)
     Room   Bath   WBub   Humid   ABub
     2.358   2.514   2.382   2.694   2.718

fd	fa	fh	Pwb	Pab	CNC		range		s
0.664	0.200	0.045	740.1	757.7	0.245E+00	0.210E+00	0.290E+00		0.266E-01
0.686	0.200	0.030	740.1	757.7	0.150E-01	0.100E-01	0.300E-01		0.756E-02
0.665	0.200	0.045	740.5	757.7	0.232E+00	0.160E+00	0.280E+00		0.352E-01
0.643	0.200	0.060	740.8	757.7	0.318E+01	0.289E+01	0.351E+01		0.217E+00
0.622	0.200	0.075	741.2	757.7	0.266E+02	0.234E+02	0.289E+02		0.174E+01
0.601	0.200	0.090	742.0	757.7	0.140E+03	0.129E+03	0.155E+03		0.615E+01
0.581	0.200	0.105	742.7	757.7	0.391E+03	0.348E+03	0.427E+03		0.188E+02
0.560	0.200	0.120	743.1	757.7	0.170E+04	0.159E+04	0.180E+04		0.653E+02
0.540	0.200	0.135	743.8	757.7	0.306E+04	0.292E+04	0.320E+04		0.835E+02
0.501	0.200	0.165	745.1	757.7	0.922E+04	0.878E+04	0.988E+04		0.302E+03
0.444	0.200	0.210	747.2	757.7	0.358E+05	0.338E+05	0.375E+05		0.122E+04
0.372	0.200	0.271	749.6	757.7	0.766E+05	0.741E+05	0.790E+05		0.124E+04
0.303	0.200	0.330	751.8	757.7	0.107E+06	0.104E+06	0.111E+06		0.257E+04
0.237	0.200	0.390	754.4	757.7	0.131E+06	0.129E+06	0.134E+06		0.186E+04
0.205	0.200	0.420	755.3	757.7	0.136E+06	0.133E+06	0.141E+06		0.251E+04

Time finished: 11.20

Thermistor readings (VDC): (1,2,3,5,6)
     2.381   2.536   2.386   2.717   2.741

Expt.#:   20.28   Date: Mar.21, 1990
Time started: 10.00   Plab: 736.0 mm Hg

Temperatures (C) : (1,2,3,5,6)
     Room   Bath   WBub   Humid   ABub
     25.19   25.36   25.03   26.39   25.52

fd	fa	fh	ftot	rh	ra	CNC	-	/	+
0.637	0.325	0.046	1.011	0.046	0.312	0.245E+00	0.350E-01		0.450E-01
0.657	0.325	0.029	1.012	0.029	0.312	0.150E-01	0.500E-02		0.150E-01
0.638	0.325	0.046	1.011	0.046	0.312	0.232E+00	0.720E-01		0.480E-01
0.619	0.325	0.064	1.010	0.063	0.313	0.319E+01	0.294E+00		0.326E+00
0.601	0.325	0.081	1.009	0.080	0.313	0.267E+02	0.322E+01		0.233E+01
0.582	0.325	0.098	1.008	0.097	0.313	0.144E+03	0.118E+02		0.155E+02
0.564	0.325	0.114	1.008	0.114	0.313	0.419E+03	0.488E+02		0.414E+02
0.546	0.325	0.131	1.006	0.131	0.314	0.170E+04	0.109E+03		0.101E+03
0.528	0.325	0.148	1.006	0.148	0.314	0.306E+04	0.136E+03		0.144E+03
0.492	0.325	0.181	1.005	0.180	0.314	0.922E+04	0.442E+03		0.658E+03
0.440	0.325	0.230	1.003	0.229	0.315	0.358E+05	0.202E+04		0.168E+04
0.373	0.325	0.296	1.003	0.293	0.315	0.766E+05	0.250E+04		0.240E+04
0.307	0.325	0.358	1.001	0.354	0.315	0.107E+06	0.258E+04		0.442E+04
0.242	0.325	0.420	1.001	0.414	0.316	0.131E+06	0.222E+04		0.278E+04
0.210	0.325	0.450	1.000	0.444	0.316	0.136E+06	0.350E+04		0.450E+04

Time finished: 11.20

Temperatures (C): (1,2,3,5,6)
     25.42   25.58   25.07   26.62   25.75